Loughborough University

This item was submitted to Loughborough's Research Repository by the author.
Items in Figshare are protected by copyright, with all rights reserved, unless otherwise indicated.

One-step hydroxylation of benzene to phenol using N2O

PLEASE CITE THE PUBLISHED VERSION

PUBLISHER

Loughborough University

LICENCE

CC BY-NC-ND 4.0

REPOSITORY RECORD

AL-Hazmi, Naeem. 2011. “One-step Hydroxylation of Benzene to Phenol Using N2O”. figshare.
https://hdl.handle.net/2134/8299.

Loughborough University

This item was submitted to Loughborough's Institutional Repository (https://dspace.lboro.ac.uk/) by the author and is made available under the following Creative Commons Licence conditions.

creative commons

COMMONS DEED

Attribution-NonCommercial-NoDerivs 2.5

You are free:

- to copy, distribute, display, and perform the work

Under the following conditions:



Attribution. You must attribute the work in the manner specified by the author or licensor.



Noncommercial. You may not use this work for commercial purposes.



No Derivative Works. You may not alter, transform, or build upon this work.

- For any reuse or distribution, you must make clear to others the license terms of this work.
- Any of these conditions can be waived if you get permission from the copyright holder.

Your fair use and other rights are in no way affected by the above.

This is a human-readable summary of the Legal Code (the full license).

Disclaimer

For the full text of this licence, please go to:
http://creativecommons.org/licenses/by-nc-nd/2.5/



One step hydroxylation of benzene to phenol using N_2O

By

Naeem AL-Hazmi

A Doctoral Thesis

Submitted in partial fulfilment of the requirements for award of Doctoral of Philosophy of Loughborough University

Department of Chemical Engineering

2011

© by Naeem AL-Hazmi (2011)

Acknowledgment

I would like to begin by thanking Almighty God for all his blessings and grace upon me in this life. I would like also to thank the Saudi Arabian Government for funding me through my PhD Work.

I would like to thank the Chemical Engineering Department at Loughborough University together with my Supervisors, Dr Danish Malik and Professor Richard Wakeman for their guidance and advice. My work with each of them allowed me to gain different experiences. I wish to express my sincere gratitude to Professor Wakeman for giving me valuable advice and support for my project. I wish to thank Dr Danish Malik for giving me very useful feedback during my work, also for thorough feedback on my Thesis. He was with me step by step – Thank you Dr Malik.

Additionally, I would like to thank Chris Manning, Tony Eyer, Dave Smith and the laboratory supervisor Sean Creedon for all their training and help with the laboratory equipment and with the experimental part of this thesis.

Finally, I especially want to dedicate my dissertation to my family (especially my brother Yasser AL-Hazmi) for all the patience and encouragement they showed me during the years I spent doing my PhD. I want to thank my FATHER (RABEEH AL-HAZMI) for his love, caring, help and support which allowed me to carry on, through both the good and difficult days, when he was in the life. He passed a way, but I believe that he is still with me. My thanks to my mother Haddia AL-Auida for her love and caring. I am blessed to have her as a mother. I want to thank all my brothers and sisters for their love and support in the past and present.

I would like to thank my friends, Waleed AL-Laffi and Katherine Hayes for their caring and support. Also I would like to thank my friends Fahad, Reda, Hakem, my fellow PhD students at the Chemical Engineering Department at Loughborough University.

Abstract

There is an increasing commercial interest in finding alternative ways to produce phenol that overcome the disadvantages of the current cumene process used to synthesize phenol. The drivers for the change are both economic and environmental. A direct oxidation route for producing phenol from benzene is based on using N_2O as an oxidizing agent in the gas phase in the presence of modified Fe-ZSM5 zeolite. One of the main objectives was to examine the effect of different Si/Al ratios, temperatures and iron content on the selective conversion of benzene to phenol with a desire to achieve high selectivity and minimise catalyst deactivation. Also one of the research objectives was to identify the active sites in the catalyst and design the catalyst which is able to delay coke formation. The methodology was to incorporate iron directly at extra-framework positions via liquid ion-exchange. In this project, a series of selective Fe-ZSM5 catalysts with different Si/Al ratios have been prepared and evaluated for selective formation of phenol. The catalyst samples were characterized (by Atomic Absorption Spectroscopy (AAS), Malvern mastersizer and Nitrogen adsorption using N_2 at 77 K via Micromeritics to determine the elemental composition, average particle size, BET surface area and pore size distribution) and their catalytic activities compared. A quantitative comparison between the number of active sites using isopropylamine decomposition method shows that active sites increase as the Si/Al ratio increased and also as the iron content increased. The influence of coke formation and concentration of iron-containing active sites (*α*-sites) on the hydroxylation of benzene to phenol by nitrous oxide was studied. Catalysts synthesized with high Si/Al ratios (80) and with low iron content (~0.1 wt%) showed good long term stability (reduced deactivation rates) and demonstrated good phenol selectivity and reaction rates (6 mmol/g.h). Catalysts with high amounts of iron (~1%) showed considerable deactivation particularly at high reaction temperatures (450°C). High reaction temperatures (450°C) in comparison with 350°C were found to favour higher reaction rates however, catalysts with high iron content were particularly prone to deactivation at this temperature.

The novelty of this work was based on the high benzene to phenol selectivity in the range of (80 - 92 %) with high benzene conversion (~80%) and with high average productivity (typically 6 mmol/g.cat.h or higher) using a low concentration of benzene and nitrous oxide compared with literature (~3 mmol/g.cat.h) such as (Hensen *et al*., 2005) using the same reaction conditions. The regeneration of coked catalysts has been made. Catalysts regeneration using oxidation followed by reduction seemed to be promising compared with oxidation by N_2O and O_2 methods. This concludes that the phenol productivity and the catalyst regeneration depends on the catalyst preparation and active sites concentrations.

A kinetic model for phenol production from benzene was developed. The simulation work has shown that the conversion of benzene (~60%) was lower than its conversion in the experimental work (~80%) using 0.2g of catalyst. This demonstrates that the catalyst preparation significantly affects the nature of active centers of the surface of Fe/ZSM-5. The simulation results show that the small amount of catalyst is active for phenol production from benzene.

Table of contents

1 Introduction to Research Problem 1

1.1 Problem description and catalyst comparison 4
1.1.1 Background (History) of phenol production 4
1.1.2 Background (History) of cumene manufacturing process 6
1.1.3 New process development: single step oxidation processes using a novel catalysts 8
Novel catalysts 11
1.2 Reactor technology 19
1.3 Research objectives 22
1.4 Conclusions 22

2 Literature Review on One Step Oxidation of Benzene to Phenol Using N_2O as Oxidising Agent 23

2.1 Heterogeneous catalysis using H_2O_2 and N_2O in one step oxidation of benzene to phenol. 23
2.1.1 Titanium silicate (TS-1) (liquid phase) 23
2.1.2 Nitrous oxide using zeolites as catalysts (gas phase oxidation) . 24
2.1.3 Structure and properties of zeolites 28
2.1.4 Catalyst preparation methods 30
2.1.5 Formation of active sites 32
2.1.6 Deactivation of zeolites 34
2.1.7 The selectivity and productivity of phenol 37
2.1.8 Physical and chemical characterisation of the catalyst 39
2.2 Reaction mechanism of benzene oxidation using N_2O 40
2.2.1 Modelling of reaction kinetics [Benzene hydroxylation (using N_2O as oxidising agent) to phenol with consideration of competing reaction.] 40
2.3 Conclusions 49

3 Materials and Methods 50

3.1 Catalysts preparation 50
3.1.1 H-ZSM-5 catalysts preparation 52
3.1.2 Fe/ZSM-5 catalysts preparation 54
3.2 Granulation process 56
3.3 Characterization of Fe/ZSM-5 57
3.3.1 Particle size characterisation 57
3.3.2 Elemental composition (AAS) 58
3.3.3 Surface area measurement (Nitrogen physisorption) 59
3.3.4 Chemisorption method 60
3.4 Experimental setup to evaluate benzene reaction with nitrous oxide using zeolite catalysts. 63
3.5 Regeneration of coked catalysts 65
3.6 Standard preparation and calibration method using (GC) 66

4 Catalysts Characterisation Results and Discussion 71

4.1 Elemental analysis using AAS 71
4.2 Particle size analysis using malvern 73
4.3 Surface area and pore structure using (BET) 80
4.4 Determination of the nature of active sites 84

5 Experimental Results and Discussion for Direct Oxidation of Benzene to Phenol using N_2O 92

5.1 Phenol production using Fe-ZSM-5 catalysts 92
5.2 Phenol productivity (rate of phenol formation) 96
5.2.1 Effect of iron content on phenol productivity 96
5.2.2 Effect of Si/Al ratio on phenol productivity 99
5.2.3 Effect of iron content and temperature on phenol productivity 102
5.3 Benzene conversion and phenol selectivity 106
5.4 Coke formation 108
5.5 Catalyst regeneration 109
5.6 Kinetics of benzene hydroxylation to phenol 111
5.6.1 Kinetics of benzene hydroxylation using research Project data 111
5.6.2 Rate law from experimental data with the rate – limiting step .. 116
5.6.3 Derivation of the kinetic model 120
5.7 Conclusions 128

6 Conclusions and Recommendations for Future Work 129

6.1 Conclusions 129
6.2 Recommendations for future work 131

References 132

Appendixes 143

Appendix A: Modeling for reaction kinetics using a fixed bed reactor data. 143
Appendix B. Experimental setup and procedure 146
Appendix C: Samples characterisations 175
Appendix D: Experimental results 179
Appendix E. Published work 186

List of Figures

Figure 1.1 Phenol production using cumene process 2
Figure 1.2 One step oxidation of benzene to phenol by using molecular oxygen 9
Figure 1.3 Micro-reactor for producing phenol by oxidation of benzene. 20
Figure 1.4 Producing phenol by oxidation of benzene 21
Figure 2.1 One-step hydroxylation of benzene to phenol using H_2O_2 23
Figure 2.2 One-step hydroxylation of benzene to phenol using N_2O 25
Figure 2.3 Basic Zeolite Structure 29
Figure 2.4 Structre type MFI (www.iza-online.org) 29
Figure 2.5 A possible mechanism for ion exchange in an aqueous solution of iron (III). 31
Figure 2.6 Formation of pair of α- sites in the form of a dinuclear iron complex 33
Figure 2.7 The schematic representation of coking and regeneration of ZSM-5 36
Figure 2.8 Isopropylamine decomposing to Propylene and ammonia 39
Figure 2.9 Schematic representation of elementary reactions constituting the main reaction 41
Figure 2.10 Schematic representation of elementary reactions constituting the side reaction of N_2O 43
Figure 2.11 Schematic representation of elementary reactions constituting the Consumption of phenol 44
Figure 2.12 Schematic representation of elementary reactions constituting the side reaction of phenol2 (catechol) 45
Figure 2.13 Schematic representation of elementary reactions constituting the side reaction of $phenol_2$ (*p*-benzoquinone) 45
Figure 3.1 Photograph of the series numbers of catalyst samples before and after preparation using ion exchange. 51
Figure 3.2 Procedure to prepare HZ30 and HZ80 catalyst samples using liquid ion exchange method 53

Figure 3.3 Procedure to prepare FeZ30 and FeZ80 catalyst samples using liquid ion exchange method 55
Figure 3.4 A Granulation process for ZSM-5 catalyst samples 56
Figure 3.5 Surface area and pore size analyzer. 60
Figure 3.6 Vapor generation apparatus. 61
Figure 3.7 A line diagram of the chemisorption method to find the number of active sites. 61
Figure 3.8 Photograph of the chemisorption apparatus to quantify acidic sites in the catalyst. 62
Figure 3.9 A line diagram of the fixed bed reactor system. 64
Figure 3.10 Digital photo of the fixed bed-reactor system 65
Figure 3.11 A sample chromatogram of all analyzed species. 66
Figure 3.12 Calibration plot of benzene (0.6 – 2 wt%) (GC) 67
Figure 3.13 Calibration plot of benzene (2 – 15 wt%) (GC) 67
Figure 3.14 Calibration plot of phenol (1 – 10 wt%) (GC) 68
Figure 3.15 Calibration plot of hydroquinone (0.1 – 1 wt%) (GC)..... 68
Figure 3.16 Calibration plot of catechol (0.1 – 1 wt%) (GC)..... 69
Figure 3.17 Calibration plot of p-benzoquinone (0.1 – 1.5 wt%) (GC)..... 69
Figure 3.18 Calibration plot of He (MFC) 70
Figure 3.19 Calibration plot of N_2O (MFC) 70
Figure 4.1 Cummulative curve of particle size distribution for (NH4ZSM-5 30) – before preparation..... 73
Figure 4.2 The particle size analysis for (NH4ZSM-5 30) – before preparation. 73
Figure 4.3 Cummulative curve of particle size distribution for (NH4ZSM-5 80) – before preparation..... 74
Figure 4.4 The particle size analysis for (NH4ZSM-5 80) – before preparation. 74
Figure 4.5 Cummulative curve of particle size distribution for (FeZ30 0.1%) – post preparation. 75
Figure 4.6 The particle size analysis for (FeZ30 0.1%) –post preparation. 75
Figure 4.7 Cummulative curve of particle size distribution for (FeZ80 0.1%) – post preparation. 76
Figure 4.8 The particle size analysis for (FeZ80 0.1%) –post preparation. 76

Figure 4.9 Cummulative curve of particle size distribution for (FeZ30 1%) – post preparation. 77
Figure 4.10 The particle size analysis for (FeZ30 1%) –post preparation. 77
Figure 4.11 Cummulative curve of particle size distribution for (FeZ801%) – post preparation. 78
Figure 4.12 The particle size analysis for (FeZ80 1%) –post preparation. 78
Figure 4.13 Pore size characterisation for (NH_4Z30) 81
Figure 4.14 Pore size characterisation for (NH_4Z80) 81
Figure 4.15 Pore size characterization for Z30 before and after preparation . 82
Figure 4.16 Nitrogen adsorption isotherm for Z30 before and after preparation 82
Figure 4.17 Nitrogen adsorption isotherm for Z30 & 80 before and after preparation 83
Figure 4.18 Multiple Isopropylamine injections at 200°C with and without catalyst 84
Figure 4.19 Desorption of propylene in temperature programmed decomposition for NH_4Z30. 85
Figure 4.20 Desorption of propylene in temperature programmed decomposition for 0.1%FeZ30. 86
Figure 4.21 Desorption of propylene in temperature programmed decomposition for 1%FeZ30. 86
Figure 4.22 Desorption of propylene in temperature programmed decomposition for NH_4Z80. 87
Figure 4.23 Desorption of propylene in temperature programmed decomposition for 0.1%FeZ80. 87
Figure 4.24 Desorption of propylene in temperature programmed decomposition for 1%FeZ80. 88
Figure 4.25 Desorption of propylene in temperature programmed decomposition for Z30 with different iron contents. 89
Figure 4.26 Desorption of propylene in temperature programmed decomposition for Z80 with different iron contents. 89
Figure 4.27 Desorption of propylene in temperature programmed decomposition for Z80 and 30 90

Figure 4.28 Desorption of propylene in temperature programmed decomposition for 0.1% FeZ30 and 80. 90
Figure 4.29 Desorption of propylene in temperature programmed decomposition for 1% FeZ30 and 80. 91
Figure 5.1 The invariability of the feed composition of benzene as a function of time. 93
Figure 5.2 Benzene and phenol concentrations vs. time on stream (reaction conditions: 450°C, atmospheric pressure, feed gas =60ml/min, using 0.1% Fe/Z30). 94
Figure 5.3 Phenol productivity for repeated experiments vs time on stream (reaction conditions: 450°C, atmospheric pressure, feed gas =60ml/min, using 0.1% Fe/Z30). 94
Figure 5.4 By-products productivity vs time on stream (reaction conditions: 450°C, atmospheric pressure, feed gas =60ml/min). 95
Figure 5.5 Phenol productivities vs time on stream using Si/Al ratio 30. 97
Figure 5.6 Phenol productivities vs time on stream using Si/Al ratio 80. 97
Figure 5.7 Phenol productivities vs time on stream using 0.1% Fe/ZSM-5. . 100
Figure 5.8 Phenol productivities vs time on stream using 0.1%FeZ80. 100
Figure 5.9 Phenol productivities vs time on stream using 1% Fe/ZSM-5. 101
Figure 5.10 Phenol productivities vs time on stream at 450°C. 102
Figure 5.11 Phenol productivities vs time on stream at 350°C. 103
Figure 5.12 Productivity of phenol as a function of iron contents in FeZ30 in 1 and 2.5 h. 104
Figure 5.13 Active sites as a function of different iron contents in FeZ30. ... 104
Figure 5.14 Effect of temperature on the productivity and selectivity at reaction time of 0.5s. 105
Figure 5.15 Benzene to phenol conversion as a function of time on stream for FeZ80 at 450 °C. 106
Figure 5.16 Benzene to phenol conversion as a function of time on stream for FeZ80 at 350 °C. 107
Figure 5.17 Productivity of phenol and coke formation as a function of time on stream using1%FeZ30. 108
Figure 5.18 Phenol Productivity using the sample before and after catalyst regeneration for 0.1%FeZ80 using reduction method. 109

Figure 5.19 Phenol Productivity using the sample before and after catalyst regeneration for 0.1%FeZ80. 110
Figure 5.20 Plot of rate vs. benzene partial pressure at 1h using 0.1%FeZ80 111
Figure 5.21 Arrhenius plot rate constants (k1) as a function of temperature. 114
Figure 5.22 Conversion profile (reaction conditions: 1 mol% benzene, 7 mol% nitrous oxide, atmospheric pressure, feed gas =60ml/min). 126
Figure 5.23 Temperature profile (reaction conditions: 1 mol% benzene, 7 mol% nitrous oxide, atmospheric pressure, feed gas =60ml/min). 126
Figure 5.24 Benzene and phenol concentration profile (reaction conditions: 1 mol% benzene, 7 mol% nitrous oxide, atmospheric pressure, feed gas =60ml/min). 127

List of Tables

Table 1.1 Comparison of performance of various catalysts in the open literature for the hydroxylation of benzene to phenol (liquid phase reaction) . 12
Table 1.2 Literature described catalytic systems for hydroxylation of benzene with O2 and H2 15
Table 3.1 Nomenclature identifying catalyst samples prepared using ion exchange. 50
Table 4.1 Catalyst elemental composition. 71
Table 4.2.Total pore volumes, area, and pore sizes of the various zeolite catalysts. 80
Table 4.3 The amount of acid sites determined from isopropylamine decomposition. 91
Table 5.1 Effect of reaction temperature on the reactor performance. 105
Table 5.2 Stoichiometric Table for a flow system 123

1 Introduction to Research Problem

Phenol is industrially important in the synthesis of many drugs, dyes and insecticides. Phenol is used primarily to produce phenol-formaldehyde resins. It is also used in the manufacture of nylon and other synthetic fibers, as well as in slimicides (chemicals that kill bacteria and fungi in slimes). Phenol is an important intermediate for the synthesis of petrochemicals, agrochemicals, and plastics. Examples of using phenol as an intermediate are in the production of Bisphenol A, phenolic resins, alkylphenols, caprolactam and aniline. Other uses include utilizing phenol as disinfectant, as an antiseptic, and in medicinal preparations, such as mouthwash and sore throat lozenges (Schmidt, 2005). Worldwide production of phenol is around 11 million tonnes annually (Zakoshansky, 2009). Traditionally phenol is produced mainly via the three-stage cumene process as shown in Figure 1.1. The average annual growth from 1995 to 2000 and 2001 to 2006 were 4.2% and 3%, respectively (www. The innovation – group.com, 2008). The cumene process produces around 90% of the phenol used in the world (Liptakova *et al*., 2004). Starting from benzene, the cumene process involves:.

- Alkylation of benzene with propylene in the vapour phase to form cumene, catalyzed over an acid catalyst, phosphoric acid (H_3PO_4). However before 1990 cumene was produced by the gas-phase reaction of benzene with propylene. Today the alkylation process is catalyzed using zeolite catalysts and the reaction is carried out in the liquid phase (Zakoshansky, 2009).
- Oxidation of cumene to cumene hydroperoxide (a non-catalytic reaction with air) using molecular oxygen.
- Cleavage of cumene hydroperoxide to phenol and acetone, progressed with homogeneous acid catalysis using sulfuric acid.

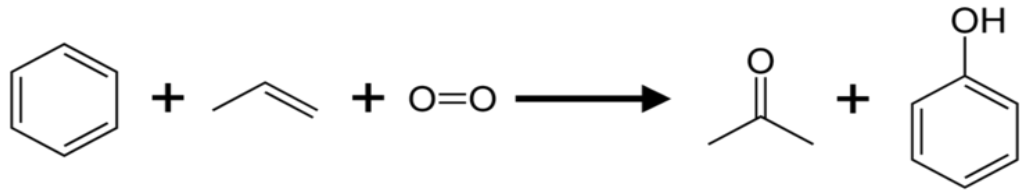


Figure 1.1 Phenol production using cumene process

The current technology uses a multi-step cumene process resulting in difficulty in achieving high phenol yields in relation to the benzene consumed and also high energy consuming and needs a high capital investment due to the multi step nature (Niwa *et al.*, 2002). The cumene process has a number of inherent disadvantages such as high investment costs because of the complexity of the process and the use of a relatively expensive reactant like propylene. From a process safety perspective, formation of the hazardous intermediate cumene hydroperoxide is explosive whilst the formation of the by-product propanone (acetone) in a 1:1 stoichiometry (0.62 tonne acetone / tonne phenol) is also a weakness of the process. The annual growth rate for phenol has not been matched by a similar increase in demand for acetone. There is concern that supply of acetone may exceed demand. If the market demand for acetone is less than that of phenol, then the cumene process profitability is in doubt. Therefore, the process economics of the cumene process significantly depends on the marketability of the acetone by-product (Kleinloh, 2000).

Hence alternatives to the cumene process such as a single-stage oxidation process using non-toxic and easily available reagents like oxygen and water or hydroxylation of benzene to phenol with nitrous oxide in the gas phase using ZSM-5 (MFI) type zeolites as catalysts are of research interest. Other routes include the catalytic hydroxylation of benzene with hydrogen peroxide (H_2O_2) in the liquid phase using titanium–silicate as a catalyst (Jia *et al*., 2004). Currently, there is research interest in utilizing iron-based ZSM-5 catalysts for the process using N_2O. Most of research efforts have been aimed at the investigation of Fe-ZSM-5 catalysts in benzene hydroxylation

and only a few papers are devoted to other Fe containing zeolites (Fe-Y, Fe-Mordenite, Fe-Ferrierite, Fe-Beta, Fe-MCM-41 and Fe-MCM-22). Fe/ZSM-5 zeolites have attracted a lot of attention because of their high activity and stability in the direct hydroxylation of benzene to phenol (Yang *et al*., 2006).

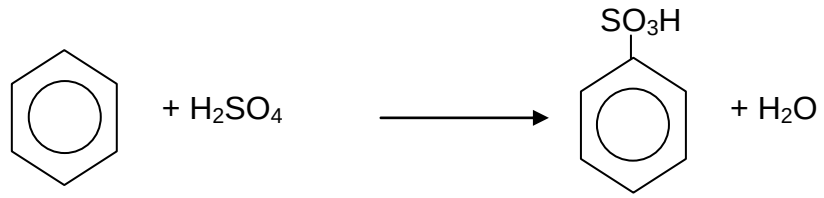
The novelty of iron-based ZSM-5 catalysts is discussed later on in this report. Direct oxidation of phenol from benzene with N_2O has significant economic and environmental benefit if it is compared to the widely used cumene process (Jia *et al*., 2004). This reaction has been investigated previously, usually in conventional fixed-bed reactors (Panov *et al*., 1988 and Panov, 2000., Notte, 2000). However in the literature there is a wide range of reported materials of catalyst preparation, activation and reported catalytic activity to increase the selectivity and minimize catalyst deactivation. In this one-step process using N_2O with near 4% and 98% conversion of benzene and selectivity to phenol respectively, phenol is obtained whilst minimizing the formation of by- products thereby having the potential of overcoming the disadvantages of the conventional three-step cumene process. One step oxidation of benzene is more desirable for the phenol production without byproducts (Yuichi *et al*., 2010). Solutia and the Borescov Institute of Catalysis (BIC) developed this new process jointly (Panov, 2000). The major hurdles are related to the stability of the catalyst, inhibition of side reactions and availability of cheap N_2O (Panov, 2000).

1.1 Problem description and catalyst comparison

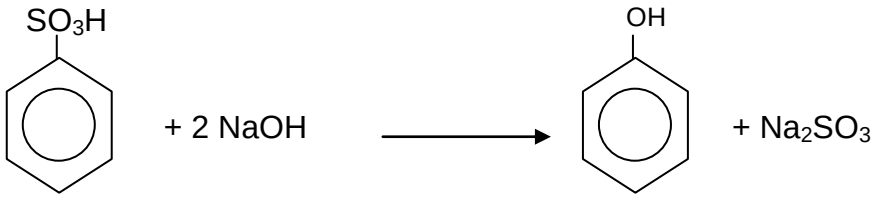
1.1.1 Background (History) of phenol production

Phenol was discovered in 1834, having been isolated from coal tar, and named “carbolic acid”. Synthetic phenol preparation constitutes an important chapter in the history of organic reactions. Below is a summary of the historical development of phenol processes:-

The Sulfonation Process - The first one implemented on an industrial scale by BASF in 1899. This process was used for about 80 years, but the main disadvantage was the poor atom economy (36%) of the reaction (which is the percent ratio of the molecular mass of the desired product to the molecular mass of the reactant). This means that considerably less than half the mass of the reactants ends up as the desired product. In practice the yield is more likely to be 88%, giving an atom economy of 32.3% (Panov *et al*., 1988 and Panov, 2000).

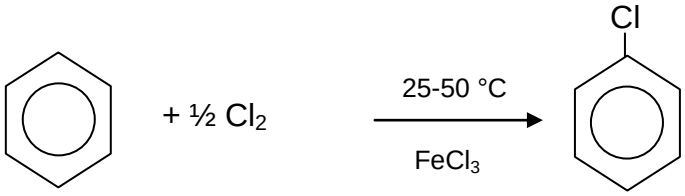


(1.1)

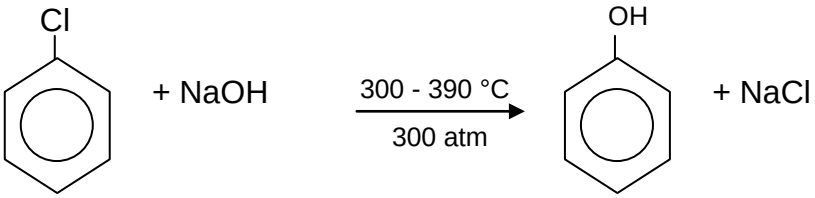


(1.2)

The Chlorination Process – Put in operation in 1924 by USA Dow Chemical. Independently, a similar technology was developed in Germany (Kirk-Othmer, 2005).In this process benzene is converted to chloro benzene, which is then reacted in the presence of sodium hydroxide to form phenol. This process is no longer used because of the adverse economics of chlorine and alkali production (Morrison *et al*., 1992).

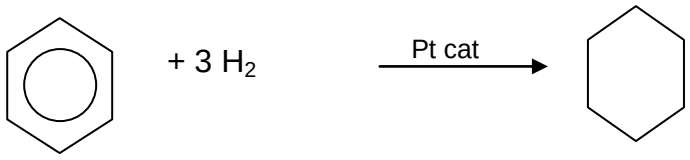


(1.3)

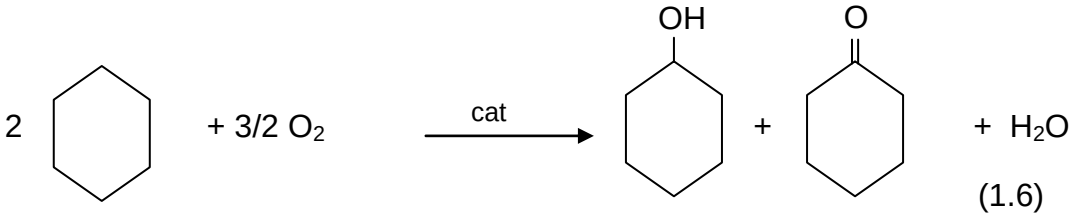


(1.4)

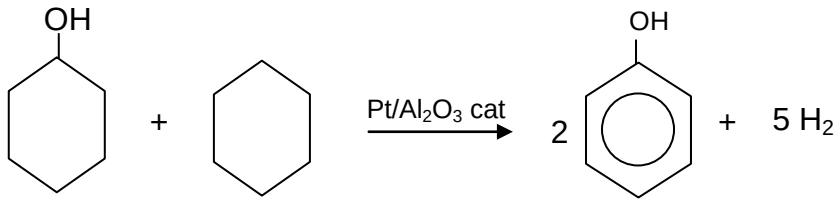
The Cyclohexanone Process – Phenol is produced in the last step by dehydrogenation process. It was used by Monsanto during the sixties in Australia for a few years before being replaced (Panov *et al*., 1988 and Panov, 2000).



(1.5)

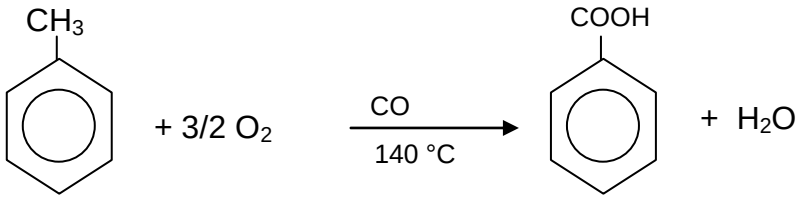


(1.6)

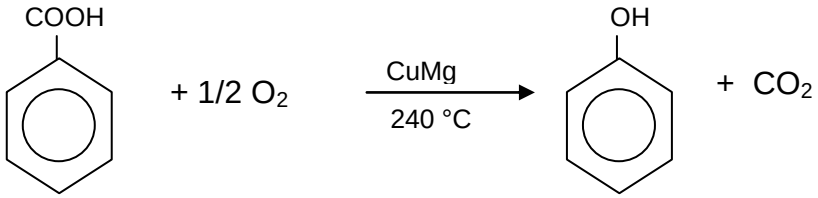


(1.7)

The Benzoic Acid Process – It is the only process based on a non-benzene raw material that was commercialized in Canada in 1961. However it has very slight contribution to the global phenol production never exceeding 5%, while the remaining is attributed to cumene process (Panov *et al*., 1988 and Panov, 2000).



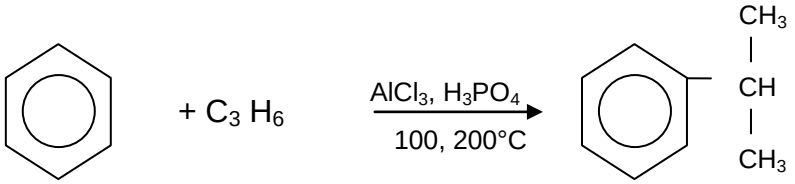
(1.8)



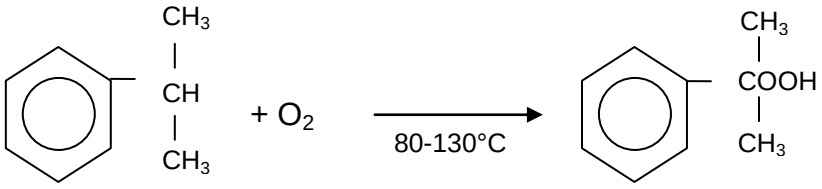
(1.9)

1.1.2 Background (History) of cumene manufacturing process

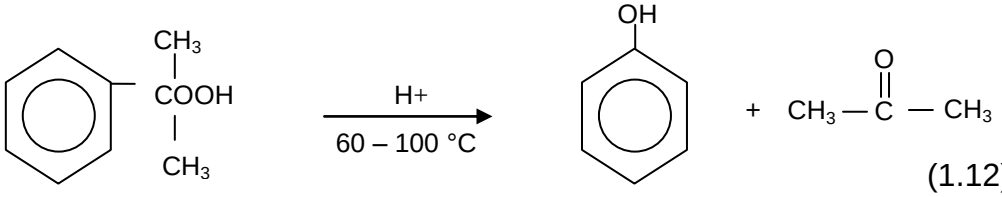
The Cumene Process – Comprises three steps as follows:



(1.10)

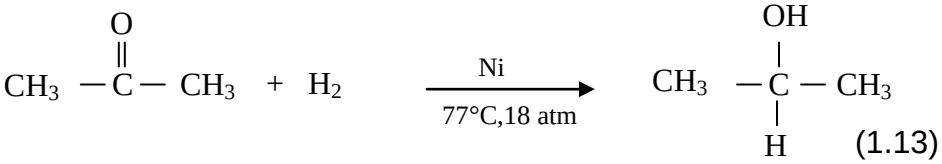


(1.11)

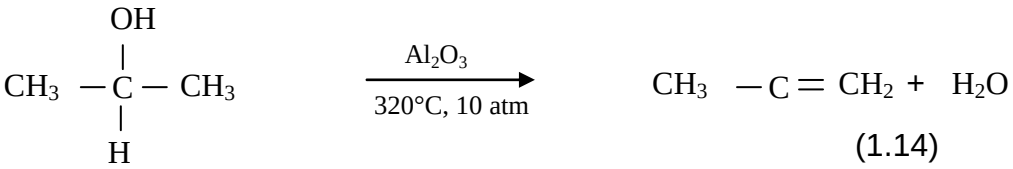


(1.12)

The cumene process was developed in the former Soviet Union in 1942. The first industrial plant was put in operation in 1949. Stalin prize was granted to a large team of scientists in 1951 (Panov, 2000). However in Europe, the process was developed in the late 40s, sometimes called “Hock’s process”. Commercial use commenced in the early 50s in the USA. For many decades the cumene process has been the standard way to manufacture phenol. Almost 70% of the global phenol production originates in the USA and Europe (Panov, 2000). The cumene process has several disadvantages including the following: adverse environmental impact, explosive intermediate products, multi-step reaction process whose disadvantages include high-energy consumption and a large amount of acetone as a by-product which has a smaller demand, so the economics of the process depends on the marketability of acetone. In 1992 Mitsui Company introduced acetone recycle to manufacture phenol. This includes two additional steps (a hydrogenation and a dehydration step) to convert acetone into the feedstock propylene:-



(1.13)



(1.14)

But the 5-step technology is not the best solution as it increases the complexity of the process and requires a hydrogenation step. The direct oxidation process has significant commercial advantages over the processes reviewed so far.

1.1.3 New process development: single step oxidation processes using a novel catalysts

Oxidation reactions are of considerable importance at an industrial level and correspond to a huge market for products. Oxidation reactions are widely used in industry and are widely studied in academic and industrial laboratories. Research in oxidation processes has resulted in the development of many new selective oxidation processes. Environmental protection relies mainly on oxidation reactions. A difficult field of catalytic chemistry is the selective oxidation of hydrocarbons. The main difficulty here lies in the creation of selective catalysts. A variety of oxygen sources such as O_2, H_2O_2, O_3, and N_2O are used for the reaction (Panov, 2000). Most heterogeneous catalysts contain a transition metal, supply an oxygen species that has a negative charge such as O^- or O^{2-}.

Catalyzed oxidation reactions are today one of the most rapidly advancing fields in catalysis. There is currently considerable interest in using a gas-phase catalytic oxidation process for phenol manufacture. The gas-phase reaction process has the considerable potential advantages over the corresponding liquid-phase process from an economic point of view. A new route for producing phenol directly from benzene may be based on using N_2O as an oxidizing agent in the gas phase (in the presence of modified ZSM-5 or ZSM-11 zeolite) catalysts containing such elements as Ga, B, In, Cr, Fe, Sc, Co, Ni, Be, Zn, Cu, Sb, As or V (Gubelmann *et al*., 1991 and Rana *et al*., 2010). Other routes includ direct liquid phase hydroxylation of benzene with H_2O_2 in the presence of titanium silicate or supported vanadium oxide catalysts, however the cost of the H_2O_2 is higher than for N_2O (Salehirad *et al*., 2004).

A new process for manufacturing phenol from benzene in a single utilizing a heterogeneous catalyst and a selective oxidation reaction using molecular oxygen as the oxidant is shown in Fig.1.2. (Leanza *et al*., 2001 and Ehrich *et al*., 2002).

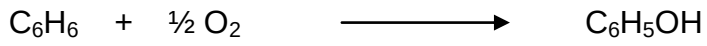


Figure 1.2 One step oxidation of benzene to phenol by using molecular oxygen

If successful, this one-step process would require much less energy and produce less waste than the conventional cumene process. The proposed process is also attractive in that, in principle, it produces no by-products with more than 95% phenol selectivity (Guanjie *et al.,* 2010). The large quantity of acetone produced in the cumene process is a major driving force behind the search for new catalytic processes such as a one-step synthesis of phenol without the formation of by-products. The direct oxidation of benzene may be carried out in two ways: (1) Oxidation by dioxygen, and (2) monooxygen donors.

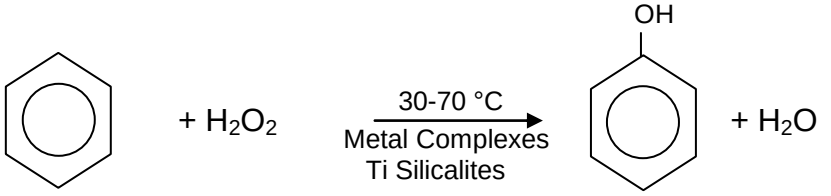
Oxidation by molecular oxygen (O_2)

Research on benzene oxidation by molecular oxygen dates back to 1865 (Panov, 2000). Since that time, several attempts were made to find an effective way to perform this most academically attractive and industrially important reaction. The problem is one of achieving yields due to the reactivity of phenol toward oxidation compared with benzene itself. The conversion of benzene is only 0.3% at 500 °C in the presence of oxygen and the selectivity of phenol using N_2O as oxidant is 98%, while with O_2 as oxidant, only complete oxidation occurs (Mehmet *et al*., 2010). Moreover, direct oxidation by molecular oxygen has previously been tried in both gas and liquid phases, but the results have not been promising to merit practical further development.

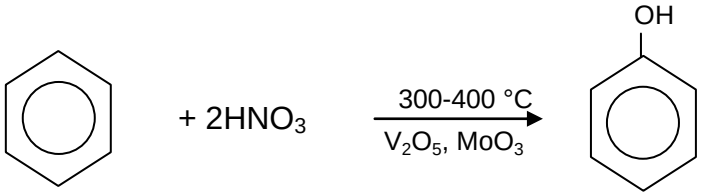
Monooxygen donors

Monoxygen donors, as illustrated in eq. 1.15 – eq. 1.18, are capable reagents to convert benzene to phenol. Direct liquid phase hydroxylation of benzene with H_2O_2 has received particular attention since the discovery that titanium silicate is a good catalyst for the process (eq. 1.15), (Salehirad *et al*., 2004). Use of nitric acid as an oxygen donor was first patented in 1925 (eq. 1.16). Other monooxygen donor catalysts include V_2O_5 and MoO_3 are the

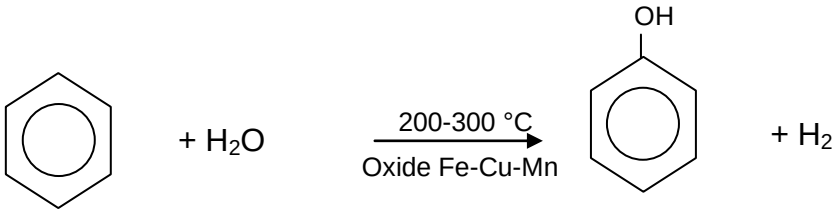
most effective catalysts for this gas phase oxidation providing a 83% phenol selectivity at a 92% benzene conversion, but the oxidant used was HNO_3, which is toxic martial (Panov, 2000). Panove (2000) reported achieving oxidation of benzene using water, but in this case, a high yield of phenol formation occurred at the expense of the solid material oxygen rather than water oxygen and may thus not be truly catalytic (eq. 1.17). Benzene hydroxylation by nitrous oxide (N_2O) was the basis of benzene to phenol one step conversion process (eq. 1.18) (Jia *et al*., 2004).



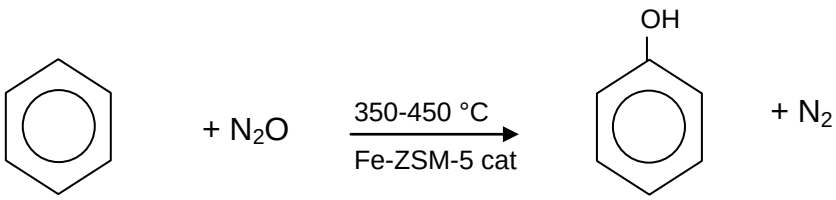
Low H_2O_2 Selectivity (1.15)



X-52%, S-90%, first patent: 1925 (1.16)



X-15%, S-97% (1.17)



X-27%, S-98% (1.18)

Novel catalysts

The direct oxidation of benzene can be achieved using several different oxidizing agents, but none of these has yet proven economically feasible on a large scale. Considerable research is going on into finding catalysts that might allow the direct oxidation of benzene to phenol. An extensive range of catalysts may be used for the preparation of phenol from benzene as discussed later in this report.

The role of a catalyst is to increase the rate of a reaction. The catalyst is usually present in small quantities and is not consumed by the reaction. A catalyst allows reactions to take place more efficiently e.g. under milder conditions than would otherwise be required.

In recent years, there has been a growing research interest in finding a suitable solid catalyst for the selective oxidation of benzene to phenol under mild reaction conditions, with clean oxidants like O_2 and H_2O_2. Rodriguez (1998) reported that carbon materials may be useful as heterogeneous catalysts. The larger surface area and higher porosity helps in higher dispersion of active phases. The surface chemistry of carbon materials can be ascribed to the surface oxygen containing chemical groups, which can be acidic, basic or neutral. The interactions between the surface groups and the active phase could also have a synergistic effect on the catalytic activity of these materials. Choi *et al*., (2005) used activated carbon as supports for transition metals in the liquid phase to produce phenol from benzene with H_2O_2 as the oxidant. Results indicated that activated carbons may be a good alternative to MCM-41 as a catalyst support for this reaction. The activated carbon supported transition metal catalysts, Vanadium and Iron gave a higher yield of phenol about 4% and 16% respectively compared to that of transition metal (Vanadium) impregnated on MCM-41 catalysts about 1% as shown in Table1.1 (Choi *et al*., 2005). A comparison of yields of phenol on various catalysts by liquid phase reaction cited in the literature is presented in Table 1.1.

Table 1.1 shows that the results obtained on the surface modified catalysts indicated a dominant role of surface oxygen groups and the impregnated iron in catalyzing the benzene hydroxylation reaction, for phenol synthesis, which have a higher yield (y >15%) compared with non-modified catalysts (Choi *et al*., 2005 and Schmidt, 2005). TS-1 (Titanium–Silicate) yield seemed high (y= ~ 64%) vs others (y≤ 10%) as shown in Table1.1.

Table 1.1 Comparison of performance of various catalysts in the open literature for the hydroxylation of benzene to phenol (liquid phase reaction)

Catalyst	**Reaction Temperature (°C) and (oxidant)**	**Conversion(X), selectivity(S) and yield(Y) (%)**	**Reference**
Cu-zeolite	30 °C (O_2)	Y = 1.69	(Ohtani *et al*., 1995)
Pd/SiO_2	45 °C (O_2 and H_2)	X = 7.0, S = 88.5, Y = 6.2	(Miyake *et al*., 1995)
$CuO–Al_2O_3$	30 °C (O_2)	Y = 1.0	(Miyahara *et al*.,2001)
V/SiO_2	30 °C (O_2 and H_2)	Y = 8.2	(Masumoto *et al*., 2002)
V/MCM-41	30 °C (O_2 and H_2)	Y = 8.6	(Masumoto *et al*., 2002)

Catalyst	**Reaction Temperature (°C) and (oxidant)**	**Conversion(X), selectivity(S) and yield(Y) (%)**	**Reference**
Polymer bound Vanayl acetylacetonate	70 °C (30% H_2O_2)	Y = 10.0	(Kumar *et al*., 1997)
TS-1 **(Titanium–Silicate)**	60 °C (30% H_2O_2)	X = 74.4, S = 85.6, Y = 63.7	(Bhaumik *et al*., 1998)
V/MCM-41	70 °C (30% H_2O_2)	X = 1.39, S = 93, Y = 1.29	(Lee *et al*., 2000)
V/MCM-48	70 °C (30% H_2O_2)	X = 0.44, S = 93, Y = 0.41	(Lee *et al*., 2000)
AMM catalyst Cu_3Si **(AMM**)Amorphous microporous mixed oxides	60 °C (30% H_2O_2)	X = 7.1, S = 21.13, Y = 1.5	(Stockmann *et al*., 2000)
0.5 wt.% V on activated carbon	65 °C (30% H_2O_2)	Y = 3.9	(Choi *et al*., 2005)
5 wt.% iron on activated carbon	65 °C (30% H_2O_2)	Y = 15.8	(Choi *et al*., 2005)
5.0Fe/NACH-600N (5 wt.% iron impregnated on NACH-600N)	65 °C (30% H_2O_2)	X = 50.0, S = 40.0, Y = 20.0	(Choi *et al*., 2005)

Catalyst	**Reaction Temperature (°C) and (oxidant)**	**Conversion(X), selectivity(S) and yield(Y) (%)**	**Reference**
TS-1 **(Titanium–Silicate)**	80 °C (methanol/water)	x = 4 S= 90	(Barbera *et al*., 2010)
$FeSO_4/SiO_2$	70 °C H_2O_2	Y= 14 S= 100	(Liu *et al*., 2010)
(CuAPO-11) copper substituted aluminophosphate molecular sieves	70 °C H_2O_2	X= 10.5 S= 100	(Qi *et al*., 2009)
CuO Catalytic polymeric membranes	35 °C H_2O_2 in an ultrafiltration membrane reactor	X=2.3	(Molinari *et al*., 2009)
MCM-41 Mesoporous Molecular Sieves Modified with Iron and Cobalt Compounds	75 °C (40% H_2O_2)	X=11	(Sirotin *et al*., 2009)
Sodium metavanadate	25 °C (H_2O_2)	*Y=13.5* *S= 94*	(Jian *et al*., 2006)
vanadium catalyst catalyst solution (300 mL of 10 mol VCl3 /m3-aq)	40 °C	Productivity= 40 (mol/g.h)	Tanarungsun *et al*., 2010)

Table 1.2 Literature described catalytic systems for hydroxylation of benzene with O2 and H2

Catalyst	Conditions	Productivity (mol phenol/(1 g-atom Pt or Pd)) h	Conversion of benzene (%)	References
Liquid-phase oxidation				
Pd–Cu/SiO_2	25 °C	4	0.02	(Kunai *et al*., 1990)
Pt–V_2O_5	HOAc, 60 °C	67	0.07	(Hideyki *et al*., 1994)
Pd, Pt–V_2O_5/SiO_2	HOAc, 60 °C	46	0.14	(Hamada *et al*., 1993) Japan Patent
Pt/ZrO_2 + $V(acac)_3$	HOAc, 60 °C	400	0.45	(Hamada *et al*., 1993) USA Patent
Pt, Rh, Ir, Pd or Ru + V_2O_5, Y_2O_3, Nb_2O_5, WO_3, La_2O_3 or MoO_3/SiO_2	HOAc, 60 °C	264	0.6	(Miyake *et al*., 1995)
Pd/Ti-silicalite	H_2O + HCl, 25 °C	13	0.36	(Tatsumi *et al*.,1993)
Pd/Al_2O_3 + $V(acac)_3$ or $FeCl_2$	HOAc, 65 °C	50	2.3	(Remias *et al*., 2003)

Catalyst	**Conditions**	**Productivity (mol phenol/(1 g-atom Pt or Pd)) h**	**Conversion of benzene (%)**	**References**
Gas-phase oxidation				
(0.2% Pt–20% PMo_{12})/SiO_2 (100), 1.5 g	200 °C	60	4.4	Kuznetsova *et al*., 2009)
Pt–PMo_{12}/SiO_2 and Pd–PMo_{12}/SiO_2	180–250 °C	380	0.3	Kuznetsova *et al*., 2005)
Pt/VO_x/SiO_2 or Pd/VO_x/SiO_2	150–200 °C	60	0.68–0.97	(Ehrich *et al*., 2002)
Pd membrane	150–200 °C		3–13%	(Niwa *et al*., 2002)
(1% Pt–20% PMo_{12})/SiO_2 (400), 1.3 g	200 °C	4	1.3	(Kuznetsova *et al*., 2009)
Pd–Cu/SiO_2	200 °C	80	0.9	(Kitano *et al*., 1994 and Boricha *et al*., 2010)

Table 1.2 shows that the comparison of the productivity and conversion in the liquid and gas phase. Table shows that the catalyst productivity for Pd–Cu/SiO_2 catalyst is much less for similar catalysts when the reaction is conducted in the liquid phase. However the same high selectivity is achieved for both of them. The conversion of benzene is typically close to 1%, and is

much higher (3–13%) in the work using a Pd membrane reactor at an over-stoichiometric ratio of O_2 and H_2. In term of Pd and Pt as support for the catalysts, liquid phase shows better productivity compare with gas phase (Niwa *et al*., 2002).

There has been much research conducted on direct hydroxylation of benzene to phenol. The major thrust has been the development of an appropriate modified catalyst using transition metals. The palladium, copper or iron supported zeolite materials (Leanza *et al*., 2001 and Yamanaka *et al*., 2002) have been recent targets for catalyst development. Most reactions usually need liquid solvents (i.e., liquid phase environment) and special hydroxylation agents, like H_2O_2, and some reactions using N_2O and NO_2 as special agents in the gas phase to get high phenol yields (Zhang *et al*., 2010) Some heteropolyacid catalysts were reported to produce phenol at yields of over 10% using molecular oxygen, but the catalysts showed fatal structural instabilities (Lee *et al*., 2003).

There are many catalysts that may be used for the synthesis of phenol from benzene. In addition to other catalysts that have been discussed earlier in this report, “Zeolites” are of considerable earliest with nitrous oxide (N_2O) as the oxidizing agent. Benzene in the vapor phase is oxidized to phenol and nitrogen (Jia *et al*., 2004). Direct oxidation of phenol from benzene with N_2O as the oxidizing agent may have considerable economic and environmental benefit if it is compared to the widely used cumene process. zeolites are hydrate crystalline materials that are built from a three dimensional framework of (SiAl) O_4, tetrahedral with all four oxygen atoms shard by adjacent tetrahearal (as discussed later in the Chapter 2.1.3). However unprompted zeolite show limited applications so addition of promoters such as transition metal ions are necessary. Many papers are published on the characterization and reactivity of such transition metal containing zeolites. The introduction of iron into extra framework positions of zeolites can be achieved by impregnation, ion exchange and hydrothermal synthesis (Ramirez., 2006). Among those, iron in the MFI zeolites is of considerable

interest to catalysis. Productivity of phenol, concentration of active sites, and the rate of N_2O decomposition depend on iron loaded to the catalyst (Dubkov *et al*,. 2002). Guanjie *et al,.* (2010) reported that the blockage of micropore volume because of coking on the catalyst surface is the main reason for catalyst deactivation. The second reason for causing the oxidation of the product and coking on the active sites is the strong adsorption of phenol and dihydroxybenzene on the catalyst's superficial active sites. Dubkov *et al*., (2002) reported that the nature of Fe in active sites based on Mossbauer spectra, and also suggested that the extra-framework dinuclear Fe species, formed by high temperature calcinations, and bearing bridging oxygens, are the active sites for benzene hydroxylation. Guanjie *et al,.* (2010) suggested that not only the amount of Iron but also the catalyst structure is important in the creation of an active catalyst. Other reactions routes include direct liquid phase formation of phenol from benzene using H_2O_2 (as oxidant) with titanium silicate (TS-1) as a catalyst. Nitrous oxide (N_2O) and hydrogen peroxide (H_2O_2) are discussed further in Chapter 2.

1.2 Reactor technology

There are different types of flow reactors such as fluidized bed and fixed bed (tubular) reactors employing heterogonous catalysts. A fixed bed reactor also called a packed bed reactor is essentially a pipe that is packed with solid catalyst particles. This heterogeneous reaction system is used normally to catalyze gas reactions. This reactor has difficulties with temperature control. The advantage of the packed bed reactor is that for most reaction it gives the highest conversion per weight of catalyst of any catalytic reactor. A fluidized bed reactor (FBR) can handle large amounts of feed and solid and has good temperature control. Fluidized bed reactors are considerably more efficient than fixed bed reactors due to fluidized bed reactors do not clog as easily as fixed bed reactors and the catalyst is usually troublesome to replace using fixed bed reactor, but fluidized bed reactors are more difficult to design than fixed bed reactors. Producing phenol directly from benzene was using usual fixed-bed reactors (Panov *et al*., 1988 and Panov, 2000).

The direct hydroxylation of benzene to phenol using molecular oxygen by atmospheric pulse DC corona discharge using a plasma reactor has been investigated (Lee *et al*., 2003). The conversion of benzene increased with the increase of oxygen content and input voltage but the selectivity of phenol decreased due to the formation of polymerized products (Lee *et al*., 2003). Flow rates of oxygen and inert gases were controlled by mass flow controllers and evaporated benzene was carried by inert gas flow. The plasma reactor and benzene flowing tubes were heated to 60°C to prevent the condensation of benzene. The liquid phase products and unreacted benzene were collected at the liquid trap which was kept under 0°C using dry ice suspended in ethanol. Meanwhile, a study using plasma reaction system has showed noteworthy performances in direct hydroxylation of benzene using molecular oxygen. The application of atmospheric plasma techniques into direct hydroxylation of benzene to phenol was required but an application has not been reported yet.

However, these days and in future, many chemicals including phenol may be produced in relatively small reactors. Microreactors are widely studied as a new reactor (Ehrfeld *et al*, 2000), because it has many advantages such as rapid heat transfer, also this method saves on capital cost by reduces energy use, reduces waste, and can easily be scaled up by series of reactors. The technology can also be applied to the manufacture of other materials.

Niwa *et al.,* (2002) reported a one-step catalytic process to convert benzene to phenol using a Pd membrane, giving a higher yield than the cumene process. In this system hydrogen and oxygen were supplied separately; hydrogen was fed into a stream of a substrate and oxygen gas mixture through a metallic thin layer.

One potential microreactor to produce phenol involves the use of a small diameter (2 mm), porous tube of alumina coated with a layer of palladium metal. A mixture of benzene and oxygen is fed through the tube, and hydrogen gas is passed over the tube. See Fig.1.3.

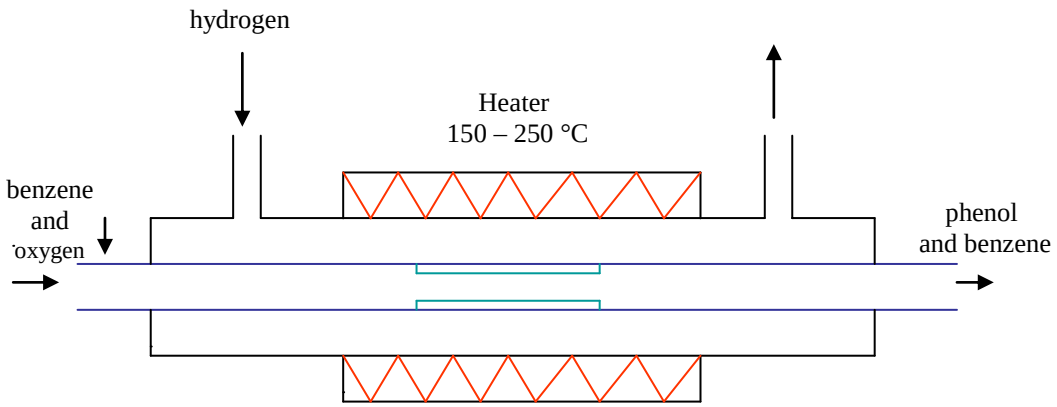


Figure 1.3 Micro-reactor for producing phenol by oxidation of benzene.

The tube is heated to 150 – 250 °C. Hydrogen permeates through the alumina tube coated with a layer of palladium metal, and is converted to atomic hydrogen by the palladium catalyst. The hydrogen atoms react with oxygen gas, releasing oxygen atoms, which in turn react with the benzene

forming benzene epoxide. This isomerizes to phenol as shown in Fig.1.4. (Niwa *et al*., 2002).

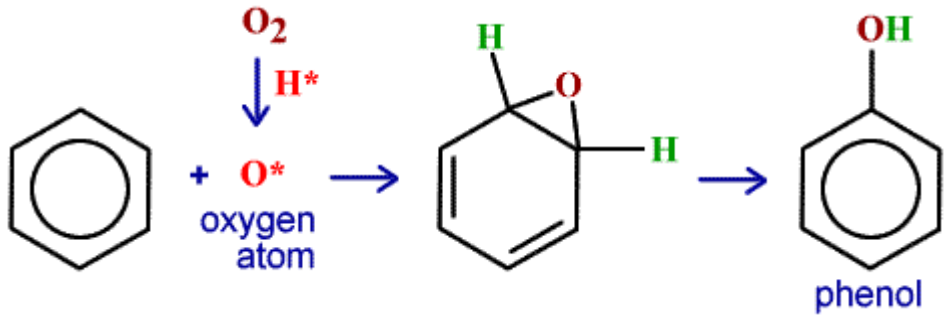


Figure 1.4 Producing phenol by oxidation of benzene

The boiling points of phenol (182°C) and benzene (80°C) mean that phenol is easily separated from un-reacted benzene, and the final liquid phenol is in a highly pure form. On the other hand, Hiemer *et al*. (2004) studied direct oxidation of benzene to phenol using Fe-ZSM-5-coated stainless-steel microreactor. Using a microreactor with the ability to remove the heat directly from the catalyst to the wall of the reactor offers the possibility to conduct the hydroxylation of benzene under isothermal conditions. Since there is almost no temperature raise this allows to work at elevated initial temperatures and at high concentrations of the reactants without needing to dilute the reactants. As nitrous oxide and benzene can form explosive mixtures at high concentrations of N_2O (Uriate.,1998), using a microreactor is inherent safe and offers the possibility to work at high concentrations of nitrous oxide leading to high space–time yields.

The selectivity of nitrous oxide to phenol is strongly reduced at high temperature due to more oxidation of phenol (by products). So, using a microreactor instead of other tubular reactors increases the selectivity of nitrous oxide to phenol for not having a temperature rise along the reactor. The selectivity with a microreactor is more than double the selectivity achieved in the tubular reactor at a starting temperature of around 723 K (Ehrfeld *et al*, 2000).

1.3 Research objectives

An experimental tubular reactor has been designed for the evaluation of catalyst selectivity for the gas phase reaction of benzene to phenol using nitrous oxide. The experimental rig design included consideration of a gas handling system feeding the fixed-bed reactor linked to an on-line GC gas analyser. This thesis examines the effect of different Si/Al ratios and iron content on the selective conversion of benzene to phenol with a desire to achieve high selectivity and minimise catalyst deactivation which is able to delay coke formation. A series of selective Fe-ZSM5 catalysts with different Si/Al ratios have been prepared and evaluated for selective formation of phenol using ion exchange method. The characterisation of physicochemical properties such as surface acidity and the quantity of active sites (active oxygen donor a-sites) has been done to understand the effect of Si/Al ratio, temperature and iron content on the catalyst performance.

1.4 Conclusions

A common problem in heterogeneous catalysis is the lack of comparability of materials prepared in different laboratories and the catalytic performance studied under different reaction conditions. Reliable comparative physicochemical characterisation data accompanied by measurement of catalyst performance for a variety of materials previously reported in literature to have given good phenol selectivity have as yet not been published. Many attempts have been made to elucidate the active structure and functioning of the redox sites, but no definite conclusions have been drawn yet. Hence, the objective of the research problem chapter was to compare the performance of previously studied catalysts in terms of conversion, selectivity and yield both in liquid phase and gas phase hydroxylation of benzene to phenol. One-step oxidation of benzene to phenol in the gas phase with N_2O as oxidant over iron-zeolite has been identified to be the best catalyst in term of conversion of benzene, selectivity and productivity of phenol.

2 Literature Review on One Step Oxidation of Benzene to Phenol Using N_2O as Oxidising Agent

2.1 Heterogeneous catalysis using H_2O_2 and N_2O in one step oxidation of benzene to phenol.

2.1.1 Titanium silicate (TS-1) (liquid phase)

A potential route of direct liquid phase formation of phenol from benzene uses H_2O_2 (as oxidant) with titanium silicate (TS-1) as a catalyst (see Fig.2.1.). This route is preferred to the conventional cumene process because it minimizes pollution (Wang *et al*., 2010). Titanium silicate (TS-1) is one of the most important catalysts for hydroxylation of benzene to phenol, on the basis of its well established efficiency in term of yield and selectivity in a series of oxidation processes with hydrogen peroxide, such as alkenes epoxidation, alkanes oxidation, alcohol oxidation and phenol hydroxylation (Bianchi *et al*., 2000). The experiments show the benzene conversion and selectivity to phenol is lower than using N_2O and cost of using H_2O_2 is even higher than that of N_2O (Jia *et al*., 2004 and Wang *et al*., 2010).

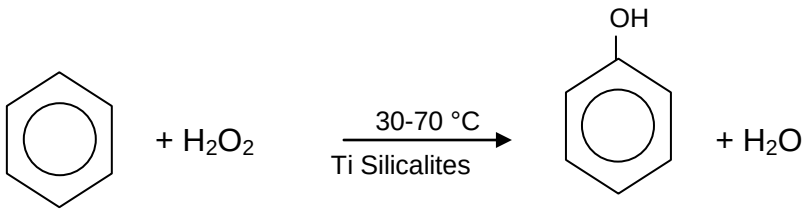


Figure 2.1 One-step hydroxylation of benzene to phenol using H_2O_2

A problem with the direct benzene oxidation is the cost of H_2O_2; however, this disadvantage might be overcome by integrating the H_2O_2 production with the downstream use in benzene oxidation, or by generation of H_2O_2 (by reaction between hydrogen and oxygen), catalyzed by noble metals. Another problem in benzene hydroxylation with H_2O_2 is the low selectivity to phenol. This may be explained by the formation of the by-products due to the strong adsorption of phenol on the active sites of the catalyst (phenol is more reactive toward oxidation than benzene), and therefore a strict control

over both reaction conditions and benzene conversion is necessary to achieve an acceptable selectivity to phenol (Barbera *et al*., 2010).

2.1.2 Nitrous oxide using zeolites as catalysts (gas phase oxidation)

A review of the scientific literature shows that iron-based ZSM-5 zeolite catalysts are promising candidates for the catalytic oxidation of benzene to phenol (Wącław *et al*, 2004). Iron complexes formed inside zeolite channels are thought to be responsible for the catalytic oxidation of benzene to phenol. Ribera *et al*., (2000) prepared Fe/ZSM-5 zeolites by hydrothermal synthesis. Samples with a SiO_2/Al_2O_3 ratio of ≤100 contained 0.5 –1 wt % of iron with high selectivity (>99%) and high phenol yield (up to 27%). The iron content was determined by atomic absorption spectroscopy. Iron is required for formation of extra framework species that are active in selective conversion of benzene to phenol. Higher amount of iron loaded into the catalyst create more active sites that cause further oxidation of products and coke formation. Pirutko *et al*. (2002) shows that only a small fraction of the Fe is active in the selective oxidation of benzene to phenol. The rate of coke formation decreased with decreasing reaction temperature and increasing concentration of benzene. Productivity can also be increased with decreasing the SiO_2/Al_2O_3 ratio. Investigation of the oxidation of benzene to phenol utilizing this Fe-ZSM-5 zeolite catalyst with N_2O as the oxidant on the coking behavior is very valuable to improve the stability of the catalyst and to optimize the reaction in terms of theory and practice (Guanjie *et al,.* 2010).

The catalytic activity was found to be related to the acid-base properties of the catalyst (Wącław *et al*, 2004). Similar results have been given by some researchers, and have proved commercially that iron-based ZSM-5 zeolites are the best catalysts so far for the oxidation of benzene to phenol, with nearly 100% benzene selectivity for phenol. Different Ion exchange methods have been proposed for the preparation of Fe/ZSM-5 catalysts : gas phase, liquid phase and solid phase (Reitzmann *et al.*, 2000).

Hydroxylation of benzene to phenol may be achieved using zeolites with nitrous oxide (N_2O) as the oxidizing agent (see Fig.2.2.). Direct oxidation of phenol from benzene with N_2O as the oxidizing agent has great economic and environmental benefit if it is compared to the widely used cumene process. During the last two decades, one of the most interesting new reagent for the selective oxidation of benzene is N_2O, because it contains 36 wt% oxygen and for hydroxylation of benzene to phenol, the by-product would be N_2. A disadvantage in using N_2O is its high cost. The process uses metal modified zeolite catalysts, such as V_2O_5/ MoO_5/ ZSM-5 and Fe_2O_3/ MoO_3/ ZSM-5, which transfer atomic oxygen, from the decomposition of the N_2O on the catalyst surface to benzene. The active catalyst appears to be the metal species occupying the pores in the zeolite structure (Panov *et al*., 1988 and Panov, 2000).

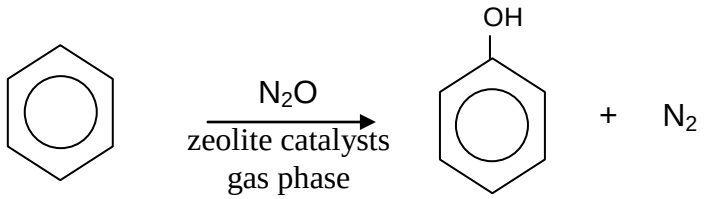


Figure 2.2 One-step hydroxylation of benzene to phenol using N_2O

This reaction is of particular value to Solutia, as they are a major producer of adipic acid, used in nylon production, and N_2O is produced as a waste by-product of the adipic acid manufacturing process. This cannot simply be released into the atmosphere, as it is a pollutant under strict control. The waste gas (N_2O) would be used as an inexpensive source for an alternative oxidant demonstrating an example of process integrated environmental protection, so its use to make phenol removes the need to treat it as waste, and generates a valuable product. N_2O is a waste by-product of the adipic acid manufacturing process and is therefore an ideal source. It must otherwise be disposed of as a waste stream by conversion first to nitric oxide and then nitric acid (Schmidt, 2005). The global N_2O emission from adipic acid plants is not sufficient for producing 9 MMT (Million Metric Tons) phenol per year. Worldwide production of phenol is around 11 million tonnes

annually using the cumene process (Zakoshansky, 2009). Phenol needs technological processes for N_2O synthesis at the unit capacity up to 100 KT/y. Solutia and BIC recently developed a new large-scale catalytic process for the synthesis of nitrous oxide via selective oxidation of ammonia over a Mn-Bi-O/a-Al2O3 catalyst (Parmon, 2005).

Louis *et al.*, (2001) studied the one-step oxidation of benzene to phenol with N_2O over iron-zeolite (Fe/MFI) and H-zeolite (HMFI) catalysts. He also studied the original sample ZSM-5 catalyst, which contains an Fe impurity. Catalysts were probed at 723 K and near atmospheric pressure using a fixed bed micro-flow reactor. The benzene to phenol reaction was found to be of the consecutive type. Perathoner *et al.*, (2003) suggested that in all types of catalysts only very small amount of iron sites are responsible for the selective oxidation of benzene to phenol and the remaining extra-framework iron species, especially the samples prepared by hydrothermal synthesis, play a role in blocking sites responsible for catalyst deactivation, because catalysts prepared by hydrothermal synthesis show a lower rate of deactivation than those prepared by liquid ion exchange (LIE). The catalyst is deactivated by coke deposition. The catalyst can be easily regenerated using O_2 or N_2O, which can be generated via interaction on N_2O with the iron sites or OH, which can be generated at the Bronsted site on the catalyst (Ivanov *et al.*, 2003) and also by water vapor in the feed, resulting in a stable performance. It is assumed that H_2O displaces phenol from the sites (Louis *et al.*, 2001). The calcinations flowed by pretreatment in an aritifical air flow (100 ml/min, 20 vol% O_2 in He) at a heating rate of 1 °C min^{-1} from room temperature to 823 K, for at least 2 h, was necessary for the ZSM-5 catalyst before the reaction. Considering only the reaction to phenol and not regarding consecutive reactions of phenol there is a net release of energy when phenol is produced. Including the inevitable and also undesired consecutive oxidation of phenol to mainly dihydroxybenzene (catechol, hydroquinone andresenol), p-benzoquinone and carbon dioxide, the release of energy is even higher. Hiemer *et al.,* (2004) have reported that using a reactor with poor heat transfer out of the reactor, the release of energy from the

hydroxylation reaction raises the reactor temperature significantly; it means temperature control is important. At 673 K the overall reaction enthalpy of the hydroxylation of benzene to phenol is 259 kJ mol^{-1}, the enthalpies of undesired further oxidations of phenol are even higher. Hiemer *et al.,* (2004) have reported that working at a starting temperature of 723 K with a mixture of benzene and nitrous oxide of 1:1 in a laboratory tubular reactor oxidizes phenol totally to CO_2 because of the rest of the N_2O (N_2O adsorbs again in the active site of the surface area), so the selectivity of nitrous oxide to phenol is typically only 30% because of coke formation due to the high concentration of nitrous oxide and high temperatures. Low concentrations of nitrous oxide may be more beneficial. In order to avoid high temperatures and to achieved high selectivity, the temperature has to be reduced by e.g. reducing the amount of nitrous oxide added (Hiemer *et al.,* 2004). As soon as all the N_2O has reacted there can be no further increase in the reactor temperature.

The catalytic oxidation process e.g. single step oxidation of benzene to phenol using N_2O as oxidant shows several advantages when compared to the cumene process, such as, one step only, low capital expenses, no acetone by product, and no highly reactive intermediates. The process has also very good environmental features. N_2O pollution abatement is an important environmental problem due to the high greenhouse potential of N_2O and its ozone-depleting properties (Jia *et al*, 2004). Producing phenol from N_2O is suggested only if the expensive N_2O is available as an industrial waste product in adipic acid plants (economical and environmental production).

2.1.3 Structure and properties of zeolites

The name of zeolite is from the Greek zien (meaning: to boil) and lithos (stone) to describe minerals that frothed when heated. Zeolites are proven useful catalysts due to their porosity (microporous nature) and surface acidity. It is a broad term used to describe a family of minerals called tectosilicates. These minerals contain small pores which provide a generous surface area. Zeolites are constructed of tetrahedral AlO_4-5 and SiO_4-4 molecules bound by oxygen atoms. Each AlO_4 tetrahedron in the framework bears a net negative charge which is balanced by extra-framework exchangeable cations, mainly Na, K, Ca or Mg. These cations are held within the central cavities and surrounded by water molecules. The cations are mobile and may usually be exchanged by other cations. Currently, there are 40 known natural zeolites and in excess of 150 synthetic zeolites (Christie, 2002). There are numerous naturally occurring and synthetic zeolites, each with a unique structure. The pore sizes commercially available range from approximately 3 Å to approximately 8 Å. Some of the commercial materials are: A, beta, mordenite, Y, and ZSM-5. The main zeolite formula is [M_2/nO. Al_2O_3.xSiO_2.yH_2O], where M defines the “compensating” cation with valence n. The structural component is Mx/n[(AlO_2)x(SiO_2)y].zH_2O. Figure 2.3 shows that zeolites can be custom made by manipulating the structure, silica-alumina ratio. Other metals can also be incorporated into zeolites to obtain specific catalytic properties (Zhu *et al.*, 2004). Zeolites not only act as shape selectivity catalyst, but also act as acid catalysts for chemical reaction if the loosely localized cations in the zeolites are exchanged with protons (www.iza-online.org).

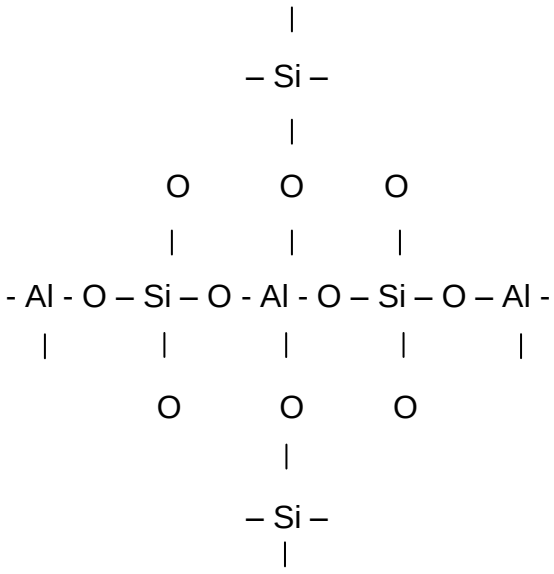


Figure 2.3 Basic Zeolite Structure

Figure 2.4 shows that the MFI (ZSM-5) structure has a three dimensional pore system consisting of sinusoidal 10 rings channels (5.1 -5.5 Å) and intersecting straight 10 rings channels (5.3 × 5.6 Å) (www.iza-online.org).

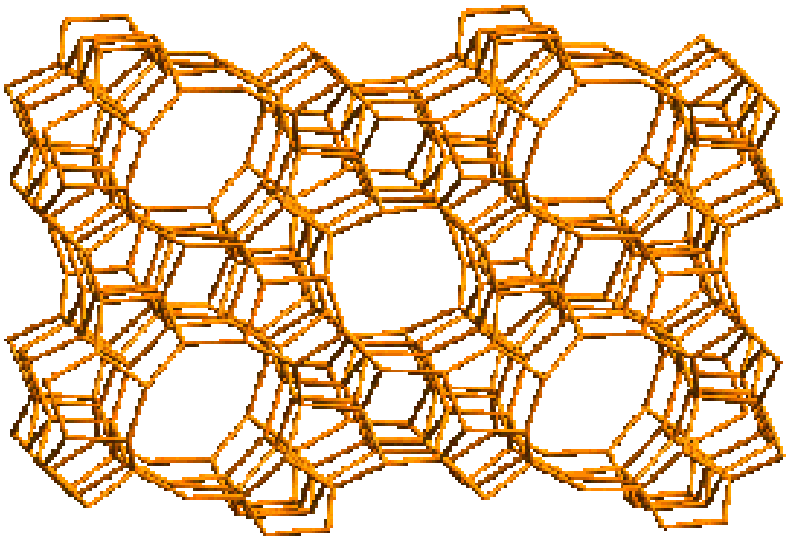


Figure 2.4 Structre type MFI (www.iza-online.org)

The motivations for using zeolite catalysts are primarily profit and environmental regulation compliance. Zeolites can help produce products at more mild temperatures and pressures which lower operating costs.

They also are used for their superior control of reaction selectivity which saves on feed costs and by reducing waste streams, saving on treatment costs (Zhu *et al.*, 2004).

The Si/Al ratio is an important characteristic of the zeolites. The charge imbalance due to the presence of aluminum in the zeolite framework determines the ion exchange properties of the zeolite and induces potential acidic sites. As Si/Al ratio increases, the cation content decreases. The thermal stability increases and the surface selectivity changes from hydrophilic to hydrophobic (Zhao *et al.*, 1993).

Many zeolites are thermally stable to over 500 °C. Some are stable in an alkaline environment, and some are stable in acidic media. Zeolites can be regenerated using relatively easy methods such as heating to remove adsorbed materials, ion exchanging with sodium to remove cations, or pressure swing to remove adsorbed gases. There are a number of different ways that zeolites can be modified. The framework of the zeolite can be modified by synthesizing zeolites with metal cations other than aluminum and silicon in the framework. The framework of the zeolites can be modified by dealumination to increase the silica and increase the hydrophobic nature of the zeolite. There are many proprietary methods to modify zeolites that impart unique characteristics to them. The combination of many properties, among them: the microporous character of the uniform pore dimensions, the ion exchange properties, the ability to develop internal acidity, the high thermal stability, the high internal surface area. These make zeolites unique among inorganic oxides.

2.1.4 Catalyst preparation methods

Zeolites have proven to be good hosts for active species of transition metals which are able to catalyze such reactions. The preparation methods using the metal elements can be divided into two groups: the metal elements can be introduced through post-synthetic treatment methods or during the zeolites synthesis. The activity, selectivity and stability of the catalytically

active species strongly depend on their structure. There are four types of catalysts preparation: liquid ion exchange, chemical vapour deposition, solid state and hydrothermal synthesis.

Different Ion exchange methods have been reported in literature for the preparation of Fe/ZSM-5: gas phase, liquid phase and solid phase (Reitzmann *et al.*, 2002). Fe/ZSM-5 catalyst preparation by ion exchange in the liquid phase would have been an attractive route because of its relatively simple experimental condition, as the redox chemistry of iron in water may not be so complicated. Reitzmann *et al.*, (2002) reported that the method preparation for Fe/ZSM-5 catalyst using LIE (Liquid Ion Exchange) was the best in term of catalyst stability, conversion of benzene and phenol selectivity. Figure 2.5 shows a possible mechanism for ion exchange in aqueous solution of iron (III) (Mircea *et al.,* 2005). This catalyst preparation for Fe/ZSM-5 from H/ZSM-5 in hydrogen form using Fe $(NO_3)_3.9H_2O$. Typically 10-15 g solid to 1 L liquid was mixed. The mixture was heated at 60-80 ^oC using heating plate with a magnetic stirred for 6 h followed filtration of the solid phase using 0.1 µm cellulose filter. This step was repeated one more time. The filtrated catalyst was washed with distilled water and then dried in an oven at 120 ^oC for 2 h. The sample was calcined by heating in an oven at 700 ^oC, 800 ^oC and 900 ^oC for 12 h to activate the sample. Other workers have also shown iron activation by steam treatment results in catalyst displaying a high selectivity (>99%) and up to 27% phenol yields. (Yuranov *et al*., 2004).

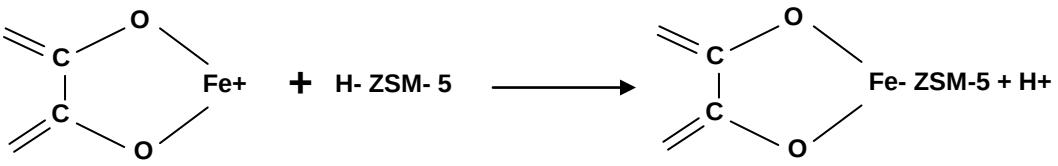


Figure 2.5 A possible mechanism for ion exchange in an aqueous solution of iron (III).

2.1.5 Formation of active sites

In literature there are a number of studies related to use of iron containing ZSM-5 zeolites in the catalytic formation of phenol from benzene (Keqiang *et al.*, 2008). Iron complexes formed inside zeolite channels are thought to be responsible for benzene to phenol oxidation. Recent research performed on two different zeolite matrices (templated and non-templated) with Fe-Si base without aluminum or replaced with Ga, B and Ti and also with different Si/Al ratio (40 and 45) which were obtained by means of ionic exchange using iron cations (Pirutko *et al*., 2002). ZSM-5 zeolite sample with high Si/Al ratio resulting from substitution of iron ions via solid state exchange resulted in highly active and relatively stable catalysts for benzene to phenol hydroxylation (Pirutko *et al*., 2002). Iron loaded zeolites have recently attracted renewed attention due to their outstanding catalytic properties (Sun *et al.*, 2008). The structure of active sites is less clear. There are three types of iron active sites in the zeolite: (a) Isolated ions in tetrahedral lattice position, (b) Isolated ions or small complexes inside the channels, and (c) dispersed oxide particles on the outer surface of the zeolite (Ione *et al* ., 1987).

Many reactions had to be carried out in the past by mixing reactants in the presence of mineral acids. In addition to Bronsted acid and Lewis acid sites of catalyst, the pore system may play a role for the selectivity of acid catalyst reactions. The formation of transition state could be accrued by liquid phase acid catalyzed reactions, hence the introduction of a pore system containing the acid site requires the transition state to be able to fit into the pore system. Fe is very likely bonded with oxygen as FeO. Iron has metallic standards that can be mainly found on the form Fe foil, FeO, Fe_2O_3, Fe_3C, and Fe_xN (x = 2 to 4). In crystalline solids, Fe can occur as Fe^0, Fe^{2+}, Fe^{3+}, and as a mixture of Fe^{2+} and Fe^{3+}. Comparison of the data from the Fe foil, FeO, and Fe_2O_3 show that, as the oxidation state of Fe increases, the absorption edge shifts to higher energy. In going from the metallic to the ferrous state and then to

the ferric state, there is a positive shifts of the Fe absorption (Tsuzuki *et al.,* 1984).

The structure and role of the active site for the benzene to phenol reaction is still an object of discussion. Apelian *et al*., (1996) reported that the total acidity decreased as the calcination temperature increased, and the acidity is connected to the amount of accessible residual framework Fe (and Al), more than to the total amount of iron. *α*-sites are known to form at the stage of high temperature zeolite activation as shown in Figure.2.6. At this stage Fe ions migrate from the crystalline lattice into zeolite micropores, where *α* sites form. At high-temperature activation, due to the presence of defects, iron atoms migrate over the crystal and may move from the lattice into the micropore space, forming dinuclear complexes stabilized at the charge compensating sites (Dubkov *et al*., 2003). Figure 2.6 shows a possible mechanism of the active site formation; formation of a binuclear iron complex A by both synthesis and post-synthesis of the zeolite. Overweg *et al*., (2004) suggested that Fe atom is migrated from tetrahedral positions or an external Fe insertion using solid ion exchange for Fe/ZSM-5, Fe-silicalite and Fe-β. Complex A is thought to be transformed into a reduced complex B via oxygen desorption. The process of a-site formation and Fe (II) stabilization appeared to depend on the chemical composition of the matrix and post-treatment methods. The reduced iron atoms of complex B appear to be inert to dioxygen and this is further oxidized by nitrous oxide into complex C. (Lioubove *et al.,* 2003 and Overweg *et al.,* 2004).

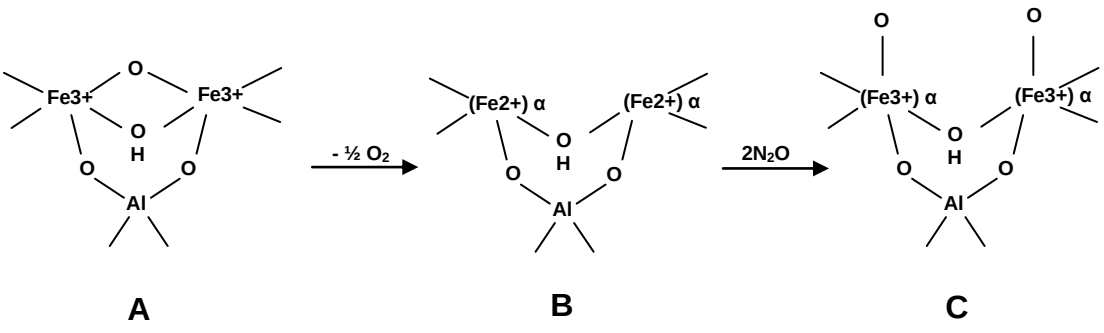


Figure 2.6 Formation of pair of α- sites in the form of a dinuclear iron complex

Sun *et al*, (2008) reported the catalyst activity per gram of iron increases as the iron concentration decreases. This indicates that only a fraction of iron is catalytically active in the direct oxidation of benzene to phenol. However, since only a fraction of iron is catalytically active, this suggests that not all oxidized iron (II) to iron (III) species were able to generate active oxygen species needed for the oxidation of benzene to phenol. Only a small fraction of iron (II) to iron (III) species oxidized were able to generate active oxygen for phenol production from benzene (Jerome *et al.,* 2005). High iron content leads to an excess of active sites promote to coke formation which is resulted coupling of phenol with benzene or another by-products presence in reaction area. Reaction mechanism is discussed further in the reaction Chapter 2.2. Panov *et al*., (2000) reported that deactivation resulted from decreasing the number of active sites on the catalyst. At the same time, the activity of a single active site was found to remain constant.

2.1.6 Deactivation of zeolites

Some processing conditions may lead to unwanted "side-effects," such as dealumination, zeolite destruction, agglomeration of supported metals etc. These side-effects decrease the catalyst lifetime and, therefore, increase the total cost of industrial production. Coke formation is strongly dependent on the three factors: zeolite structure, the reaction conditions, and the nature of the reactants (Ivanov *et al*., 2003).

Consideration of the regeneration ability of zeolite catalysts coked during the oxidation reaction is important. Moulijn *et al* (2001) reported that, catalyst deactivation can be caused by (A) decrease in the number of active sites, (B) decrease in the quality of the active sites, (C) decrease in the accessibility of the pore space containing the active sites. Ivanov *et al*., (2003) reported two ways to regenerate the catalyst, using N_2O and O_2. In the case of catalyst regeneration with nitrous oxide, a complete restoration of catalytic activity required the removal of only 30–35% coke. In the case of regeneration using oxygen, catalytic activity was fully restored after removal of 60–65% of the total coke amount. Sayyar *et al*., (2008) reported that the catalysts were

weighted before and after regeneration to determine the weight of coke formation. Panov *et al*., (2000) suggested the activation takes place at active sites. In the case of completely coked samples, active sites (micropore) are blocked by coke and do not participate in activation of catalyst. Removal of even a small coke fraction makes active sites easily reached.

Guanjie *et al.,* (2010) suggested that catalytic activity and concentration of active sites on the samples decrease with an increase in coke content. Catalytic activity of partially regenerated samples was not directly proportional to the coke amount on a sample only but also to further hydroxylation of phenol to dihydroxybenzene (p-benzoquinone, catechol and hydroquinone) by strong adsorption of phenol in Bronsted acid sites (the activation centers). The deactivation may be resulted from decreasing the number of active sites on the catalyst (Panov *et al*., 2000).

Some studies have been undertaken to prolong the reaction mechanism and to eliminate the presence of specific active sites. Time studies support iron complexes adsorbed in the micropore space of the zeolite (Ivanov *et al*., 2003) may impact catalytic activity to the catalyst. Studies of catalytic oxidation found that the catalyst activity gradually decreases with time due to catalyst deactivation by coke (Hensen *et al.,* 2005). As the active sites are unblocked, the regeneration rate increases and reaches its maximum. Figure 2.7. shows a schematic representation of coking and regeneration of ZSM-5: (A) initial sample before reaction; (B) the coked sample after the reaction; and (C) the sample after regeneration (Ivanov *et al*., 2003).

Meloni *et al* (2003) found that for Fe-ZSM5 catalysts, addition of steam to the feed improved catalyst activity, selectivity, and durability and also that the surface acidity was not responsible for activity in the main reaction, but it affected catalyst deactivation by coking. Catalyst deactivation derived mainly from the decomposition-condensation of phenol onto Bronsted acid sites; the stronger the latter (strong adsorption of phenol), the quicker was the coking rate. Finally, the concentration of Bronsted acid sites decreased with increasing pretreatment temperature, showing clearly that they are not

responsible for catalytic activity for the main reaction (not regarding the consecutive reactions). Coke deposition increased as the reaction temperature increased, especially at higher than 450 °C and this is proof that phenol oxidizes further and forms more deposition coke as the reaction temperature increases, which results in less selectivity for phenol and this is due to benzene hardly cracks in the experimental temperature range compare with phenol (Guanjie *et al.,* 2010).

Sometimes the pore system consists of interconnecting channels without cavities, as in the ZSM5 framework, in this case the deactivation occurs first through limitation of the access to the active sites and then by blockage of the access to the sites of the channel intersection in which the coke molecules are sitting. In fact, it is known that in MFI (ZSM-5) zeolites the soluble coke molecules remain trapped within the micropores (pore size < 20 Å) (Sun *et al.*, 2008).

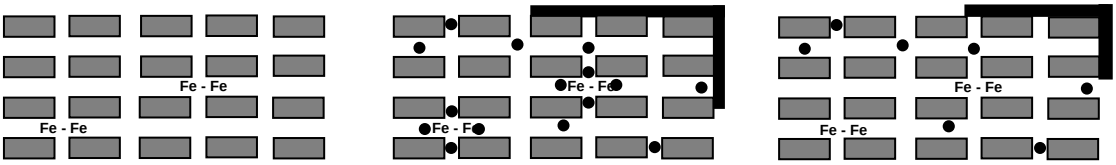


Figure 2.7 The schematic representation of coking and regeneration of ZSM-5

The understanding of different issues related to coke, such as formation mechanisms, location and structure is needed in order to develop more efficient regeneration process and to provide a scientific foundation for the further development and the industrial application of these kinds of catalysts.

2.1.7 The selectivity and productivity of phenol

Zeolites have been tested as catalysts for the one step oxidation of benzene to phenol with N_2O and the most promising were MFI-structured zeolites, like Fe-silicalite or Fe-ZSM5. Selectivity was found to be higher than 90%. According to Panov, (1998), small extraframework Fe clusters, called *α*-sites, can dissociate N_2O at low temperatures. This would produce (O)*α* species responsible for the selective oxidation of benzene to phenol. Other researchers proposed that Brønsted acid sites or extraframework aluminum-based Lewis acid sites are involved, so attributing the catalytic activity to surface acidity only (Hensen *et al.,* 2005).

The catalytic role of iron species at extraframework positions for selective benzene oxidation to phenol with nitrous oxide as oxidant has been investigated in many recent studies. For the low reaction temperature, the phenol productivity was found to be very low (Hensen *et al.,* 2005). The activity measurements (catalyst testing) for one step oxidation of benzene to phenol was performed using fixed bed reactor in mixture of 1 vol% benzene and 4 vol% nitrous oxide in helium flow with a total flow rate of 100 ml/min. The productivity of phenol decreases strongly from 4.35 to 2.44 mmol/g.h with increasing iron loading (Sun *et al*,. 2008).

One step hydroxylation of benzene to phenol was achieved using low concentration of benzene and nitrous oxide, the molar C_6H_6/N_2O/He feed ratio was 1/3/36 at 450°C (Krishana *et al*., 2004). An increase in iron content upon calcination in O_2 at 450°C in this reaction leads to decrease in phenol productivity over time on stream and also a strong increase in the benzene conversion (~26%), and a very low phenol yield (~7%). On the other hand upon steam treatment at 650°C, the phenol yield increase (~13%), but the benzene conversion strongly decreases (~15%) with high iron loaded to the catalyst (Krishana *et al*., 2004 and Sun *et al*., 2008). Dubkov *et al*., (2002) suggested that the reduction of the Bronsted acid sites increases the number of the active sites and phenol productivity. They concluded that a part of Fe (II) which are responsible to create active sites were converted to Fe (III). It

was seen from their experiments that these a-O are unstable at temperature higher than 300°C. High-temperature treatment radically enhances the phenol productivity, mainly by increasing the selectivities towards phenol (Notte, 2000). The decrease in the rate of phenol formation with increasing iron content for the high-temperature treated catalyst is mainly due to the decrease in the selectivity of benzene to non-selective products (Zhu *et al* ., 2004). Mircea *et al*., (2005) discuss the benefits of isomorphously substituting low iron content in the zeolites to increase the catalyst selectivity. Only at high temperature (> 673 K) small amounts of by-products (mainly benzoquinone and benzofuran) were detected. Total oxidation of benzene to carbon dioxide and water was the main undesired reaction (Ivanov *et al*., 2003).

2.1.8 Physical and chemical characterisation of the catalyst

In the literature, Fe/ZSM-5 zeolites catalyst is comprehensively characterized and investigated for the structure properties and surface acidity by nuclear magnetic resonance spectroscopy (NMR), fourier transform infrared spectroscopy (FTIR) and temperature programmed desorption (NH_3-TPD) measurements. The iron Fe/ZSM-5 was also investigated for the elemental composition, BET surface area and pore size distribution by X-Ray Diffraction (XRD), inductivity coupled plasma emission spectroscopy (ICP), atomic absorption spectroscopy (AAS) and nitrogen adsorption using N_2 adsorption-desorption at 77 K via Micromeritics (physisorption).

The determination of the active sites concentration, reactivity and TPD studies were carried out using a Micromeritics ASAP 2010 analyser provided with a quartz plug- flow reactor and using mass spectrometer (MS) to analyse the gas phase compositions (Hensen *et al*., 2004). There are three ways to determine the active sites using TPD: A) ammonia, B) non-reactive amines such as pyridine and t-butyl, C) reactive vapors using isopropylamine (IPA), this amines are reactive and cleavage to propylene and ammonia over Bronsted acid sites as shown in Figure.2.8. The most recent technique for measuring Bronsted acid site concentrations is the temperature programmed decomposition of amines. The number of acid sites was calculated from the peak of propene molecules obtaining from IPA decomposition (www.micromeritics.com and Hensen *et al*., 2004).

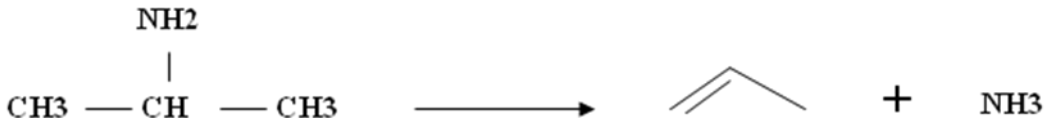


Figure 2.8 Isopropylamine decomposing to Propylene and ammonia

2.2 Reaction mechanism of benzene oxidation using N_2O

This section review the scientific literature relate to the kinetics of the benzene – nitrous oxide reaction. Additionally, a fixed-bed model is described to evaluate catalyst performance.

2.2.1 Modelling of reaction kinetics [Benzene hydroxylation (using N_2O as oxidising agent) to phenol with consideration of competing reaction.]

Investigation of the literature on oxidation of benzene to phenol using a zeolite catalyst with N_2O as the oxidant has been carried out. The catalytic activity was found to be related to the acid-base properties of the catalyst (Wącław *et al*, 2004). The hydroxylation of benzene to phenol is thought to accure at Bronsted acid centers (BAC) of the zeolite. However there is no clear answer can be given to the question about the corresponding active sites. To improve the performance of zeolites catalysts using Ion exchange methods are the most common techniques used to change the acidity of zeolites (Reitzmann *et al* , 2000).

ZSM-5 a zeolite is one of the most important catalyst for the direct oxidation of benzene to phenol in the gas phase using nitrous oxide (N_2O) as the oxidant (see Equation 2.1).

$$C_6H_{6\,(g)} + N_2O_{(g)} \xrightarrow[\text{Fe/ZSM-5 cat}\\ \text{gas phase}]{450\ ^{\circ}C} C_6H_5OH_{(g)} + N_{2(g)}\ldots \qquad (2.1)$$

A mechanism for Reaction (2.1), which is typical for oxidative catalytic reactions, is discussed by Reitzmann *et al.,* (2002). The suggested reaction mechanism involves the following steps (the main reaction (MR), the side reaction of N_2O (SN) and the side reaction of phenol (SP_1)) and (SP_2). Additional side reactions of phenol (SP_2) on two different types of sites S_0 and S_1:

1- (MR), the main reaction (see Figure 2.9) is the hydroxylation of adsorbed benzene with the chemisorbed oxygen species to form phenol.

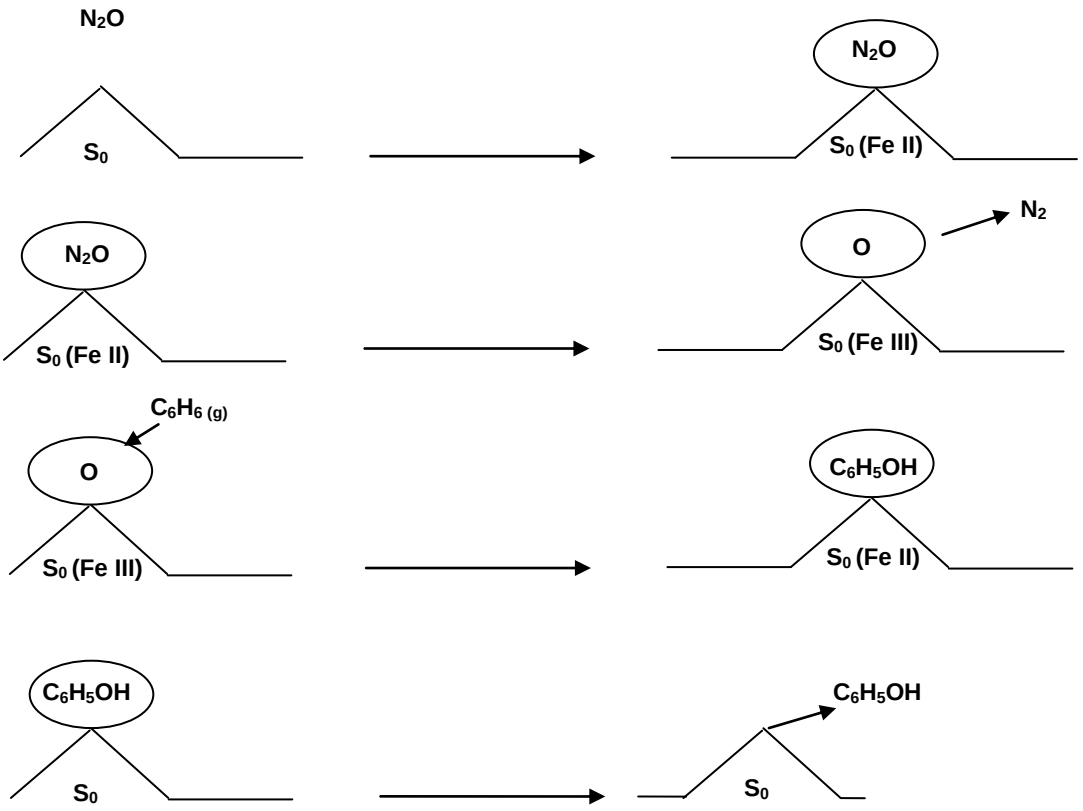


Figure 2.9 Schematic representation of elementary reactions constituting the main reaction

Where (Figure 2.9) above represents the adsorption for nitrous oxide on site S_0 and the key step for a decomposition of nitrous oxide (N_2O) into nitrogen and an active form of oxygen, probably on a Lewis acid site (Reitzmann *et al.,* 2002) as mentioned in Figure 2.6 above. Benzene adsorbed on site (S_0), which in turn, reacts with the active form of oxygen. After that the adsorbed phenol is formed. Finally the desorption of the phenol product and liberation of active site S_1 on which phenol can be adsorbed again (SP_1, consumption of phenol) because of the strong adsorption of phenol and slow diffusion and may be the only solution to avoid the liberation of active sites is by control the acidity during the catalyst preparation. The site S_1 probably represents a special iron species, which is present in trace amounts in H-(Al)ZSM-5 and is increased by iron-exchange in Fe-(Al)ZSM-5 according to (Panov *et al.*,1988

and 2000). This would explain the higher consumption rates on iron exchanged ZSM-5. The understanding of the role of active sites and control of the acidity is still under investigation.

It has been shown that the active site of oxygen, deposited on the catalyst by its reaction with nitrous oxide (N_2O), can hydroxylate benzene directly at room temperature, while the only product which can be recovered from the catalyst by extraction would be the phenol (Reitzmann *et al* 2002). These studies gave evidence that benzene oxidation to phenol occurs with the presence of active site of oxygen. Additionally, it is assumed that sorption equilibrium of phenol is also reached.

$$N_2O \leftrightarrow Z - N_2O$$
$$B + Z \leftrightarrow Z - B$$
$$Ph + Z \leftrightarrow Z - Ph$$

The sorption is described by the Langmuir theory resulting in the surface coverages

$$\Theta_{Z,B} = \frac{K_B \chi(B)}{1 + K_B \chi(B) + K_{Ph} \chi(Ph) + K_{N_2O} \chi(N_2O)} \quad \text{.....(2.2)}$$

$$\Theta_{Z,Ph} = \frac{K_{Ph} \chi(Ph)}{1 + K_B \chi(B) + K_{Ph} \chi(Ph) + K_{N_2O} \chi(N_2O)} \quad \text{.....(2.3)}$$

Since the sorption constant of N_2O is very small compared with those of the aromatics, sorption of N_2O should not influence the interaction of the aromatics. Therefore, $K_{N_2O}\chi(N_2O)$ in Eqs. (2.2) and (2.3) can be neglected. Reitzmann *et al*, (2002) have reported that the saturation of benzene and phenol coverage is reached (formation of any by products is very low). Therefore, the "1" in Eqs. (2.2) and (2.3) can be neglected, which means that free sorption sites are no more available $(\alpha Z_{,free} = 0)$. This leads to the following expressions for the surface coverage for the aromatics

$$\Theta_{Z,B} = \frac{1}{1+\left(K_{Ph}\chi(Ph)/\,K_B\chi(B)\right)} \quad \text{.....(2.4)}$$

$$\Theta_{Z,Ph} = \frac{1}{1+\left(K_B\chi(B)/\,K_{Ph}\chi(Ph)\right)} \quad \text{.....(2.5)}$$

2- (SN), the side reaction of N_2O. In case of high concentration of N_2O compare with benzene, the nitrous oxide will adsorb again to the new active sit S_1. At high molar fractions (concentration) of N_2O, direct oxidation of phenol to CO_2 by chemisorbed oxygen also occurs. Activation of adsorbed N_2O leading to the formation of chemisorbed oxygen species at the site S_1 (see Figure 2.10).:

$$S_0 - N_2O + S_1 \rightarrow S_0 + N_2 + S_1 - O$$

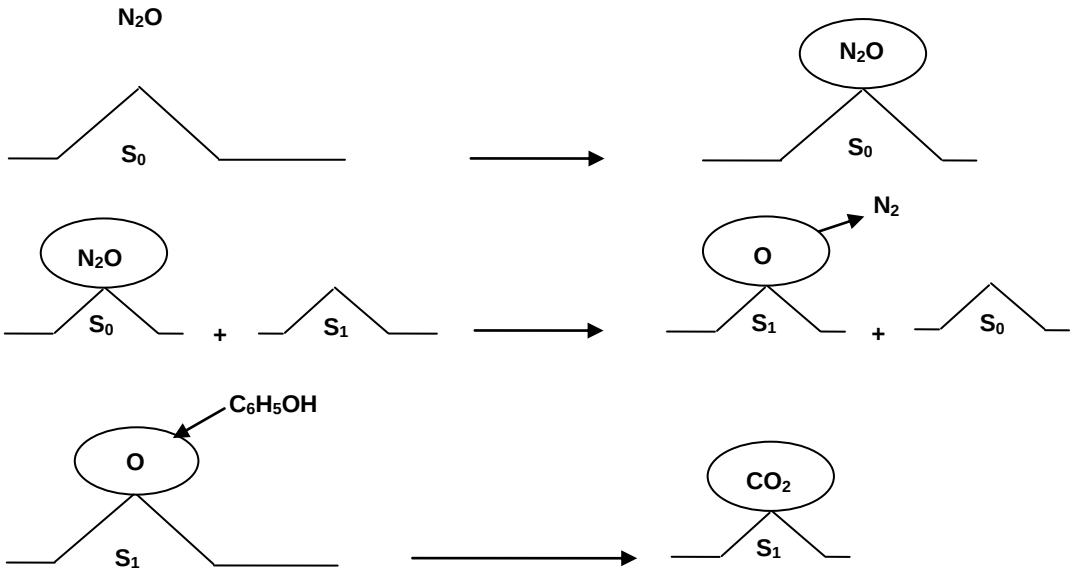


Figure 2.10 Schematic representation of elementary reactions constituting the side reaction of N_2O

Although it has been assumed that the sorption of N_2O has no influence on the interaction of aromatics with zeolite, adsorption of N_2O has to precede the formation of the chemisorbed oxygen species.

$$\Theta_{Z,N_2O} = \frac{K_{N_2O}\chi(N_2O)}{1+K_{N_2O}\chi(N_2O)} \quad \text{.....(2.6)}$$

Adsorbed N_2O dissociates at the active site (S_1) leading to the formation of chemisorbed oxygen species and nitrogen is released (rate r_0)

$$r_o = K_o \Theta Z, N_2 O \alpha S_{1,free} \quad \text{.....(2.7)}$$

$$\alpha S_{1,O} + \alpha S_{1,free} = 1 \quad \text{.....(2.8)}$$

3- (SP_1), the side reaction of phenol is the consecutive reaction of phenol without the participation of chemisorbed oxygen. SP_1 should be attributed to the accumulation of phenol inside the ZSM-5 particle due to strong adsorption and slow diffusion of phenol on active site S_1 (see Figure 2.11), which subsequently leads to oligomerisation products ($C_xH_yO_z$).

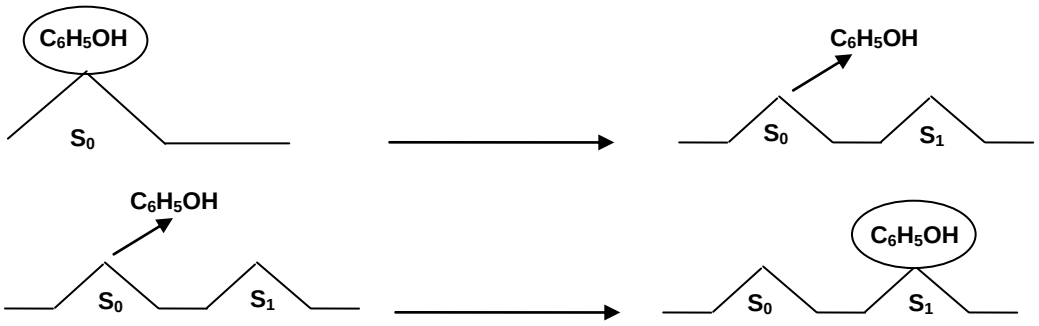


Figure 2.11 Schematic representation of elementary reactions constituting the Consumption of phenol

4- (SP_2), side reaction of $phenol_2$. Additional side reactions of phenol and chemisorbed oxygen are the consecutive hydroxylation of phenol by oxygen to catechol ($C_6H_4(OH)_2$) and *p*-benzoquinone ($C_6H_4O_2$). Hydroquinone is subsequently oxidised to *p*-benzoquinone (see Figures 2.12 and 2.13).

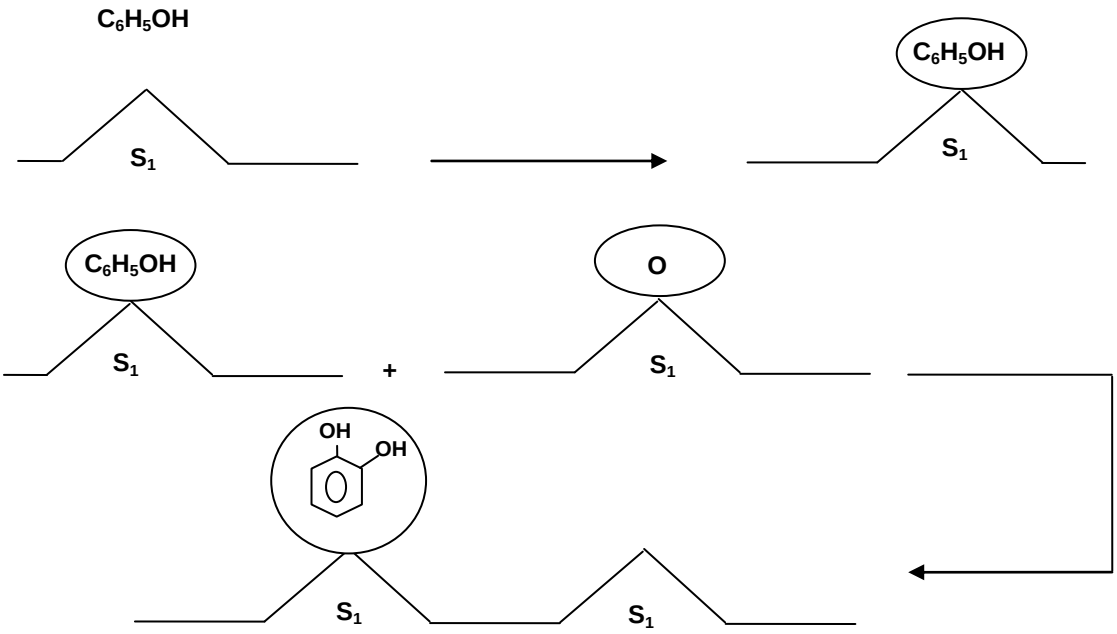


Figure 2.12 Schematic representation of elementary reactions constituting the side reaction of phenol2 (catechol)

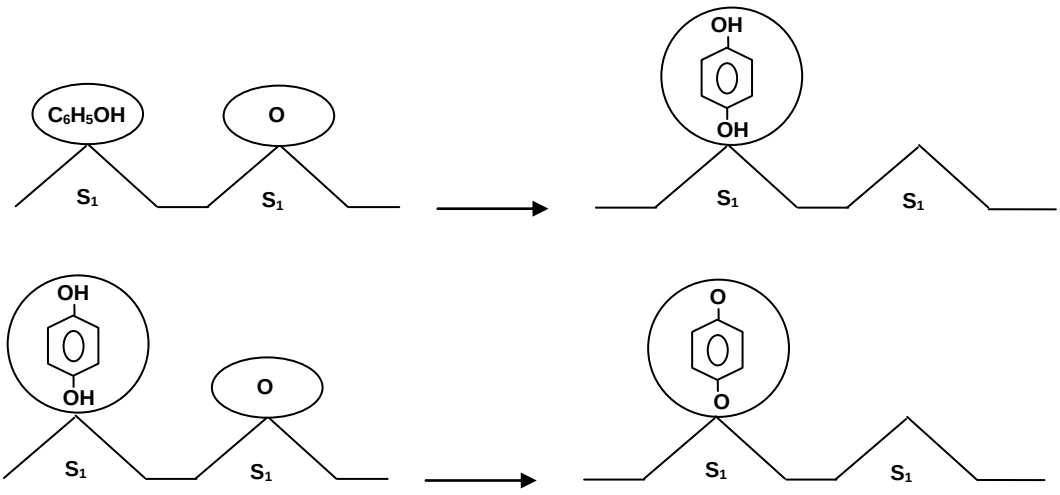


Figure 2.13 Schematic representation of elementary reactions constituting the side reaction of $phenol_2$ (*p*-benzoquinone)

Consumption of the chemisorbed oxygen (Main reaction (MR)):

$$r_{MR} = K_{MR}\Theta_{Z,B}\alpha S_{1,O} \quad (2.9)$$

Consumption of the chemisorbed oxygen (Side reaction (SN)):

$$r_{SN} = \hat{K}_{SN}\left(\Theta_{Z,}C_X H_Y O_Z\right)\alpha S_{1,O} \quad (2.10)$$

Consumption of phenol (accumulation, oligomerisation: SP1):

$$r_{SP_1} = K_{SP_1}\Theta_{Z,Ph} \quad (2.11)$$

Consecutive hydroxylation (formation of p-benzoquinone: SP2):

$$r_{SP2} = K_{SP2}\Theta_{Z,Ph}\alpha S_{1,O} \quad (2.12)$$

oxygenate species are present that r_{SN} is no more dependent on $\Theta_{Z,}C_X H_Y O_Z$. This simplifies Eq. (9) to

$$r_{SN} = K_{SN}\alpha S_{1,O} \quad (2.13)$$

$$\alpha S_{1,O} = \frac{K_O}{K_{MR}\Theta_{Z,B} + K_{SN} + K_O\Theta_{Z,N_2O}}.\Theta_{Z,N_2O} \quad (2.14)$$

Applying Eqs. (2.4) and (2.6) the coverage of N_2O and benzene can be calculated. The consecutive hydroxylation (Eq. (2.12)) is not considered due to its negligible contribution to the overall reaction. Defining a new pseudo-rate constant $\hat{K}_O$ Eq. (2.14) can be transformed to

$$\alpha S_{1,O} = \hat{K}_O.\Theta_{Z,N_2O} \quad (2.15)$$

The constant $\hat{K}_O$ represents the ratio between the rate constants of formation and consumption of chemisorbed oxygen. The molar rates of N_2O and benzene consumption and phenol formation are:

$$-R_B = K_{MR}\Theta_{Z,B}\alpha S_{1,O} \quad \text{.....(2.16)}$$

$$-R_{N_2O} = K_{MR}\Theta_{Z,B}\alpha S_{1,O} + K_{SN}\alpha S_{1,O} + 2K_{SP2}\Theta_{Z,Ph}\alpha S_{1,O} \quad \text{.....(2.17)}$$

$$-R_{Ph} = K_{MR}\Theta_{Z,B}\alpha S_{1,O} - K_{SP1}\Theta_{Z,Ph}. - K_{SP2}\Theta_{Z,Ph}\alpha S_{1,O} \quad \text{.....(2.18)}$$

are expressed in detail by considering each coverage $\Theta_i, \alpha S_{1,O}$. Equations (2.19 - 2.21) show the molar rates of N_2O and benzene consumption and phenol formation.

$$-R_B = K_{MR}\hat{K}_O \frac{K_{N_2O}\chi(N_2O)}{1+K_{N_2O}\chi(N_2O)} \times \frac{1}{1+(K_{Ph}\chi(Ph)/K_B\chi(B))} \quad \text{.....(2.19)}$$

$$-R_{N_2O} = K_{MR}\hat{K}_O \frac{K_{N_2O}\chi(N_2O)}{1+K_{N_2O}\chi(N_2O)} \times \frac{1}{1+(K_{Ph}\chi(Ph)/K_B\chi(B))}. + K_{SN}\hat{K}_O \frac{K_{N_2O}\chi(N_2O)}{1+K_{N_2O}\chi(N_2O)} + 2K_{SP2}\hat{K}_O \frac{K_{N_2O}\chi(N_2O)}{1+K_{N_2O}\chi(N_2O)} \times \frac{1}{1+(K_B\chi(B)/K_{Ph}\chi(Ph))} \quad \text{.....(2.20)}$$

$$-R_{Ph} = K_{MR}\hat{K}_O \frac{K_{N_2O}\chi(N_2O)}{1+K_{N_2O}\chi(N_2O)} \times \frac{1}{1+(K_{Ph}\chi(Ph)/K_B\chi(B))}. - K_{SP1}\frac{1}{1+(K_B\chi(B)/K_{Ph}\chi(Ph))} - K_{SP2}\hat{K}_O \frac{K_{N_2O}\chi(N_2O)}{1+K_{N_2O}\chi(N_2O)} \times \frac{1}{1+(K_B\chi(B)/K_{Ph}\chi(Ph))} \quad \text{.....(2.21)}$$

Nomenclature

B≡ benzene

k ≡ kinetic constant

Ph ≡ phenol

r ≡ rate of reaction

S_i ≡ site for species (i) adsorption

S_1 ≡ site for side of reaction adsorption

$\chi(i)$ ≡ mole fraction of species (i)

Z≡ zeolite

Greeks Symbols

$\Theta_{Z,B}$ ≡ the surface coverage

$\alpha Z_{1,free}$ ≡ free active sites of zeolite

$\alpha_{Z1,O}$ ≡ chemisorbed oxygen

2.3 Conclusions

For industrial processes, heterogeneous catalysts have some advantages over homogeneous catalysts such as catalyst recovery and recycling. The effect of coke on catalytic and texture properties of ZSM-5 zeolites in the reaction of benzene oxidative hydroxylation by nitrous oxide was studied. The catalysts were regenerated in oxygen and in nitrous oxide. N_2O was found to be a more efficient reactivation reagent than O_2. Hence, the objective of the literature review was to identify promising catalyst preparation methods that were subsequently used in the present study to prepare a series of materials for testing under similar reaction conditions (not reported in previous in literature). Fe-ZSM5 catalyst samples with different Si/Al ratios and different iron contents have been studied for the one step oxidation of benzene to phenol using N_2O as the oxidant. Fe-ZSM5 catalysts with affect of different Si/Al ratios, iron contents and temperature have been identified and studied for selective formation of phenol. The literature review shows that catalysts synthesized with high Si/Al ratios and with low iron content have good long term stability (reduced deactivation rates) and demonstrated good phenol selectivity and reaction rates of phenol (productivity). Catalysts with high amounts of iron showed considerable deactivation particularly at high reaction temperatures. The chemisorption method that has been used in the present study to measure the active sites concentration was identified. The balance between Bronsted acidity and the quantity of active oxygen donor α-sites seem to depend on the Si/Al ratio and the presence of the iron within the catalyst matrix. The possible mechanism for hydroxylation of benzene to phenol has been discussed. The proposed mechanism (the model equations using the main reaction and the consecutive reactions) yields rate expressions that are discussed later in Chapter 5.6 for simulation and rate parameter estimation. The structure of the active site for the benzene to phenol reaction is still an object of discussion. Mechanistic details are still unclear, including such important aspects as *α*-sites structure and nuclearity.

3 Materials and Methods

In this chapter, a brief description of catalyst preparation method, catalyst characterisation, standard preparation and calibration of gas phase concentrations using GC (Gas Chromatography) is presented. The experimental setup used to evaluate the catalyst performance is described.

3.1 Catalysts preparation

A series of Fe/ZSM-5 catalysts were prepared to evaluate the influence of catalyst properties on the production of phenol from benzene by one step hydroxylation. H-ZSM-5 followed by Fe/ZSM-5 catalysts (varying iron content, 0.1% and 1% by weight) were prepared employing an ion exchange method. ZSM-5 in ammonium form (NH_4-ZSM-5) was procured from Zeolyst International USA. In the initial studies, liquid phase (aqueous) ion exchange was employed to convert NH_4-ZSM-5 (30 and 80 Si/Al ratio) to Fe/ZSM-5 (replacing NH_4^+ with Fe^{3+}). The iron source has been used was Fe $(NO_3)_3$ for iron (III). Furthermore, monovalent cations can be exchanged more easily into a zeolite than divalent or trivalent cations because the positive charge of multivalent cations has to be balanced by specially separated negative charge of the zeolite matrix. Therefore formation of hydroxo-ions as $Fe(OH)^+$ is favoured. Table 3.1 and Figure 3.1 shows a summary of the catalysts prepared using the liquid ion exchange (LIE) method.

Table 3.1 Nomenclature identifying catalyst samples prepared using ion exchange.

Fe / ZSM-5 catalyst (LIE)			
Si / Al ratio (30) [NH_4Z30]		**Si / Al ratio (80)** [NH_4Z80]	
[FeZ30- 0.1%]	[FeZ30- 1%]	[FeZ80- 0.1%]	[FeZ80- 1%]
1	2	3	4

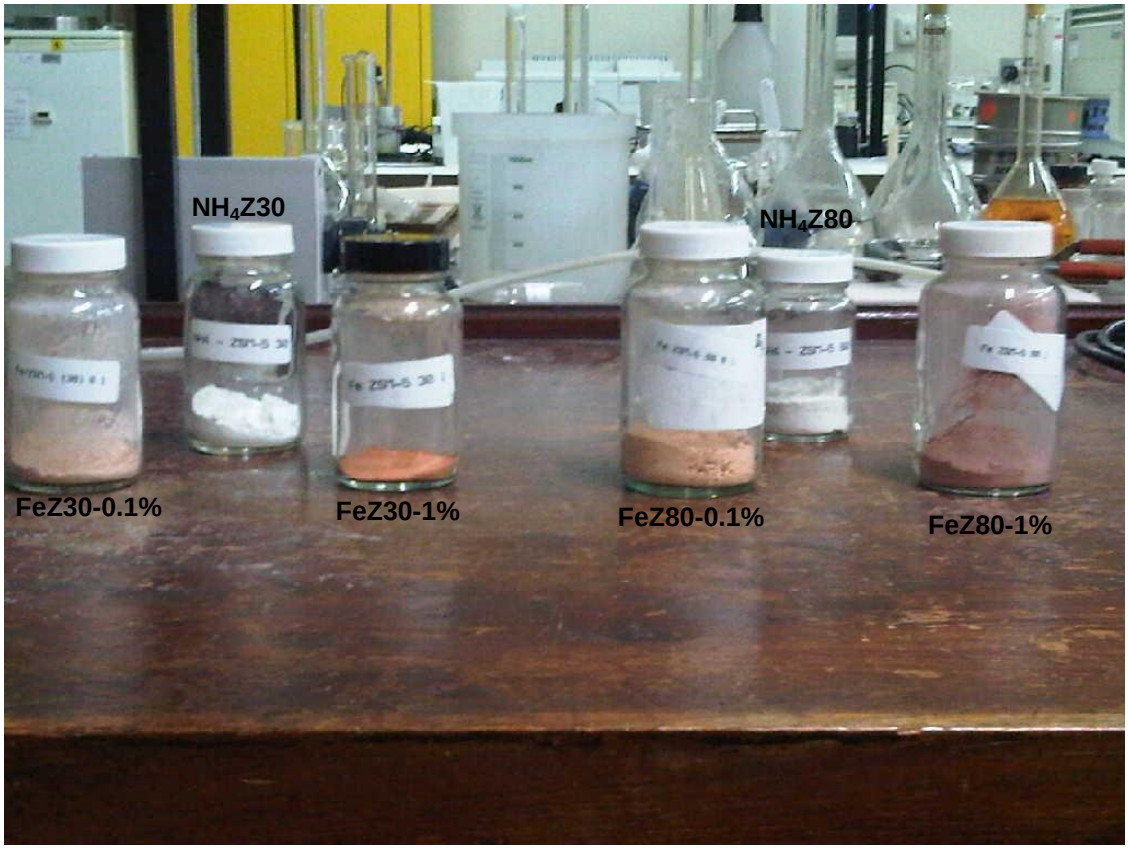


Figure 3.1 Photograph of the series numbers of catalyst samples before and after preparation using ion exchange.

Nomenclature

[NH_4Z30] = ZSM-5 in ammonium form (Si/Al ratio 30)

[NH_4Z80] = ZSM-5 in ammonium form (Si/Al ratio 80)

[FeZ30- 0.1%] = ZSM-5 with 0.1 wt% of Fe using LIE (Si/Al ratio 30)

[FeZ30- 1%] = ZSM-5 with 1 wt% of Fe using LIE (Si/Al ratio 30)

[FeZ80- 0.1%] = ZSM-5 with 0.1 wt% of Fe using LIE (Si/Al ratio 80)

[FeZ80- 1%] = ZSM-5 with 1 wt% of Fe using LIE (Si/Al ratio 80)

3.1.1 H-ZSM-5 catalysts preparation

HZ30 and HZ80 were prepared using LIE method (Louis *et al* , 2001) to remove any sodium as shown in Figure 3.2. The preparation method is as follows:

1- 10 g of the zeolite NH_4-ZSM-5 (30 or 80 - Si/Al) was mixed with 40ml of 0.1 M NH_4Cl in a beaker (volume = 100ml).
2- The mixture was heated to 80^oC using a hot plate with a magnetic stirrer and kept at 80^oC for 5h. The sample was filtered through a 0.1 µm cellulose filter (Whatman International, 542 grade).
3- 40ml of [NH_4Cl] were added to the sample after filtration. The mixture was heated to 80^oC for 5h (with agitation at 450 rpm), and was filtered again.
4- Step 3, was repeated one more time.
5- The filtered catalyst was washed with distilled water for 45 min (in a sintered glass column) to remove any residual NH_4Cl. The sample was then dried in an oven at 120^oC for 2 h.
6- The sample was calcined at a heating rate of 10 °C min^{-1} from room temperature to 550^oC in an oven (CARBOLITE furnace, purchased from Elite Thermal Systems Limited, model (TSH12/50/300-2416 CG)) for 5 h to form H-ZSM-5.

Nomenclature

[HZ30] = ZSM-5 in hydrogen form using LIE (Si/Al ratio 30)
[HZ80] = ZSM-5 in hydrogen form using LIE (Si/Al ratio 80)

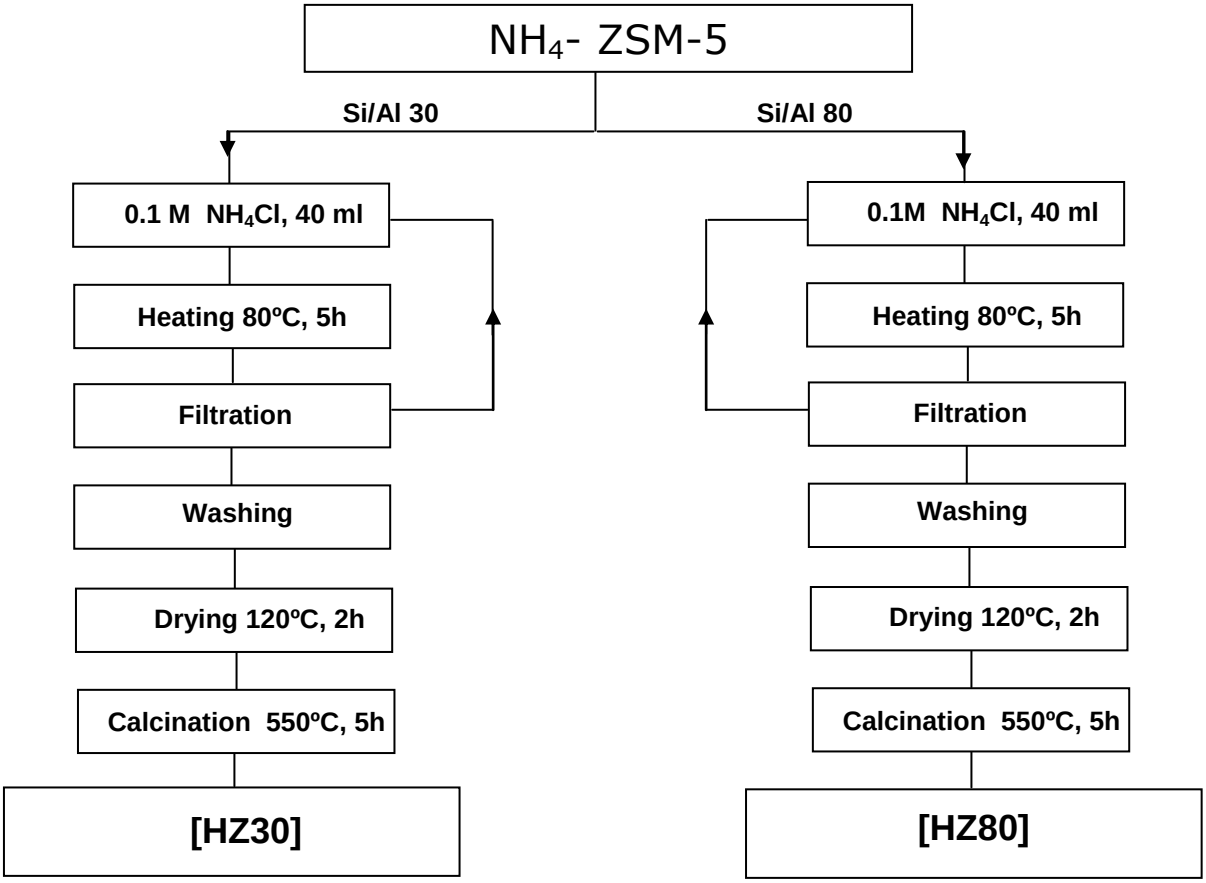


Figure 3.2 Procedure to prepare HZ30 and HZ80 catalyst samples using liquid ion exchange method

3.1.2 Fe/ZSM-5 catalysts preparation

Figure 3.3 shows the preparation method for Fe/ZSM-5 [0.1% Fe-Z30, 1% Fe-Z30, 0.1% Fe-Z80 and 1% Fe-Z80] using LIE (Liquid Ion Exchange). The preparation method follows the method of Reitzmann *et al.* , (2002) with some modifications:

1. 10 g of the zeolite H/ZSM-5 (30 or 80 - Si/Al) was mixed with 10 and 40 ml of 0.2M $Fe(NO_3)_3$ (98% purity) in a beaker (volume = 100ml).
2. The mixture was heated to 60^{o}C using a hot plate with a magnetic stirrer and kept at 60^{o}C for 6h. The sample was filtered though a 0.1 µm cellulose filter (Whatman International, 542 grade).
3. The same volume of (98% purity) Fe $(NO_3)_3$ were added to the sample after filtration. The mixture was heated to 60^{o}C for 6h (with agitation at 450 rpm), and was filtered again.
4. Step 3, was repeated one more time.
5. Acid treatment of the catalysts was done using $Na_2S_2O_4$ and HNO_3 for 40 and 60 minutes respectively at 50^{o}C to remove any residual.
6. The filtered catalyst was washed with distilled water for 45 min (in a sintered glass column) to remove any residual Fe $(NO_3)_3$. The sample was then dried in an oven at 120^{o}C for 2.5 h.
7. The sample was calcined at a heating rate of 10 °C min^{-1} from room temperature to 900^{o}C in an oven (CARBOLITE furnace, purchased from Elite Thermal Systems Limited, model (TSH12/50/300-2416 CG)) for 15 h to activate the sample.

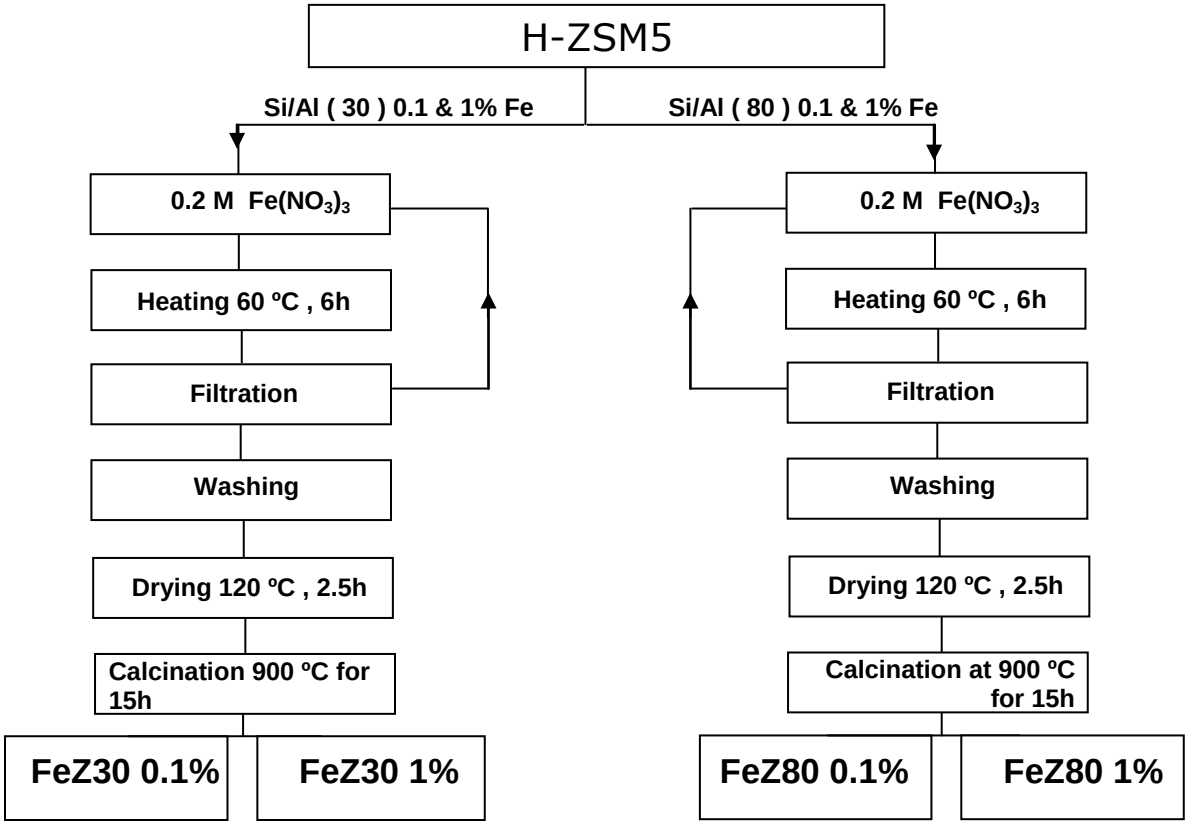


Figure 3.3 Procedure to prepare FeZ30 and FeZ80 catalyst samples using liquid ion exchange method

3.2 Granulation process

The particle size for the NH_4-ZSM-5 (30 and 80 Si/Al ratio) catalysts supplied by Zeolyst International USA was within the range 0.1- 10µm. The particle size was grown to 365 µm directly after catalyst preparation using the LIE method from NH_4-ZSM- to Fe/ZSM-5. The preparation method seems to have had a significant effect on the shape of the particle size; this may be due to coagulation. Indiscriminately the word coagulation has been used for such a long time to describe the coagulation effects of density of the particle by causing the formation of loosely bound units which behave as aggregates (Akers, 1979). Coagulation is a process in which small particles join together to form larger agglomerates. The most important types of additives in coagulation are the salts of multivalent metal ions such as Ca^{2+}, Fe^{2+}, Fe^{3+} and Al^{3+} (Wakeman and Tarleton, 1999).

The catalyst particles of 60 - 250 µm were used to evaluate the influence of catalyst performance on phenol production. The granulation process for Fe/ZSM-5 catalyst particles was successfully done using three steps as shown in Figure 3.4.

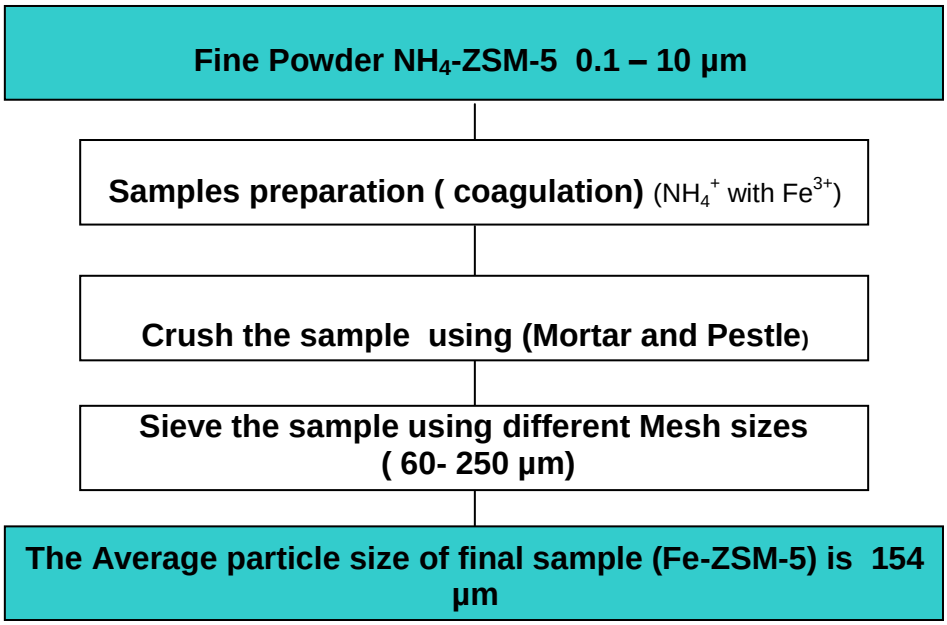


Figure 3.4 A Granulation process for ZSM-5 catalyst samples

3.3 Characterization of Fe/ZSM-5

NH_4ZSM5 and Fe/ZSM-5 zeolite catalysts were characterized to determine the elemental composition of theses materiales, the average particle size, and the BET surface area and pore size distribution using Atomic Absorption spectroscopy (AAS), Malvern mastersizer and Nitrogen adsorption (using N_2 at 77 K via Micromeritics) respectively. The determination of the active sites concentration were carried out using Temperature Programmed Desorption (TPD) using propylamine as reactive vapor.

3.3.1 Particle size characterisation

The stability, chemical reactivity and material strength of many materials are affected by the size and characteristics of the particles within them. Particle characterisation has different aspects e.g. particle size, particle shape, particle size distribution, particle concentration, particle surface characteristics and particle density. These factors affect the behavior of the particles and are considerably important for petroleum and chemical applications. The fact is that, many, if not all, effects of a change in size of particles and distribution can be related to particle shape change (Hawkins 1993). Particle size analysis equipment (i.e. Malvern) is of fundamental importance in particle technology, as it provides the values used in the calculations. Malvern Method is based on the Laser technique to determine the size distribution of particles. In this method *D* is the particle size, which is instead of *x* in some books, and *D(v,0.1)* is the particle diameter of the distribution of 10% of the sample. The other parameters are same as in Malvern table. Moreover, *D(v,0.5)* is the median size, *D(4,3)* is the mean diameter by volume or mass, *D(3,2)* is the mean diameter by surface area per volume that is called Sauter mean diameter.

Using Mastersizer analysis software of Malvern method and Excel worksheet, a table can be created for each material, which is used to predict the specific surface area of particles by using the Suter mean diameter $D(3,2)$.

$D = x$

$D(v,0.1) = x_{10}$,10%

$D(v,0.5) = x_{50}$,50%. Median size

$D(4,3)$ Mass = volume = the median diameter $\bar{x}_3 = \sum \bar{x}_i.m_i$

$D(3,2)$ Sauter mean diameter by surface area (median diameter)

$x_{sv} = \frac{6}{S_v}$ Sauter Mean Diameter (m)

$S_v = 6.\sum \frac{m_i}{x_i}$ = Specific Surface Area (1/m)

$$m_i(mass.fraction.in.grade) = \frac{particles.volume.under.size2}{\sum particles.volume} - \frac{particles.volume.under.size1}{\sum particles.volume}$$

From these equations and by using Mastersizer analysis data, tables for each material can be generated which in turn are used to predict the specific surface area of particles. The average particle size D[4,3] with sauter mean diameter (equivalent surface area mean diameter) D[3,2] of the ZSM-5 catalysts were measured based on area related to the light scattering properties of the particle (see appendix C.1). Particle size measurements were carried out using a Malvern mastersizer model (MMSS Particle Size Analyizer, includes flow sciences enclosure hood, Model FS5000-87) that has a range from 100 nm to 900 µm of particle size.

3.3.2 Elemental composition (AAS)

The determination of the bulk elemental composition of zeolites is important to verify the synthesis formulations, the bulk Si/Al ratio, the cations concentration, degree of ion exchange and the detection of contaminant elements such as impurities and poisons. A series of samples with different Si/Al ratios (30&80) and different iron contents (0.1&1 wt%) were digested overnight at room temperature using a concentrated mixture of HCl and HNO_3 (ratio 4:1vol%), during which the colour of solution changed to pink (Griepink *et al*., 1984). This process is called (aqua regia). The solution was

boiled gently under reflux for 2 h before dilution and analysis by Atomic Absorption Spectrophotometer (AAS VARIAN SPECTRA AA.200. Graphite furnace GTA 100, Autosampler, PC. YoC: 1996). The elemental compositions (Si, Al, Fe and Na contents) of the ZSM-5 catalysts were determined. AAS require that the sample must be introduced in liquid form.

3.3.3 Surface area measurement (Nitrogen physisorption)

The BET surface area measurement is key in understanding the behaviour of a material, as material reacts with its surroundings via its surface, a higher surface area material is more likely to react faster, dissolve faster and adsorb more gas than a similar material with a lower surface area. The SSA of the samples was calculated employing the BET method (mathematical model for the process of gas sorption). The Brunauer-Emmett-Teller (BET) method, based on multilayer N_2 adsoption, is inadequate to describe the adsorption process in medium-pore zeolites due to the restricted pore size using a Micrometrics ASAP 2010 analyzer. The surface area (m^2/g) and pore volume (m^2/g) of the samples were measured by nitrogen adsorption at 77K, in the range 0-1 bar, after degassing the samples in vacuum at 200°C for 16 hours using a surface area and pore size analyzer as shown in Figure 3.5. This physical adsorption of a gas over the entire exposed surface of a material and the filling of pores is called physisorption. The first stage in the interpretation of a nitrogen isotherm is the identification of the physisorption mechanism which is monolayer-multilayer adsorption, capillary condensation or micropore filling. Capillary condensation is involved as a secondary process in the filling of mesopores (pore width in the range 2 – 50 nm). The BET method cannot be used to provide a reliable evaluation of the surface area if the solid contains pores of molecular dimensions such as narrow micropores < 2 nm.



Figure 3.5 Surface area and pore size analyzer.

3.3.4 Chemisorption method

Determination of the Fe(II) sites in the six types of the catalysts was performed by Temperature Programmed Desorption (TPD), type number three (reactive vapors) as discussed in Chapter 2 using propylamine. Figure 3.6 shows the apparatus for vapour generation. The apparatus was equipped with a thermocouple, reflux condenser, and flask for the probe liquid. Three steps were followed for the determination of the Fe(II) sites method; A) the samples were degassed at 100 °C for 1 h using Helium followed by heating using a temperature ramp programmed to 500 °C at a ramp rate of 10 °C/min. The sample was held at that temperature for 2 h to activate the sample. Finally the sample was cooled to 200°C in a stream of helium; B) in this step the sample was saturated with propylamine vapour using at least ten injections of vapour into the samples; C) TPD was performed by ramping the sample temperature at 10°C/min to 500°C. The gas exiting the apparatus was passed through a mass spectrometer (MS) to identify and quantify the desorbed species and hence to evaluate the density of acid sites. Line diagram of the chemisorption method together with a schematic

representation of the apparatus are shown in Figure 3.7 and Figure 3.8 respectively.

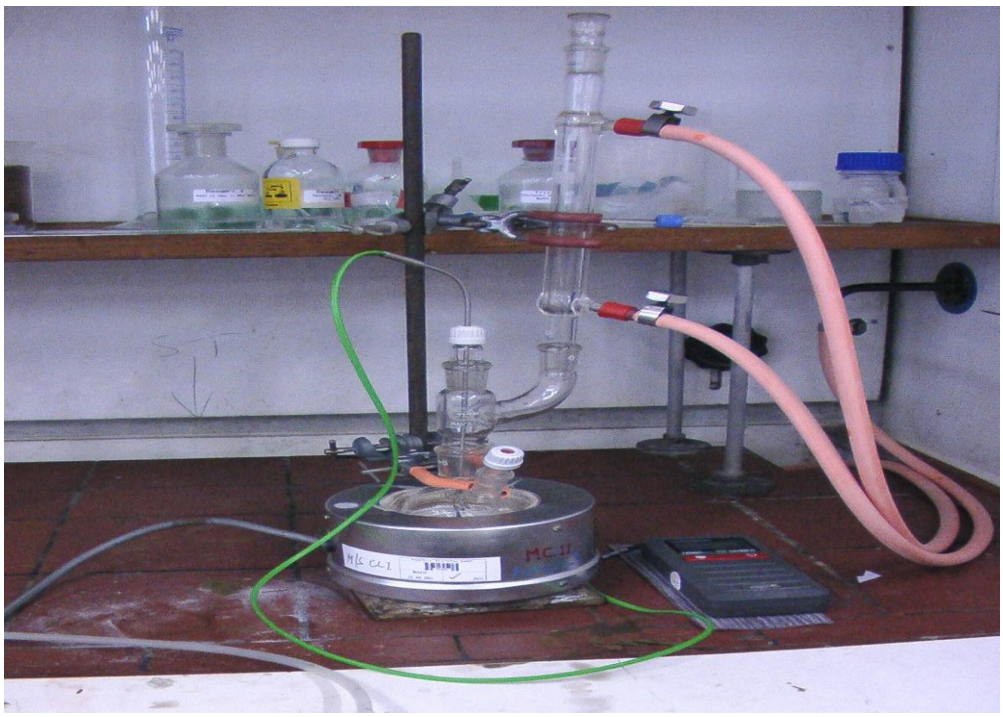


Figure 3.6 Vapor generation apparatus.

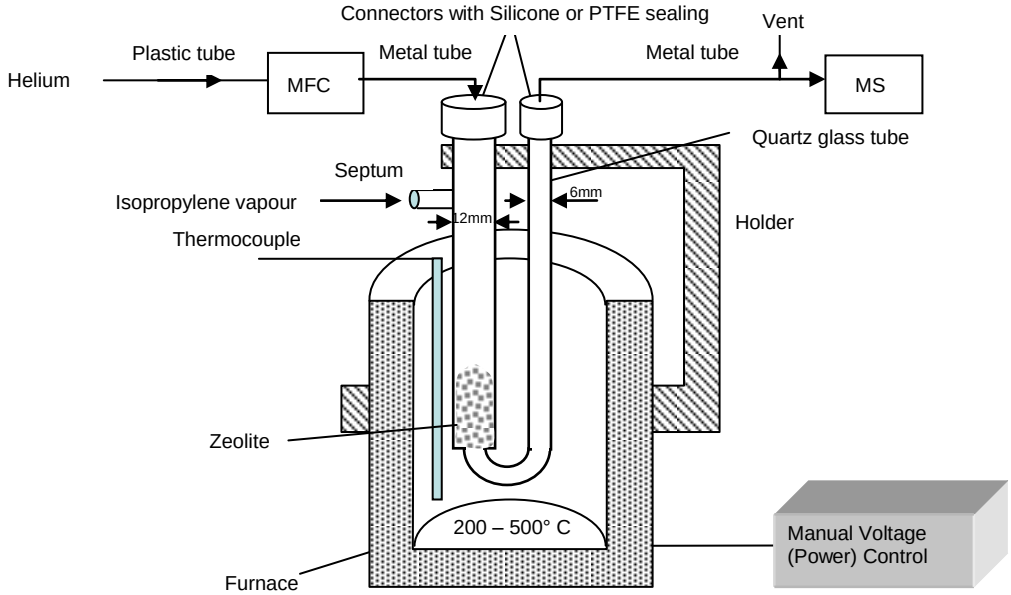


Figure 3.7 A line diagram of the chemisorption method to find the number of active sites.



Figure 3.8 Photograph of the chemisorption apparatus to quantify acidic sites in the catalyst.

3.4 Experimental setup to evaluate benzene reaction with nitrous oxide using zeolite catalysts.

Catalyst performance was evaluated using an experimental packed bed reactor (PBR). For each experiment, 200 mg of 0.1–0.2 mm diameter catalyst particles were packed into a stainless steel reactor with an inner tube diameter of 2 mm. Reaction conditions and their effects on conversion, productivity, and selectivity were studied. The setup used for the kinetic study consisted of a feed section, an analytical section, and a small-scale fixed bed reactor. Since the catalyst particles used were (60 -250 µm), no bypassing near the wall must be taken into account $\frac{d_R}{d_P} =$ ~ (10 - 40) (Reitzmann *et al.,* 2002).

The feed gas composition was varied by varying the flow rates of helium and N_2O regulated by mass flow controllers (MFC) (AALBORG, 0 – 200 ml/min). The benzene feed rate was influenced by the flow of helium gas through the benzene bubbler equilibrated at 50°C. The reactor feed and exit gas mixtures were sampled and analyzed on-line using a GC (Gas Chromatograph). The gases and vapours were separated using a DB-1701 capillary column (J&W Scientific). The effect of reaction temperature at 350°C and 450°C was studied. The feed gas contained 7 mol% N_2O and the rest was a mixture of benzene/helium. The total flow rate exiting the reactor was 60 ml/min. Experiments were performed using Fe/ZSM-5 (0.1 and 1 % w/w Fe) with a feed gas containing 10 ml/min N_2O, 50 ml/min Benzene/He at atmospheric pressure. A matrix of experiments was followed to evaluate the effect of reaction temperatures (350 and 450°C), iron content (0.1 and 1 % w/w Fe) and different Si/Al (30 and 80) ratio on phenol productivity, selectivity and benzene conversion on the catalysts. The low concentrations of benzene and nitrous oxide were used and also the values in the matrix of experiments were selected in order to minimize the possible effect of consecutive reactions of further hydroxylation of phenol intermediate. Samples were collected every hour during the 20 h of reactor operation. The

catalysts were tested using a feed containing an excess of nitrous oxide in comparison with benzene (~1 mol% benzene compared with 7 mol% N_2O). The catalytic tests were made using a feed containing low concentrations of benzene and nitrous oxide in order to minimize the possible effect of consecutive reactions of phenol hydroxylation. The reaction temperature of 450°C was chosen as a reference temperature, because the majority of the data available in the literature is at this reaction temperature. In addition, this reaction temperature represents a good compromise between the activity of the catalyst and the deactivation rate. The reactor was placed in a furnace (purchased from Elite Thermal Systems Limited, model (TSH12/50/300-2416 CG) with a maximum temperature of 1100°C and minimum ramp rate of 0.1°C/min. The oven temperature was calibrated (details in Appendix B.1). All the pipe work between the ovens and GC were insulated with quartz wool. All fittings for this system were bought from Swagelok. Line diagram of the complete fixed bed reactor system together with a schematic representation of the apparatus are shown in Figure 3.9 and Figure 3.10 respectively. For more details about the startup and shutdown procedures for the experimental rig design, and also about the previous rig designs, of line diagrams [1 - 3] refer to Appendix B.2.

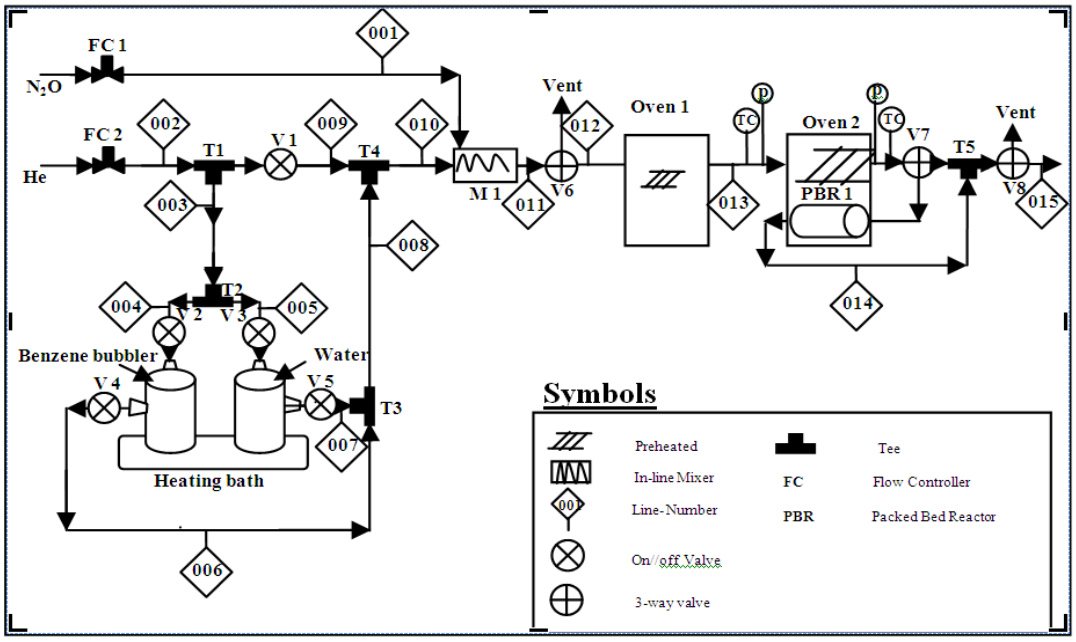


Figure 3.9 A line diagram of the fixed bed reactor system.

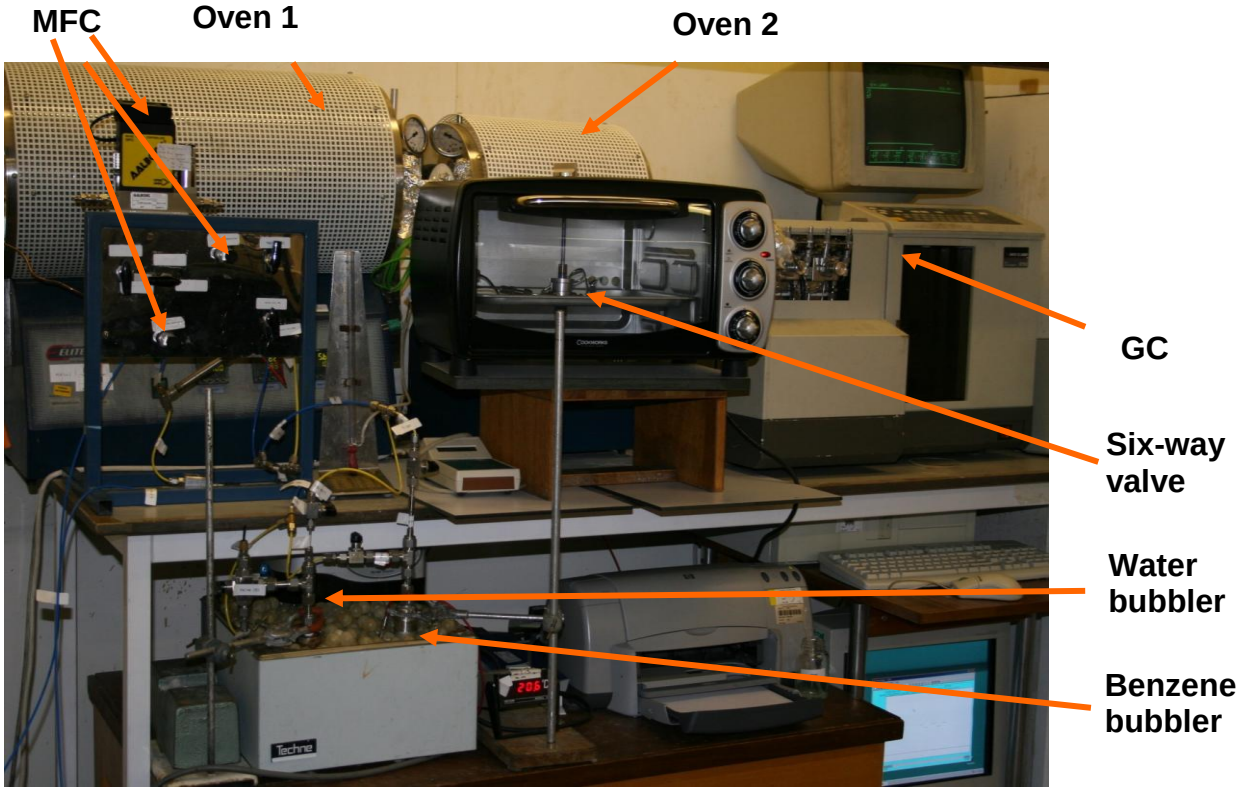


Figure 3.10 Digital photo of the fixed bed-reactor system

3.5 Regeneration of coked catalysts

Catalyst deactivation due to coke formation poses the problem of catalytic activity restoration (see Chapter 2). The catalyst samples with coke content was taken after 20 h on stream. After 20 h on stream the reaction mixture was replaced with helium, the reactor temperature was raised up to 450°C, and the catalyst was purged for 30 min. The carbon-containing deposits remaining at the surface under these conditions were considered to be carbon. 0.1%FeZ80 catalyst was regenerated by two methods: using oxygen diluted with helium (oxidation) followed by hydrogen diluted with helium (reduction). Regeneration was done in the same flow reactor where the reaction was performed, using 0.2 g of coked catalyst and total flow rate 60 ml/min. Reaction conditions were 450°C and oxygen concentration 1.7 % in He. The sample then was heated to 600 °C, after that the system was cooling down to 300°C for hydrogenation (temperature programmed reduction), and to 450°C for reaction at a heating rate of 10 °C/min.

3.6 Standard preparation and calibration method using (GC)

The GC was calibrated in order to determine the compositions of the reactant feed and the product effluents. The mass flow controllers (MFCs) were also calibrated. The analytical method of the GC were: Injection temperature (300°C), column temperature (250°C), detector temperature (300°C) and helium flow rate (30 ml/min). The gas Chromatography (GC) equipped with DB-1701 (J&W) column was calibrated using 1µL of benzene, phenol, catechol, hydroquinone and p-benzoquinone – ethanol solutions. Figure 3.11 shows an example of chromatogram of all analyzed species (see Appendix B3 for more chromatograms). The retention times of benzene, phenol, catechol, hydroquinone and p-benzoquinone components were 3.2, 8.3, 11, 12 and 7.1 mints respectively. The range of standards used for benzene were (0.2 – 15 wt %). The calibration data of benzene was plotted as shown in (Figures 3.12 & 3.13) using as Perkin Elmer, 8700-GC. Figures (3.14 to 3.17) show that the calibration data of different range of standards for phenol (1–10 wt%), catechol (0.1–1 wt%), hydroquinone (0.1–1 wt%) and p-benzoquinone (0.1–1.5 wt%) In ethanol as the solvent. The experiments were repeated six to eight times for each concentration of each solution.

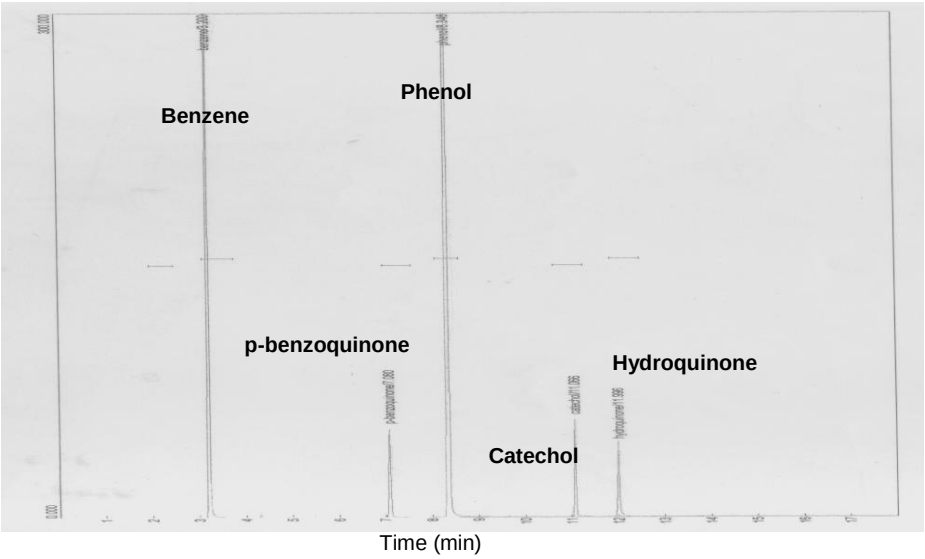


Figure 3.11 A sample chromatogram of all analyzed species.

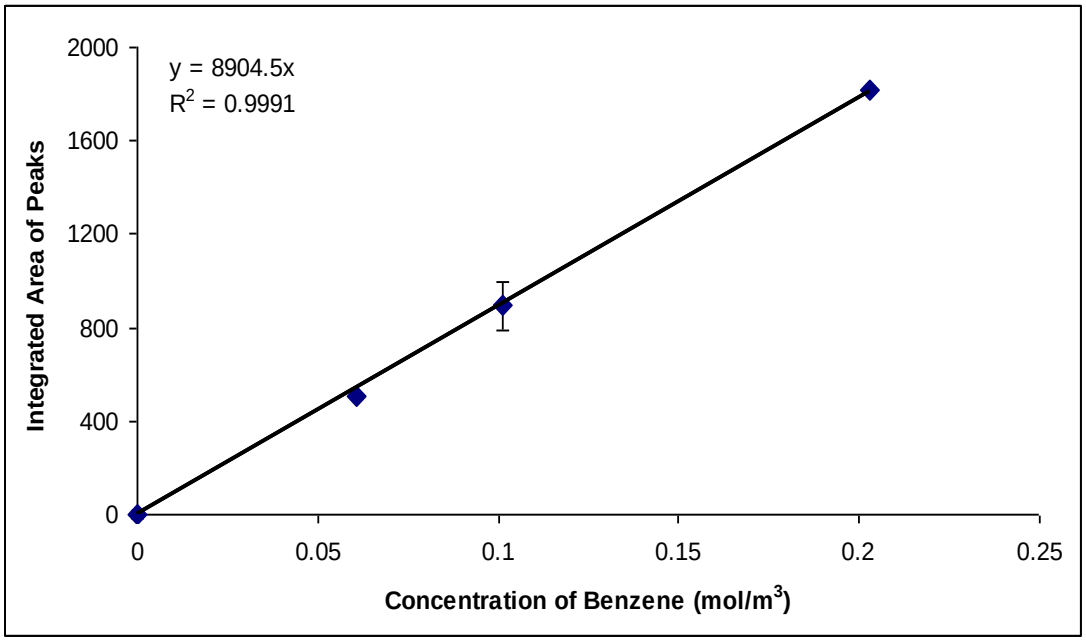


Figure 3.12 Calibration plot of benzene (0.6 – 2 wt%) (GC)

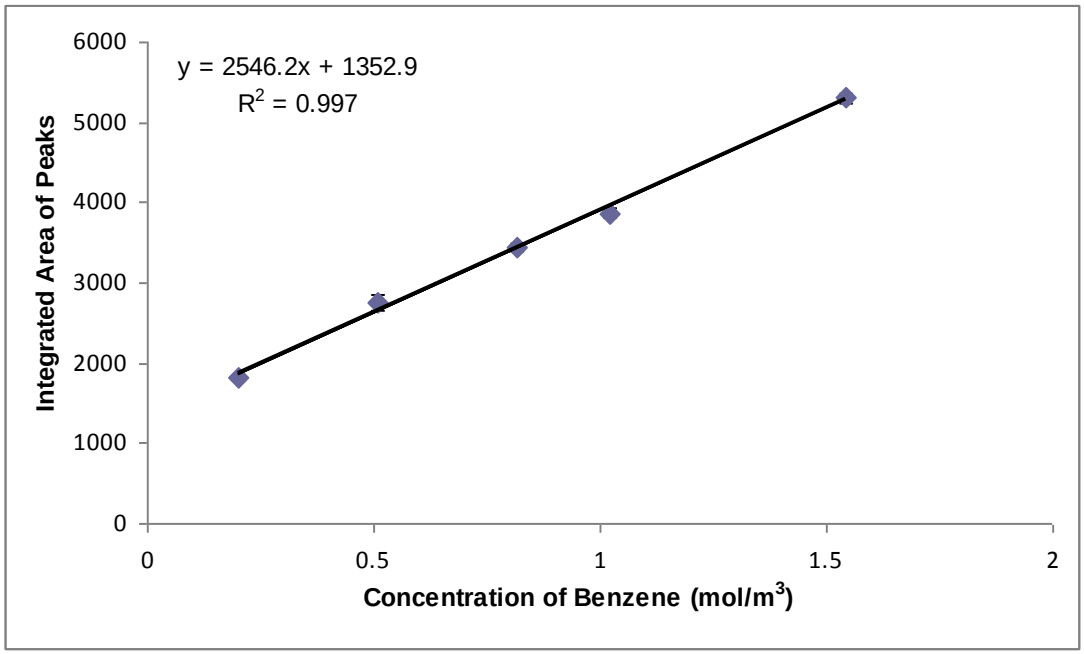


Figure 3.13 Calibration plot of benzene (2 – 15 wt%) (GC)

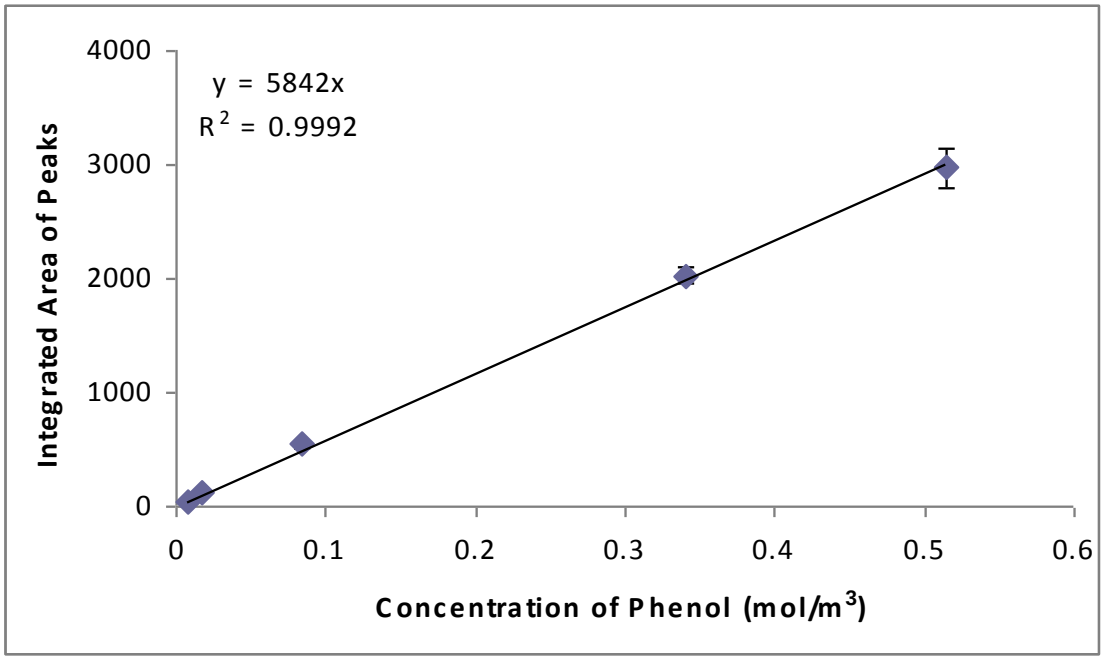


Figure 3.14 Calibration plot of phenol (1 – 10 wt%) (GC)

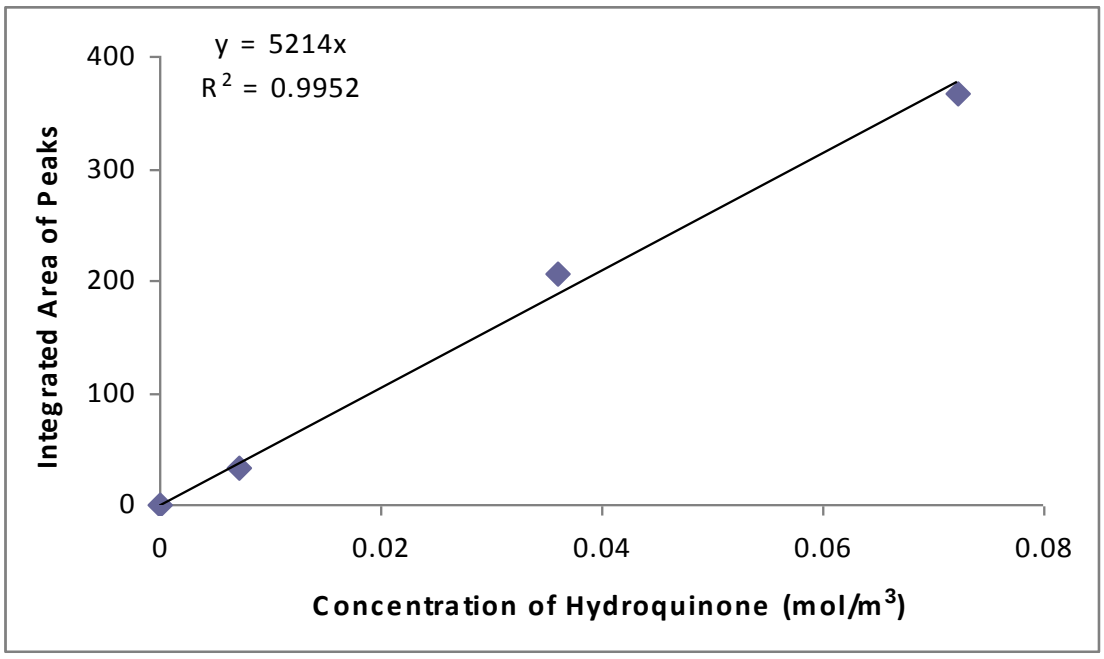


Figure 3.15 Calibration plot of hydroquinone (0.1 – 1 wt%) (GC)

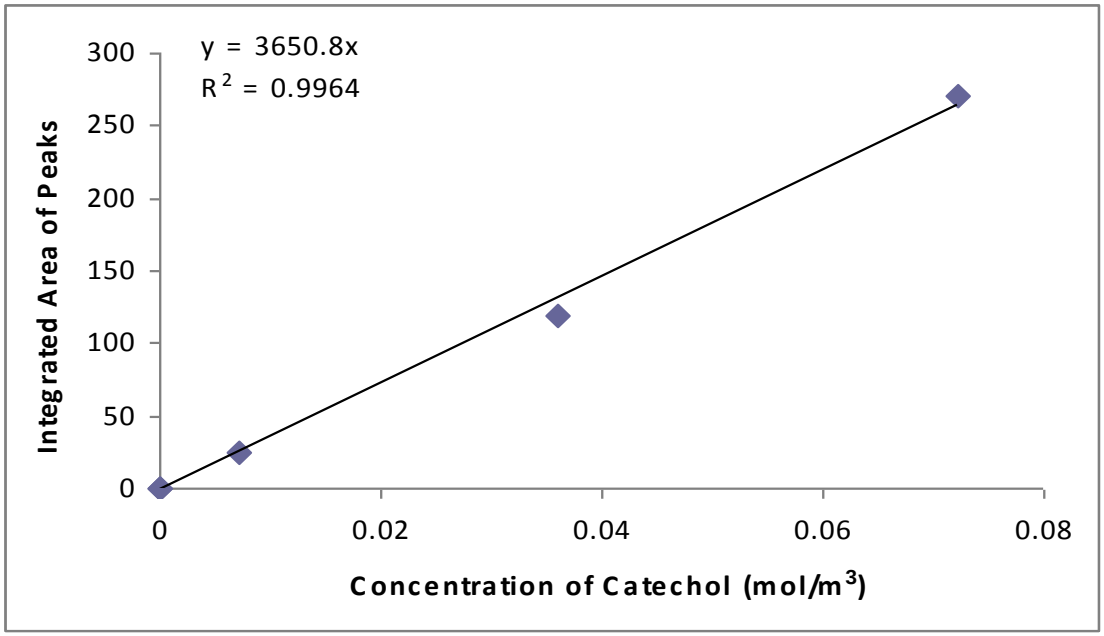


Figure 3.16 Calibration plot of catechol (0.1 – 1 wt%) (GC)

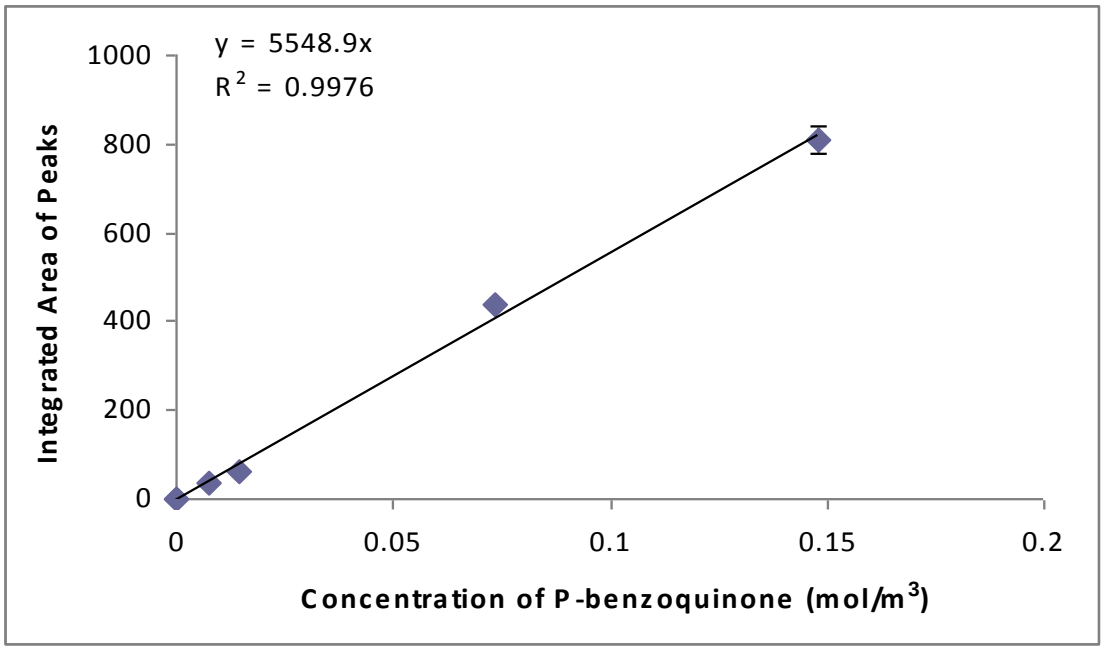


Figure 3.17 Calibration plot of p-benzoquinone (0.1 – 1.5 wt%) (GC)

MFCs give a reading which indicates how much of the valve inside these controllers is opened and hence how much gas is flowing through this opening. Each gas was allowed to enter to the specified MFC from its source which usually was a gas cylinder. The time measurements were repeated three times at each reading of the MFC. Figures 3.18 & 3.19 show the calibration data for MFCs for helium and nitrous oxide respectively. For more details about the standard preparation with calibration and MFCs refer to Appendix B.3.

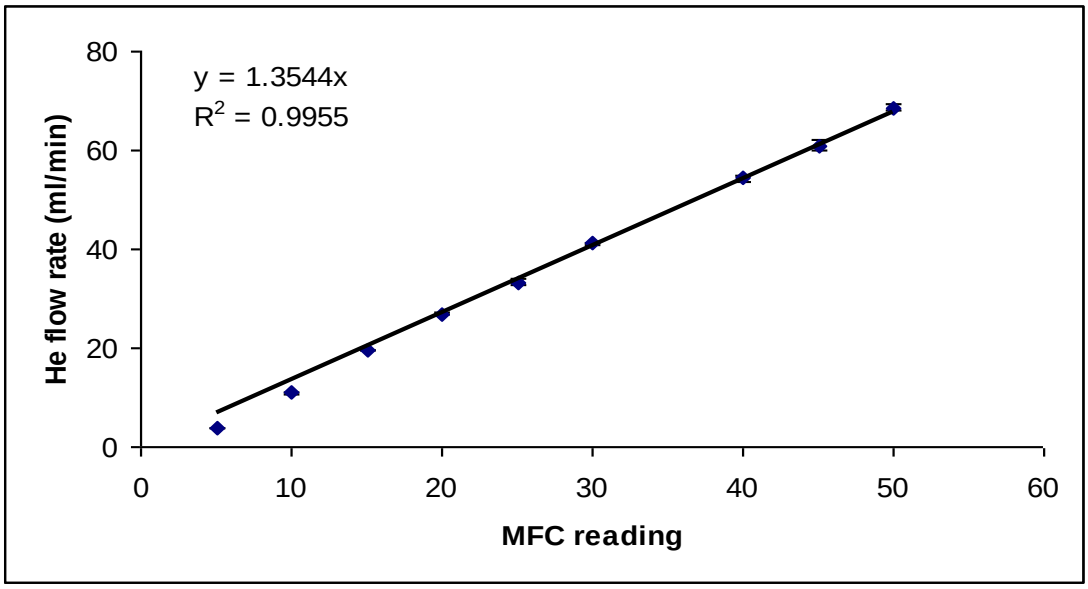


Figure 3.18 Calibration plot of He (MFC)

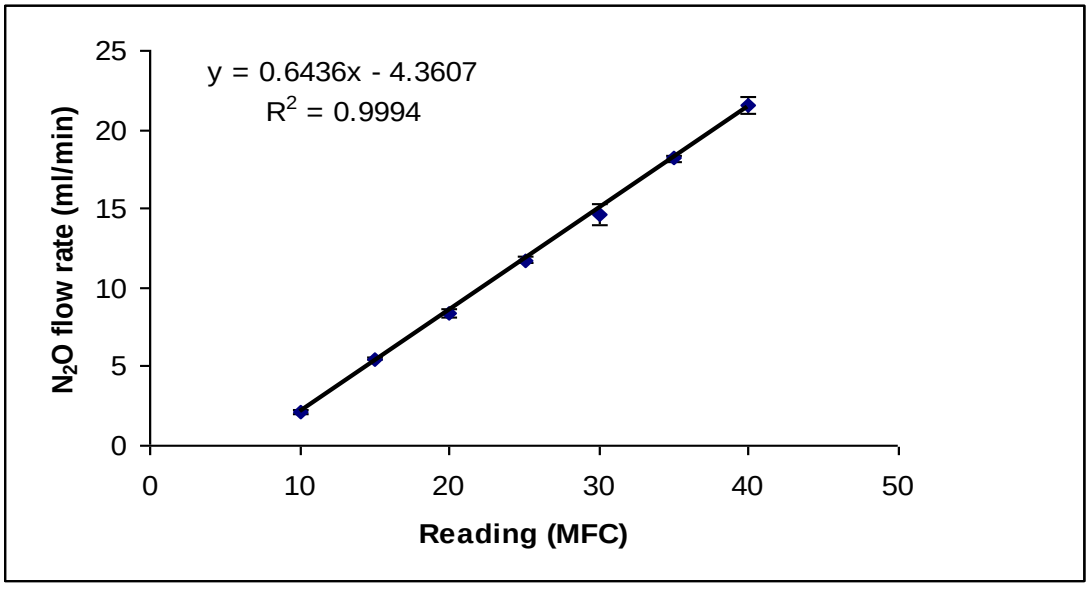


Figure 3.19 Calibration plot of N_2O (MFC)

4 Catalysts Characterisation Results and Discussion

4.1 Elemental analysis using AAS

Fe/ZSM-5 of different Si/Al ratio may possibly have similar Fe content. Dedecek *et al.,* (2001) reported that the Al distribution in silicon – rich zeolite depends on the chemical composition and condition of the synthesis. In this work, samples with different Si/Al ratios and different iron content were used. The elemental composition (Si, Al, Fe and Na content) of the ZSM-5 catalysts before and after ion exchange preparation was determined by atomic absorption spectroscopy (AAS) (see Chapter 3) as shown in Table 4.1.

Table 4.1 Catalyst elemental composition.

Sample (ZSM-5)	**Na (wt%)**	**Fe (wt%)**	**Al (wt%)**	**Si (wt%)**	**Al/Fe mol/mol**	**Si/Fe mol/mol**	**Fe/Al mol/mol**
Si/Al 30	0.06	0.02	1.31	34	108	1179	0.01
Si/Al 80	0.05	0.09	1.11	53	26	2703	0.04
FeZ30 0.1%	0.04	0.16	0.74	27	10	341	0.10
FeZ80 0.1%	0.04	0.15	0.75	46	10	615	0.10
FeZ30 1%	0.03	1.15	0.67	26	1	45	0.83
FeZ80 1%	0.03	0.85	0.69	47	1	110	0.60

The results show that the Na contents for both Si/Al ratio (30 & 80) are almost the same ~ 0.06 in the NH_4-ZSM-5 catalysts before ion exchange. The Na and Al contents decreased with Fe increasing and were not affected by the Si/Al ratio. The Si/Al ratio 80 sample had more iron impurity (0.09) than Si/Al ratio 30 (0.02). The ratio of Al/Fe decreased with an increase of the iron content and it was not found to be related to the Si/Al ratio. This means that the iron may have replaced the Al. Table 4.1 shows comparatively similar results to literature. Prikhodko *et al.,* (2006) reported that the elemental composition for FeZSM-5 prepared by LIE using 0.53 wt% Fe with 40 Si/Al ratio was 130 Si/Fe and 0.26 Fe/Al. The Fe content in the final catalysts (Table 4.1) showed a good accuracy of the catalysts prepared by LIE, thus confirming the efficiency of the preparation procedure in inserting the desired amount of Fe into the zeolite framework.

4.2 Particle size analysis using malvern

Figures 4.1 to 4.4 show the fraction by mass and the cumulative curve for the NH_4-ZSM-5 catalyst supplied by Zeolyst International USA Company. The particle size distribution was in the range 0.1 µm – 10 µm. The mean particle size by mass for the sample before preparation was 2.9 µm. The specific surface area per unit mass was 12.6 m^2/g and sauter mean diameter was 0.75 µm using the area related to the light scattering properties of the particle (Malvern equipment).

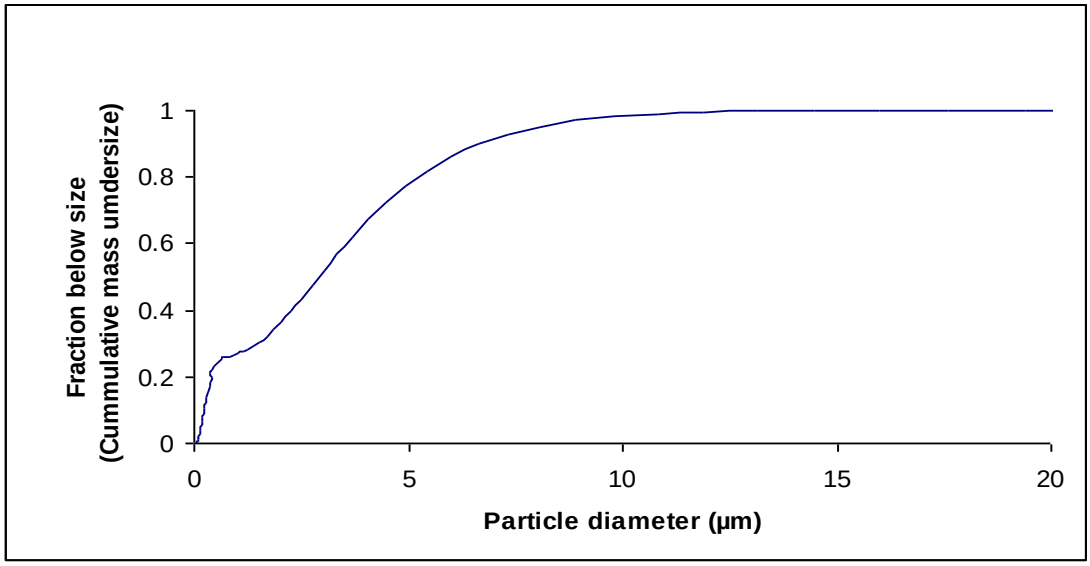


Figure 4.1 Cummulative curve of particle size distribution for (NH4ZSM-5 30) – before preparation.

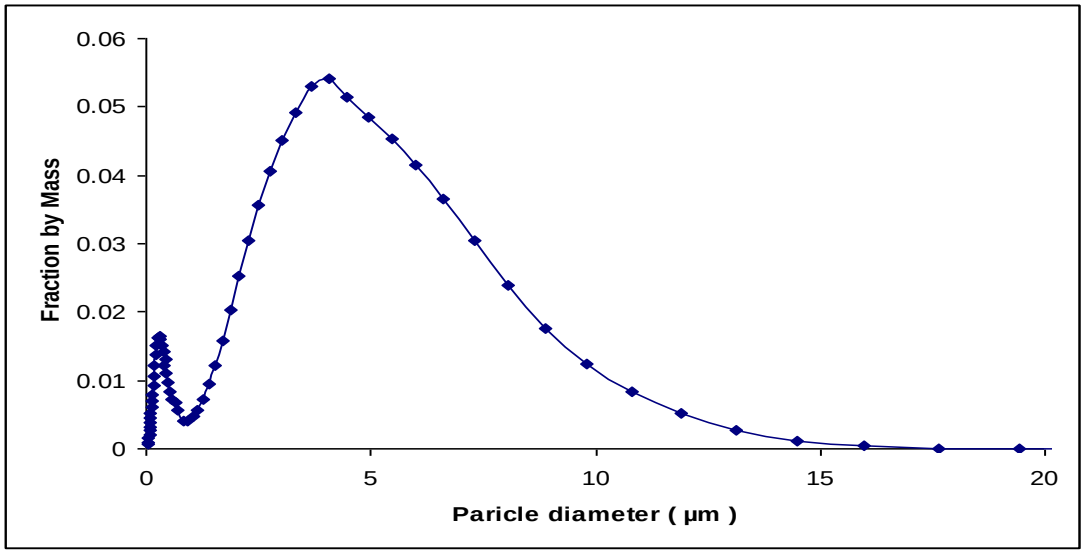


Figure 4.2 The particle size analysis for (NH4ZSM-5 30) – before preparation.

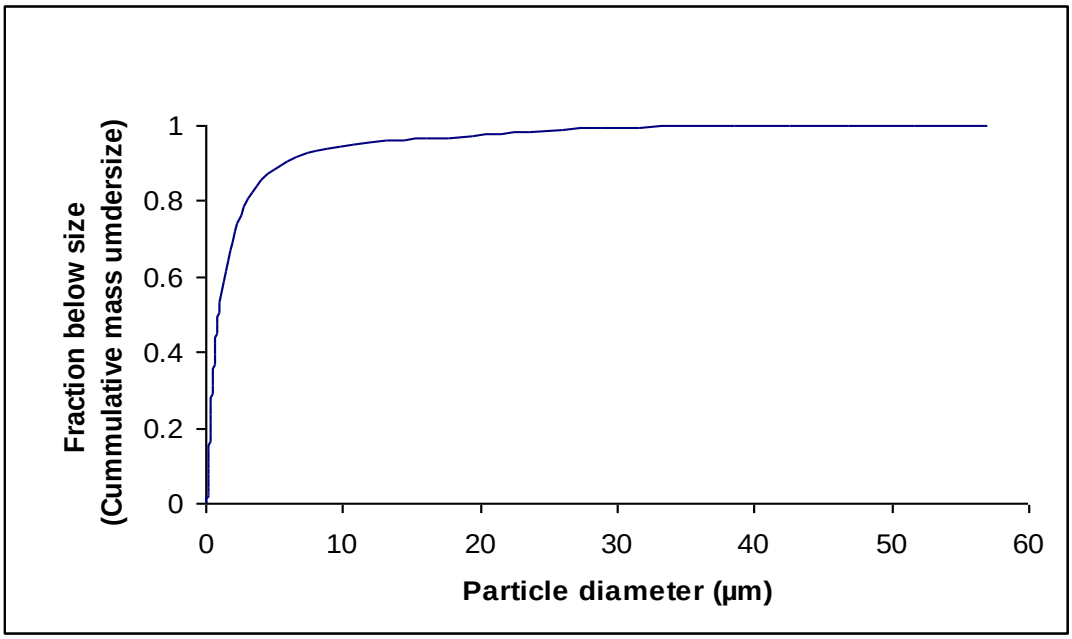


Figure 4.3 Cummulative curve of particle size distribution for (NH4ZSM-5 80) – before preparation.

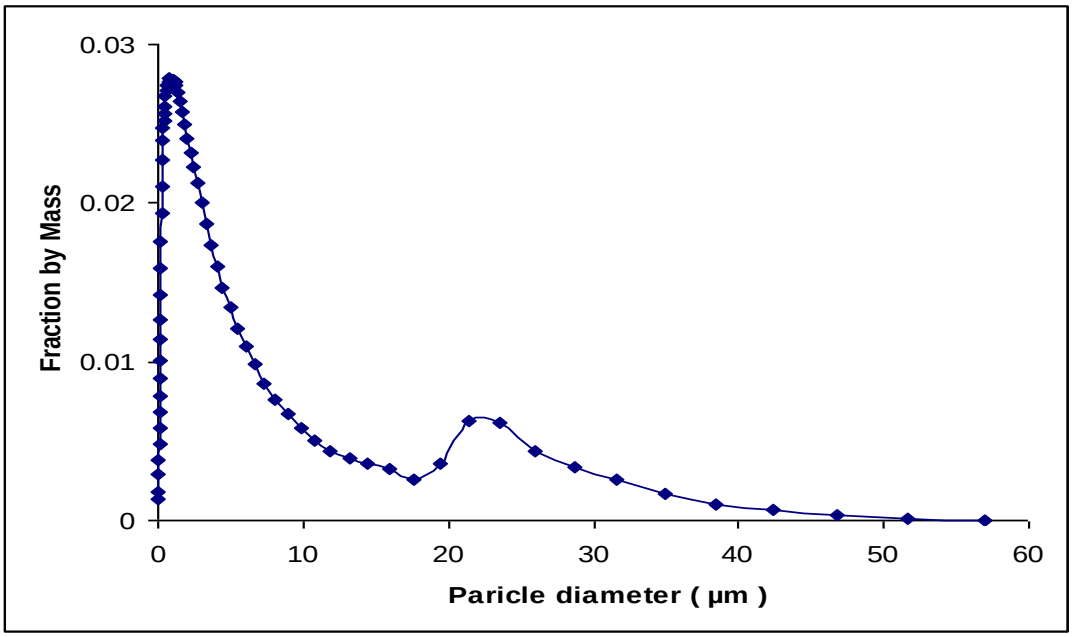


Figure 4.4 The particle size analysis for (NH4ZSM-5 80) – before preparation.

ZSM-5 zeolites catalysts (MFI) with various Fe and Al contents were prepared by liquid ion exchange. Figures 4.5 and 4.12 show the fraction by mass and the cumulation profile for the sample after a preparation (Fe/ZSM-5). The mean particles size by mass for the all samples after preparation were 145 - 167 µm. The specific surface area per unit mass was 0.22 m^2/g and sauter mean diameter was 33 µm. For more details about Malvern Mastersizer table with calculations refer to Appendix C.1.

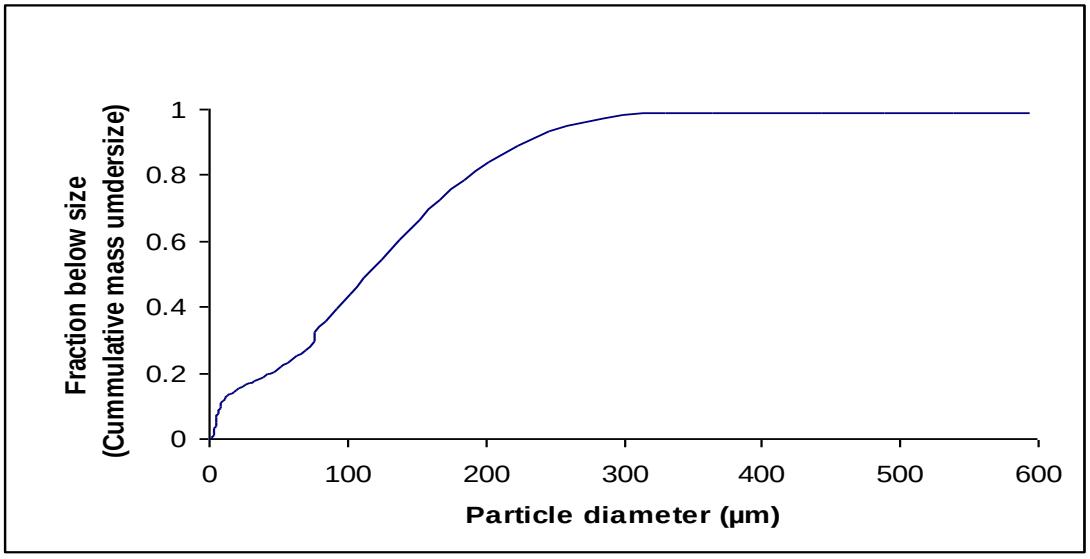


Figure 4.5 Cummulative curve of particle size distribution for (FeZ30 0.1%) – post preparation.

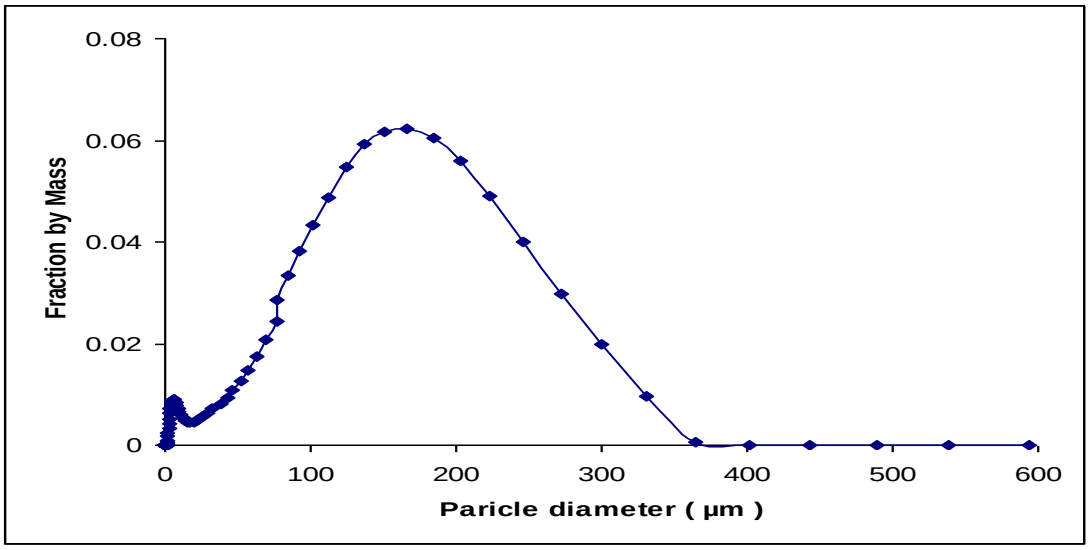


Figure 4.6 The particle size analysis for (FeZ30 0.1%) –post preparation.

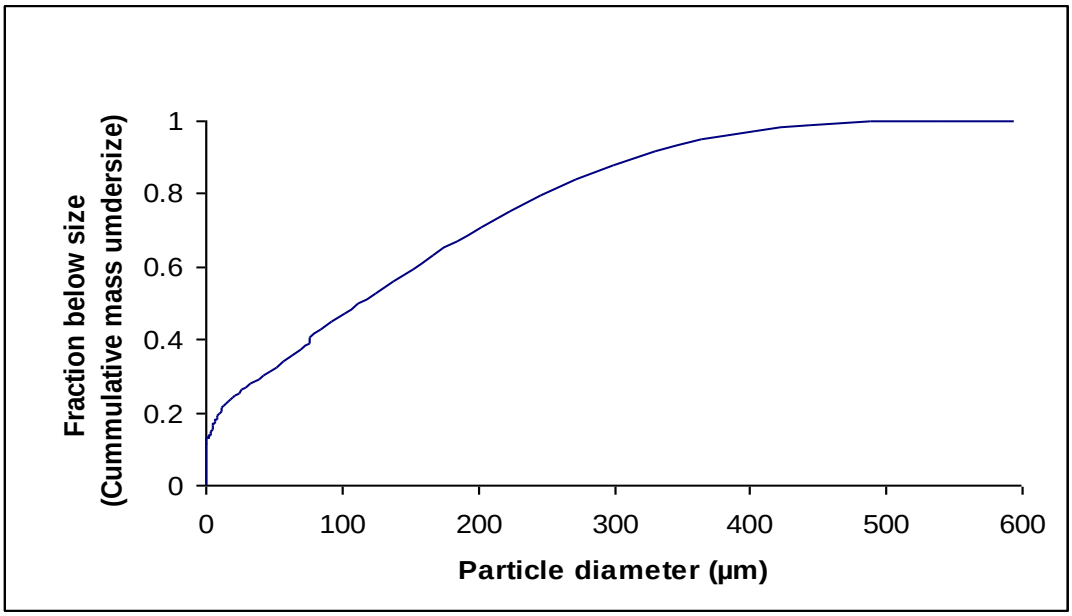


Figure 4.7 Cummulative curve of particle size distribution for (FeZ80 0.1%) – post preparation.

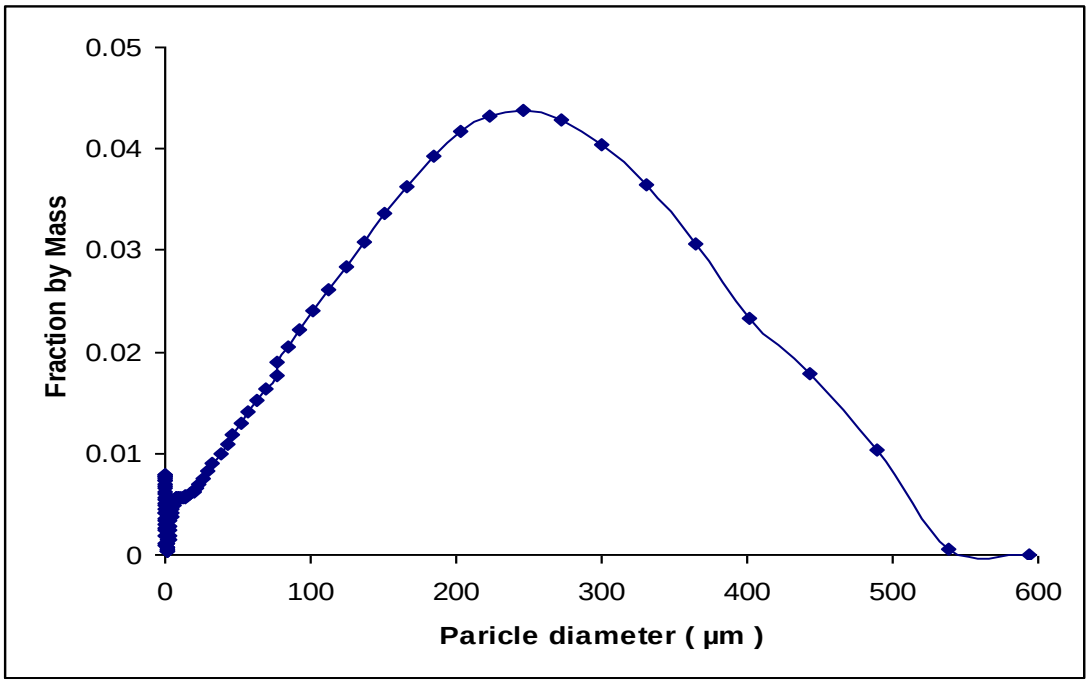


Figure 4.8 The particle size analysis for (FeZ80 0.1%) –post preparation.

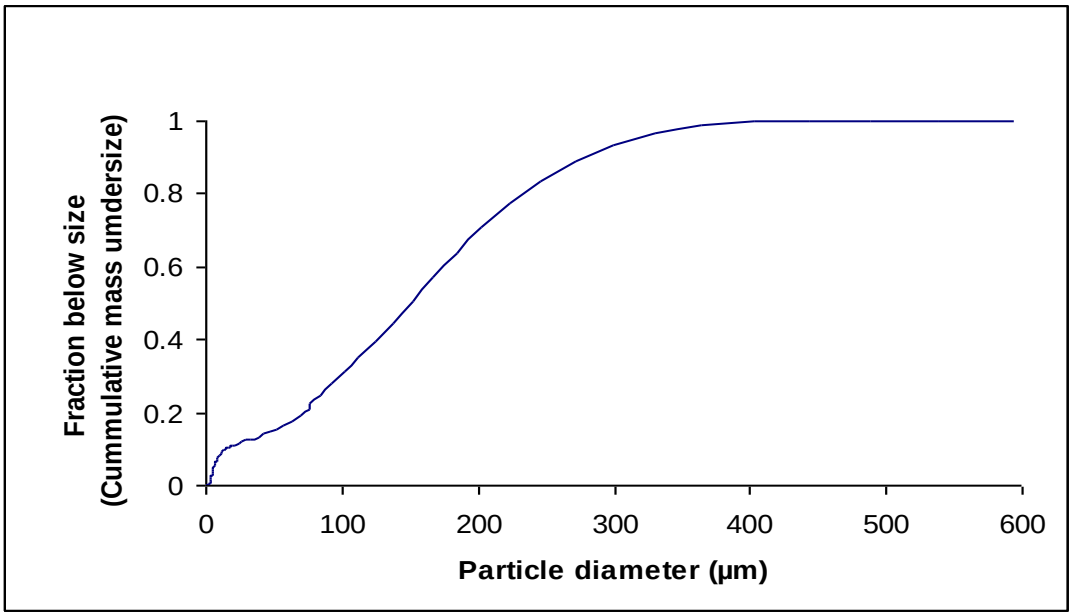


Figure 4.9 Cummulative curve of particle size distribution for (FeZ30 1%) – post preparation.

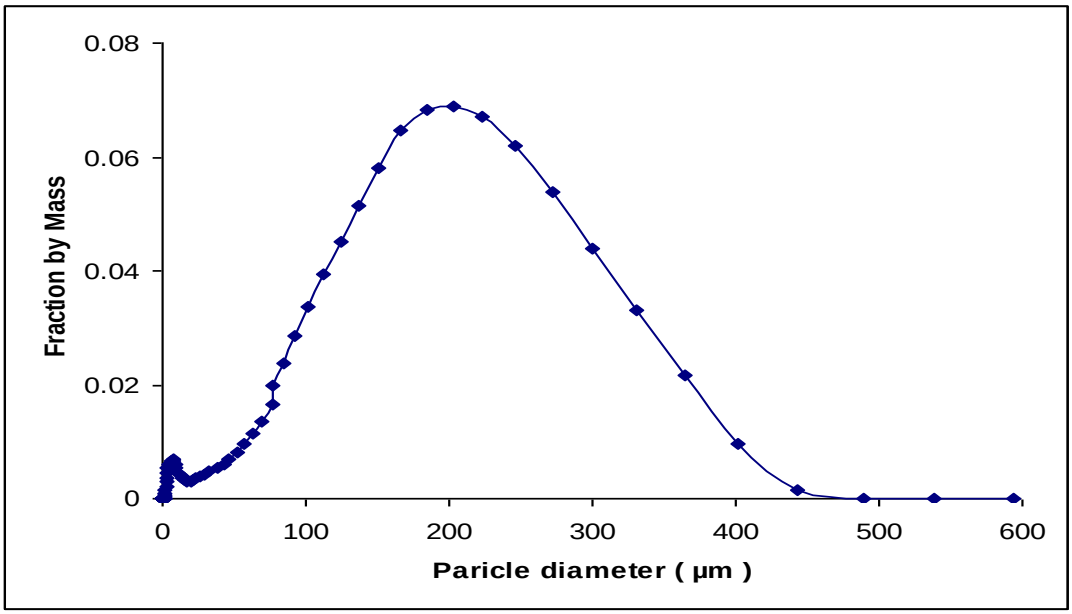


Figure 4.10 The particle size analysis for (FeZ30 1%) –post preparation.

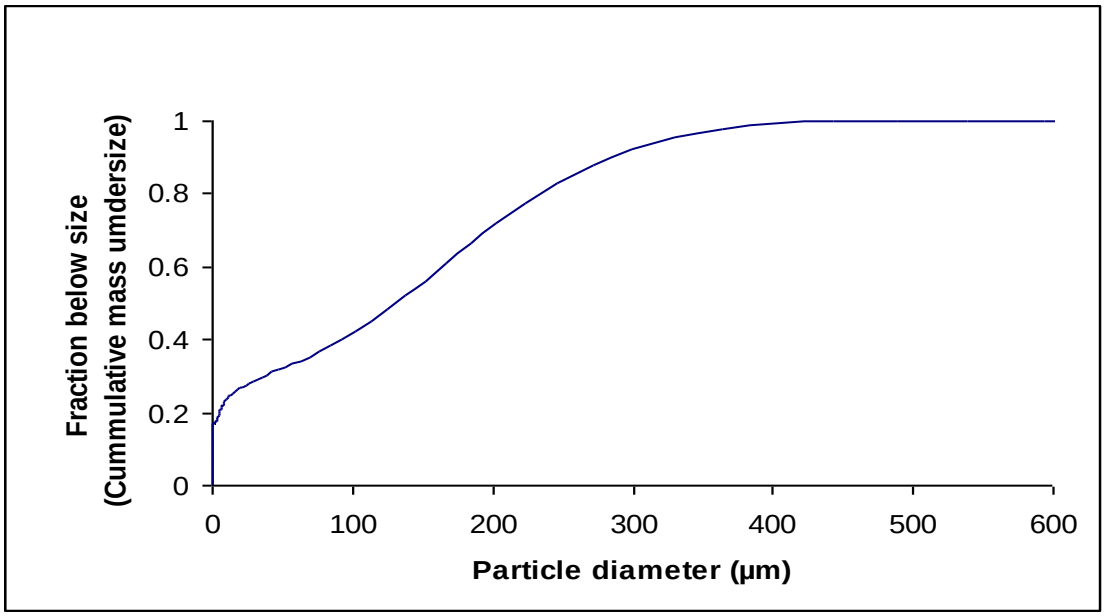


Figure 4.11 Cummulative curve of particle size distribution for (FeZ801%) – post preparation.

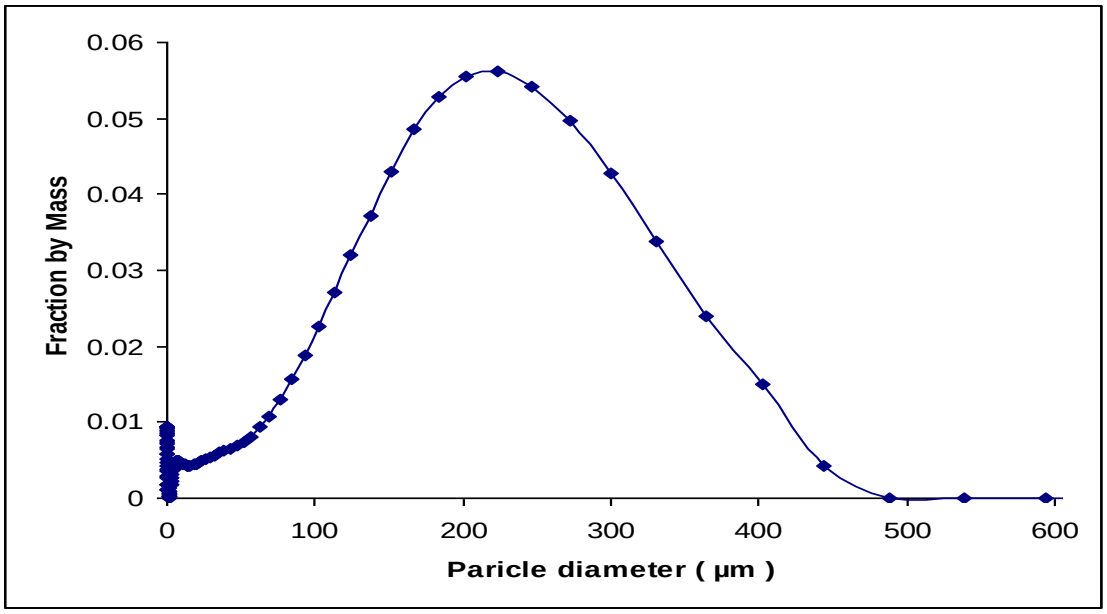


Figure 4.12 The particle size analysis for (FeZ80 1%) –post preparation.

Particle size characterisation is very important to select the catalyst for use in a mini fixed-bed reactor system and to increase the selectivity. As a conclusion, clearly all the particles for ZSM-5 catalyst samples after preparation (Fe/ZSM-5) are less than 300µm, hence, 1.00 as a fraction, are less than this size. The Malvern results consistently present a uni-model drop size distribution. The (Sauter mean diameter) equivalent spherical diameter per surface area per unite volume (or mass) is the most appropriate for the reaction engineering. The small spherical particles (154 µm) of Fe/ZSM-5 catalyst are packed in the packed bed reactor. The chemical reaction takes place on the surface of the catalyst. The reaction rate is based on the amount of the solid catalyst rather than the volume of the reactor. The particle size may influences on the reaction kinetics.

4.3 Surface area and pore structure using (BET)

The internal surface area and pore structure of the catalyst samples were investigated by nitrogen adsorption. The results are summarised in Table 4.2 for ZSM-5 catalysts before and after preparation using LIE. Incorporation of the Fe species into the micropore space is reflected by slightly lower of the surface area and micropore volume or probably related to some degree of pore blocking.

Table 4.2.Total pore volumes, area, and pore sizes of the various zeolite catalysts.

Sample (ZSM-5)	Total BET area (m^2/g)	Total pore volume (cm^3/g)	Mesopore size (Å)
Si/Al 30	338	0.23	22
Si/Al 80	409	0.24	35
FeZ30 0.1%	336	0.22	21
FeZ80 0.1%	404	0.23	34
FeZ30 1%	334	0.22	19
FeZ80 1%	401	0.22	32

Figures 4.13 and 4.14 show the pore size for the NH_4-ZSM-5 (Si/Al ratio, 30 & 80) catalysts. Figure 4.15 shows that comparison between ZSM-5 (Si/Al ratio, 30) catalyst before and after preparation.

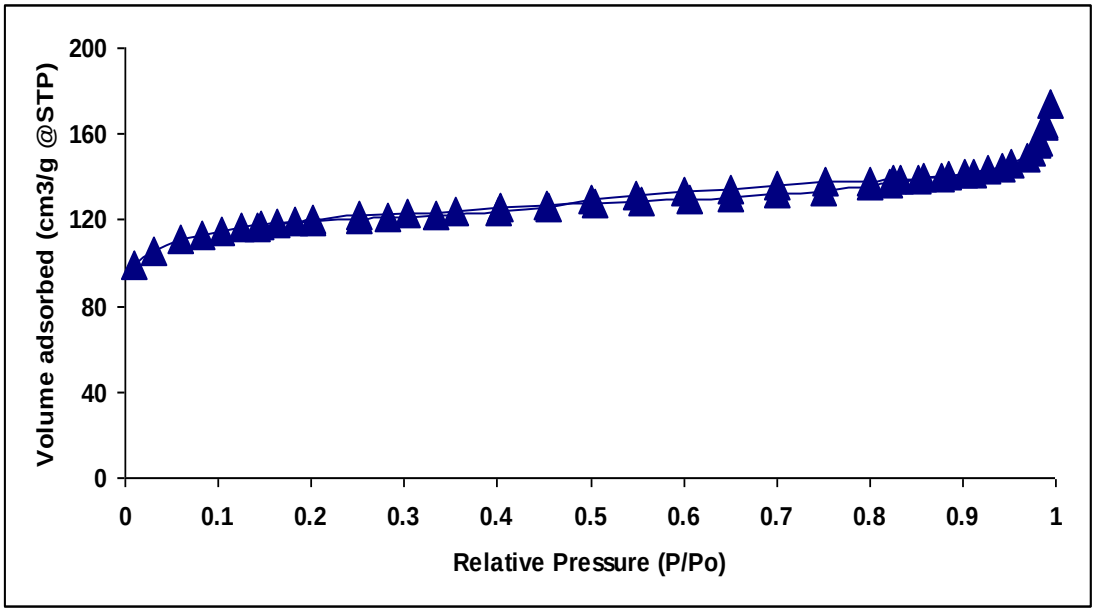


Figure 4.13 Pore size characterisation for (NH_4Z30)

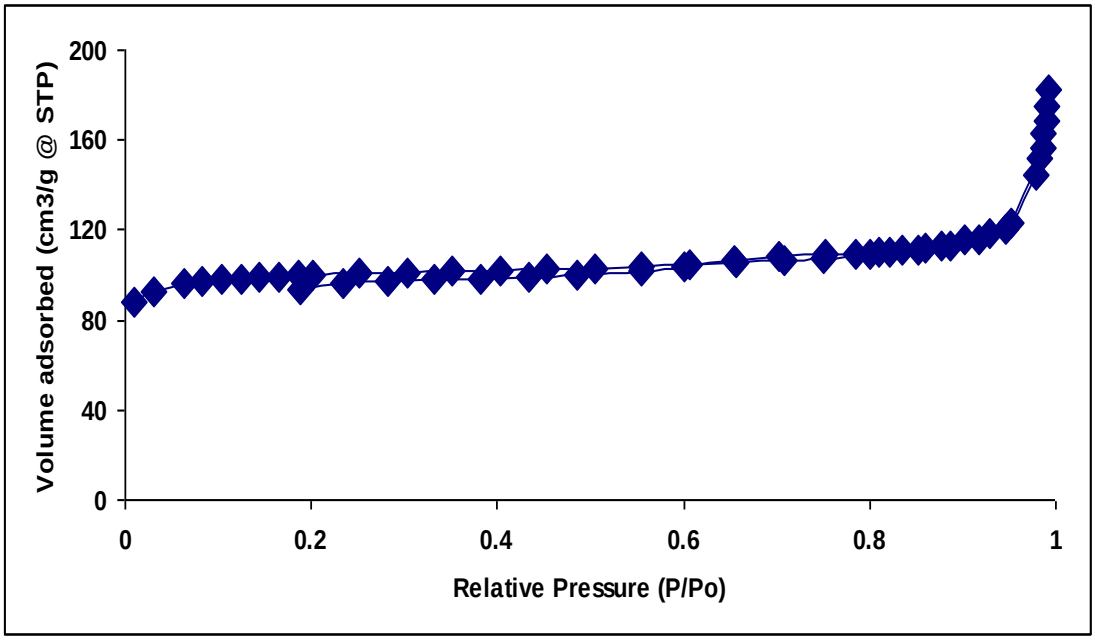


Figure 4.14 Pore size characterisation for (NH_4Z80)

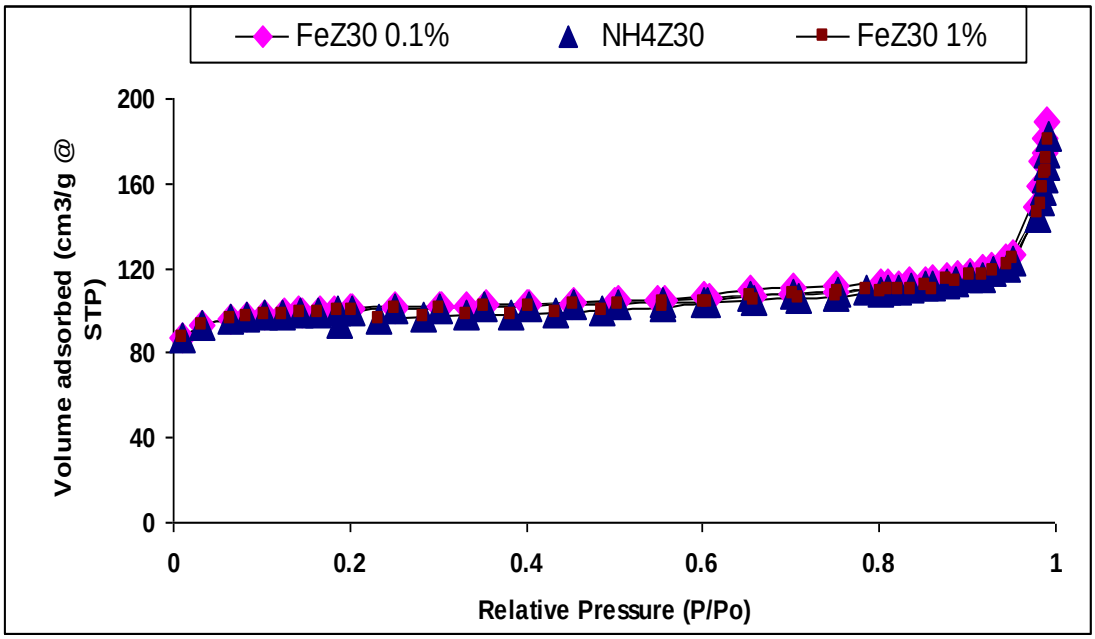


Figure 4.15 Pore size characterization for Z30 before and after preparation

Figure 4.16 shows that the comparison between ZSM-5 (Si/Al ratio, 30) catalyst before and after Preparation and Figure 4.17 shows comparison between ZSM-5 (Si/Al ratio, 30&80) catalyst before and after Preparation using N_2 adsorption isotherm . For more details see Appendix C.2.

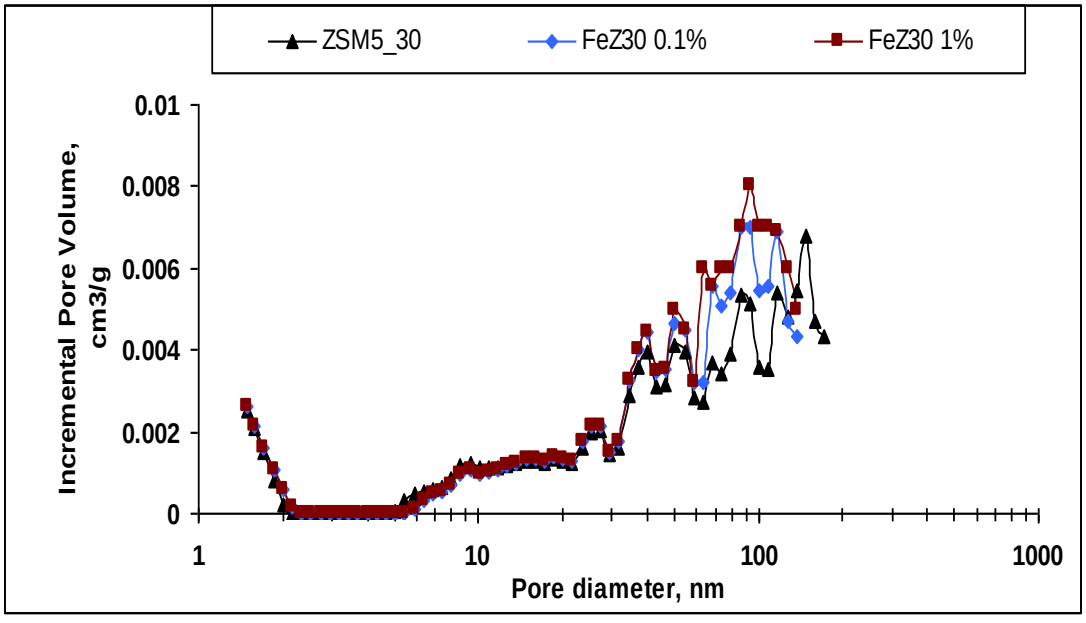


Figure 4.16 Nitrogen adsorption isotherm for Z30 before and after preparation

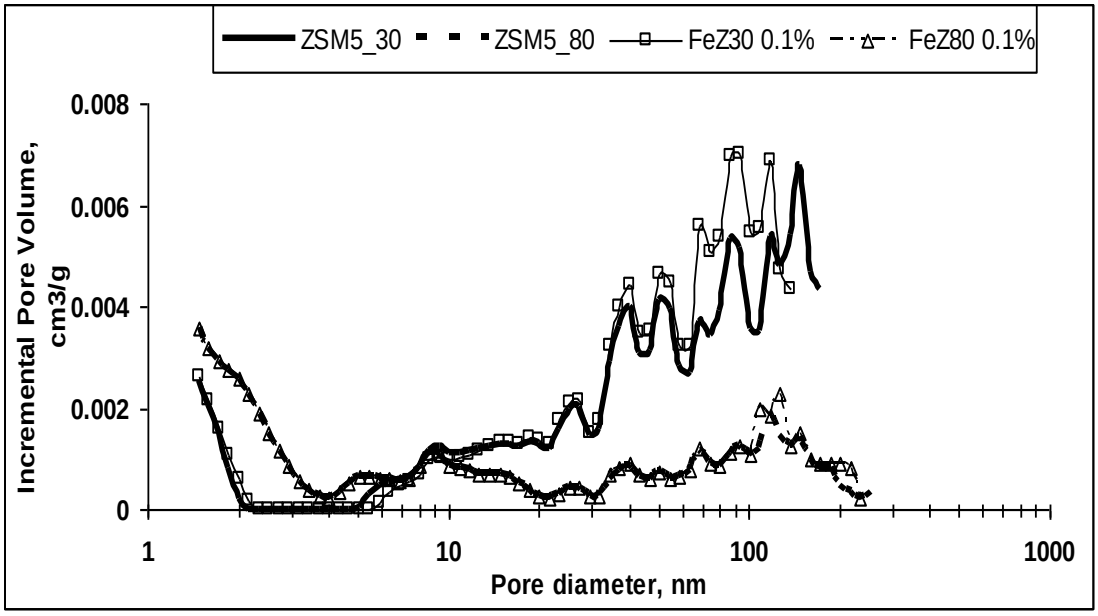


Figure 4.17 Nitrogen adsorption isotherm for Z30 & 80 before and after preparation

The results show the total surface area and the pore volume for the NH_4-ZSM-5 (Si/Al ratio, 80) catalysts were measured to be 409 m^2 g^{-1} and 0.24 cm^3 g^{-1}. The ZSM-5 (Si/Al ratio, 30) catalyst before preparation were 338 m^2 g^{-1} and 0.23 cm^3 g^{-1}, and after preparation using 1%wt Fe were 334 m^2 g^{-1} and 0.22 cm^3 g^{-1}. Also these results show that the preparation seems not to have had a significant effect on the catalyst accessible area and pore structure of the ZSM-5 (Si/Al ratio, 30 & 80) catalyst before (as supplied by Zeolyst International USA Company) and after preparation using LIE. The results show that the differences in the mini and micropore structures for ZSM-5 (Si/Al 30) and ZSM-5 (Si/Al 80) catalyst samples may point to changes in the nature of extra-framework species and this may result in differences in mass transfer within the particles. Creation of larger pores occurs with removal of aluminium (dealumination) from framework positions. It can also be interpreted by migration of small iron species from the micropores to the external surface.

4.4 Determination of the nature of active sites

Temperature programmed decomposition of adsorbed isopropylamine (IPA) was used to determine the strength and amount of acidic sites. The number of acidic sites was calculated from the number of propylene molecules deriving from IPA decomposition. Hensen *et al*., (2004) have reported that exactly one IPA molecule is chemisorbed per acid site. Figure 4.18 shows an example of isopropylamine peaks before and after catalysts saturated by injection of isopropylamine vapour at 200°C (Chapter 3.3.4). Dobkov *et al.,* (2003) shows a comparatively similar method and results to the present work.

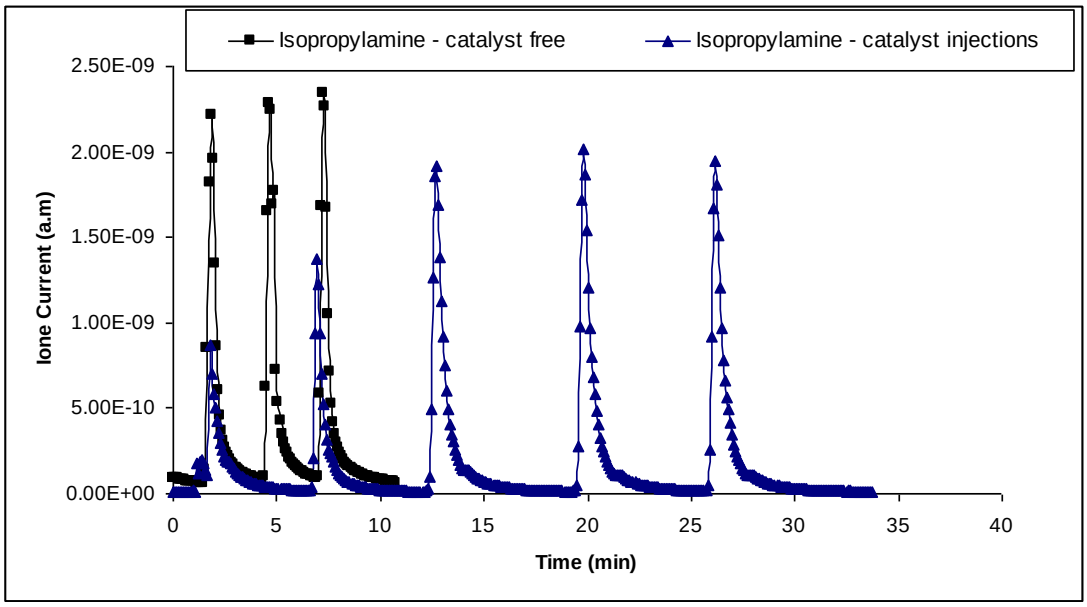


Figure 4.18 Multiple Isopropylamine injections at 200°C with and without catalyst

Figure 4.18 shows that the ZSM-5 catalyst was activated and then saturated by ten injections of Isopropylamine vapour into the sample. The figure displays that isopropylamine peaks before catalyst was found to be ~2.3 $\times 10^{-9}$ and after catalysts saturated was ~2 $\times 10^{-9}$. To obtain quantitative data, multiple injections of 15 ml volume (V_{cal}) of the Isopropylamine at 200°C were done without and with catalyst as shown in Figure 4.18. It can be seen from the figure that the repeated injections of the Isopropylamine vapour have almost similar in area. The areas were averaged to give a general conversion factor (V_{cal}/A_{cal}) and then compared with propylene peaks (A_{pms}) after IPA decomposition (Figures 4.19 to 4.24). For more details about the original data (Print screen) and calculations refer to Appendix C.2.

Figures 4.19 to 4.24 show that with increasing Fe content, the concentration of propylene peaks and ammonia linearly increased (this correlates to an increase in the number of active sites) for both Si/Al ratio 30 & 80. The results were fitted by a linear relationship between the concentration of active sites and the amount of Fe species as shown in Table 4.3.

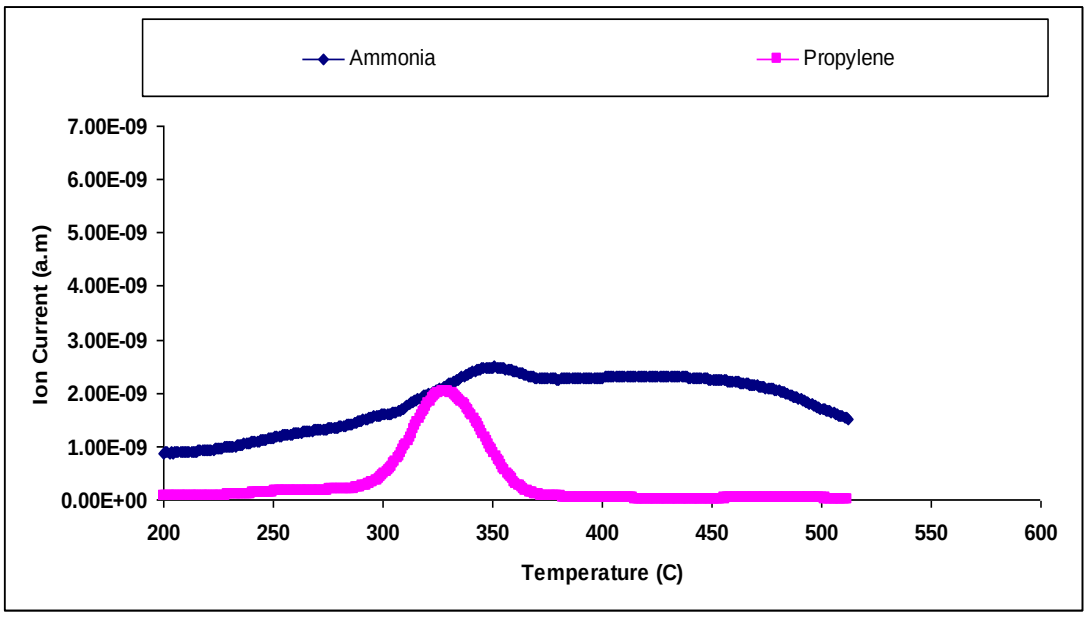


Figure 4.19 Desorption of propylene in temperature programmed decomposition for NH_4Z30.

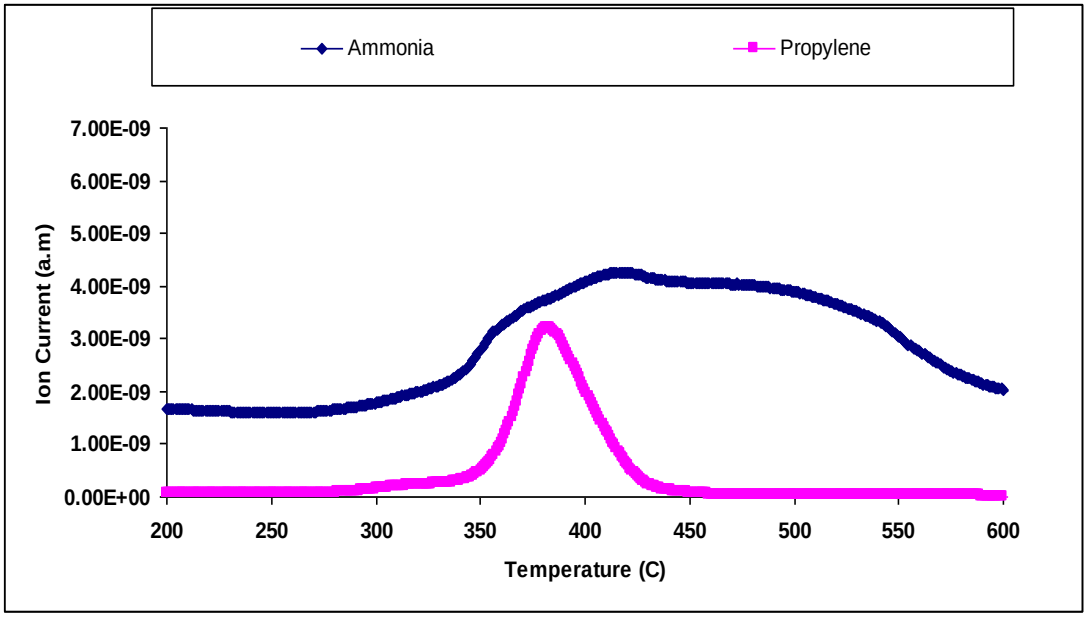


Figure 4.20 Desorption of propylene in temperature programmed decomposition for 0.1%FeZ30.

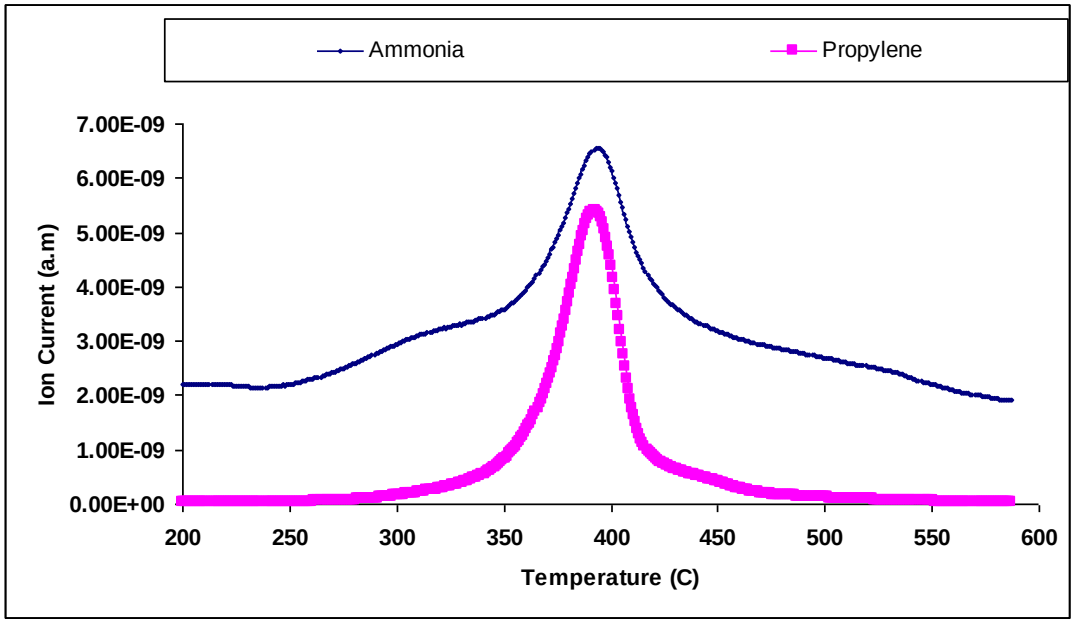


Figure 4.21 Desorption of propylene in temperature programmed decomposition for 1%FeZ30.

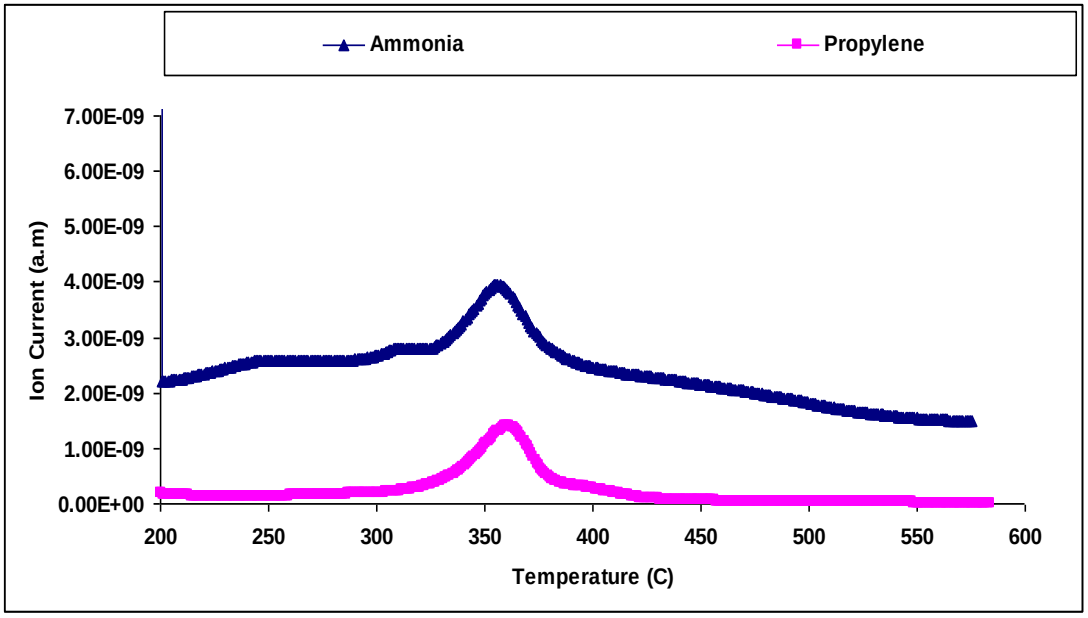


Figure 4.22 Desorption of propylene in temperature programmed decomposition for NH_4Z80.

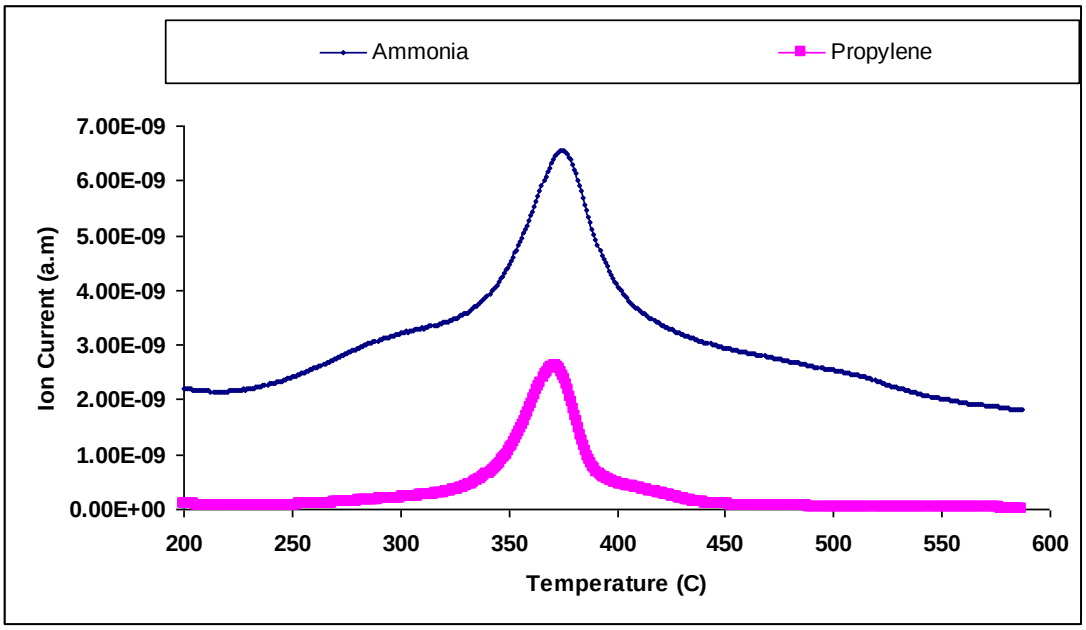


Figure 4.23 Desorption of propylene in temperature programmed decomposition for 0.1%FeZ80.

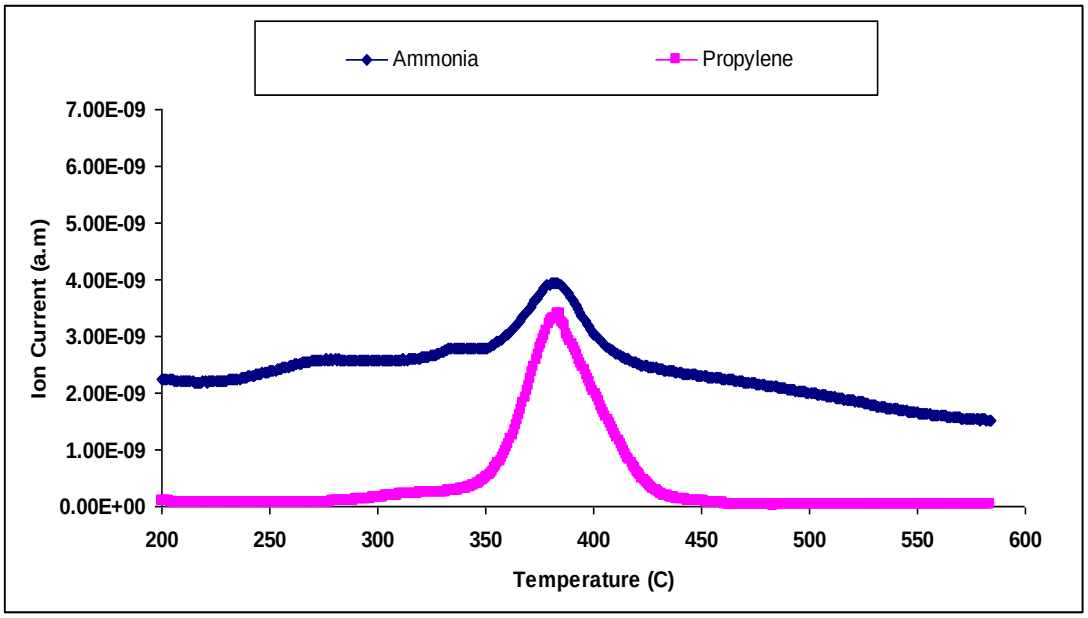


Figure 4.24 Desorption of propylene in temperature programmed decomposition for 1%FeZ80.

Figures 4.25 & 4.26 show a comparison between different iron contents using Si/Al ratio 30 and 80 respectively. These results show that the propylene peaks have different areas. It can be seen from the results that the area increased with increasing amounts of iron. The propylene peaks also occurred at different temperatures. The reaction delay (The propylene peaks shift) with increasing the iron content for ZSM-5 (30) and (80) as shown in Figures 4.25 and 4.26. The shift of the propylene peaks occurred possibly due to changes in the nature of extra-framework species or due to differences in mass transfer within the particles.

The importance of understanding and predicting the performance of Fe/ZSM-5 catalyst samples was determined by the quantity and strength of acid sites. For several reactions such as the reaction of hydroxylation of benzene to phenol (as discussed on Chapter 5.2), the reaction rate increases linearly with Al and Fe content (acid sites) in Fe/ZSM-5 catalyst. The activity depends on many factors, but the Bronsted-acid site density is usually one of the most important parameters.

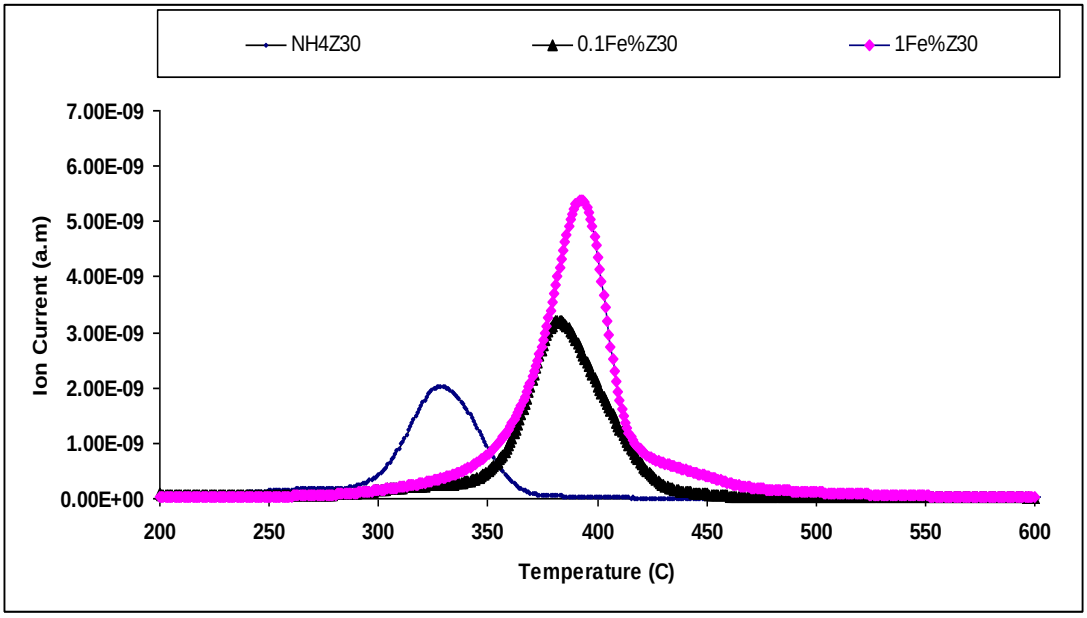


Figure 4.25 Desorption of propylene in temperature programmed decomposition for Z30 with different iron contents.

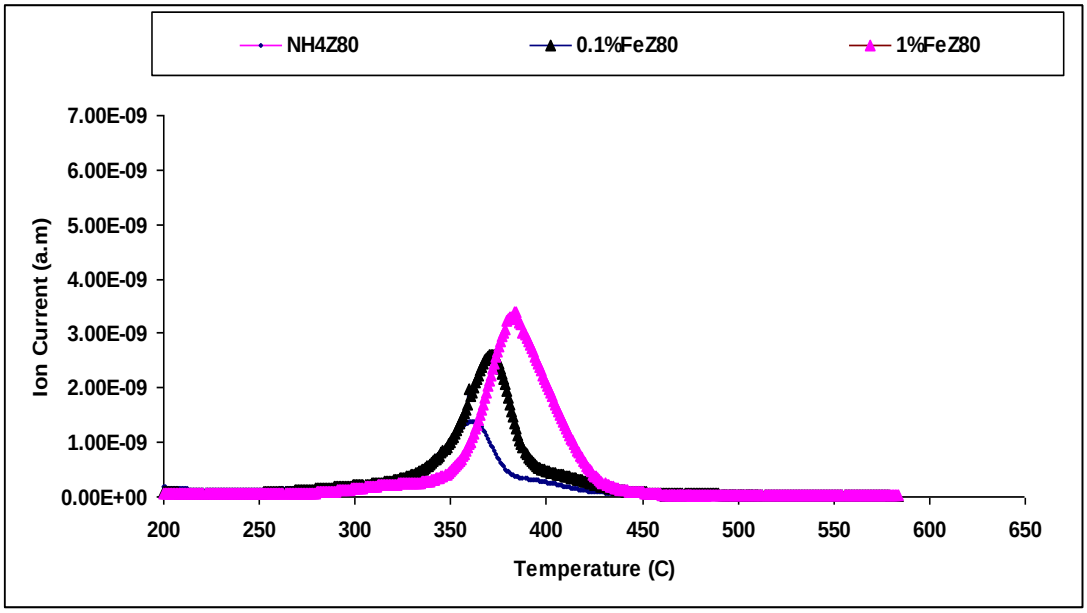


Figure 4.26 Desorption of propylene in temperature programmed decomposition for Z80 with different iron contents.

High Si/Al ratio 80 shows smaller propylene peaks (areas) compared to Si/Al ratio 30 before and after ion exchange as shown in Figures 4.27 – 4.29. Bronsted sites are well known as being the important sites for the catalytic reactions. The catalyst acidity was influenced by the (Si/Al) ratio. Lower Si/Al ratio and higher iron contents provide higher Bronsted acid sites (active sites).

The ratio of Al/Fe decreased with an increase of the iron content. This means that the iron may have replaced the Al during ion exchange preparation of catalyst as shown in Table 4.1. These results also show that the propylene peak for Z30 occurred earlier at lower temperature (~320°C)) compared to Z80 (~350°C), but with increasing iron content, the catalyst with high Si/Al ratio 80 occurred earlier compared to the peak for Si/Al ratio 30. These results prove that the iron content and Si/Al ratio have a significant effect on the concentration of the active site.

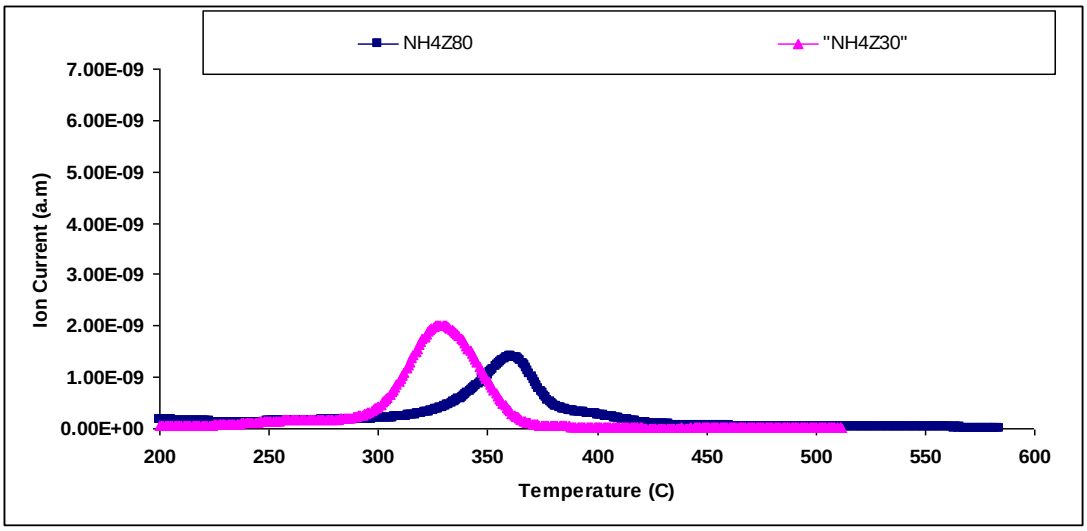


Figure 4.27 Desorption of propylene in temperature programmed decomposition for Z80 and 30.

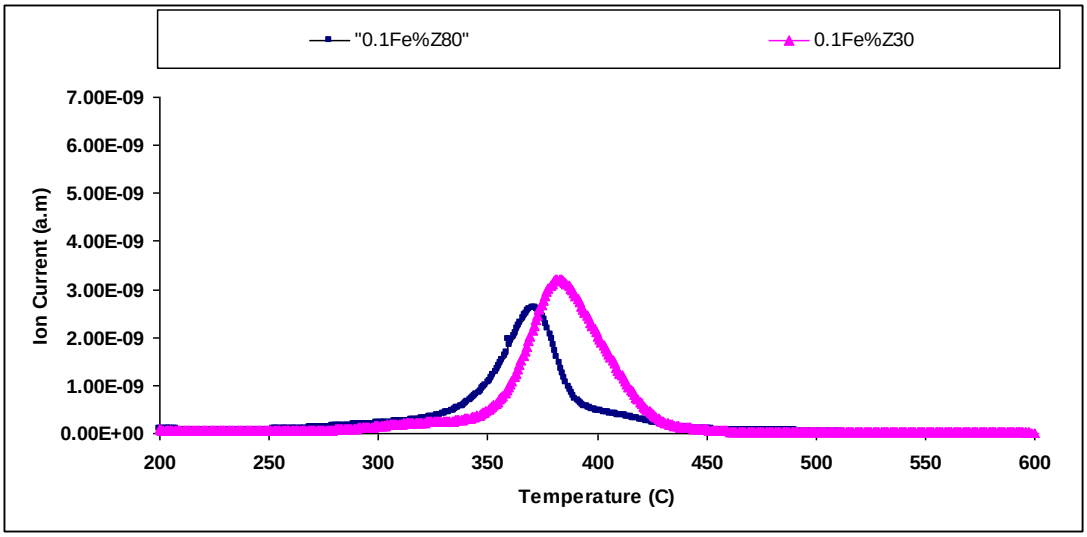


Figure 4.28 Desorption of propylene in temperature programmed decomposition for 0.1% FeZ30 and 80.

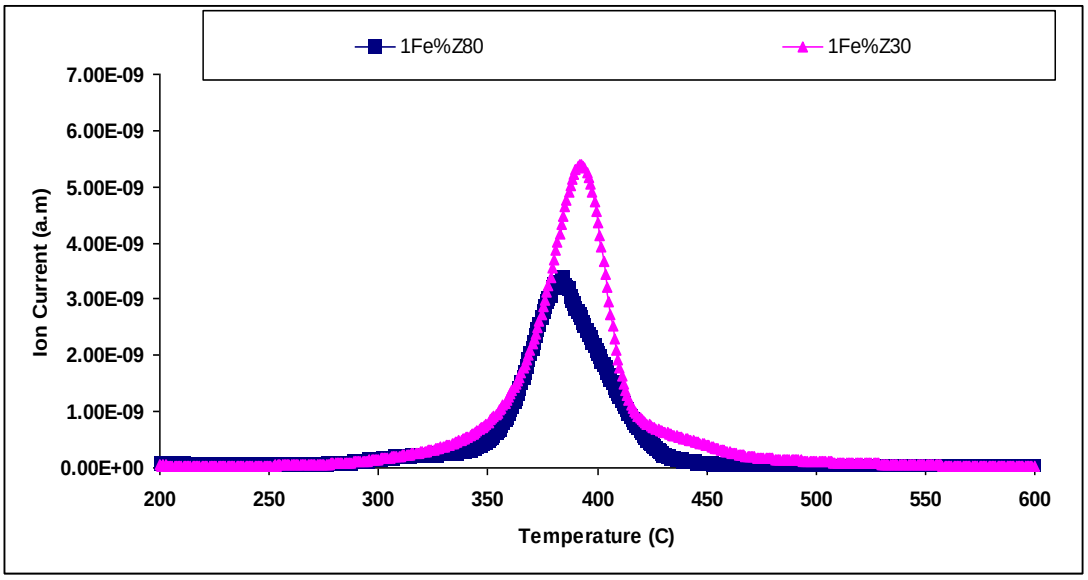


Figure 4.29 Desorption of propylene in temperature programmed decomposition for 1% FeZ30 and 80.

In conclusion, Table 4.3 summarizes the number of active sites obtained via the decomposition of isopropylamine for the various catalysts. This work shows that the Bronsted acidity of the ZSM-5 zeolite is an essential catalyst activity for the hydroxylation of benzene to phenol reaction (as discussed on Chapter 5.2.3). The whole set of the results obtained suggested that the preparation procedure significantly affects the nature of active centers and chemical characteristics of the surface of Fe-containing ZSM-5 zeolite. The values for the Fe/ZSM-5 catalysts are close to the values reported in literature (Sun *et al*., 2008 and Zhu *et al*., 2004). The initial high activity of the Fe/ZSM-5 catalysts may be due to the present of Fe^{+2} centers (active sites).

Table 4.3 The amount of acid sites determined from isopropylamine decomposition.

Samples	Z30	Z80	0.1%FeZ30	0.1%FeZ80	1%FeZ30	1%FeZ80
Amount Fe (10^{18}site/g)	10	7.5	16	13	28	18

5 Experimental Results and Discussion for Direct Oxidation of Benzene to Phenol using N_2O

The one step oxidation of benzene to phenol using the Fe/ZSM-5 catalyst was performed in a fixed bed reactor. The feed gas contained ~1 mol% benzene and 7 mol% N_2O with 60 ml/min total flow rate. Samples were collected every 2 h during the 20 h period of experiment. (see Chapter 3.4 for the reaction conditions and experimental procedure). A matrix of experiments was designed to evaluate the effect of temperature, Si/Al ratio and iron content on phenol selectivity using 0.2 g of (Fe/Z30/80–calcined at 900°C/ particle size -154µm).The low concentrations of benzene and nitrous oxide were used in order to minimize the possible effect of consecutive reactions of further hydroxylation of phenol intermediate. Trace amount of the main reaction by –products include dihydroxybenzenes such as catechol, hydroquinone and p-benzoquinone have been found. Another undesirable reaction is the formation of coke on the catalyst surface.

5.1 Phenol production using Fe-ZSM-5 catalysts

The invariability of the feed composition as a function of time was evaluated (see Figure 5.1). The flow rate of N_2O was set at 10 ml/min and that of helium fed through a benzene bubbler (bubbler temperature set at 50°C) was 50 ml/min. The feed preheater temperature was set at 300°C using oven 1 and the reactor temperature was set at 450°C using oven 2 as described in Chapter 3. The sampled feed composition was found to be steady over the duration of the experiment (see appendix D.1).

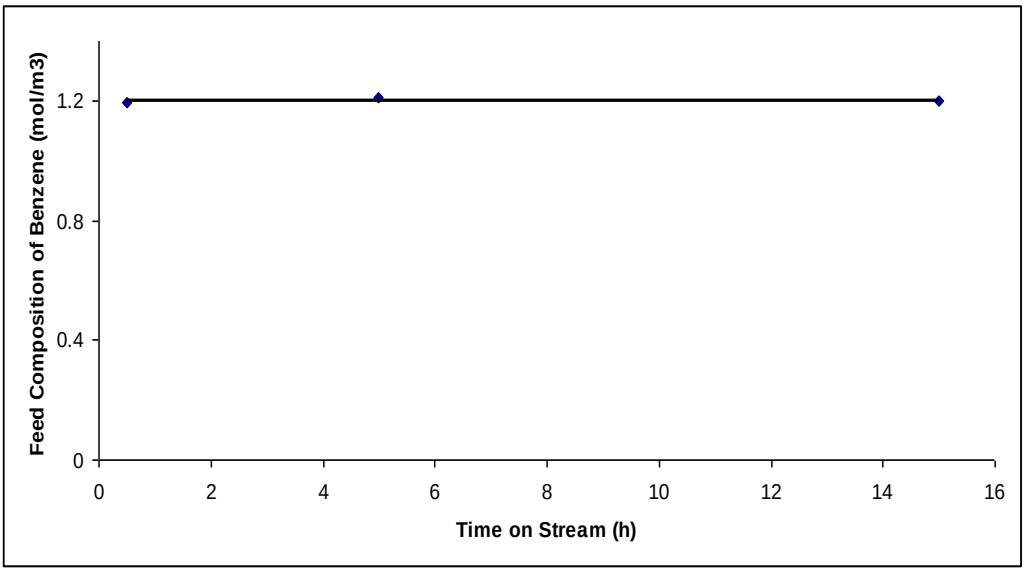


Figure 5.1 The invariability of the feed composition of benzene as a function of time.

Figure 5.2 shows that reactant, products, by-products and conversion over the time on stream at 450°C using (0.1% Fe/Z30- cal 900°C/154µm). Benzene effluent increased with phenol decreasing. High conversion of benzene (about 80%) and a high effluent concentration of phenol were observed. Trace amounts of by-products (catechol, hydroquinone and p-benzoquinoe) < 1% were observed and the selectivity of benzene to phenol was high (about 90%). The reproducibility of these results is demonstrated in Figure 5.3 which shows the results for experiments using 0.2 g of 0.1% Fe/Z30–cal 900°C/154µm. The results show the high initial rate of phenol production (rate of phenol formation) was (11.5 mmol /g. h) at 450°C with high average productivity of phenol (~ 6 mmol /g. h).

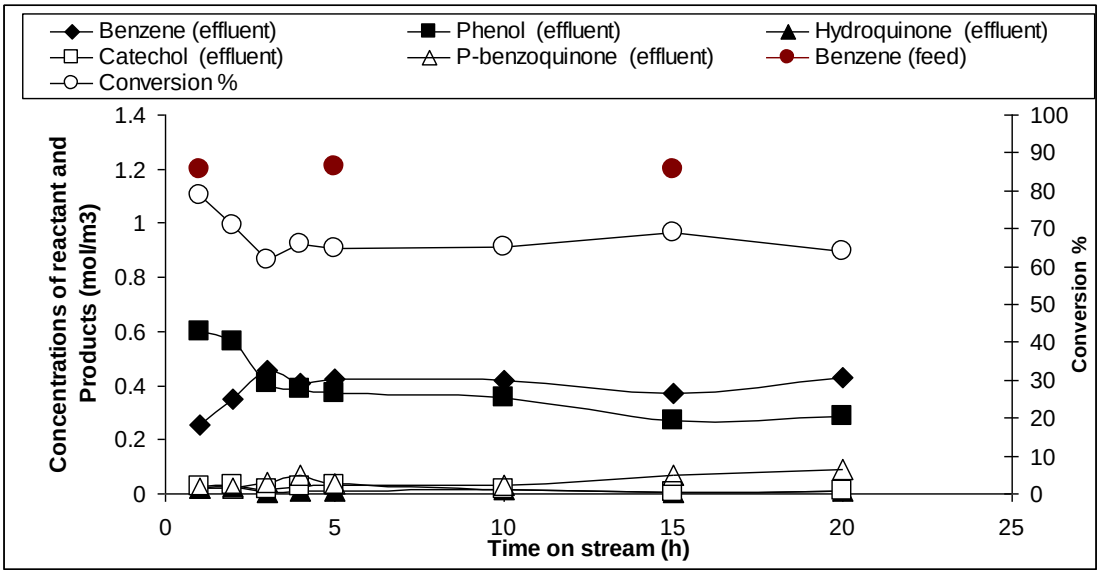


Figure 5.2 Benzene and phenol concentrations vs. time on stream (reaction conditions: 450°C, atmospheric pressure, feed gas =60ml/min, using 0.1% Fe/Z30).

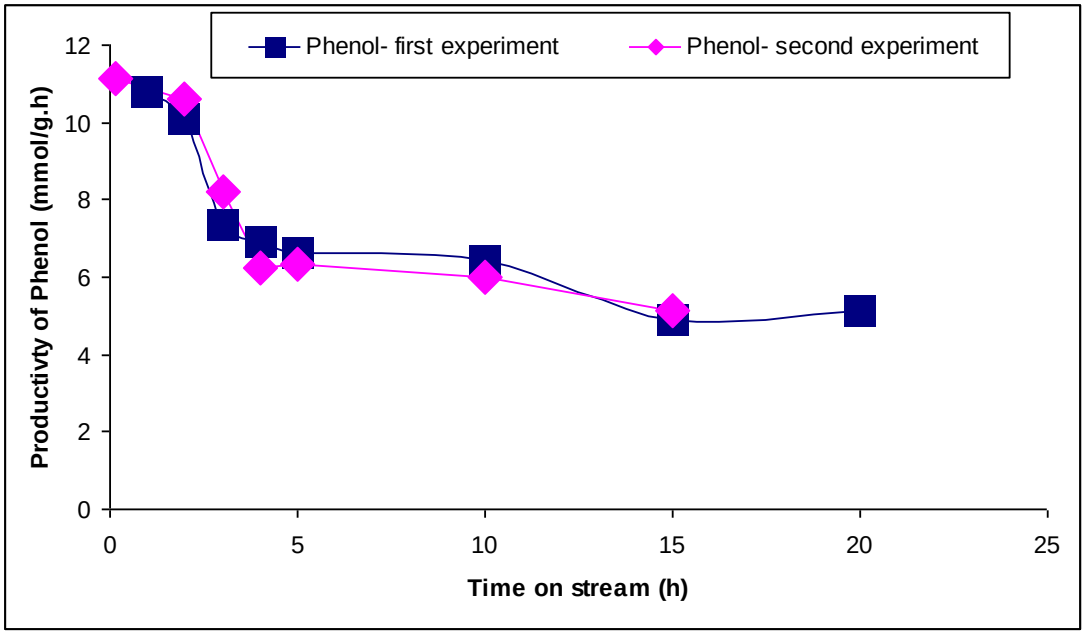


Figure 5.3 Phenol productivity for repeated experiments vs time on stream (reaction conditions: 450°C, atmospheric pressure, feed gas =60ml/min, using 0.1% Fe/Z30).

Figure 5.4 shows the byproducts (catechol, hydroquinone and p-benzoquinone) over time on stream**.** The results support that the observed hydroquinone decreased whilst *p*- benzoquinone increased. This may be explained by the formation of the hydroquinone by-product which subsequently oxidises to *p*-benzoquinone due to the strong adsorption of hydroquinone on the active sites of the catalyst. This matched with the reaction mechanism of the hydroxylation of benzene to phenol from literature review (as discussed in Chapter 2.2). Figures 5.3 and 5.4 show that after 5 h the phenol production rate decreased which the by-products, catechol and *p*-benzoquinone increased their concentration. The deactivation may be due to coke formation of the catalyst which decreased the number of active sites on the catalyst surface. In addition, further hydroxylation of phenol to dihydroxybenzene (p-benzoquinone, catechol and hydroquinone) by strong adsorption of phenol on the Bronsted acid sites (the activation centers) as shown in Figure 5.4.

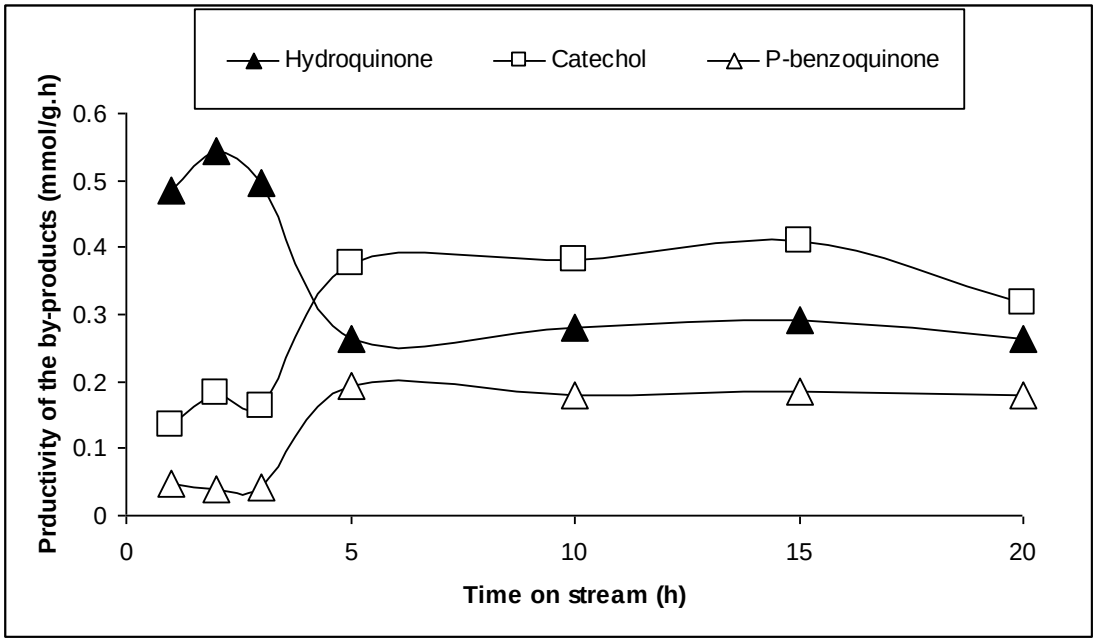


Figure 5.4 By-products productivity vs time on stream (reaction conditions: 450°C, atmospheric pressure, feed gas =60ml/min using 0.1% Fe/Z30).

5.2 Phenol productivity (rate of phenol formation)

5.2.1 Effect of iron content on phenol productivity

For samples Z30 the initial rate of phenol production was higher (see Figure 5.5) at 450°C (11.5 mmol /g. h) compared with 350°C (about 8.5 mmol /g. h). All samples showed significant deactivation within the first 5 hours reacted by a lower rate of phenol production. However, catalyst samples with lower iron content (~ 0.1%) showed a lower tendency to deactivate in comparison with the samples with higher iron content (~1 %). The 0.1% Fe sample at 450°C showed a higher rate of phenol production (11.4 mmol /g. h), this production rate remained nearly constant for the first two hours of time on stream and then decreased to 6 mmol /g.h at 5 h. The productivity thereafter remained nearly constant between 5 h and 20 h on stream at this value. In comparison, the initial production rate of phenol for this sample (0.1%Fe/Z30) at 350°C was about 7 mmol/g.h and the production rate decreased to about 4.2 mmol /g.h after the intial period of deactivation (lasting again around 5 h). The 1%Fe/Z30 sample showed similar behaviour except that the degree of deactivation at 450°C was markedly more severe (see Figure 5.5). It appeared that the amount of iron in the sample affected the degree of deactivation. The decrease in the rate of phenol formation with increasing iron content using a high-temperature (450°C) may be due to the decrease in the selectivity of benzene to non-selective products. Catalyst deactivation can be caused by a decrease in the number of active sites, decrease in the quality of the active sites and decrease in the accessibility of the pore space containing the active sites. For catalyst samples with Si/Al ratio 30, lower iron content and high reaction temperature favour higher reaction rates and reduced tendency for catalyst deactivation. This indicates that only a fraction of iron is catalytically active in the direct oxidation of benzene to phenol.

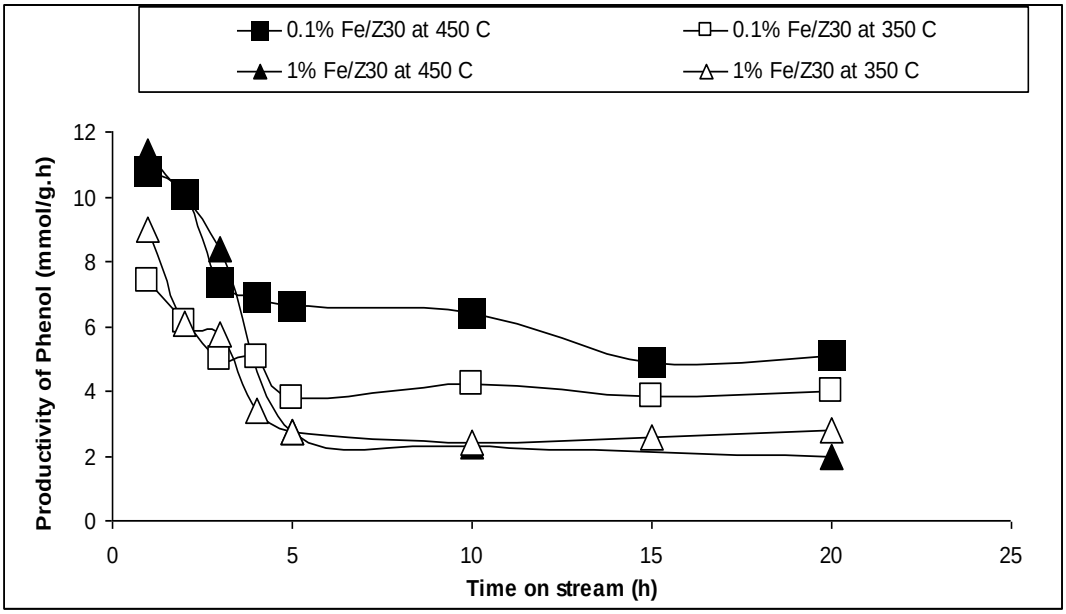


Figure 5.5 Phenol productivities vs time on stream using Si/Al ratio 30.

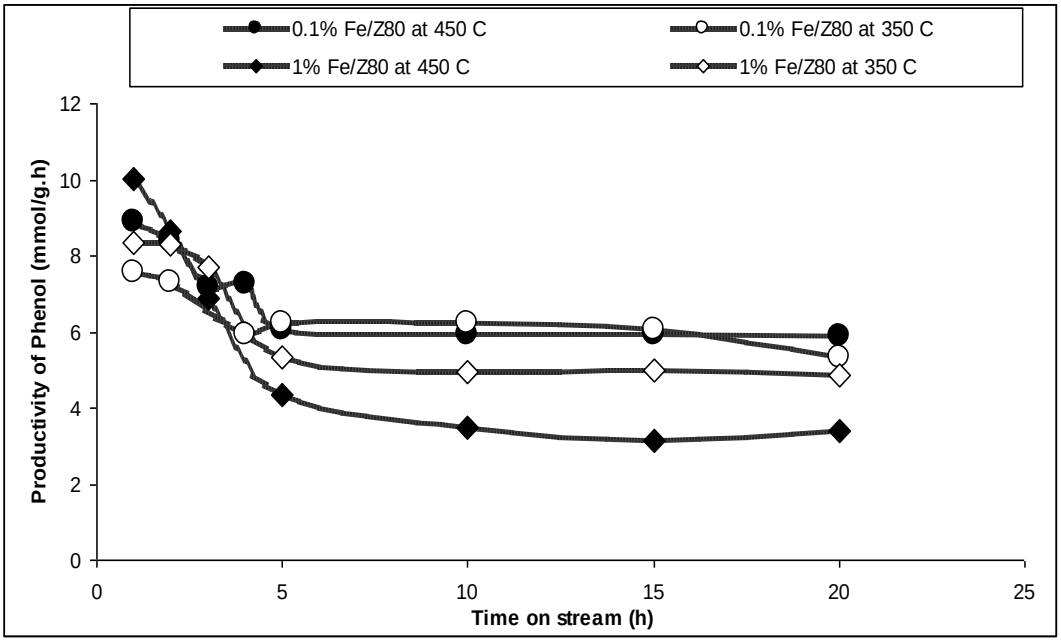


Figure 5.6 Phenol productivities vs time on stream using Si/Al ratio 80.

For samples Z80 the initial rate of phenol production was higher (see Figure 5.6) at 450°C (~10 mmol /g. h) for 1%Fe/Z80 compared with 350°C (about 8 mmol /g. h). All samples showed considerable deactivation within the first 5 hours reacted by a lower rate of phenol production. However, catalyst samples with lower iron content (~ 0.1) showed a lower tendency to deactivate in comparison with the samples with higher iron content (~1). The 0.1% Fe sample at 450 °C showed a higher rate of phenol production (~9 mmol /g. h), this production rate decreased to 6 mmol /g.h at 5 h. The productivity thereafter remained nearly constant between 5 h and 20 h on stream at this value. In comparison, the initial production rate of phenol for this sample (0.1%Fe/Z80) at 350°C is slightly below about 8 mmol/g.h and the production rate decreased to slightly above 6 mmol /g.h at 5 h after the intial period of deactivation (lasting again around 5 h). The 1%Fe/Z80 sample shows similar behaviour except that the degree of deactivation at 450°C was markedly more severe (see Figure 5.6) and the post 5 h production rate was less than 4 mmol /g. h. It appeared again that the amount of iron in the sample affected the degree of deactivation. However, since only a fraction of iron is catalytically active, this suggests that only a small fraction of iron (II) to iron (III) species oxidized were able to generate active oxygen for phenol production from benzene. High iron content leads to an excess of active sites (see Chapter 4.4) promoting coke formation which has due to the reaction by-products (p-benzoquinone, catechol and hydroquinone). For catalyst samples with Si/Al ratio 80 lower iron content and a high reaction temperature favour higher reaction rates and reduced tendency for catalyst deactivation, however, unlike Si/Al ratio 30 the effect of temperature between 5-20 h was less pronounced.

5.2.2 Effect of Si/Al ratio on phenol productivity

At 450°C Fe/Z30 (~11 mmol/g.h) showed (see Figures 5.7 and 5.8) a higher initial reaction rate compared with Fe/Z80 (~9 mmol/g h). However, after 5 h the phenol production rate for both samples decreased to ~6 mmol/g.h. Composition measurements of the reactor outlet streams at 15 h and 20 h suggest the Fe/Z30 showed a slightly worse performace in terms of deactivation with phenol production rates around 5 mmol/g.h. The 0.1%Fe/Z80 and 0.1%Fe/Z30 have similar reaction rates at 350°C however, the sample 0.1%Fe/Z80 very little deactivation and reaction rate remained stable at around ~6 mmol/g h. The sample 0.1%Fe/Z30 showed deactivation with the rate between 5-20 h steady at around ~4 mmol/g h. Thus, for catalyst samples with low iron content (~ 0.1), the Si/Al ratio seems to have an effect on catalyst deactivation. Catalyst samples with high Si/Al ratio showing lower deactivation rates. It was concluded that not only the amount of iron but also the catalyst structure is important in the creating of an active catalyst.

Pirutko *et al*., (2002) reported Fe/ZSM-5 zeolite structure can be synthesised on the Fe-Si bas without aluminium or replaced with Ga, B, and Ti. The distinction in the zeolite activity relate to the fact that the formation of Fe-containing active sites strongly depends on the Bronsted acidity and proceeds with different efficiency in the various matrics. Finally, the presence of Al, Ga, B and Ti does not effect the composition and properties of iron containing active sites but increases their concentration due to more favourable distribution of Fe in the zeolite matrix. The results showed that a high initial productivity was achieved using higher amounts of Al (Si/Al 30) at high temperature (450°C) in the zeolite matrix (see Figures 5.7 and 5.8).

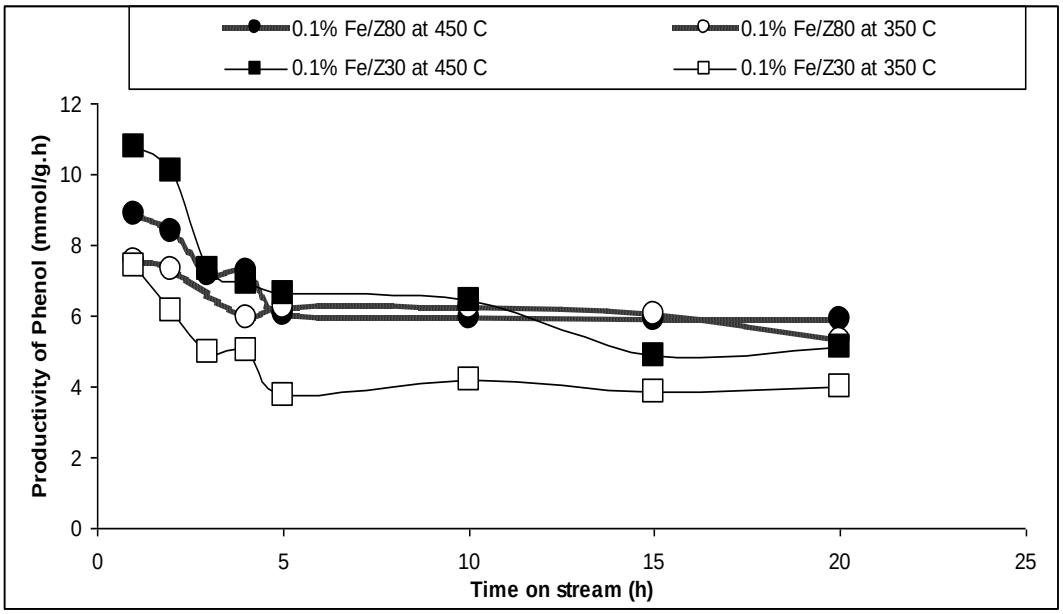


Figure 5.7 Phenol productivities vs time on stream using 0.1% Fe/ZSM-5.

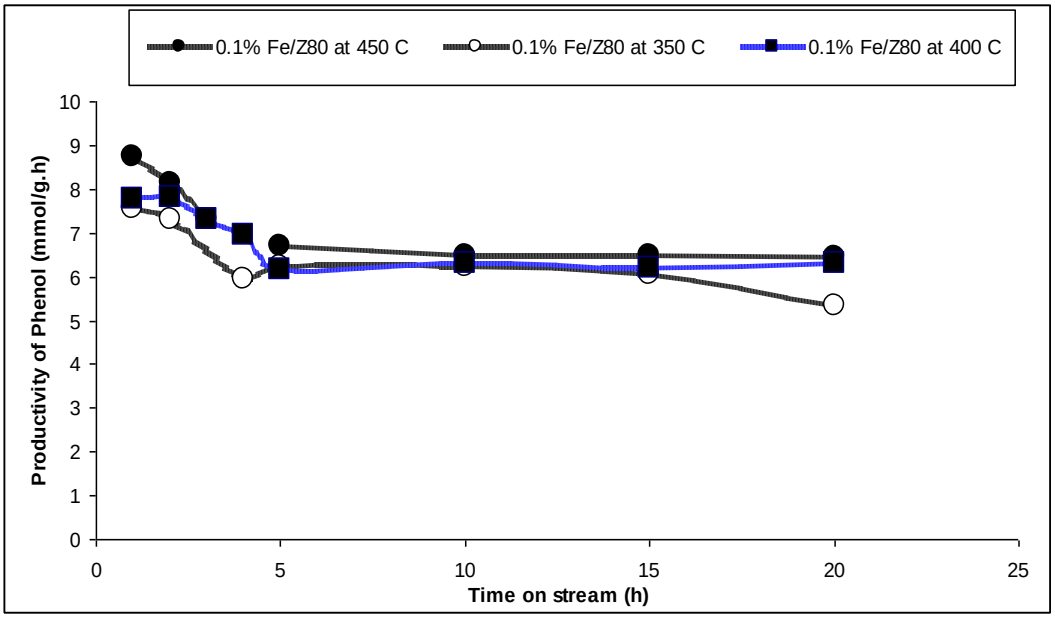


Figure 5.8 Phenol productivities vs time on stream using 0.1%FeZ80.

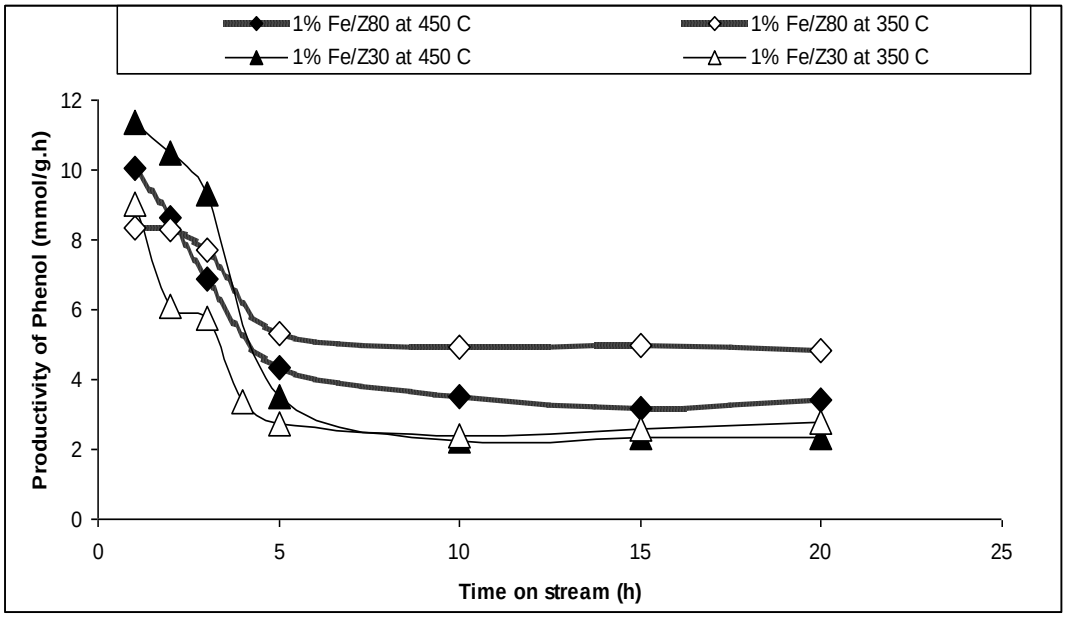


Figure 5.9 Phenol productivities vs time on stream using 1% Fe/ZSM-5.

At 450°C Fe/Z30 (~11.5 mmol/g h) showed (see Figure 5.9) a higher initial reaction rate compared with Fe/Z80 (~10 mmol/g h). However, after 5 h the phenol production rate for both samples decreased Fe/Z30 (~2 mmol/g h) and Fe/Z80 (~4 mmol/g h). The rate of deactivation is considerable more marked in comparison with catalyst samples having lower iron content (see Figures 5.7 and 5.8). The 1%Fe/Z80 and 1%Fe/Z30 have similar reaction rates at 350°C however, the sample 0.1%Fe/Z80 showed less deactivation and the reaction rate in the stable range (5-20 h) was around ~5 mmol/g h. The sample 0.1%Fe/Z30 showed similar deactivation at the lower temperature with reaction rate in the stable range (5-20 h) around ~2 mmol/g h. Thus, for catalyst samples with high iron content (~1) the Si/Al ratio seems to have an effect on catalyst deactivation. Catalyst samples with high Si/Al ratio showing lower deactivation rates. It was observed that an increase in the initial productivity is obtained for higher amounts of Al (Si/Al 30) at high temperature (450°C) in the zeolite matrix (see Figure 5.9).

Traces of by products (p-benzoquinone, hydroquinone and catechol) were detected in the outlet stream from the reactor for all catalysts and at all temperatures.

5.2.3 Effect of iron content and temperature on phenol productivity

At 450°C samples with low iron content (irrespective of Si/Al ratio) seemed to yield higher phenol reaction rates over the long term (5-20 h) and demonstrated greater stability in terms of catalyst resistance to deactivation (see Figure 5.10). However, samples Z80 seemed to show slightly higher reaction rates compared with Z30 post 10 h of catalyst operation. At 350°C samples with high Si/Al ratio (Z80) seemed to yield higher phenol reaction rates (irrespective of iron content) over the long term (5-20 h) and demonstrated greater stability in terms of catalyst resistance to deactivation (see Figure 5.11).

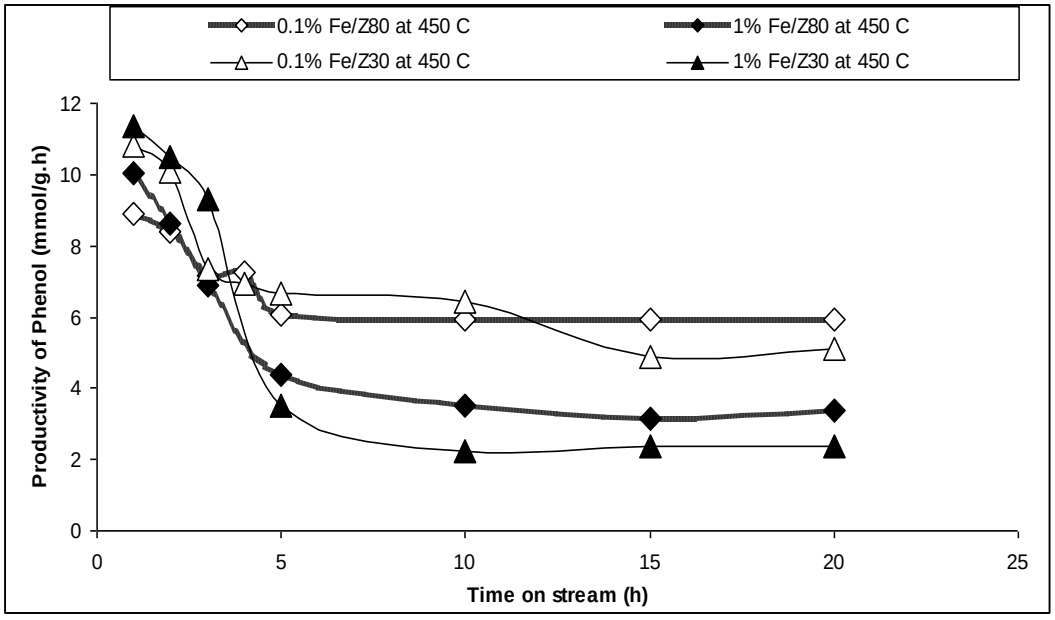


Figure 5.10 Phenol productivities vs time on stream at 450°C.

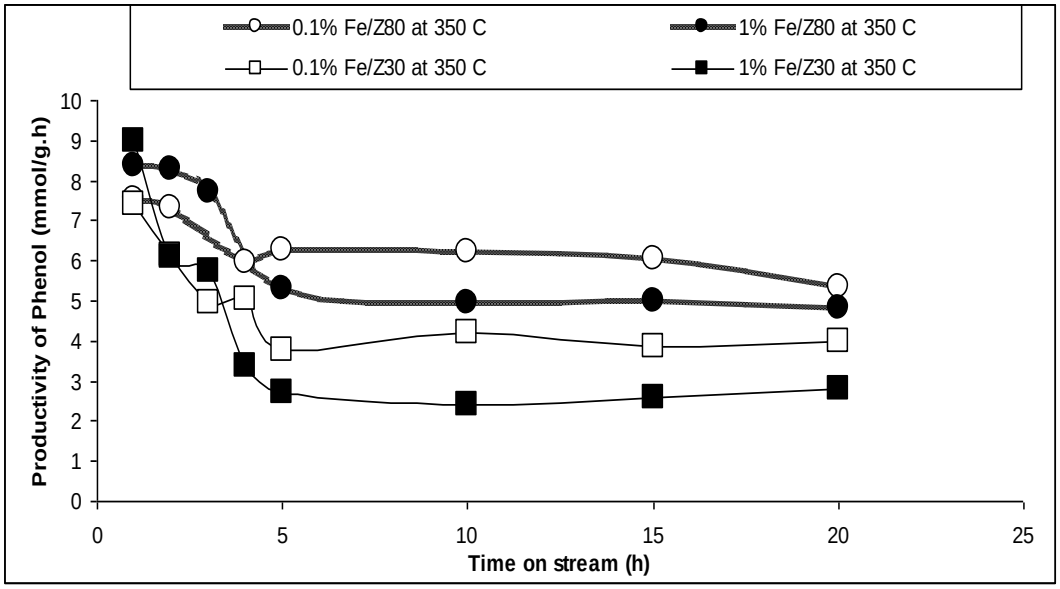


Figure 5.11 Phenol productivities vs time on stream at 350°C.

In conclusion, catalysts with high amounts of iron showed considerable deactivation. High reaction temperatures (450°C) favoured higher reaction rates, however, catalysts with high iron content were particularly prone to deactivation at this temperature. The balance between Bronsted acidity and the quantity of active oxygen donor α-sites seemed to be depend on the Si/Al ratio and the presence of the iron within the catalyst matrix.

Figure 5.12 shows the relation between the initial rate of phenol formation and the iron content for FeZ30 using 0.1 and 1wt% of iron. The results showed a nearly increase of the rate of phenol formation on the Fe concentration after 1 h of running reaction. Increasing the iron content up to 1 wt% was accompanied by increasing of the phenol productivity. Figure 5.12 also shows almost an optimum for iron loaded to the catalyst after 2.5 h of running reaction and higher amount of iron or number of active sites was shown a negative effect on catalyst half-life. Active sites increased by increasing iron content as shown in Figure 5.13. Active sites and iron content results were discussed in Chapter 4. Hensen *et al*., (2005) reported that increasing Fe wt% in the extra-framework of the zeolite at the same reaction condition results higher N_2O decomposition, while a decrease in the productivity was observed as shown for the recent work in Figure 5.12. The

main reason could be some a-oxygen was consumed for converting phenol to dihydroxybenzene or coke formation. The location and structure of the Fe sites is important for their redox activity, as revealed by a much higher activity of the catalyst after high temperature calcinations. The nature of the Fe in the active sites was discussed in Chapter 2.

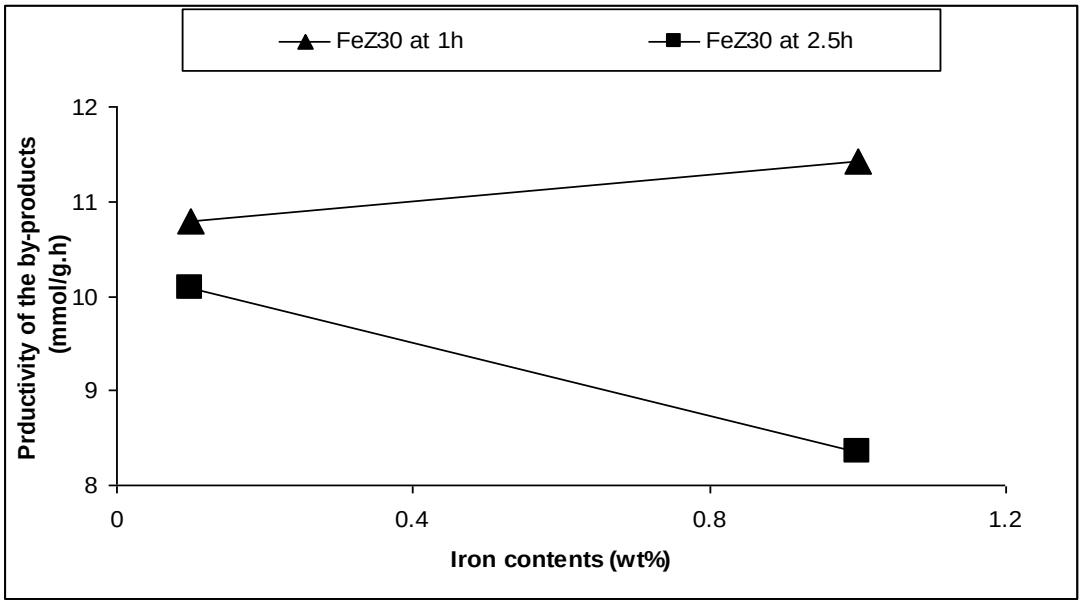


Figure 5.12 Productivity of phenol as a function of iron contents in FeZ30 in 1 and 2.5 h.

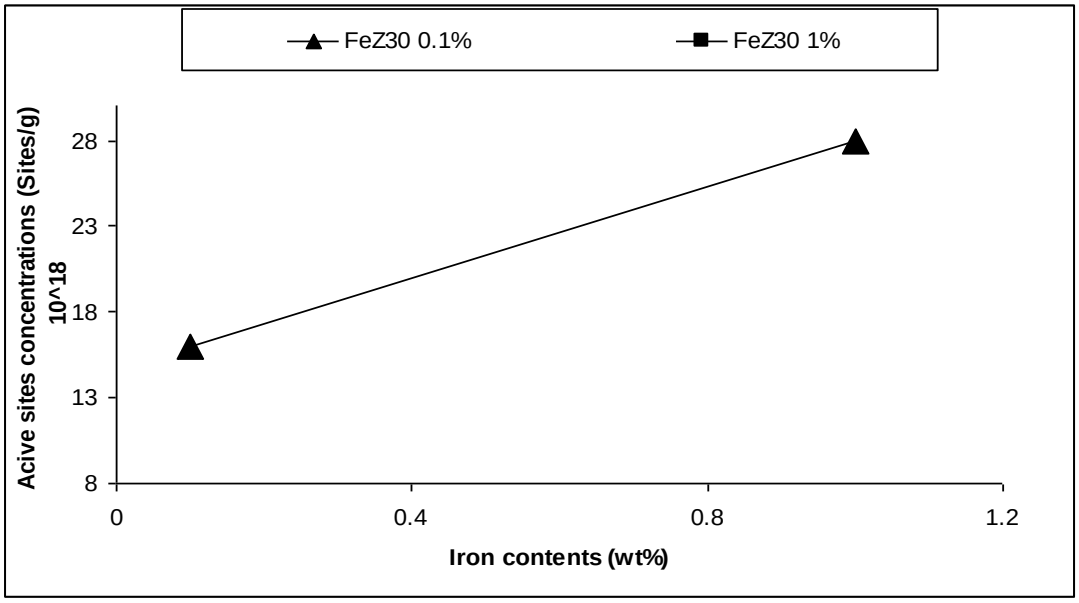


Figure 5.13 Active sites as a function of different iron contents in FeZ30.

Table 5.1 presents the data on phenol productivity, and selectivity. The reactor was loaded with FeZ80- 0.1% and reaction was run at 450 °C, atmospheric pressure and feed composition of 10 ml/min N_2O and 50 ml/min He/C_6H_6. It can be seen from Table 5.1, that temperature has a positive linear effect on phenol productivity, while it has negative effect on selectivity toward phenol. Figure 5.14 shows phenol formation was increased by increasing the temperature. Comparing the data presented in Table 5.1 it can be seen that the formation of byproducts dihydoxybenzene (catechol, hydroquinone and p-benzoquinone) were increased (the Arrhenius plot of apparent rate constant k_1 on temperatures is shown later in Figure 5.21).

Table 5.1 Effect of reaction temperature on the reactor performance.

Reaction Temperature (°C)	Phenol (mmol/g.h)	Dihydroxybenzene (mmol/g.h)
350	**7.5**	**0.26**
400	**8.7**	**0.69**
450	**10**	**0.85**

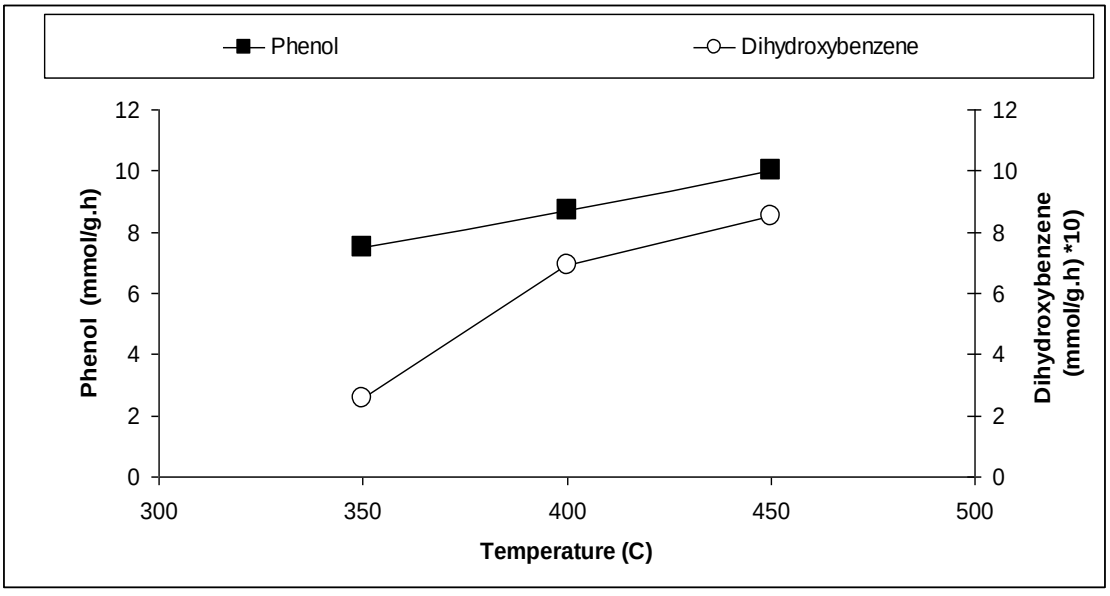


Figure 5.14 Effect of temperature on the productivity and selectivity at reaction time of 0.5s using FeZ80- 0.1%

5.3 Benzene conversion and phenol selectivity

In the present work, Fe/ZSM-5 catalysts were prepared with (0.1 & 1 wt%, Fe) using liquid ion exchange, calcined at 900°C. The reaction was run using 0.2 g of FeZ80 with different iron content and different temperatures at 350 - 450°C, atmospheric pressure and feed composition of 10 ml/min N_2O and 50 ml/min He/benzene at contact time, 0.5 s. Waclaw *et al*., (2004) reported that Fe/ZSM-5 calcined in the range of temperature from 700 - 900°C showed high activity for hydroxylation of benzene to phenol. This may be due to the effect of concentration of active a-oxygen by changing in the nature of extra-framework species or changing in the pore structure. And also they achieved (55%) benzene conversion and (98%) selectivity towards phenol. Panove *et al*., (2000) reported that the number of active sites for Fe/ZSM-5 at 900 °C calcinations was higher when compared to other temperature calcinations (500 - 800°C). Figures 5.15 and 5.16 show that samples with low iron content 0.1wt% showed lower activity (benzene conversion) in both temperatures 350 and 450°C. High conversion of benzene (~80%) and a high selectivity (overall selectivity) towards to phenol (about 90%) was observed using high iron content 1wt% as shown in Figures 5.15 and 5.16.

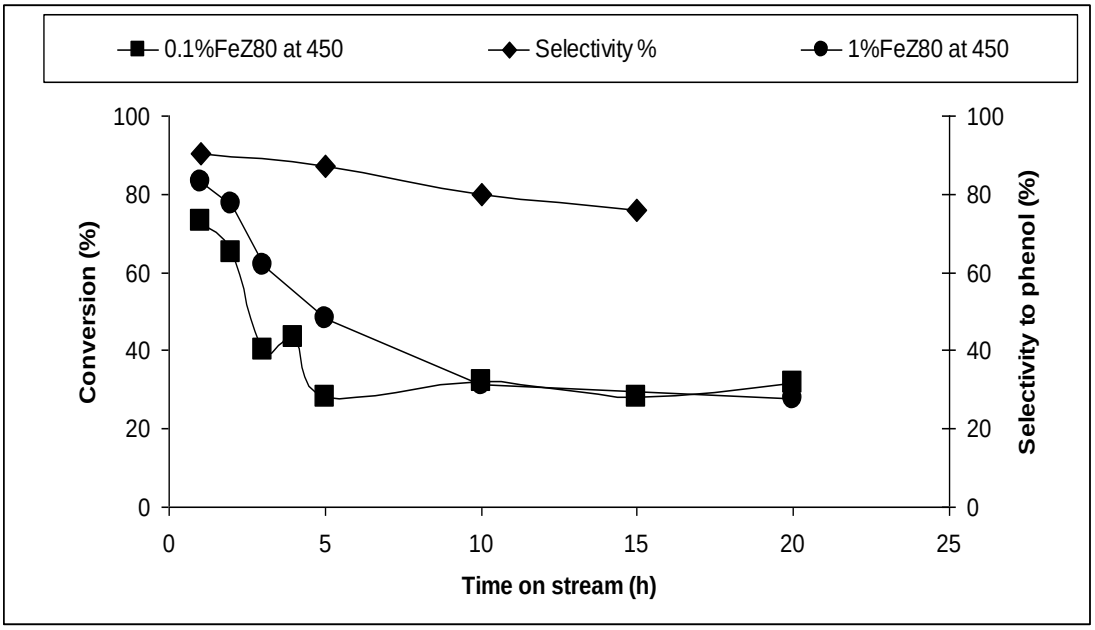


Figure 5.15 Benzene to phenol conversion as a function of time on stream for FeZ80 at 450 °C.

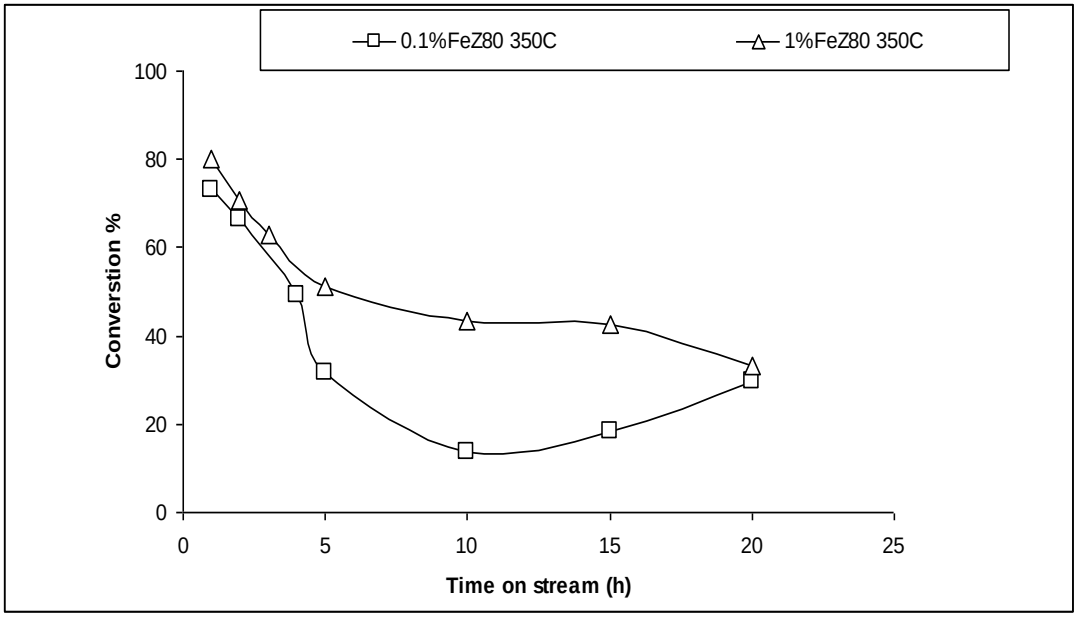


Figure 5.16 Benzene to phenol conversion as a function of time on stream for FeZ80 at 350 °C.

5.4 Coke formation

The formation of coke deposits on catalyst surfaces leads to catalyst deactivation in many hydrocarbon processes. Coke formation is dependent on the zeolite structure (Guanjie *et al*., 2010). Figures 5.17 shows the 1%FeZ30 catalyst productivity of phenol during hydroxylation of benzene to phenol as a function of time-on-stream, as example of a series Fe/ZSM-5 catalysts prepared by ion exchange and having different amount of iron (0.1 and 1 wt%) and different Si/Al ratio (30&80). Sample with low iron content and high Si/Al ratio (0.1%Fe/Z80) as explained above shows less deactivation and the reaction rate in the stable range (5-20 h) is around ~6 mmol/g h. Higher amount of Fe (III) in catalysts significantly increases the initial productivity of phenol, but a lower half-life was observed from the experimental data. The reaction using 1%FeZ30 at 450°C was run for duration of 1, 5 and 15 hours and the samples have been weighed before and after the reaction to calculate the coke formation (Figure 5.17).

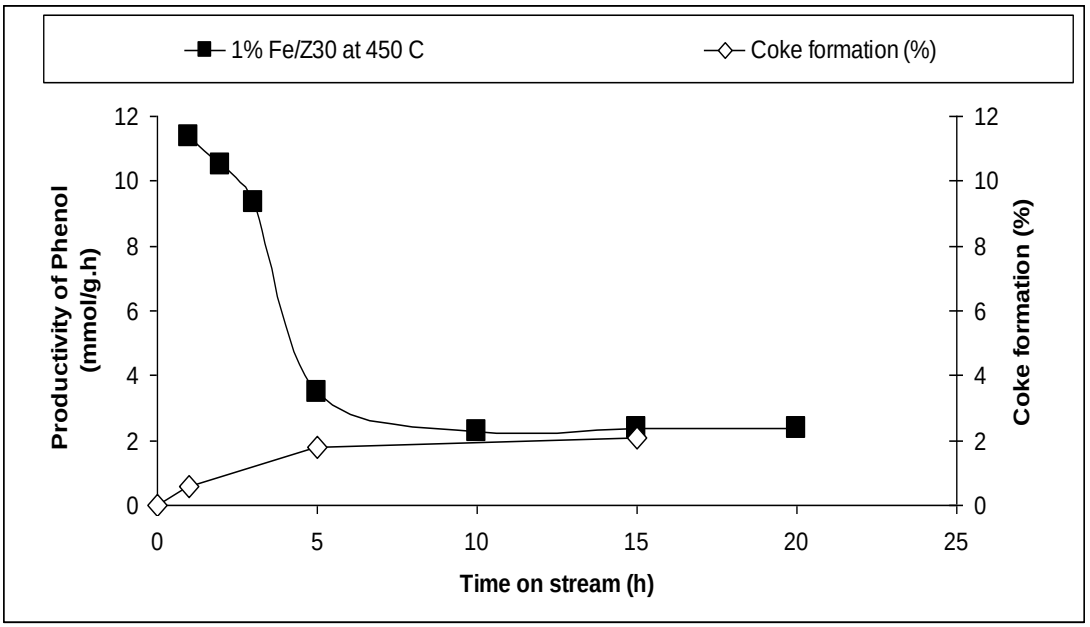


Figure 5.17 Productivity of phenol and coke formation as a function of time on stream using1%FeZ30.

5.5 Catalyst regeneration

Catalyst regeneration was studied on the sample with the maximum coke content (2.1 wt.%), which was obtained after 20 h on stream. 0.1%FeZ80 catalyst was regenerated by two steps: using oxidation followed by reduction method as explained in chapter 3.5.

$$Fe^{\circ} + \frac{1}{2}O_2 \xrightarrow{600^{\circ}C} FeO \Rightarrow TPO$$

$$FeO + H_2 \xrightarrow{300^{\circ}C} Fe^{\circ} + H_2O \Rightarrow TPR$$

Figure 5.18 shows comparison of 0.1%FeZ80 catalyst before and after regenerations 1 and 2 using Oxidation by O_2 followed by hydrogenation. The sample regenerated in this method shows almost similar results to fresh catalyst.

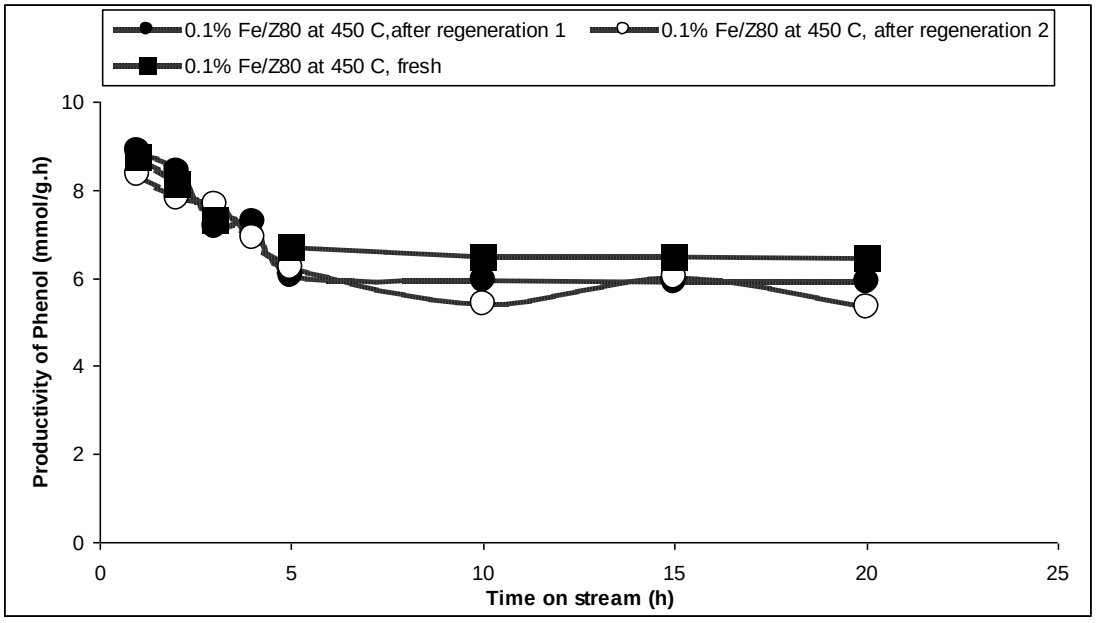


Figure 5.18 Phenol Productivity using the sample before and after catalyst regeneration for 0.1%FeZ80 using (oxidation, then reduction method).

Inanov et al., (2003) reported that there are two methods for the catalyst regeneration using oxygen diluted with helium and nitrous oxide diluted with helium as well. They reported that a higher activity was achieved using nitrous oxide rather than oxygen.

In this work, catalyst regeneration was carried out using N_2O, O_2 and the reduction method (oxidation followed by reduction - see Chapter 3.5). Figure 5.19 shows that the (oxidation followed by reduction) was found to be a more efficient reactivation reagent than N_2O and O_2. The reason may be because of the water being produced after the temperature programmed oxidation TPO followed by the temperature programmed reduction TPR, it was assumed that water replaced the carbon on the active sites of the surface area.

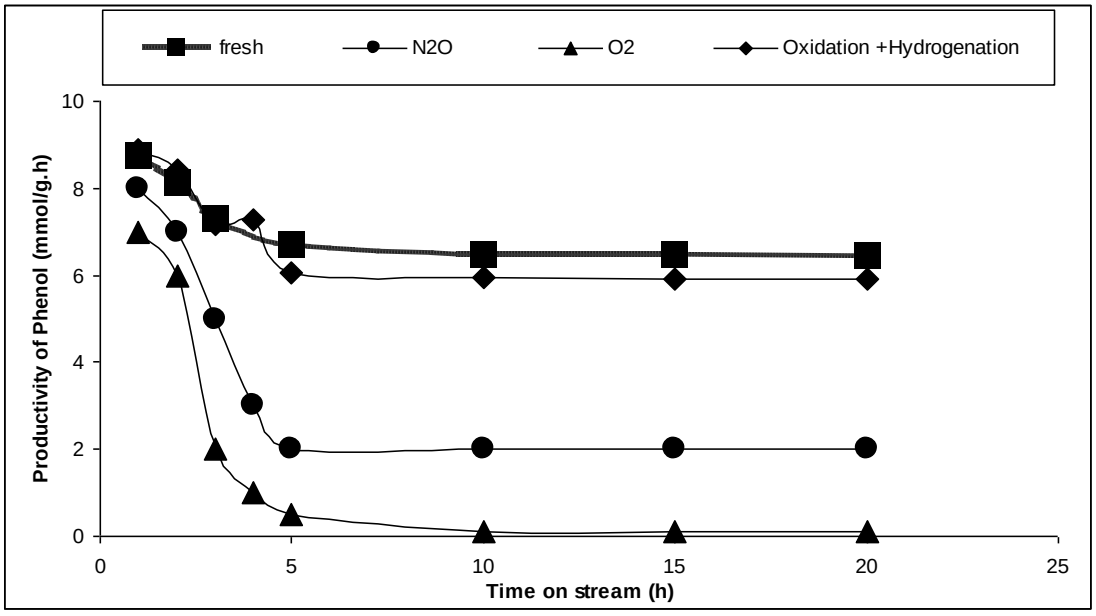


Figure 5.19 Phenol Productivity using the sample before and after catalyst regeneration for 0.1%FeZ80.

5.6 Kinetics of benzene hydroxylation to phenol

5.6.1 Kinetics of benzene hydroxylation using research Project data

One step oxidation of benzene to phenol was performed using a fixed bed reactor. A mixture of C_6H_6/He (50 ml/min) and N_2O (10ml/min) was used at 450°C for 20 h at atmospheric pressure. The total flow was 60 ml/min, contact time (0.5 s) and the molar C_6H_6/N_2O/He feed ratio was 1/7/92. Finely powdered 200mg of 0.1%Fe/Z80 catalyst was used for the reaction. The partial pressure of benzene is changed by changing the He flow through the benzene bubbler while an additional He line is maintained to balance the changes and keep the total flow constant. The rate seemed to be independent of the benzene partial pressure, this may be due to the sites are all saturated with benzene. This product is plotted logarithmically against benzene partial pressures in Figure 5.20, which shows that the reaction rate is zero order in benzene.

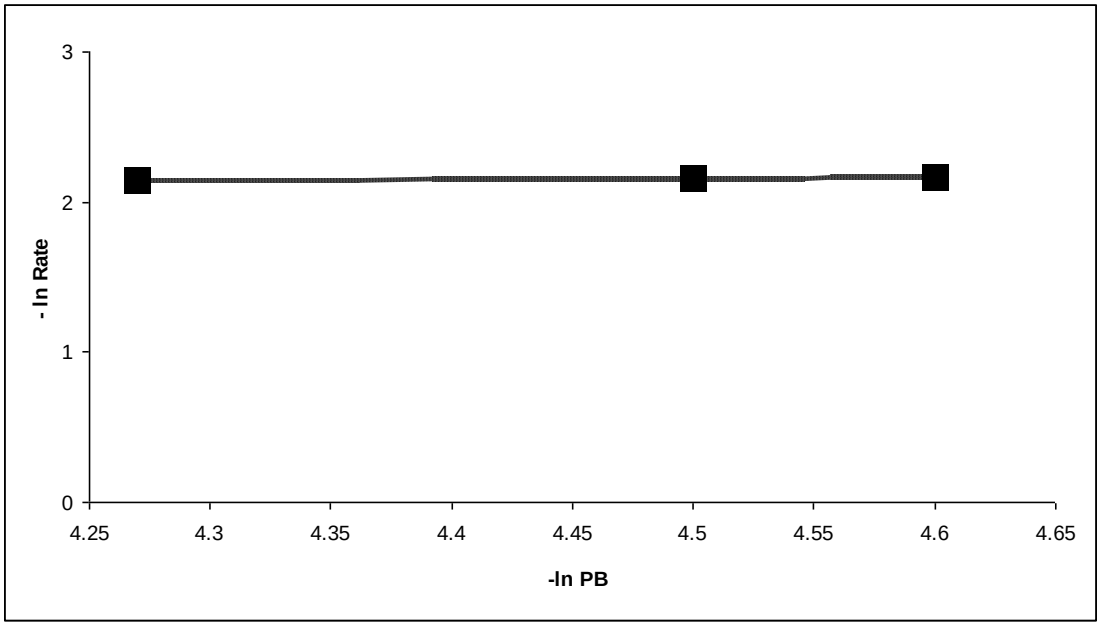


Figure 5.20 Plot of rate vs. benzene partial pressure at 1h using 0.1%FeZ80

The rate of catalytic reaction depends on the concentration of sorbed components and the concentration of active sites. The concentration of sorbed components depends on the gas phase concentration and the sorption equilibrium constant, which is temperature dependent.

The hydroxylation of benzene to phenol experiments have an excess of nitrous oxide resulted in the first order reaction behaviour. The net rate of phenol production is assumed to be approximately equal to the net rate of nitrous oxide consumption due to the selectivity of N_2O to phenol is ≥ 95%. Therefore, the net rate of phenol production is also first order in N_2O concentration (Yakovlev *et al*., 2001). Different literature review suggested that productivity increases linearly with feed gas N_2O less than 10 mol%. Panove *et al*., (2000) also reported that Fe/ZSM-5 is first order behaviour for nitrous oxide.

Literature references regarding the kinetics at conditions used in the present study are insufficient (Perez-Ramirez *et al*., 2003). The majority of studies were carried out in excess N_2O, where the yield increases with benzene concentration. On the other hand, a detailed kinetic study of an Fe/ZSM-5 catalyst under conditions of excess benzene has been published (Ivanov *et al*., 2003). They found that the rate of N_2O consumption is first order with respect to N_2O; it decreases with increasing benzene and phenol concentration. They also note that the rate of formation of catechol, hydroquinone and p-benzoquinone increases with the mole fraction of phenol, indicating a consecutive reaction. The kinetic equation for the rate of N_2O consumption in a (FBR) reactor with first order behaviour and also the sorption of nitrous oxide in the zeolite obeys Henry's Law with its concentration within the zeolite micropores can be written as:

$$r_{N_2O} = -\frac{dP_{N_2O}}{dt} = k_1 p_{N_2O}$$

$$t = 0 \Rightarrow \left(p_{N_2O} = p^0{}_{N_2O}\right)$$

$$k_1 = -\frac{\ln(1-x)}{t}$$

$$[N_2O] = \beta_{N_2O} P_{N_2O} v N_0$$

The unit of r_{N_2O} is partial pressure change per unit time. Contact time is also defined as catalyst bed volume (cm^3) / feed gas flow rate (cm^3/s). β_{N_2O} is the Henry's constant; N_0 the maximum sorption capacity of the zeolite micropores; v is the fraction of free micropore volume not occupied by molecules of benzene and phenol. Ivanov *et al*., (2003) said that the assumption of N_2O sorption obeying Henry's Law at the high temperatures of reaction seems to be reasonable. They suggested that the rate limiting step is the reaction between sorbed N_2O and unoccupied a-sites, and also the concentration of unoccupied catalyst active sites is constant.

In this work, the net rate of benzene and nitrous oxide consumption are assumed to be approximately equal to the net rate of phenol production (stoichiometry of the reaction are the same, 1:1).

$$C_6H_6 + N_2O \longrightarrow C_6H_5OH + N_2$$

$$bB + aA \longrightarrow cC + dD$$

$$-r_{N_2O} = -r_{C_6H_6} = r_{C_6H_5OH}$$

The rate seemed to be independent of $C_{C_6H_6}$, Therefore, the rate of phenol production can be written as

$$r_{C_6H_5OH} = k_1 P_{N_2O}$$

The rate of phenol production increased with increasing reaction temperatures. k_1 has been evaluated from the measured rate and partial pressure of N_2O. For the experimental results obtained in the current study, using the Arrhenius plot of apparent rate constant k_1 on temperatures (350, 400 and 450°C) is shown in Figure 5.21. The straight line fit between ln(k_1) and inverse absolute temperature and the slop of this plot gives a value of the apparent activation energy.

$$-r_B = \lfloor k(T)][\, fn(C_{N_2O}) \rfloor$$

$$k(T) = Ae^{-E_A/RT}$$

$$\ln k = \ln Ae^{-E_A/RT}$$

$$\ln k = \ln A - \frac{E}{R}\left(\frac{I}{T}\right)$$

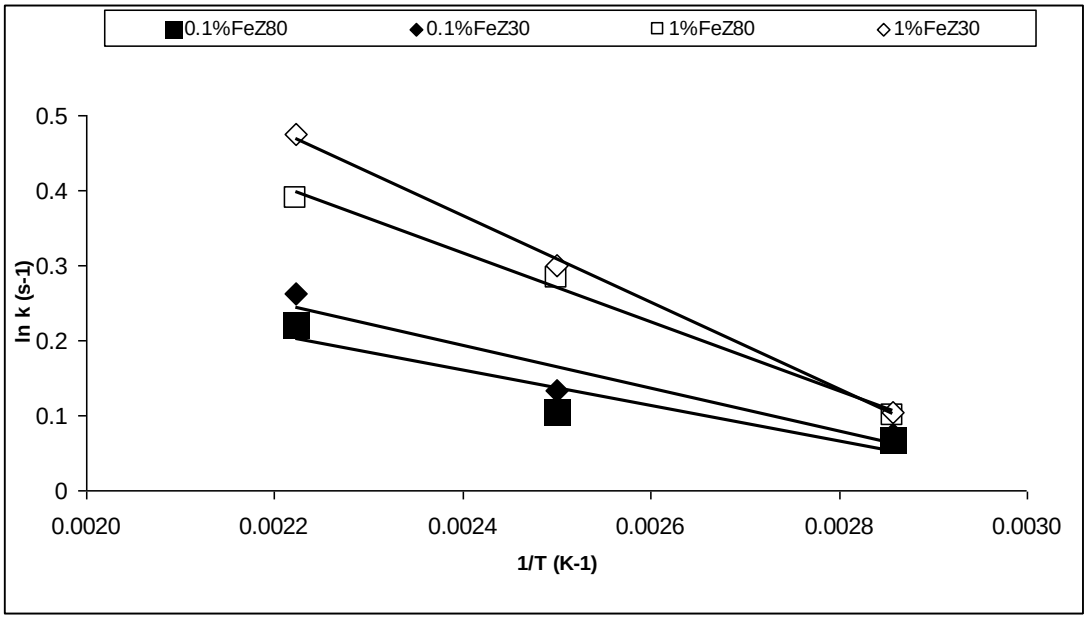


Figure 5.21 Arrhenius plot rate constants (k1) as a function of temperature.

The experiments also show that the apparent activation energy of the of the Fe/ZSM-5 catalysts is in the range (21 - 27) KJ/mol as shown in Figure 5.21, depending on the Fe/ZSM-5 catalysts (varying iron content, 0.1&1 wt% and Si/Al ratio, 30 & 80) preparation. It was calculated that activation energy for 0.1%FeZ80, 0.1FeZ30, 1%FeZ80, 1%FeZ30 were 21.06, 22.91, 24.65 and 26.95 kJ/mol respectively. Mehmet *et al.,* (2010) reported experimental results showing that the N_2O decomposition is a first order reaction. The apparent activation energy for the Fe/ZSM-5 catalysts was found to be 27 % kJ/mol, depending on the preparation methods.

If we assumed that the lack of dependence on benzene concentration true for all catalyst samples, then the rate of phenol production can be written as

$$r_{C_6H_5OH} = k_1 P_{N_2O}$$

5.6.2 Rate law from experimental data with the rate – limiting step

The reaction mechanism of benzene oxidation using nitrous oxide was discussed in Chapter 2.2. The mechanism of the hydroxylation process is based on the decomposition of N_2O to a monatomic chemisorbed O_2 and release of N_2. Gas phase benzene adsorbs on the chemisorbed oxygen. The next step involves phenol formation, and also desorption of phenol from the active sites and diffusion out of the zeolite channels. These steps are important for the kinetics of the process because of the relatively strong interaction of phenol surface sites within the zeolite catalyst. Chang *et al.,* (1994) reported that the decomposition of N_2O increased with increasing reaction temperatures, while the high concentration of N_2O in the feed (more than 10 mol %) does not effect the decomposition. Another study suggested that productivity increases linearly with feed gas N_2O less than 10 mol% (Panove *et al*., 2000).

The rate of N_2O decomposition can be written as

$$r = kP_{N_2O}$$

$$k = k_0 e^{-E_A / RT}$$

Rate law from experimental data (literature review)

The rate law of benzene depends on the benzene concentration only and was found not to be related to the nitrous oxide concentration (Louis *et al.,* 2001).

$$-r_B = \frac{k_3 C_B}{1 + \frac{k_3}{k_n} C_B} \qquad \textbf{(5.1)}$$

The rate law parameters for the reaction rate of benzene (eq 5.1) regarding the main reaction of benzene to phenol (Louis *et al.*, 2001):

$$k_3 = 2.3 \times 10^{-7} m^3 g^{-1} s^{-1}$$

$$k_n = 5.2 \times 10^{-7} mol\ g^{-1} s^{-1}$$

The rate – limiting step

The rate-limiting step considers a gaseous reactant (such as benzene) flowing through a bed of solid catalyst (zeolite). The chemical procedures involve activated adsorption of reactant with or without dissociation, surface reactions on active sites, and activated desorption of the products. A possible mechanism (see Chapter 2.2) has been hypothesized to explain the form of the observed rate expression (reaction rate of reactant ($\mathbf{-r_A}$), adsorption ($\mathbf{r_{AD}}$), surface reaction ($\mathbf{r_S}$)) and desorption ($\mathbf{r_D}$)) as shown below:

$\mathbf{-r_A = r_{AD} = r_S = r_D}$

Because there is no accumulation of reacting species on the surface, the rates of each step in the sequence are all equal. The overall reaction is

$$C_6H_6 + N_2O \longrightarrow C_6H_5OH + N_2$$

Elementary reaction steps

Adsorption: $B + S \leftrightarrow B.S$

Surface reaction: $B.S + S \leftrightarrow P_h.S + S$

Desorption: $P_h.S \leftrightarrow P_h. + S$

Assume a rate-limiting step.

The rate law for the adsorption step is

$$r_{AD} = k_{BA}\left[C_V P_B - \frac{C_{B.S}}{K_A}\right] \text{ Adsorption, where } K_A = \frac{k_A}{k_{-A}} \qquad (5.2)$$

The rate law for the surface reaction step is

$$r_S = k_S\left[C_{B.S} - \frac{C_{P.S}}{K_S}\right] \text{ Surface reaction, where } K_S = \frac{k_S}{k_{-S}} \qquad (5.3)$$

The rate law for the desorption step is

$$r_D = k_D\left[C_{P.S} - \frac{P_P C_V}{K_{DC}}\right]$$ Desorption, where $K_{DC} = \frac{k_D}{k_{-D}}$ and the phenol adsorption equilibrium constant is just the reciprocal of the phenol desorption constant $K_{PAD} = \frac{1}{K_{DC}}$

$$r_D = k_D\left[C_{P.S} - K_{PAD} P_P C_V\right] \qquad (5.4)$$

Assumed that the surface reaction – limited mechanism, since more than 75% of all heterogeneous reaction that are not diffusion-limited (are surface reaction-limited).

The rate law for the surface reaction step is

$$r_S = k_S\left[C_{B.S} - \frac{C_{P.S}}{K_S}\right] \text{ From equation (5.3)}$$

Using the other steps that are not limiting to find $C_{B.S}$ and $C_{P.S,}$ for surface reaction- limited reaction the adsorption specific rate k_A and desorption specific rate k_D are large compared with k_S :

Using $\frac{r_{AD}}{k_A} \cong 0 \cong \frac{r_D}{k_D}$ to find $C_{B.S}$ and $C_{P.S}$

Adsorption to obtain CB.S

$$r_{AD} = k_{BA}\left[C_V P_B - \frac{C_{B.S}}{K_A}\right] \Rightarrow C_{B.S} = K_A C_V P_B \quad (5.5)$$

Desorption to obtain CP.S

$$r_D = k_D\left[C_{P.S} - K_{PAD} P_P C_V\right] \Rightarrow C_{P.S} = K_{PAD} P_P C_V \quad (5.6)$$

Site balance, the only variable left to eliminate is C_V :

$$C_t = C_V + C_{B.S} + C_{P.S}$$

substituting for the concentrations of the $C_{B.S}, C_{P.S}$

$$C_t = C_V + K_A C_V P_B + K_{PAD} P_P C_V$$

$$C_V = \frac{C_t}{1 + K_A P_B + K_{PAD} P_P}$$

The rate law for the surface reaction step is

$$r_S = k_S\left[C_{B.S} - \frac{C_{P.S}}{K_S}\right]$$

Benzene rate law for the surface reaction

$$r_S = -r_B = k_S\left[K_A P - \frac{K_{PAD} P_P}{K_S}\right] C_V$$

$$r_S = -r_B = \frac{\overbrace{k_S C_t K_A}^{k}\left[P_B - \frac{P_P}{Kp}\right]}{1 + K_A P_B + K_{PAD} P_P}$$

$$Kp = \frac{K_S}{K_{PAD}}$$

$$r_S = -r_B = \frac{k\left[P_B - \frac{P_P}{Kp}\right]}{1 + K_A P_B + K_{PAD} P_P}$$

Neglecting the reverse reaction we have the rate law for surface- reaction limited mechanism.

$$r_S = -r_B = \frac{k\ p_B}{1 + K_A P_B} \qquad (5.7)$$

The correct mechanism and rate-limiting step were done by comparing the rate law derived in equation (3.7) $r_S = -r_B = \frac{k\ p_B}{1 + K_A P_B}$ with experimental data (literature review) in equation (3.1) $-r_B = \frac{k_1 C_B}{1 + \frac{k_1}{k_n} C_B}$

5.6.3 Derivation of the kinetic model

In the kinetic investigation, the simulations using the kinetic equations in differential form for fixed bed reactor were used to estimate the effect of weight of catalyst on the conversion, temperature and compositions of the reactant feed and product effluents. And also to compare the simulation results with the experimental results. All model parameters were estimated from literature by non-linear regression of the measured reactants and products concentrations in the fixed bed reactor.

In this case, reaction rate (eq 5.1) regarding the main reaction of benzene to phenol only.

Rate constants from literature

$k_1 = 2.3 \times 10^{-7}\ m^3 g^{-1} s^{-1}$

$k_n = 5.2 \times 10^{-7}\ mol\ g^{-1} s^{-1}$

Reaction rate of benzene (eq 5.1)

$$-R_B = \frac{k_1 C_B}{1 + k_2 C_B}$$

$$k_2 = \frac{k_1}{k_n} = \frac{m^3 g^{-1} s^{-1}}{mol\ g^{-1} s^{-1}} = 0.44 m^3 / mol$$

$$-R_B = \frac{k_1 C_B}{1 + k_2 C_B} = \frac{m^3 g^{-1} s^{-1}}{m^3 / mol} \frac{mol / m^3}{mol / m^3} = mol / g.cat.s$$

Differential form of the mole balance for packed bed reactor (PBR),
(molar flow rate of benzene (B) over catalyst weight)

$$\frac{dF_B}{dW} = r_B'$$

For flow system,

$$F_A = F_{A_0} - F_{A_0} X$$

Differential form of the design equation will be

$$\frac{dX}{dW} = \frac{-r_B'}{F_{B_0}}$$

$$-F_{B_0}\frac{dX}{dW} = r_B'$$

Reaction rate of benzene (eq 5.1)

$$-r_B' = \frac{k_1 C_B}{1+k_2 C_B} = -r_B = \frac{k\ p_B}{1+K_A P_B}$$

$$F_{B_0}\frac{dX}{dW} = \frac{k_1 C_B}{1+k_2 C_B}$$

Ideal gas equation

$$PV = nRT \Rightarrow P = \frac{n}{V}RT \Rightarrow P_B = C_B RT$$

$$C_B = \frac{P_B}{RT}$$

Divided by time

$$P_0 q_0 = F_{T_0} R T_0$$

$$P\,q\ = F_T\, RT$$

$$\frac{P_0 q_0}{P\,q} = \frac{F_{T_0} T_0}{F_{T_0}(1-\Im X)T}$$

Partial pressure of benzene

$$P_B = C_{B_0} RT(1-X)\frac{T_0}{T} y \Rightarrow P_B = P_{B_0}(1-X)y\frac{T_0}{T}$$

The total vlometric flow rate is

$$q = q_0(1+\Im X)\frac{P_0}{P}\frac{T}{T_0}$$

For flow system the mole fraction

$$\Im = y_{B_0}\delta = 0$$

$$q = q_0\frac{P_0}{P}\frac{T}{T_0}$$

Expressed the concentration of species (A, B, C, D) for flow system in terms of converstion

$$C_B = \frac{C_{B_0}(1-X)}{(1+\Im X)}\frac{P}{P_0}\frac{T_0}{T}$$

$$C_B = C_{B_0}(1-X)y\frac{T_0}{T}$$

$$y = \frac{P}{P_0}$$

$$P_B = C_{B_0}RT\frac{(1-X)}{(1+\Im X)}y\frac{T_0}{T}$$

$$P_P = P_{B_0}Xy\frac{T_0}{T}$$

$$P_{B_0} = (y_{B_0})(P_0)$$

An analytical solution equation for the pressure for isothermal operation can be written as:

$$y = \frac{P}{P_0} = (1-aW)^{\frac{1}{2}}$$

Table 5.2 presents the stoichiometric relationships between reacting molecules for hydroxylation of benzene to phenol reaction. This table shows that the molecules of species are formed during a chemical reaction. The stoichiometric relationships for reacting species are developed that give the change in the number of moles of each species (i.e. A, B, C and D). Species B (benzene) are taken as the basis of calculation (i.e. limiting reactant) to formulate the stoichiometric table as shown in Table 5.2.

$$C_6H_6 + N_2O \longrightarrow C_6H_5OH + N_2$$

$$B + A \longrightarrow C + D$$

Table 5.2 Stoichiometric Table for a flow system

Species	in	change	outlet
(N_2O) A	$F_{A0} = \Theta_A F_{B_0}$	$-F_{B0}X$	$F_A = F_{B0}(\Theta_A - X)$
(C_6H_6) B	F_{B0}	$-F_{B0}X$	$F_B = F_{B0}(\Theta_B - X)$
(C_6H_5OH) C	$F_{C0} = \Theta_C F_{B_0}$	$F_{B0}X$	$F_C = F_{B0}(\Theta_C + X)$
(N_2) D	$F_{D0} = \Theta_D F_{B_0}$	$F_{B0}X$	$F_D = F_{B0}(\Theta_D + X)$

Concentrations of reactant feed and product effluents

By expressed the concentration of species (A, B, C, D) for flow system in terms of converstion

Concentration of nitrous oxide

$$F_A = C_A.q$$

$$C_A = \frac{F_A}{q} = \frac{F_{B_0}[\Theta_A - X]}{q_0}\left(\frac{P}{P_0}\right)\left(\frac{T_0}{T}\right)$$

Conc. of benzene

$$C_B = \frac{F_B}{q} = \frac{F_{B_0}[\Theta_B - X]}{q_0}\left(\frac{P}{P_0}\right)\left(\frac{T_0}{T}\right)$$

Conc. of phenol

$$C_C = \frac{F_C}{q} = \frac{F_{B0}[\Theta_C + X]}{q_0}\left(\frac{P}{P_0}\right)\left(\frac{T_0}{T}\right)$$

Conc. of nitrogen

$$C_D = \frac{F_D}{q} = \frac{F_{B_0}[\Theta_D + X]}{q_0}\left(\frac{P}{P_0}\right)\left(\frac{T_0}{T}\right)$$

$$\Theta_i = \frac{F_{i_0}}{F_{B_0}}$$

Reaction rate considering competing reactions

Phenol may react consecutively with the chemisorbed oxygen to catechol ($C_6H_4(OH)_2$), hydroquinone ($C_6H_4(OH)_2$) and *p*-benzoquinone ($C_6H_4O_2$). Equations (2.19 - 2.21) show the molar rates of N_2O and benzene consumption and phenol formation (see Chapter 2.2). These equations show that the rate expressions regarding the consecutive reactions of phenol. The hydroxylation of phenol may be due to the strong adsorption and slow diffusion of phenol on the active site (Reitzmann *et al.,* 2002). The conversion, temperature and profile of the concentrations of benzene and phenol are shown as a function of catalyst weight in Figures (5.22 - 5.24) respectively considering the consecutive reaction in equation 2.19.

$$-R_B = K_{MR}\hat{K}_O \frac{K_{N_2O}\chi(N_2O)}{1+K_{N_2O}\chi(N_2O)} \times \frac{1}{1+(K_{Ph}\chi(Ph)/K_B\chi(B))} \quad \text{.....(2.19)}$$

$$-R_{N_2O} = K_{MR}\hat{K}_O \frac{K_{N_2O}\chi(N_2O)}{1+K_{N_2O}\chi(N_2O)} \times \frac{1}{1+(K_{Ph}\chi(Ph)/K_B\chi(B))} . + K_{SN}\hat{K}_O \frac{K_{N_2O}\chi(N_2O)}{1+K_{N_2O}\chi(N_2O)} +$$
$$2K_{SP2}\hat{K}_O \frac{K_{N_2O}\chi(N_2O)}{1+K_{N_2O}\chi(N_2O)} \times \frac{1}{1+(K_B\chi(B)/K_{Ph}\chi(Ph))} \quad \text{.....(2.20)}$$

$$-R_{Ph} = K_{MR}\hat{K}_O \frac{K_{N_2O}\chi(N_2O)}{1+K_{N_2O}\chi(N_2O)} \times \frac{1}{1+(K_{Ph}\chi(Ph)/K_B\chi(B))} . - K_{SP1}\frac{1}{1+(K_B\chi(B)/K_{Ph}\chi(Ph))} -$$
$$K_{SP2}\hat{K}_O \frac{K_{N_2O}\chi(N_2O)}{1+K_{N_2O}\chi(N_2O)} \times \frac{1}{1+(K_B\chi(B)/K_{Ph}\chi(Ph))} \quad \text{.....(2.21)}$$

Nomenclature

B= benzene

W= weight of catalyst

k ≡ kinetic constant

F_B = molar flow rate of benzene

P_B = partial pressure of Benzene

P_i = partial pressure of species

P_h ≡ phenol

$-r_B$ ≡ rate of reaction

S= active site of the surface area

$\chi(i)$ ≡ mole fraction of species (i)

X= conversion

Z≡ zeolite

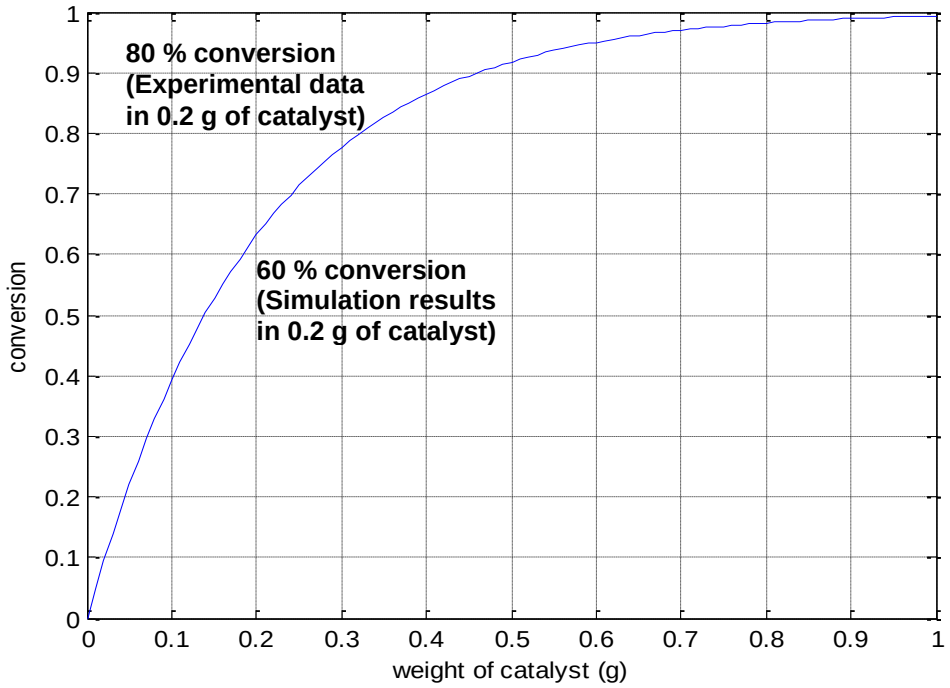


Figure 5.22 Conversion profile (reaction conditions: 1 mol% benzene, 7 mol% nitrous oxide, atmospheric pressure, feed gas =60ml/min).

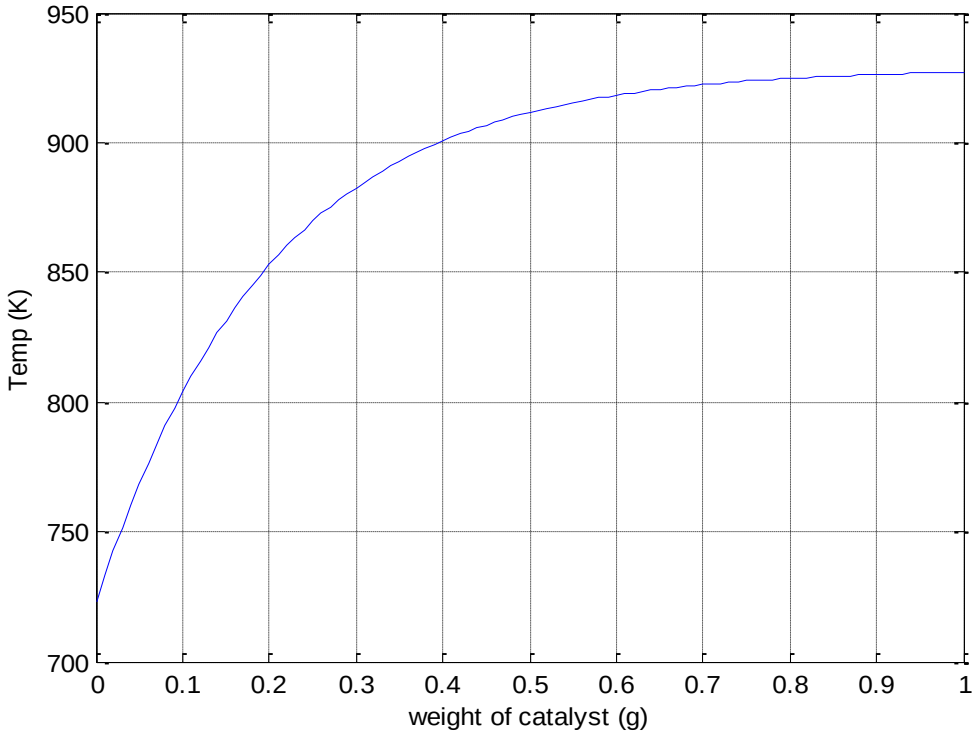


Figure 5.23 Temperature profile (reaction conditions: 1 mol% benzene, 7 mol% nitrous oxide, atmospheric pressure, feed gas =60ml/min).

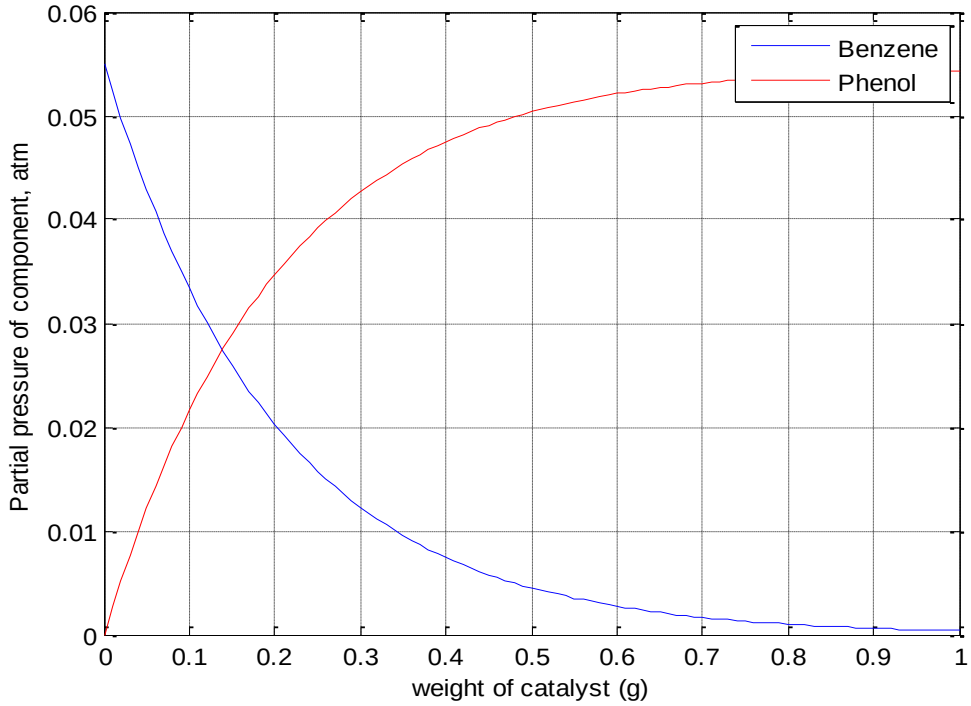


Figure 5.24 Benzene and phenol concentration profile (reaction conditions: 1 mol% benzene, 7 mol% nitrous oxide, atmospheric pressure, feed gas =60ml/min).

The conversion of benzene is shown as a function of catalyst weight (g) in Figure (5.22). The temperature and concentrations profiles of benzene and phenol are shown in Figure (5.23 and 5.24) respectively using the consecutive reaction (See the Appendix A). The simulation results are for the experimental conditions (as discussed earlier in Chapter 5) used in the experimental system. The model was used for an adiabatic reactor.

The results show that the temperature and the conversion increased as the weight of catalyst was increased. Figure 5.22 shows that the simulation results showed lower activity (benzene conversion) ~ 60% compared with experimental results ~80% using 0.2 g of Fe/ZSM-5 catalyst. Figure 5.23 shows that the weight of catalyst influences on the temperatures. However, the phenol productivity decreases with increasing reaction temperature. Phenol detection commenced at small amount of catalyst (see Figure 5.24). This indicates that the small amount of catalyst is active in the direct oxidation of benzene to phenol.

5.7 Conclusions

Fe-ZSM5 catalyst samples with different Si/Al ratios and different iron contents have been studied for the one step oxidation of benzene to phenol using N_2O as the oxidant. The hydroxylation of benzene to phenol takes place at elevated temperatures (350, 400 and 450 °C) and atmospheric pressure, with the benzene to phenol selectivity in the range of (80 - 92 %) with high benzene conversion (~80%) and with high average productivity (typically 6 mmol/g.cat.h or higher) using a low concentration of benzene and nitrous oxide compared with literature (~3 mmol/g.cat.h) such as (Hensen *et al*.,2005). Catalysts synthesized with high Si/Al ratios and with low iron content seem better suited in terms of long term operation. Catalysts regeneration using oxidation followed by reduction method seemed to be promising compared with N_2O and O_2 methods and may be this concludes that the regeneration method depends on the catalyst preparation and active site concentrations.

The modelling work on phenol production as a function of catalyst weight was studied in the fixed bed reactor. The simulation results show that the small amount of catalyst is active for phenol production from benzene and also show low conversion compared to experimental work (Chapter 5.3). High pressure drop leads to an increase in the reaction temperature. The main reason of further hydroxylation of phenol intermediate may be due to a high temperature. As a conclusion, only 0.2 g of Fe/ZSM-5 catalyst was used for one step oxidation of benzene to phenol as discussed earlier in this Chapter. The effect of coke formation and active sites on the hydroxylation of benzene to phenol has experimentally been done as discussed in chapters (4 and 5), but it has not been possible to include it into the model, so far. The application of the kinetic model to the data measured in the fixed bed reactor shows its limitation concerning the deactivation starting from phenol. Therefore, the model has to be extended by coke formation kinetics.

6 Conclusions and Recommendations for Future Work

6.1 Conclusions

A series of Fe/ZSM-5 catalysts were prepared using an ion exchange method at 900 °C calcination and characterized. A matrix of experiments has been done to evaluate the influence of catalyst properties on the production of phenol from benzene by one step hydroxylation. The results suggest that only a small fraction of iron ~0.1% is active in the selective oxidation of benzene to phenol in the presence of N_2O. However, this indicated that the only a fraction of the oxidized Fe^{+2} to Fe^{+3} species was able to generate the active oxygen for the oxidation of benzene to phenol. This fraction increase with decreasing iron concentration. A method for quantitive determination of the active Fe-containing sites responsible for the formation of propene peaks species is developed based on the isopropylamine decomposition. Possibly the presence of other inactive iron species and low amount of active sites makes it very difficult to identify the active sites in Fe-zeolites accurately. Iron is required for formation of extra framework species that are active in selective conversion of benzene to phenol. High reaction temperatures (450°C) leads to higher phenol productivity using low concentrations of benzene (1 mol %) and nitrous oxide (7 mol %). However, catalysts with high amounts of iron were particularly prone to deactivation at this temperature. Higher iron content loaded into the catalyst creates higher numbers of the active sites which caused further oxidation of products towards coke. The coke formation depends on the strong chemisorptions of phenol, probably on lewis acid sites, which hinders the fast back-desorption of phenol out of the zeolite channels. It was observed that the rate of coke formation increased with increasing reaction temperature and decreasing Si/Al ratio. The main reason could be some *α*-oxygen was consumed for converting phenol to dihydroxybenzene or coke formation by high temperature. Usually, the number of Bronsted sites increase with the decreased of the Si/Al ratio, since each Al atom replacing a Si framework atom creates a Bronsted site. This indicated that the presence of Al does not effect the composition and

properties of iron containing active sites but increases their concentration due to more favourable distribution of Fe in the zeolite matrix.

The catalytic behavior of Fe/ZSM-5 catalysts thus depends on the distribution of active sites in the zeolite channels due to the presence of competing reactions during phenol synthesis and further transformations having comparable rates. The catalyst acidity was influenced by the (Si/Al) ratio. This indicated that the acidity has a direct influence on catalytic activity and favors deactivation of samples due to coke formation. The deactivation effect of coke was shown to be due to the decrease in the number of active sites on the catalyst, which results in a significant decrease in the overall catalyst activity. The catalysts were regenerated by three different methods; oxygen, nitrous oxide and also by reduction method (oxidation followed by reduction). Reduction method was found to be a more efficient reactivation reagent than N_2O and O_2. The results also showed that the catalyst containing ~1 wt% iron was the most active (initially) for both Si/Al ratio (30 & 80), reaching ~80% conversion (of benzene) at about 450 °C while maintaining high selectivity ~90%. The whole set of the results obtained suggest that the preparation procedure significantly affects the nature of active centers and chemical characteristics of the surface of Fe/ZSM-5.

A kinetic model for phenol production from benzene was developed. The simulation results show that the small amount of catalyst is active for phenol production from benzene. It can be seen from the results that the low conversion of benzene ~60% was obtained compared with experimental work ~80% using 0.2 g of catalyst. This concludes that the catalyst preparation significantly affects the nature of active centers of the surface of Fe/ZSM-5.

6.2 Recommendations for future work

- Employ Infrared (IR) and Mossbauer Spectroscopy (MS) to explore the nature and structure of active sites. The Infrared (IR) technique is used to probe adsorbed species, active intermediates and the acid base properties of the catalyst surface. Mossbauer Spectroscopy can detect the Fe with different oxidation states (Fe^{+3} and Fe^{+2}), coordination states (octahedral and tetrahedral), and aggregation, this will lead to the design of more efficient catalysts.

- Study the effect of feed composition on phenol productivity using an excess of nitrous oxide (i.e. feed gas N_2O/C_6H_6 molar ratio >1) and compare the results with an excess of benzene (i.e. feed gas N_2O/C_6H_6 molar ratio <1) in order to reduce the deactivation of the catalyst for phenol production from benzene. This can be done by changing the rig design using a benzene dosing syringe instead of a benzene bubbler to increase the concentration of benzene.

- Employ Gas Chromatography - Mass Spectroscopy (GC-MS) instead of (GC) to evaluate a solution containing a number of chemicals. By combining the two techniques, we can qualitatively and quantitatively measure both the organic and inorganic (N_2O, CO and CO_2) composition of the reactant feed and the product effluents. This leads to improve the results accuracy such as the phenol selectivity.

References

Akers R. J., 1979, The Pre-treatment of Slurries. *The Second World Filtration Congress.* Loughborough University.

Apelian R.M., Degnan F.D, US Patent 5238677, 1996, Process for the dealumination of mordenite.

Barbera, D., Cavani, F., D'Alessandro, T., Fornasari, G., Guidetti, S., Aloise, A., Giordano, G., Piumetti, M., Bonelli, B. & Zanzottera, C. 2010, "The control of selectivity in benzene hydroxylation catalyzed by TS-1: The solvent effect and the role of crystallite size", *Journal of Catalysis,* **275**, 158-169.

Bhaumik A., Mukherjee P. and Kumar R., 1998, Triphase Catalysis over Titanium–Silicate Molecular Sieves under Solvent-free Conditions, *J. Catal*. **178** (1), 101.

Bianchi D., Bortolo R., Tassinari R., Ricci M. and vignola R., 2000, Direct Oxidation of Benzene to Phenol with Hydrogen Peroxide over a Modified Titanium Silicalite Angew. *Chem., Int. Ed*. **39**, 4321.

Boricha, A.B., Bajaj, H.C., Kim, T.H., Abdi, S.H.R. & Jasra, R.V. 2010, "Preparation of highly dispersed Pd-Cu on silica for the aerobic hydroxylation of benzene to phenol under ambient conditions", *Catalysis Letters,* **137**, 202-209.

Chang Y.A., McCarty J.G., Wachsman E.D. and Wong V.L., 1994, Catalytic decomposition of nitrous oxide over Ru-exchanged zeolites. *Appl.Catal. B, Env.***4**, 283.

Choi J., Kim T., Choo K., Sung J., Saidutta M.B., Ryu S., Song S., Ramachandra B. and Rhee Y., 2005, Direct synthesis of phenol from benzene on iron-impregnated activated carbon catalysts, *Applied Catalysis A: General*, **290** (1-2), 1-8.

Dedecek J., Kaucky D. and Wichterlova B., 2001, Al distribution in ZSM-5 zeolites: an experimental study, *Chem. Commun.,***11**., 970.

Dimitrova, R. & Spassova, M. 2007, "Hydroxylation of benzene and phenol in presence of vanadium grafted Beta and ZSM-5 zeolites", *Catalysis Communications,* **8**, 693-696.

Dubkov, K.A., Ovanesyan, N.S., Shteinman, A.A., Starokon, E.V. & Panov, G.I. 2002, "Evolution of iron states and formation of alpha-sites upon activation of FeZSM-5 zeolites", *Journal of Catalysis,* **207**, 341-352.

Ehrfeld W., Hessel V. and Loewe H., 2000, Microreactors, Weinheim: Wiley VCH.

Ehrich H., Berndt H., Pohl M.-M., Jahnisch K. and Baerns M., 2002, Oxidation of benzene to phenol on supported Pt-VOx and Pd-VOx catalysts, *Appl. Catal. A: Gen*. **230** (2), 271.

Guanjie MI., Jianwei LI., Dong QIU., Biaohua C., 2010., Kinetics of Coke Formation on a Fe-ZSM-5 Zeolite Catalyst in the One-step Oxidation of Benzene to phenol with N_2O, *CHINESE JOURNAL OF CATALSIS*. **31**, 547-551.

Gubelmann, M., Popa, J.M. and Tirel, P.J., 1991, Preparation of phenols by direct N2O hydroxylation of aromatic substrates. US Patent 5,055,623.

Guisnet M. and Magnoux P., 1989, Coking and Deactivation of Zeolites Influence of the Pore Structure, *Appl.Catal.General,* **54**, 1.

Hamada M., Niwa H., Oguri M. and Miyake T., 1993, *Process for producing phenols*, USA. Pat. 5,426,245.

Hamada M., Sasaki Y. and Mitake T., 1993, *A method for manufacturing a phenol*, Jap. Pat. 5-4935.

Hensen, E.J.M., Zhu, Q., Janssen, R.A.J., Magusin, P.C.M.M., Kooyman, P.J. & van Santen, R.A. 2005, "Selective oxidation of benzene to phenol with nitrous oxide over MFI zeolites: 1. On the role of iron and aluminum", *Journal of Catalysis,* **233**, 123-135.

Hensen, E.J.M., Zhu, Q. & van Santen, R.A. 2005, "Selective oxidation of benzene to phenol with nitrous oxide over MFI zeolites: 2. On the effect of the iron and aluminum content and the preparation route", *Journal of Catalysis,* **233**, 136-146.

Hideyki N., Mitiyki N. and Motohiro K., 1994, *A method of hydroxylation of aromatic compounds*. Jap. Pat. 6-256241.

Hiemer U., Klemm E., Scheffler F., Selvam T., Schwieger W. and Emig G., 2004, Microreaction engineering studies of the hydroxylation of benzene with nitrous oxide, *Chemical Engineering Journal*, **101**, 17 – 22.

http:/ www.the- innovation – group.com/, (2008)

http:/ www.iza-online.org

http:/ www.micromeritics.com

Ione K.G. and Vostrikova L.A, 1987, Isomorphism and Catalytic Properties of Silicates of Zeolite Structure, *Advance in chemistry,* **56**, 393.

Ivanov, A.A., Chernyavsky, V.S., Gross, M.J., Kharitonov, A.S., Uriarte, A.K. &Panov, G.I. 2003, "Kinetics of benzene to phenol oxidation over Fe-ZSM 5 catalyst", *Applied Catalysis A-General,* **249**, 327-343.

Jia J., Pillai K.S. and Sachtler W.M.H., 2004, One-step oxidation of benzene to phenol with nitrous oxide over Fe/MFI catalysts, *Journal of Catalysis*, **A 221**, 119 – 126.

Jian, M., Zhu, L., Wang, J., Zhang, J., Li, G. & Hu, C. 2006, "Sodium metavanadate catalyzed direct hydroxylation of benzene to phenol with hydrogen peroxide in acetonitrile medium", *Journal of Molecular Catalysis A: Chemical,* **253**,1-7.

Kirk-Othmer., 2005, Encyclopedia of Chemical Technology, 3rd Edition, **17**, 373.

Kitano T., Nakai T., Nitta M., Mori M., Ito S. and Sasaki K., 1994, *Bull. Chem. Soc.* Jpn. **67** (10), 2850.

Kleinloh W., 2000, Proceedings of the First ICIS-LOR World Phenol/Acetone Conference, 2000, Antwerpen

Kumar Jr A., Das S.K. and Kumar A., 1997, Formation of Phenol from Benzene Catalyzed by Polymer-Bound break Vanadyl Acetylacetonate, *J. Catal*. **166**, 108.

Kunai A., Kitano T., Kuroda Y., Li-Fen J. and Sasaki K., 1990, Gas phase oxidation of benzene to phenol using Pd-Cu composite catalysts, *Catal. Lett*. **4**, 139.

Kuznetsova, N.I. & Kuznetsova, L.I. 2009, "Hydrocarbon oxidation with an oxygen-hydrogen mixture: Catalytic systems based on the interaction of platinum or palladium with a heteropoly compound", *Kinetics and Catalysis,* **50**, 1-10.

Kuznetsova, N.I., Kuznetsova, L.I., Likholobov, V.A. & Pez, G.P. 2005, "Hydroxylation of benzene with oxygen and hydrogen over catalysts containing Group VIII metals and heteropoly compounds", *Catalysis Today,* **99**, 193-198.

Leanza R., Rosetti I., Mozzola I., and Forni L., 2001, Study of Fe-silicalite catalyst for the N2O oxidation of benzene to phenol*, Appl. Catal. A: General* **205**, 93.

Lee C.W., Lee W.J., Park Y.K. and Park S.E., 2000, Catalytic hydroxylation of benzene over vanadium-containing molecular sieves, *Catal. Today* **61** (1-4), 137.

Lee D.W., Lee J.H., Chun B.H. and Lee K.Y.,2003, The characteristics of direct hydroxylation of benzene to phenol with molecular oxygen enhanced by pulse DC corona at atmospheric pressure, *Plasma Chemistry and Plasma Processing,* **23** (3), 519-539.

Lioubove, K.M., Bulushev, D.A. & Renken, A. 2003, "Active sites in HZSM-5 with low Fe content for the formation of surface oxygen by decomposing N_2O: is every deposited oxygen active?", *Journal of Catalysis,* **219**, 273-285.

Liptakova B., Bahidsky M. and Hronec M., 2004, Preparation of phenol from benzene by one-step reaction, *Applied Catalysis*, **A 263**, 33 – 38.

LIU, T., WEI, X., ZHAO, J., XIE, H., WANG, T. & ZONG, Z. 2010, "Microwave-assisted hydroxylation of benzene to phenol with H_2O_2 over FeSO4/SiO2", *Mining Science and Technology (China),* **20**, 93-96.

Louis B., Kiwi-Minsker L., Reuse P., and Renken A., 2001, ZSM-5 Coatings on Stainless Steel Grids in One-Step Benzene Hydroxylation to Phenol by N2O: Reaction Kinetics Study, *Ind. Eng. Chem. Res*., **40**, 1454-1459.

Masumoto Y., Hamada R., Yokota K., Nishiyama S. and Tsuruya S., 2002, Liquid-phase oxidation of benzene to phenol by vanadium catalysts in aqueous solvent with high acetic acid concentration, *J. Mol. Catal. A Chem*. **184**, 215.

Mehmet F.F., Isik O., and Rutger A.,2010., A Density Functional Theory Study of Direct Oxidation of benzene to Phenol by N2O on a [FeO]+1 ZSM-5 Cluster. *J.Phys.Chem.***114**., 12580-12589.

Meloni, D., Monaci, R., Solinas, V., Berlier, G., Bordiga, S., Rossetti, I., Oliva,C. & Forni, L. 2003, "Activity and deactivation of Fe-MFI catalysts for benzene hydroxylation to phenol by N_2O", *Journal of Catalysis,* vol. **214**, , 169-178.

Mircea-Teodor N., Gloria B., Gabriele R., Silvia B. and Adriano Z., 2005, New precursor for the post-synthesis preparation of Fe-ZSM-5 zeolites with low iron content, *catalysis Letters,* **103**, 33- 41.

Miyahara T., Kanzaki H., Hamada H., Kuroiwa S., Nishiyama S. and Tsuruya S., 2001, Liquid-phase oxidation of benzene to phenol by CuO–Al2O3 catalysts prepared by co-precipitation method, *J. Mol. Catal. A Chem*. **176**,141.

Miyake T., Hamada M., Sasaki Y. and Oguri M., 1995, Direct synthesis of phenol by hydroxylation of benzene with oxygen and hydrogen, *Appl. Catal. A Gen.* **131**, 33.

Morrison R., and Boyd R.T., 1992, Organic Chemistry, Sixth Edition, Prentice Hall, Englewood Cliffs, New Jersery.

Molinari, R., Poerio, T. & Argurio, P. 2009, "Liquid-phase oxidation of benzene to phenol using CuO catalytic polymeric membranes", *Desalination,* **241,** 22-28.

Moulijin J.A., Diepen A.E. and Kapteijn F, 2001, Catalyst deactivation: is it predictable?: What to do?: *Appl.Catal.A:General,***212**, 3-16.

Niwa S., Eswaramoorthy M., Nair J., Raj A., Itoh N., Shoji H., Namba T. and Mizukami F., 2002, A one-step conversion of benzene to phenol with a palladium membrane, *Science.* **295**, 105.

Notte, P.P., 2000, The AlphOx process or the one step hydroxylation of benzene into phenol by nitrous oxide; understanding and tuning the ZSM-5 catalyst activities. *Topics in catalysis*, **13**, 387-394.

Ohtani T., Nishiyama S., Tsuruya S. and Masai M., 1995, Liquid-Phase Benzene Oxidation to Phenol with Molecular-Oxygen Catalyzed by Cu-Zeolites, *J. Catal*. **155**,158.

Panov G.I., 2000, Advances in Oxidation Catalysis; Oxidation of Benzene to Phenol by Nutrous Oxide, *CATTECH* **41**, 18.

Panov G.I., Uriate A.K., Rodkin M.A. and Sobolev V.I., 1988, Generation of active oxygen species on solid surfaces. Opportunity for novel oxidation technologies over zeolites*, Catal. Today*. **41**, 365.

Parmon V.N., Panov G.I., Uriarte A., and Noskov A.S., 2005 , '' Nitrous oxide in oxidation chemistry and catalysis: application and production'' *Catal.Today*. **100**, 115-131.

Passoni L.C., Luna F.J., Wallau M., Buffon R. and Schuchardt U., 1998, Heterogenization of H6PMo9V3O40 and palladium acetate in VPI-5 and MCM-41 and their use in the catalytic oxidation of benzene to phenol, *J. Mol. Catal. A Chem.* **134**, 229.

Perez-Ramirez, J., Kapteijn, F. & Bruckner, A. 2003, "Active site structure sensitivity in N2O conversion over FeMFI zeolites", *Journal of Catalysis,* **218**, 234-238.

Pérez-Ramírez, J., Kapteijn, F., Groen, J.C., Doménech, A., Mul, G. & Moulijn, J.A. 2003, "Steam-activated FeMFI zeolites. Evolution of iron species and activity in direct N2O decomposition", *Journal of Catalysis,* **214**, 33-45.

Perez-Ramirz J., US Patent 2006088469 '' Method for preparation and activation of multimetallic zeolite catalysts, a catalyst composition and application for N_2O abatement''.

Perathoner S., Pino F., Centi G., Giordano G., Katovic A., and Nagy J.B, 2006 ;Benzene selective oxidation with N_2O ON Fe/MFI catalysts: role of zeolite and iron sites on the deactivation mechanism, *Topic Catal.,* **23**, 125-136.

Pirutko, L.V., Chernyavsky, V.S., Uriarte, A.K. and Panov, G.I., 2002,Oxidation of benzene to phenol by nitrous oxide: activity of iron in zeolite matrices of various composition. *Appl Catal A Gen*, **227**, 143–157.

Qi, X., Li, J., Ji, T., Wang, Y., Feng, L., Zhu, Y., Fan, X. & Zhang, C. 2009, "Catalytic benzene hydroxylation over copper-substituted aluminophosphate molecular sieves (CuAPO-11)", *Microporous and Mesoporous Materials,* **122**, 36-41.

Reitzmann A., Emig G., Klemm E ., Kowalak S., Nowinska K., 2000, Metal-modified zeolite catalyst for the hydroxylation of aromatics with nitrous oxide, obtained by treatment of zeolite with gaseous metal salt, e.g. iron-III chloride followed by calcination at high temperature, U.S. Pat 19829515 A1.

Reitzmann A., Emig G., Klemm E ., 2002, Kinetics of the hydroxylation of benzene with N_2O on modified ZSM-5 zeolites, *Chemical Engineering Journal*. **90**, 149-164.

Remias J.E., Pavlosky T.A. and Sen A., 2003, Catalytic hydroxylation of benzene and cyclohexane using in situ generated hydrogen peroxide: new mechanistic insights and comparison with hydrogen peroxide added directly, *J. Mol. Catal. A: Chem,* **203**,179.

Ribera A., Arends I.W.C.E., de Vries S., Perez-Ramirez J. and Sheldon R.A., 2000 , Preparation, Characterization, and Performance of FeZSM-5 for the Selective Oxidation of Benzene to Phenol with N2O , *Journal of Catalysis*, **195**, 287 – 297.

Rodríguez-Reinoso F., 1998, The role of carbon materials in heterogeneous catalysis, *Carbon,* **36** (3), 159.

Salehirad F., Aghabozorg H.R., Manoochehri M. and Aghabozorg H., 2004, Synthesis of titatnium silicate-2 (TS-2) from methylamine-tetrabutylammonium hydroxide media, *Catalysis Communications*, **5**, 359 – 365.

Sayyar, M.H. & Wakeman, R.J. 2008, "Comparing two new routes for benzene hydroxylation", *Chemical Engineering Research and Design,* **86**, , 517-526.

Schmidt R.J., 2005, Industrial catalytic process – phenol production, *Applied Catalysis A: General*, < www.sciencedirect.com>.

Sirotin S. V. and Moskovskaya I. F., 2009 "Liquid-phase oxidation of benzene and phenol on MCM-41 mesoporous molecular sieves modified with iron and cobalt compounds" *Original Russian*, **49**, 104–110.

Stockmann M., Konietzni F., Notheis J.V., Voss J., Keune W. and Maier W.F., 2000, Selective oxidation of benzene to phenol in the liquid phase with amorphous microporous mixed oxides, *Appl. Catal. A Gen.* **208**, 343.

Sun, K., Xia, H., Feng, Z., van Santen, R., Hensen, E. & Li, C. 2008, "Active sites in Fe/ZSM-5 for nitrous oxide decomposition and benzene Hydroxylation with nitrous oxide", *Journal of Catalysis,* **254**, 383-396.

Taboada, Jerome.B., Hensen, E.J.M., Arends, I.W.C.E., Mul, G. & Overweg, A.R. 2005, "Reactivity of generated oxygen species from nitrous oxide over [Fe,Al]MFI catalysts for the direct oxidation of benzene to phenol", *Catalysis Today,* **110,** 221-227.

Tanarungsun, G., Kiatkittipong, W., Assabumrungrat, S., Yamada, H., Tagawa, T. & Praserthdam, P. 2010, "A REACTION-EXTRACTION-REGENERATION SYSTEM FOR HIGHLY SELECTIVE OXIDATION OF BENZENE TO PHENOL ", *Journal of Industrial and Engineering Chemistry,* **197**, 1140-1151.

Tatsumi T., 1993, *A method for manufacturing an aromatic hydroxy compound*, Jap. Pat. 5-320082.

Tesarova E, Packova V., 1983, Gas and high performance liquid chromatography of phenols. *Chromatographia*, **17**, 269-284.

Uriate A., 1998, Pat. WO 98/15514.

Wącław A., Nowińska K., Schwieger W., 2004 , Benzene to phenol oxidation over iron exchanged zeolite ZSM-5 , *Applied Catalysis A: General*, **270,** 151 – 156.

Wakeman R.J. and Tarleton E.S, 1999, Filtration: Equipment Selection, Modelling and Process Simulation*. Elsevier Advanced Technology*.

Wang, X., Guo, Y., Zhang, X., Wang, Y., Liu, H., Wang, J., Qiu, J. & Yeung, K.L. 2010, "Catalytic properties of benzene hydroxylation by TS-1 film reactor and Pd–TS-1 composite membrane reactor", *Catalysis Today,* **156**, 288-294.

Yamanaka H., Hamada R., Nibute H., Nishiyama S. and Tsuruya S., 2002, Gas-phase catalytic oxidation of benzene over Cu-supported ZSM-5 catalysts: an attempt of one-step production of phenol, *J. Mol. Catal. A Chem*. **178**, 89.

Yang, G., Zhou, D., Liu, X., Han, X. & Bao, X. 2006, "Possible active sites in Fe/ZSM-5 zeolite for the direct benzene hydroxylation to phenol: 1. μ-Oxo [Fe, M] species (M = Fe, Al)", *Journal of Molecular Structure,* **797.**, 131-139.

Yuichi I., Yo-Hei K., Naoya T., Keita T., 2010, One step Oxidation of Benzene to Phenol over Cu/Ti/HZSM-5 Catalysts, *Catal Lett.* **134**., 324-329.

Yuranov I., Bulushev D.A., Renken A., Kiwi-Minsker L., 2004 , Benzene hydroxylation over FeZSM-5 catalysts: which Fe sites are active , *Journal of Catalysis,* **227**, 138 –147.

Yuranov, I., Bulushev, D.A., Renken, A. & Kiwi-Minsker, L. 2007, "Benzeneto phenol hydroxylation with N_2O over Fe-Beta and Fe-ZSM-5: Comparison of activity per Fe-site", *Applied Catalysis A: General,* **319**, 128-136.

Yakovlev A.L., Zhidomirove G.M. and Santen R.A., 2001, DFT calaculation on N_2O Decomposition by binuclear Fe complexes in Fe/ZSM-5, *J.Phys.Chem,* **105**., 12297-12302.

Zakoshansky, V., 2009, Phenol process celebrates Its 60th Anniversary: The role of chemical principles in technological breakthroughs, *Russian Journal of General Chemistry*, 2009, **79** (10), 2244–2266.

Zhao Y., Bamwenda G.R., Groten W.A. and Wojciechowski B.W.J.,1993, The Chain Mecanism in Catalytic Cracking: The Kinetics of 2-Methylpentane Cracking.*J.Catal.,* **140**, 243-261.

Zhu Q., van Teeffelen R.M., van Santen R.A. and Hensen E.J.M., 2004 , Effect of high-temperature treatment on Fe/ZSM-5 prepared by chemical vapor deposition of FeCl3 II. Nitrous oxide decomposition, selective oxidation of benzene to phenol, and selective reduction of nitric oxide by isobutene , *Journal of Catalysis*, **221,** 575 – 583.

Appendixes

Appendix A: Modeling for reaction kinetics using a fixed bed reactor data.

Table1.1. Fixed bed reactor data for Fe ZSM-5 catalyst (Reitzmann *et al* 2002).

Parameter	Value
$\hat{K}_O$	1-1000
K_{N_2O}	33.1
$\left(K_{Ph} / K_B\right)$	7.1
K_{MR} (mmol/(gmin))	0.211
K_{SN} (mmol/(gmin))	0.114
K_{SP1} (mmol/(gmin))	0.032
K_{SP2} (mmol/(gmin))	0.014

Modeling for reaction kinetics

```
X0 = [0]; % initial value of conversion
Wspan=[0:0.01:1];
[W, X] = ode45('fbzsmr1', Wspan, X0);

Po = 1.1;        % initial pressure, atm
xBo = 0.01;      % inlet pressure of benzene, atm
xAo = 0.07;       % inlet pressure of N2O, atm
xIo = 0.92;      % inlet presser of helium, atm
qo = 1e-6;       % inlet flow rate, m3/s
a = 9.8e-3;      % value of alpha, g-1
P = Po.*((1-a.*W).^0.5);
T = To+((X*(389.54))/(1.8953))

pA = (xAo-xBo.*X).*P;
pB = xBo*(1.-X).*P;
pC = xBo.*X.*P;
pD = xBo.*X.*P;
pI = xIo.*P;

%plot (W, T, 'b')
%xlabel ('weight of catalyst')
%ylabel ('Temp')

figure (1)
plot (W, X, 'b')
xlabel ('weight of catalyst')
ylabel ('conversion')

figure (2)
plot (W, pB, 'b', W, pC, 'r')
plot(W,pB)
```

Table using Matlab program

```
function Xder=fbzsmr1(W,X)

% Constants:

Xder = zeros(1,1);

k1 = 0.11;       % KMR
k2 = 1;          % Ko, ranges between 1-1000
k3 = 28.7;       % KN2O, mmol/g.min
k4 = 4.5;        % KPh/KBenzene

To = 298;         % temperature, K
R = 8.314;       % gas constant, J/mol.K
Po = 1.1;        % total initial pressure, atm



xBo = 0.01;      % inlet mole fraction of benzene
xAo = 0.07;       % inlet mole fraction of N2O
xIo = 0.92;      % inlet mole fraction ofhelium
qo = 1e-6;       % inlet flow rate, m3/s
a = 9.8e-3;      % value of alpha, g-1
P = Po.*((1-a.*W).^0.5);



Xder = (R*To/(xBo*Po*qo))*(k1*k2*k3*(xAo-xBo*X)/(1+k3*(xAo-
xBo*X)))*((1-X)/(1-X+k4*X));
```

Table using Matlab program

Appendix B. Experimental setup and procedure

Appendix B.1 Oven Temperature

The calibration for the 1200°C Single Zone –Horizontal Tube Furnace (Oven) has been done at constant temperature 450°C using thermocouple type (K), it's suitable for high range of temperature (-240 – 1371°C). The length for the tube furnace is 36cm. Table 2.1. and Figure 2.1. show that the relation between the temperature and the length for the tube furnace. The parameter procedure for the oven following by starting procedure have been done. Figure 2.2. shows that the block diagram for the oven.

Table 2.1. The relation between the temperature and the length for the tube furnace.

Length of the oven tube	Temperature °C
2	229
4	309
6	357
8	402
10	422
12	431
14	440
16	445
17	448
18	449
19	447
20	442
22	437
24	427
26	413
28	391
30	355
32	310
34	230

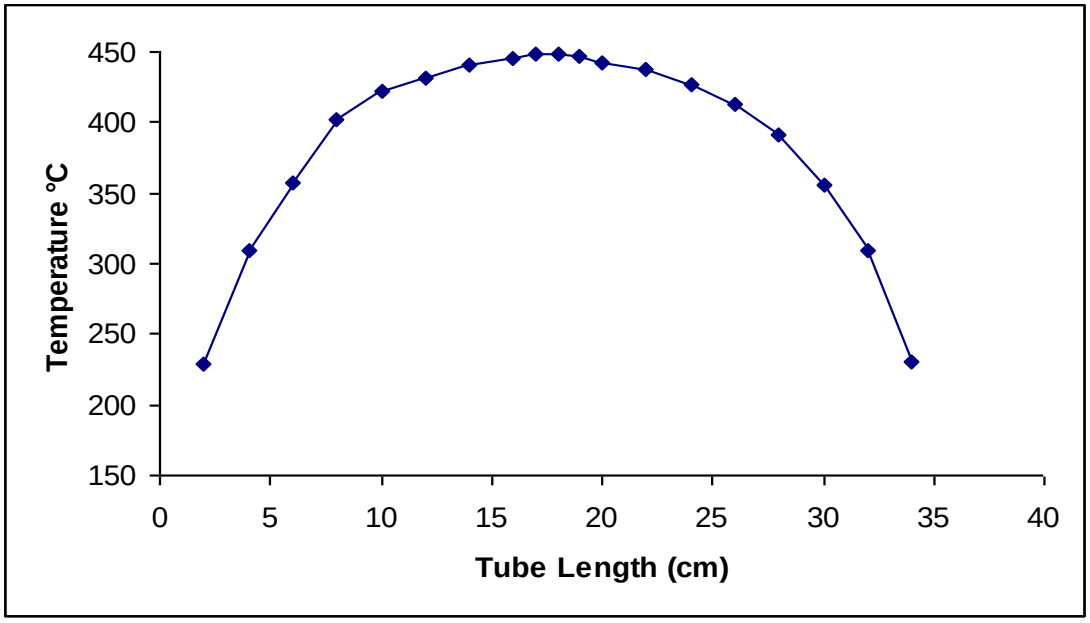


Figure.2.1. Oven temperature profile

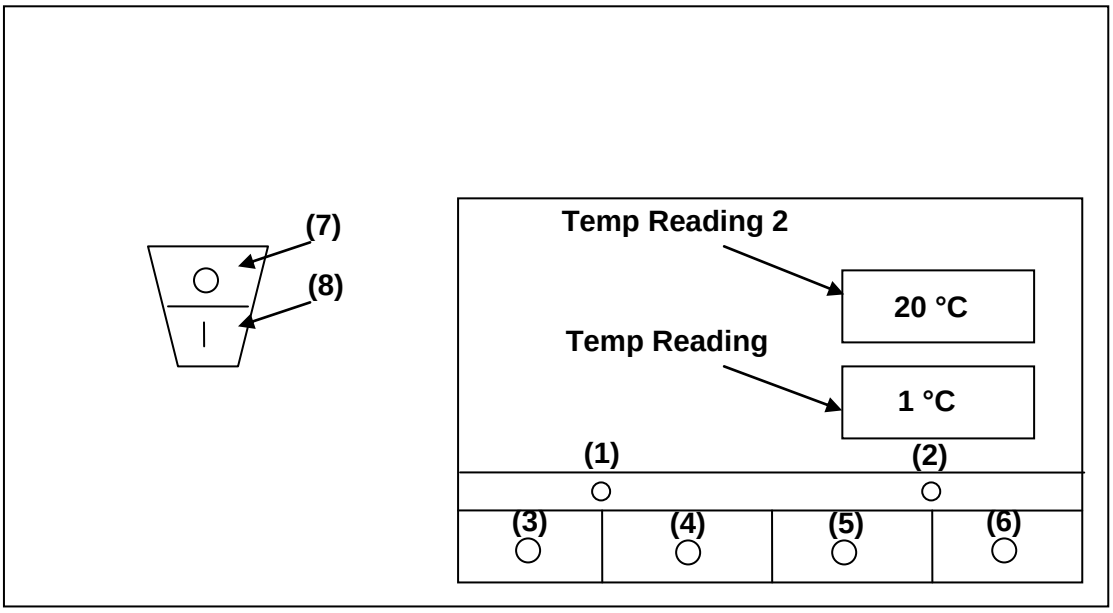


Figure 2.2. Block diagram of the 1200 ºC Single Zone-Horizontal Tube Furnaces

The Operating Procedure for the Oven:

1- Switch on the oven by pressing the button (number-8) in the figure 1.2. above and then set the parameters for the oven by doing the following:
2- Press the button (number-3) three times
3- Pressing the button (number-4), consecutively will yield the following if not press the button (number 5) in each step to find the following:

- [Hb off]
- [Hb 0]
- [rmp.u min]
- [dwl.u hours]
- [cyc.n1] this can be adjusted to give the desired cycle by pressing button (number 6) consecutively
- [SEG.n.1]
- [Type rmp.r]
- [tGt such as 450 °C] this can be adjusted to decrease or increase the temperature by pressing button (number 5 or 6) consequently
- [rate 1.0] this can be adjusted to give the desired (temperature/min) by pressing button (number 6) consecutively
- [SEG.n.2]
- [type dw E11]
- [dur such as 2.0 hours] this can be adjusted to give the desired time(h) by pressing button (number 5 or 6) consecutively, this will allow to keep the constant temperature you need for your reaction
- [SEG n.3]
- [Type rmp.r]

- [tGt 25 C] this can be adjusted to give the desired temperature by pressing button (number 5) consecutively
- [rate 1.0] this can be adjusted to give the desired (temperature/min) by pressing button (number 6) consecutively
- [SEG n.4]
- [type E End]
- [prog list]

4. Starting procedure for the oven by pressing the button (number-3) six times
5. Press the button (number-4), the display (Temperature reading 1 and 2) in figure 1.2. above will show: (Stat off)
6. Press the button (number-5), the display (Temperature reading 1) in figure 1.2. above will show: (Stat run)
7. If you want to turn it off, press the same button (number-5) again, it will appear: (Stat off)
8. Switch the oven off by pressing the button (number-7)

Heat transfer

Calculation for the length required to heat 120 ml/min of (benzene in helium and nitrous oxide) of the hydroxylation of benzene to phenol:

T_R= 450 °C

T_L= 230 °C

T_1= 100 °C

Average temperature = 165 °C

L = ? , D= 0.3cm , St =? , Re = ? , $\mu = 0.00019 \frac{s}{cm^2}$, Pr = 0.68

$$q = 2 \frac{cm^3}{s}$$

$$\frac{T_L - T_R}{T_1 - T_R} = \exp\left(-4St \frac{L}{D}\right)$$

$$-4St \frac{L}{D} = \ln\left(\frac{T_L - T_R}{T_1 - T_R}\right) = \ln\left(\frac{230 - 450}{100 - 450}\right) = -0.46$$

$$4St \frac{L}{D} = 0.46$$

$$L = \frac{0.46 \times 0.3}{4 \times St}$$

$$f = 0.08\,\mathrm{Re}^{-\frac{1}{4}}$$

$$\mathrm{Re} = \frac{4 \times q(cm^3/s)}{3.142 \times D(cm) \times \mu(cm^2/s)} = 44669$$

$$\mathrm{Re} = \frac{4 \times 2}{3.142 \times 0.3 \times 0.00019} = 44669$$

$$f = 0.08 \times 44669^{-\frac{1}{4}} = 0.006$$

$$\frac{f}{2} = 0.003$$

$$\mathrm{Pr}^{\frac{2}{3}} \times St = \frac{f}{2} = 0.003$$

$$St = 0.0039$$

$$L = \frac{0.46 \times 0.3}{4 \times 0.0039} = 8.8cm$$

Appendix B.2

Example for experimental setup and procedure (to be read in conjunction with line diagram 002)

The experimental rig consists of a gas handling system (N_2O and vapour of benzene in helium) feeding a packed bed reactor (PBR) consists of catalyst. The reactor exit gas mixture was sampled and analyzed in-line as described in chapter 4 above and also using off-line using a sample syringe as shown below. Concentrations of products was determined by GC and separating them using capillary columns DB-1701. Below the startup and shutdown procedures for the experimental rig design as shown in Figures 4.9 and 4.10 in chapter 4.

Operator procedure for filling the benzene bubbler

- Open the nuts in line [004] and line [006].
- Take the bubbler out to the fume hood and then open the nut connected directly to bubbler.
- Fill the bubbler using 50ml benzene using the measuring tube and glass fennel and then close it again. All these will be done inside the fume hood.
- Return the bubbler back between lines [004 and 006] and then close the nuts again

Catalyst replacement procedure

1- Open the nuts in line [013] and line [014] and then take the stainless steel tube out of the oven.
2- Clean the tube using air.
3- Weight the 0.2g of the ZSM-5 catalyst using the small bottle which has certain amount of catalyst and then close it, after that the catalyst will be weighted using the balance in safety way.
4- Put 200 mg Zeolite catalyst in the middle of the stainless steel tube and then hold it by quartz wool.

5- Return the reactor back between lines [013 and 014] inside the oven and then close the nuts again.

Start up procedure

- Switch on the MFC1.
- Switch on the heating bath and the oven 1.
- Set the helium (He) cylinder pressure using the pressure regulator to 2.5 bar.
- Set the nitrous oxide (N_2O) cylinder pressure using the pressure regulator to 2.5 bar.

(To measure the feed composition before reaction)

- Open (V2) in line [004] and close (V1) in line [002] to benzene bubbler and then close (V3) in line [005].
- Close (V5) in line [007] and open (V4) in line [006] and position 3-way valve (V6) in line [011] in line [012]. And then position 3-way valve (V7) in line [013]
- position 3-way valve (V8) to vent.
- Open the (He) cylinder regulator allowing (He) gas to flow through the MFC 1 in line [002] to measure the flow rate of (He) using the bubble flow.
- Open the (N_2O) cylinder regulator allowing (N_2O) gas flow through the FC 1 in line [001] to measure the flow rate of (N_2O) using the bubble flow.
- Measure the flow rate using the bubble flow before GC and then, position 3-way valve (V8) in line [015] to to 6 way valve and then to GC to measure the flow rate.

(To measure the feed composition after reaction)

- Position 3-way valve (V7) in line [013] to flow gases through line [014] to [Oven2- Packed Bed Reactor (PBR)] and then position 3- way valve (V8) to vent, to measure the flow rate and then position 3- way valve (V8) in line [015] to 6 way valve and then to GC to measure the composition for the reactant and products effluent.

(For by pass (Vent))

- Position 3-way valve (V8) in line [013] to vent.
- Position 3-way valve (V7) in line [013] and then position 3-way valve (V6) in line [012] through oven 1.
- Close the (N_2O) cylinder valve to prevent (N_2O) gas flow through the FC 1 in line [001].
- Open (V1) in line [002] and close (V2 and V4) in line [004 and 006] consequently to passing (He) directly through line [007].

Shut down procedure

- Turn (N_2O) cylinder regulator off.
- Switch off the FC1.
- Switch off the heating bath and the oven 1.
- Close (V2 and V3) in line [004 and 006] consequently and open (V1) in line [002] to passing directly through line [009 & 011].
- Position (V6) in line [011] to vent.
- Turn (He) cylinder regulator off.
- Switch off the MFC1.
- Close (V1) in lines [002].
- Close (V6) in line [011].
- Switch off all the plugs.

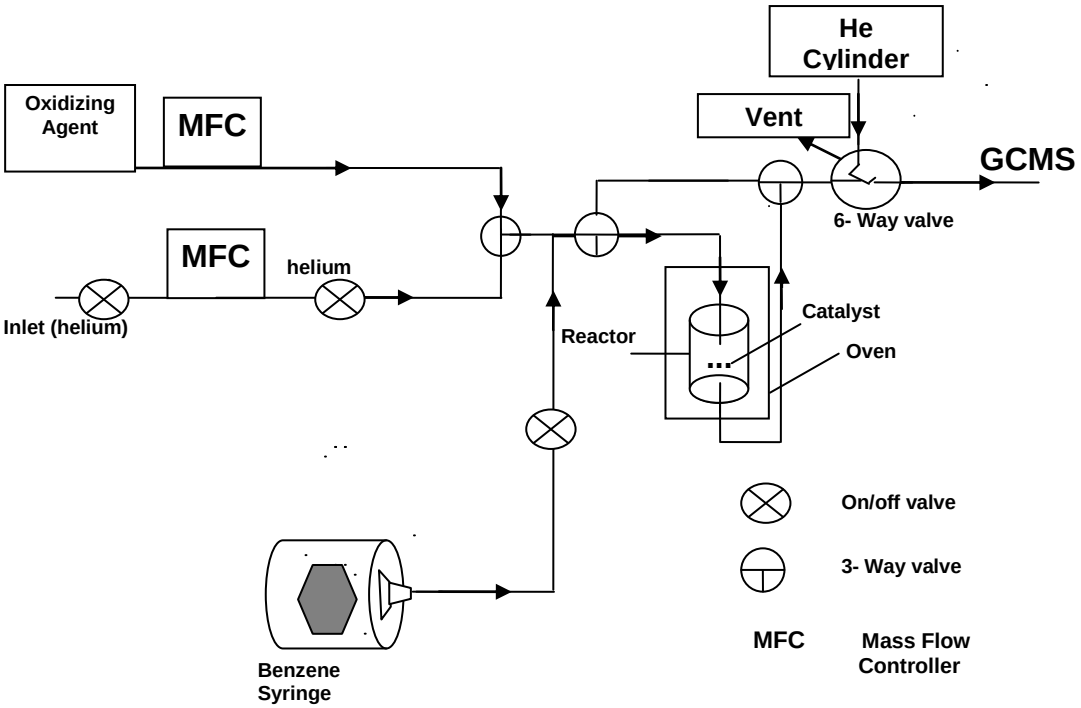


Figure 2.3 A line diagram (001) of the fixed bed reactor system.

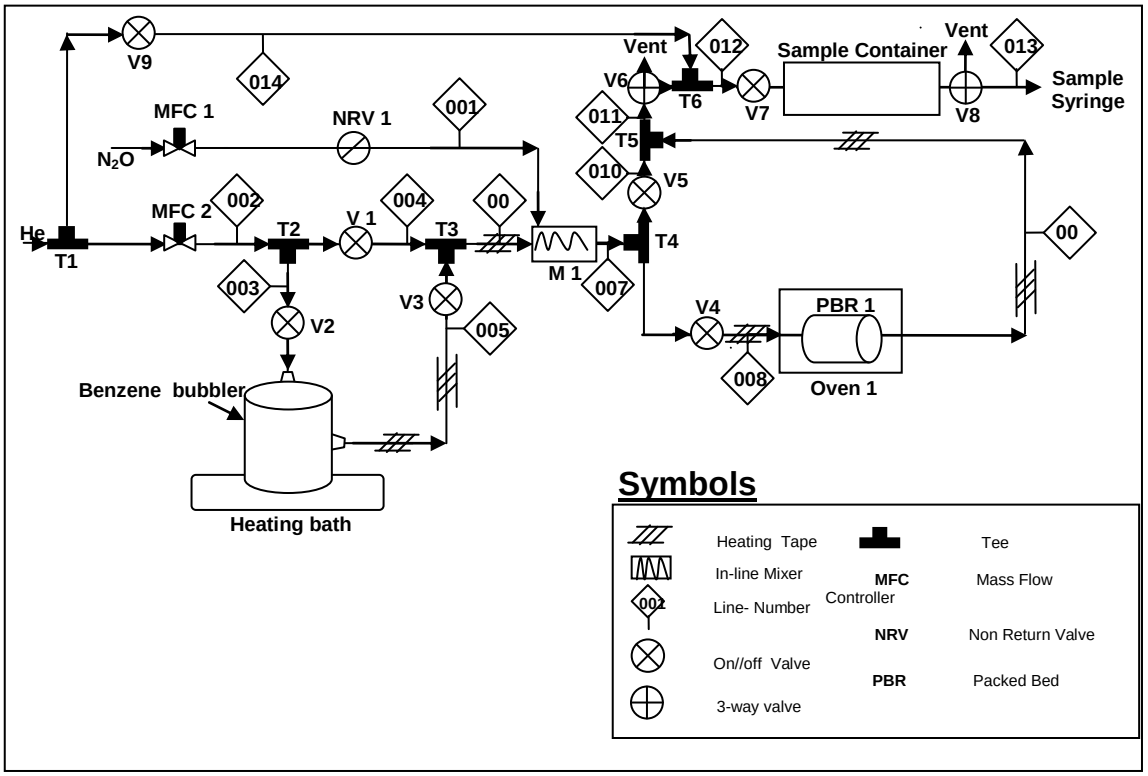


Figure 2.4. A line diagram (002) of the fixed bed reactor system.

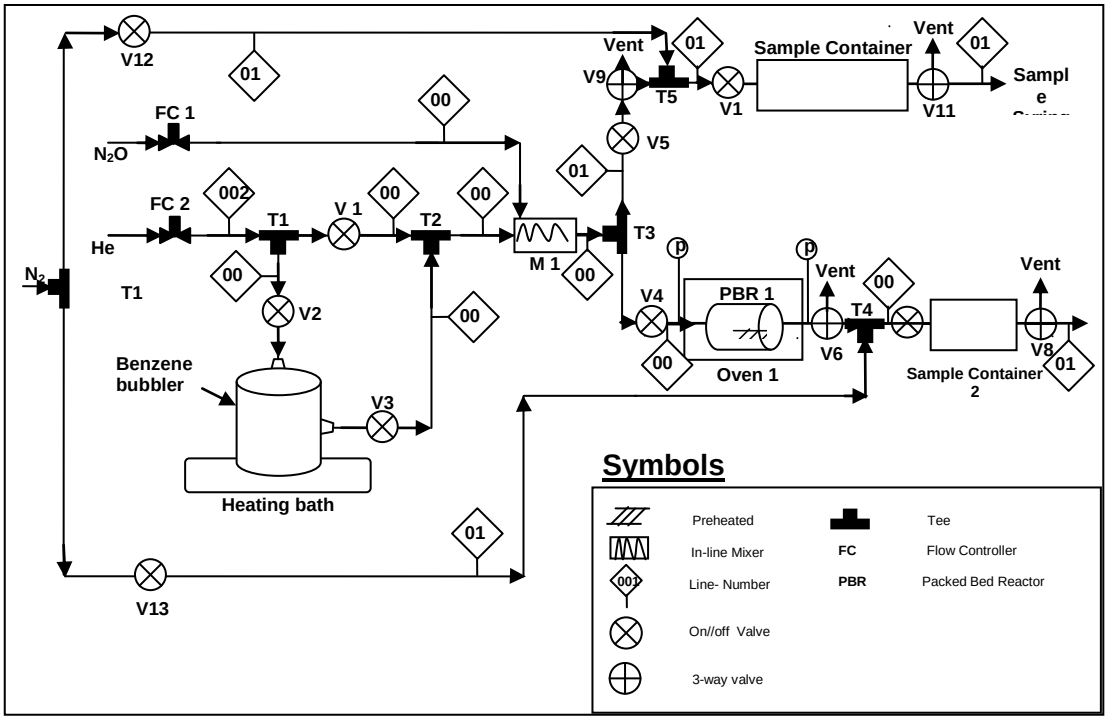


Figure 2.5. A line diagram (003) of the fixed bed reactor system.

An example for startup and shutdown procedures for line diagram (002) using off-line GC as shown in figure 2.4 in appendix B.2 .

Operator procedure for filling the benzene bubbler

- Open the nuts in line [003] and line [005].
- Take the bubbler out to the fume hood and then open the nut connected directly to bubbler.
- Fill the bubbler using 50ml benzene using the measuring tube and glass fennel and then close it again. All these will be done inside the fume hood.
- Return the bubbler back between lines [003 and 005] and then close the nuts again

Catalyst replacement procedure

- Open the nuts in line [008] and line [009] and then take the quartz tube out of the oven.
- Clean the tube using air.
- Weight the 0.5g of the ZSM-5 catalyst using the small bottle which has certain amount of catalyst and then close it, after that the catalyst will be weighted using the balance in safety way.
- Put 500 mg Zeolite catalyst in the middle of the quartz tube and then hold it by quartz wool.
- Return the quartz tube back between lines [008 and 009] inside the oven and then close the nuts again.

Start up procedure

- Switch on the MFC1.
- Switch on the heating bath and the oven 1.
- Set the helium (He) cylinder pressure using the pressure regulator to 2.5 bar.
- Set the nitrous oxide (N_2O) cylinder pressure using the pressure regulator to 2.5 bar.

(To measure the feed composition before reaction)

- Open (V1) in line [002] and close (V2) in line [003] to benzene bubbler and then close (V3) in line [005].
- Close (V4) in line [008] and open (V5) in line [010] and position 3-way valve (V6) in line [011] to vent.
- Close (V9) in line [014].
- Open the (He) cylinder regulator allowing (He) gas to flow through the MFC 1 in line [002] to measure the flow rate of (He) using the bubble flow.

- Open the (N_2O) cylinder regulator allowing (N_2O) gas flow through the FC 1 in line [001] to measure the flow rate of (N_2O) using the bubble flow.
- To measure the feed composition using the syringe, open (V2) in line [003] to benzene bubbler and then open (V3) in line [005] and close (V1) in line [004].
- Open (V5) in line [010] and close (V4) in line [008] and position 3-way valve (V6) in line [011] to [Sample Container 1] through line [012] and then open (V7) in line [012] and position 3-way valve (V8) to flow the gases through line [013].
- After 15 minutes close (V7) in line [012] and then close (V8) in line [013] to collect the sample.

(To flash the sample container (1) before reaction)

- Position 3-way valve (V6) in line [011] to vent and open (V7) in line [012] and position 3-way valve (V8) in line [013] to vent and then open (V9) in line [014] to allow (He) gas flow directly to sample container (1) through line [012].

(To measure the feed composition after reaction)

- Close (V9) in line [014] and then open (V7) in line [012] and position 3-way valve (V8) in line [013] to flow gases through line [013] and open (V4) in line [008] to [Oven1- Packed Bed Reactor (PBR)] and close (V5) in line [010] and then position 3- way valve (V6) in line [011] to the [Sample Container 1] through line [012] after view minutes, close (V7) in line [012] and then close (V8) in line [013] to collect the sample.

(For by pass (Vent))

- Position 3-way valve (V6) in line [011] to sample container through line [012] and then open (V7) in line [012] and position 3-way valve (V8) in line [013] to vent.
- Open (V5) in line [010] and close (V4) in line [008].
- Close the (N_2O) cylinder valve to prevent (N_2O) gas flow through the FC 1 in line [001].
- Open (V1) in line [004] and close (V2 and V3) in line [003 and 005] consequently to passing (He) directly through line [007].

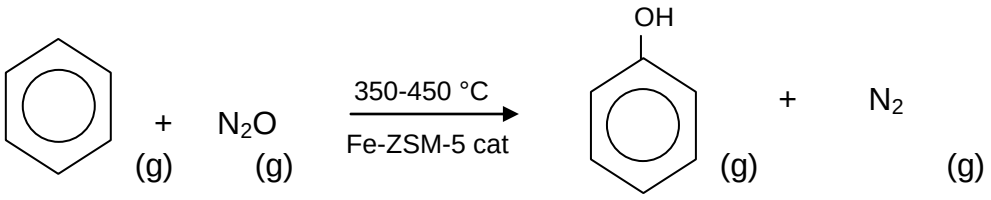
Shut down procedure

- Turn (N_2O) cylinder regulator off.
- Switch off the FC1.
- Switch off the heating bath and the oven 1.
- Close (V2 and V3) in line [003 and 005] consequently and open (V1) in line [004] to passing directly through line [007].
- Close (V5) in line [010] and then close (V7 and V8) in line [012 and 013] consequently and then open (V4) in line [008] and position (V6) in line [011] to vent.
- Turn (He) cylinder regulator off.
- Switch off the MFC1.
- Close (V1) in lines [004].
- Close (V4) in line [008] and close (V6) in line [011].
- Switch off all the plugs.

Heat of reaction and energy balance

The observed heat transfer that occurs in a closed system (with zero work) as a result of a reaction represents the energy associated with the rearrangement of the bonds holding together the atoms of the reacting molecules. For the hydroxylation of benzene to phenol (exothermic reaction), the energy required to hold the products of the reaction together is less than that required to hold the reactants together. In this section the effects of chemical reaction in the energy balance are described. The standard heat of reaction from standard heats of formation are calculated. Heat balance for adiabatic reactor and the adiabatic reaction temperature are calculated.

Heat of reaction



B + A ⟶ C + D

(M_W)

B = Benzene = 78.11 g/mol

A = N_2O = 44 g/mol

C = Phenol = 94 g/mol

D = N_2 = 28 g/mol

Heat Capacities $(kJ/mol.K) = a + bT + cT^2 + dT^3$

$$C_{P_{,B(g)}} = (74.06\times10^{-3}) + (32.95\times10^{-5})T - (25.20\times10^{-8})T^2 + (77.57\times10^{-12})T^3$$

$$C_{P_{A(g)}} = (37.66\times10^{-3}) + (4.151\times10^{-5})T - (2.694\times10^{-8})T^2 + (10.57\times10^{-12})T^3$$

$$C_{P_{D(g)}} = (29.00\times10^{-3}) + (0.2199\times10^{-5})T + (0.5723\times10^{-8})T^2 - (2.871\times10^{-12})T^3$$

$$C_{P_{C(g)}} = 0.173 kJ/mol.K$$

The standard heat of formation (kJ/mol)

$$\Delta\hat{H}_{o\,f(B)} = (+82.93_{(g)})$$

$$\Delta\hat{H}_{o\,f(A)} = (+81.5_{(g)})$$

$$\Delta\hat{H}_{o\,f(c)} = (-235.31_{(g)})$$

$$\Delta\hat{H}_{o\,f(D)} = 0_{(g)}$$

$$\Delta\hat{H}^{0}{}_{RX}(T_R) = [-235.31] - [81.5 + 82.93]$$

$$\Delta\hat{H}^{0}{}_{RX}(T_R) = -399.74 kJ/mol$$

Reaction Temperature (T) = 723 (K) = 450 °C

Reactor diameter (d= 0.2 cm)

P_0 =? And P_{exit} = 1 atm

$$P_1V_1 = n_tRT_1$$

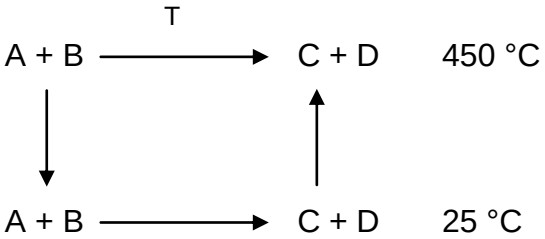
$$P_1q_1 = nRT_1$$

$$P_2q_2 = nRT_2$$

$$\frac{q_1}{q_2} = \frac{T_1}{T_2}$$

$$\frac{T_2}{T_1}q_1 = q_2$$

$$\frac{723}{298}\times1 = q_2 = 2.4 cm^3/s$$



$$\Delta\hat{H}_{RX}(T) = \Delta\hat{H}^{0}{}_{RX}(T_R) + \int_{T_R}^{T} \Delta C_P dT$$

$$\Delta\hat{H}_{RX}(T) = \Delta\hat{H}^{0}{}_{RX}(T_R) + \int_{T_R}^{T} C_{P_C} dT + \int_{T_R}^{T} C_{P_D} dT - \int_{T_R}^{T} C_{P_A} dT - \int_{T_R}^{T} C_{P_B} dT$$

$$\Delta\hat{H}^{0}{}_{RX}(25^{o}C) = -399.74$$

$$\int_{25^{o}C}^{400^{o}C} C_{P_B} dT = (74.06\times10^{-3})T\Big|_{25^{o}C}^{450^{o}C} + (32.95\times10^{-5})\frac{T^2}{2}\Big|_{25^{o}C}^{450^{o}C} - (25.20\times10^{-8})\frac{T^3}{3}\Big|_{25^{o}C}^{450^{o}C}$$

$$+ (77.57\times10^{-12})\frac{T^4}{4}\Big|_{25^{o}C}^{450^{o}C}$$

$$\int_{25^{o}C}^{400^{o}C} C_{P_B} dT = 33.33 + 33.31 - 7.65 + 0.79 = 59.78 kJ/mol$$

$$\int_{25^{o}C}^{400^{o}C} C_{P_D} dT = 11.17 kJ/mol$$

$$\int_{25^{o}C}^{400^{o}C} C_{P_A} dT = 16.85 kJ/mol$$

$$\int_{25^{o}C}^{400^{o}C} C_{P_C} dT = 375\times0.173 = 65 kJ/mol$$

$$\Delta\hat{H}_{RX}(450^{o}C) = (65 + 11.16) - (16.85) - (59.78) + (-399.74)$$

$$\Delta\hat{H}_{RX}(450^{o}C) = -400.21 kJ/mol$$

Considering only the reaction to phenol and not regarding consecutive reactions of phenol there is a release of energy of 4258 kJ per kg of phenol produced.

$$94\frac{g}{mol} = 94\frac{kg\times10^{-3}}{mol} = 0.094\frac{kg}{mol}$$

$$\frac{400.21 kJ/mol}{0.094 kg/mol} = 4258 kJ/kg$$

Energy balance

$$\dot{Q} - \dot{W}_S + \sum_{i=1}^{n} F_{i_0} H_{i_0} - \sum_{i=1}^{n} FiHi = 0$$

$$\dot{W}_S = 0$$

$$In: \sum H_{i_0} F_{i_0} = H_{A_0} F_{A_0} + H_{B_0} F_{B_0} + H_{C_0} F_{C_0} + H_{D_0} F_{D_0} + H_{i_0} F_{i_0}$$

$$Out: \sum H_i \, F_i \, = H_A \, F_A \, + H_B \, F_B \, + H_C \, F_C \, + H_D \, F_D \, + H_i \, F_i$$

$$\sum_{i=1}^{n} F_{i_0} H_{i_0} - \sum_{i=1}^{n} FiHi = F_{A_0}(H_{A_0} - H_A) + F_{B_0}(H_{B_0} - H_B) + F_{C_0}(H_{C_0} - H_C) + F_{D_0}(H_{D_0} - H_D)$$
$$+ F_{i_0}(H_{i_0} - H_i) - \underbrace{\left[H_D + H_C \, - H_B \, - H_A\right]}_{\Delta H_{RX}} F_{B_0} X$$

$$H_i = H_{i_0}(T_R) + \int_{T_R}^{T} C_{P_i} dT$$

$$H_{i_0} - H_i = \int_{T_R}^{T_0} C_P dT - \int_{T_R}^{T} C_P dT$$

$$H_{i_0} - H_i = \tilde{C}_{P_i}(T_0 - T_R) - \tilde{C}_{P_i}(T - T_0)$$

$$H_{i_0} - H_i = \tilde{C}_{P_i}(T_0 - T)$$

$$\Delta H_{RX}(T) = H_D(T) + H_C(T) - H_B(T) - H_A(T)$$

$$\Delta H^0{}_{RX}(T_R) = H^0{}_D(T_R) + H^0{}_C(T_R) - H^0{}_B(T_R) - H^0{}_A(T_R)$$

$$\Delta H_{RX}(T) = \left[H^0{}_D(T_R) + H^0{}_C(T_R) - H^0{}_B(T_R) - H^0{}_A(T_R)\right] + \int_{T_R}^{T} \left[C_{P_D} + C_{P_C} - C_{P_B} - C_{P_A}\right] dT$$

$$\Delta \hat{H}_{RX}(T) = \Delta \hat{H}^0{}_{RX}(T_R) + \int_{T_R}^{T} \Delta C_P dT$$

$$\Delta \hat{H}_{RX}(T) = \Delta \hat{H}^0{}_{RX}(T_R) + \Delta \hat{C}_P (T - T_R)$$

Case 1: for adiabatic operation $(Q = 0)$

Case 2: for non adiabatic operation $\frac{dQ}{dW} = Ua(T_a - T)$

Where **a** is the heat exchange area (wall) per weight catalyst.

$Case:1$

$$\dot{Q}-\dot{W}_S+\sum_{i=1}^{n}F_{i_0}H_{i_0}-\sum_{i=1}^{n}FiHi=0$$

$$\dot{Q}=0$$

$$\dot{W}_S=0$$

$$\sum_{i=1}^{n}F_{i_0}H_{i_0}-\sum_{i=1}^{n}FiHi=0$$

$$\Delta\hat{H}_{RX}(T)=\Delta\hat{H}^{0}{}_{RX}(T_R)+\Delta\hat{C}_P(T-T_R)$$

$$\tilde{C}_{P_A}=\tilde{C}_{P_B}(\Delta\hat{C}_P=0)$$

$$\Delta\hat{C}_P=\left(\tilde{C}_{P_D}+\tilde{C}_{P_C}-\tilde{C}_{P_A}-\tilde{C}_{P_B}\right)\left[T-T_r\right]\approx 0$$

$$\Delta\hat{H}_{RX}(T)=\Delta\hat{H}^{0}{}_{RX}(T_R)+\Delta\hat{C}_P(T-T_R)\approx\Delta\hat{H}^{0}{}_{RX}(T_R)$$

Heat Balance for adiabatic PFR case:

$$\left[\Delta H^{0}{}_{RX}(T_R)+\Delta\tilde{C}_P(T-T_R)\right]F_{B_0}X=F_{B_0}\sum\Theta_i\tilde{C}_{P_i}(T-T_0)$$

$$X\left[-\Delta H_{RX}(T)\right]=\int_{T_0}^{T}\sum\Theta_i C_{P_i}dT$$

$$X\left[-\Delta H_{RX}(T)\right]=\sum\Theta_i\tilde{C}_{P_i}(T-T_0)$$

$$(T-T_0)=\frac{X\left[-\Delta H_{RX}(T)\right]}{\sum\Theta_i\tilde{C}_{P_i}}$$

$$T=T_0+\frac{X\left[-\Delta H_{RX}(T)\right]}{\sum\Theta_i\tilde{C}_{P_i}}$$

$$\Delta\hat{H}_{RX}\left(450^{o}C\right)=-400.21kJ/mol$$

$$T=T_0+\frac{X\left[400.21\right]}{\sum\Theta_i\tilde{C}_{P_i}}$$

$$\sum\Theta_i\tilde{C}_{P_i}=\frac{F_{A_0}}{F_{B_0}}\tilde{C}_{P_A}+\tilde{C}_{P_B}+\frac{F_{C_0}}{F_{B_0}}\tilde{C}_{P_C}+\frac{F_{D_0}}{F_{B_0}}\tilde{C}_{P_D}$$

$$\left(A=N_2O\right)\rightarrow\tilde{C}_{P_A}=\frac{34.1}{723}=0.047KJ/mol.k$$

$$\left(B=C_6H_6\right)\rightarrow\tilde{C}_{P_B}=\frac{112.3}{723}=0.155KJ/mol.k$$

$$\left(C=C_6H_5OH\right)\rightarrow\tilde{C}_{P_C}=0.173KJ/mol.k$$

$$\left(D=N_2\right)\rightarrow\tilde{C}_{P_D}=\frac{29.9}{723}=0.041KJ/mol.$$

$$C_{A_0} = C_{B_0} = 1mol/m^3$$
$$q_0 = 1cm^3/s = 1\times10^{-6}m^3/s \Rightarrow F = C\times q$$
$$\left(F_{A_0} = 1\times10^{-6}mol/s\right)\left(F_{B_0} = 1\times10^{-6}mol/s\right)\left(F_{C_0} = 0\right)\left(F_{D_0} = 3.96\times10^{-5}mol/s\right)$$

$$P_0V_0 = N_{T_0}RT_0$$
$$\frac{N_{T_0}}{t} = F_{T_0}$$
$$\frac{V_0}{t} = q_0$$
$$P_0q_0 = F_{T_0}RT_0$$
$$P_0 = 2.5\times10^5 N/m^2$$
$$F_{T_0} = \frac{P_0q_0}{RT_0} = \frac{\left(2.5\times10^5\right)P_a\times\left(1\times10^{-6}\right)m^3/s}{8.314\frac{P_a\ m^3}{mol\ k}\times723k}$$
$$F_{T_0} = 4.16\times10^{-5}mol/s$$
$$\left(F_{A_0} = 1\times10^{-6}mol/s\right)+\left(F_{B_0} = 1\times10^{-6}mol/s\right)+\left(F_{C_0} = 0\right)+\left(F_{D_0} = ?\right) = F_{T_0} = 4.16\times10^{-5}mol/s$$
$$F_{D_0} = 3.96\times10^{-5}mol/s$$

$$\sum\Theta_i\tilde{C}_{P_i} = (\frac{1\times10^{-6}}{1\times10^{-6}}\times0.047)+0.155+(\frac{3.96\times10^{-5}}{1\times10^{-6}}\times0.041) = 1.8256kJ/mol.k$$

$$T = T_0 + \frac{X\left[400.21kJ/mol\right]}{1.8256kJ/mol.k}$$
$$T = 298 + 219X =$$
$$T = 298 + 175 = 473k$$

The benzene conversion is ~80 % as shown in chapter 6.

Calculation for the size (volume) of the benzene bubbler

$$q = 120 ml/\min = 120 \frac{cm^3}{\min} \times \frac{m^3}{(100)^3} = 1.2 \times 10^{-4} m^3/\min$$

$$P = CRT$$

$$Pq = FRT$$

$$P = 2.5 \times 10^5 \frac{N}{m^2}$$

$$T = 373$$

$$F = \frac{2.5 \times 10^5 \times 1.2 \times 10^{-4}}{8.314 \times 373} mol/\min$$

$$F_T = 9.7 \times 10^{-3}$$

$$F_{C6H6} = F_T \times yB \Rightarrow 9.7 \times 10^{-3} \times 0.5 = 4.84 \times 10^{-3} mol/\min$$

$$F_{C6H6} = 4.84 \times 10^{-3} mol/\min$$

$$t_{\exp} = 10 \times 60 = 600 \min$$

$$N_{C6H6} = 4.84 \times 10^{-3} \times 600 = 2.904 moles$$

$$M_{C6H6} = 2.904 \times 78 = 226.5 g$$

$$V_{C6H6} = \frac{226.5}{0.879} = 258 ml$$

The vapour pressure of Benzene

The vapour pressure of Benzene at various Temperatures was calculated in the table (2.2.) from the equations below [Ref] Physical Chemistry book and the relation between vapour pressure of Benzene and Temperature (k), different temperature of Benzene peaks (Just we have different Vapour pressure) and concentration of benzene are shown in Figure (2.6).

$$\frac{dp}{dt} = \frac{\Delta_{vap}H}{T(Rt/p)}$$

$From$

$$\frac{dp}{dt} = \frac{\Delta_{vap}H}{T\Delta_{VAP}V} \qquad \Rightarrow \Delta_{VAP}V = V_{m(g)} - V_{m(l)} \approx V_{m(g)}$$

$$\Delta_{vap}V = V_{m(g)}$$

$$V_{m(g)} = RT/P \Rightarrow \frac{dp}{dt} = \frac{\Delta_{vap}H}{T(Rt/p)} \Rightarrow \frac{dLnp}{dt} = \frac{\Delta_{vap}H}{RT^2}$$

$$\mathrm{P} = \mathrm{P}e^{-x}$$

$$X = \frac{\Delta_{VAP}H}{R}\left[\frac{1}{T} - \frac{1}{T^*}\right]$$

For example at 10 ^{0}C:

$$\mathrm{P} = 760e^{-x}$$

$$\Delta_{vap}H(KJmol^{-1}) = (+30.8)$$

$$\mathrm{P} = \mathrm{P}e^{-x}$$

$$X = \frac{\Delta_{VAP}H}{R}\left[\frac{1}{T} - \frac{1}{T^*}\right] \Rightarrow X = \frac{3.08\times10^4\ jmol^{-1}}{8.3145\ jk^{-1}mol^{-1}}\left[\frac{1}{283K} - \frac{1}{353K}\right]$$

$$at 10^{\circ}C = 57\mathrm{P}Torr = 0.074atm$$

Table (2.2) Relation between vapour pressures at various temperatures

Temperature k	Temperature ^{0}C	VAPOUR PRESSURE(atm)	VAPOUR PRESSURE(Torr)
273	0	0.046	35
283	10	0.074	57
293	20	0.117	89
303	30	0.177	135
313	40	0.2618	199
323	50	0.377	287
333	60	0.533	405
343	70	0.736	560

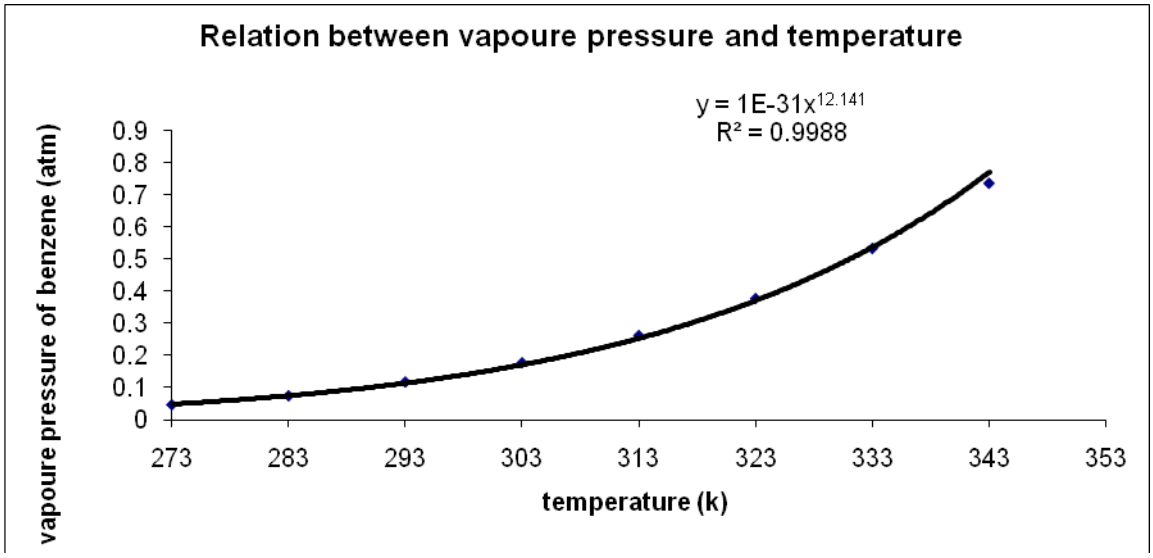


Figure (2.6) Relation between vapour pressure and temperature

Appendix B.3: Standard preparation and calibration method using (GC) and MFCs

Calibration of MFCs

He calibration for MFC

Table 2.3. calibration data of He (MFC)

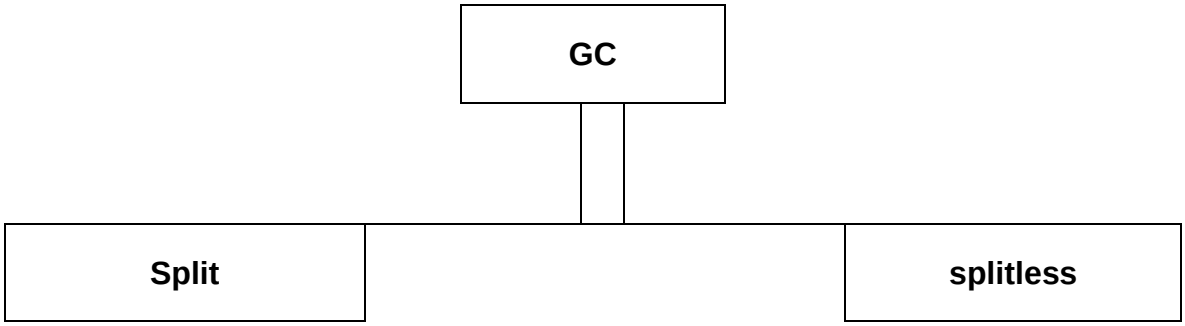
MFC Reading	He ml/min	He ml/min	He ml/min	Avr He ml/min	SD
5	3.8	3.7	3.7	3.74	0.058
10	11	10.8	10.9	10.90	0.10
15	19.5	19.4	19.5	19.47	0.058
20	27	27	26.6	26.87	0.23
25	34	33	33	33.33	0.58
30	41	41	41.5	41.17	0.29
40	54	54	55	54.33	0.58
45	60	61	62	61.00	1.00
50	69	69	68	68.67	0.58

N_2O calibration for MFC

Table 2.4. calibration data of N_2O (MFC)

MFC Reading	N_2O ml/min	N_2O ml/min	N_2O ml/min	Avr N_2O ml/min	SD
10	2	2.2	2.1	2.10	0.10
15	5.5	5.5	5.4	5.47	0.058
20	8.1	8.3	8.7	8.37	0.31
25	11.8	11.6	11.9	11.77	0.15
30	14.5	14.1	15.4	14.67	0.67
35	18	18.2	18.3	18.17	0.15
40	21.2	21.3	22.2	21.57	0.55

Method development using different method for of-line rig design with gas syringe.



GC	Split	Benzene in ethanol	He ml/min	10		25		50	
			Ramp Temperature °C/min	20	30	20	30	20	30
			Oven Temperature °C	80		80		80	
		Hydroquinone, Phenol, p-benzoquinone and Catechol in Ethanol	He ml/min	50					
			Ramp Temperature °C/min	5		10		20	
			Oven Temperature °C	250			300		
	splitless	Benzene in ethanol	He ml/min	25		50		100	
			Ramp Temperature °C/min	20	30	20	30	20	30
			Oven Temperature °C	80	80	80	80	80	80
		Hydroquinone, Phenol, p-benzoquinone and Catechol in Ethanol	He ml/min	25		50		100	
			Ramp Temperature °C/min	20	30	20	20	30	
			Oven Temperature °C	250 &300	250 &300	250 &300	250 &300	250 &300	

Standard preparation and calibration method using (GC)

The purpose of this method to determine the organic composition of the reactants and products for the hydroxylation of benzene to phenol by Gas Chromatography (GC) using [DB - 1701 (J&W)] column. Tables 2.5 to 2.9 show calibration data for injections of reactant and products standards of known composition into the GC.

Benzene

Table 2.5. GC calibration data for benzene (0.6 – 2 wt%)

Concentration wt%	Micro Moles of Benzene	Integrated Area of Peaks	SD	CV
0.6	0.06	505	14	0.03
1	0.10	895	7	0.01
2	0.20	1819	103	0.06

Table 2.6 GC calibration data for benzene (2 – 15 wt%)

Concentration wt%	Micro Moles of Benzene	Integrated Area of Peaks	SD	CV
2	0.20	1819	103	0.06
5	0.51	2747	56	0.02
8	0.82	3444	70	0.02
10	1.02	3872	65	0.02
15	1.54	5307	202	0.04

Phenol

Table 2.7. GC calibration data for Phenol (2 – 8 wt%)

Concentration wt%	Micro Moles of Phenol	Integrated Area of Peaks	SD	CV
0.1	0.01	49	4	0.08
0.2	0.02	122	7	0.06
1	0.08	542	22	0.04
4	0.34	2026	68	0.03
6	0.51	2972	173	0.06

Hydroquinone

Table 2.8. GC calibration data for Hydroquinone (0.2 – 1 wt%)

Concentration wt%	Micro Moles of Hydroquinone	Integrated Area of Peaks	SD	CV
0.1	0.01	34	3	0.07
0.05	0.07	206	9	0.04
1	0.07	368	14	0.04

p-benzoquinone

Table 2.9. GC calibration data for p-benzoquinone (0.1 – 2 wt%)

Concentration wt%	Micro Moles of p-benzoquinone	Integrated Area of Peaks	SD	CV
0.1	0.01	37	1	0.04
0.2	0.015	63	1	0.02
1	0.07	437	5	0.01
2	0.15	810	32	0.04

Calculations for Moles of Benzene

Concentration	Density kg/m^3	Mass kg	Mass g	Mass of Ethanol g	Moles	Micro Moles
1%	789.9	$7.90\times\times10^{-7}$	$7.90\times\times10^{-7}$	$7.89\times\times10^{-7}$	$1.01\times\times10^{-7}$	0.10
2%	790.8	$7.91\times\times10^{-7}$	$7.91\times\times10^{-7}$	$1.58\times\times10^{-7}$	$2.03\times\times10^{-7}$	0.20
3%	791.7	$7.92\times\times10^{-7}$	$7.92\times\times10^{-7}$	$2.38\times\times10^{-7}$	$3.05\times\times10^{-7}$	0.30
4%	792.6	$7.93\times\times10^{-7}$	$7.93\times\times10^{-7}$	$3.17\times\times10^{-7}$	$4.06\times\times10^{-7}$	0.41
5%	793.5	$7.94\times\times10^{-7}$	$7.94\times\times10^{-7}$	$3.97\times\times10^{-7}$	$5.09\times\times10^{-7}$	0.51
30%	816	$8.16\times\times10^{-7}$	$8.16\times\times10^{-7}$	$2.4\times\times10^{-7}$	$3.13\times\times10^{-7}$	3.13
35%	820.5	$8.21\times\times10^{-7}$	$8.21\times\times10^{-7}$	$2.9\times\times10^{-7}$	$3.68\times\times10^{-7}$	3.68
40%	825	$8.25\times\times10^{-7}$	$8.25\times\times10^{-7}$	$3.3\times\times10^{-7}$	$4.23\times\times10^{-7}$	4.23
45%	829.5	$8.29\times\times10^{-7}$	$8.29\times\times10^{-7}$	$3.7\times\times10^{-7}$	$4.79\times\times10^{-7}$	4.79

Example for 40% mole of benzene calculation:

$$V_B = 1ML = 1\times10^{-6}\,L = 1\times10^{-9}\,m^3$$

$$\rho_E = 789kg/m^3$$
$$\rho_B = 879kg/m^3$$
$$\rho_T = \left(0.4\times879 + 0.6\times789\right) = 825kg/m^3$$

$$M_B = V_B\times\rho_T = 1\times10^{-9}\,m^3\times825kg/m^3 = 8.25\times10^{-7}\,kg = 8.25\times10^{-4}\,g$$

$$\langle 40\%\rangle Benzene$$
$$8.25\times10^{-4}\,g\times0.4 = 3.3\times10^{-4}$$
$$moles = \frac{g}{g/mol} = \frac{3.3\times10^{-4}}{78} = 4.23\times10^{-6}\,mole$$

Example for mole fraction of benzene (Exp.1):

$$q_T = 60ml/\min = 60\frac{cm^3}{\min}\times\frac{m^3}{(100)^3} = 6\times10^{-5}m^3/\min = 1\times10^{-6}m^3/s$$

$$q_{He} = 53.5ml/\min = 53.5\frac{cm^3}{\min}\times\frac{m^3}{(100)^3} = 5.35\times10^{-5}m^3/\min = 8.92\times10^{-7}m^3/s$$

$$q_{N_2O} = 4.5ml/\min = 4.5\frac{cm^3}{\min}\times\frac{m^3}{(100)^3} = 4.5\times10^{-6}m^3/\min = 7.5\times10^{-8}m^3/s$$

$$P = CRT$$

$$Pq = FRT$$

$$P = 1\times10^5\frac{N}{m^2}$$

$$T = 298$$

$$F_{He} = \frac{\left(1\times10^5\right)\times\left(8.92\times10^{-7}\right)}{8.314\times298} = 3.6\times10^{-5}mol/s$$

$$F_{He} = 3.6\times10^{-5}mol/s$$

$$F_{N_2O} = 3.03\times10^{-6}mol/s$$

$$n_B = (\frac{area}{808.94})\times1\times10^{-6} = \left(\frac{5261}{808.94}\right)\times1\times10^{-6} = 6.51\times10^{-6}$$

$$V_g = 10cm^3 = 1\times10^{-5}m^3$$

$$C = \frac{n}{V_g} = \frac{6.51\times10^{-6}}{1\times10^{-5}} = 0.65$$

$$F_{C_6H_6}mol/s = q(m^3/s)\times C(mol/m^3) = 1\times10^{-6}\times0.65 = 6.5\times10^{-7}mol/s$$

$$F_T = F_{He} + F_{N_2O} + F_{C_2H_5OH}$$

$$F_T = 3.6\times10^{-5} + 3.03\times10^{-6} + 6.5\times10^{-7} = 3.97\times10^{-5}$$

$$y_{He} = \frac{F_{He}}{F_T} = \frac{3.6\times10^{-5}}{3.97\times10^{-5}} = 0.91$$

$$y_{N_2O} = \frac{F_{air}}{F_T} = \frac{3.03\times10^{-6}}{3.97\times10^{-5}} = 0.076$$

$$y_{C_6H_6} = \frac{F_{C_2H_6}}{F_T} = 1.63\times10^{-2}$$

$$y_T = y_{He} + y_{air} + y_{C_6H_6} = 1$$

Nomenclature

ρ_B = Density of Benzene

ρ_W = Density of Water

ρ_T = Density of mixture

M_B = Mass of Benzene

n_B = Number of Mole of Benzene

V_B = Volume of Benzene Injected

V_g = Volume of gas syringe sample

Appendix C: Samples characterisations

Appendix C.1 Particle Size Analysis

MALVERN MASTERSIZER

Reported values by the Malvern software

An example for H/ZSM-5 catalyst after first ion exchange using NH_4Cl.

D(4,3) = 20.82 microns

D(3,2) = 10.08 microns

Upper size boundary (um)	Cumulative mass undersize (%)	Mass fraction in grade (-)	Mid-point (um)	mi*xi	mi/xi
0.58	0	0			
0.67	0.08	0.0008	0.625	0.0005	0.00128
0.78	0.21	0.0013	0.725	0.000943	0.001793
0.91	0.38	0.0017	0.845	0.001437	0.002012
1.06	0.6	0.0022	0.985	0.002167	0.002234
1.24	0.87	0.0027	1.15	0.003105	0.002348
1.44	1.16	0.0029	1.34	0.003886	0.002164
1.68	1.43	0.0027	1.56	0.004212	0.001731
1.95	1.69	0.0026	1.815	0.004719	0.001433
2.28	1.96	0.0027	2.115	0.005711	0.001277
2.65	2.27	0.0031	2.465	0.007642	0.001258
3.09	2.73	0.0046	2.87	0.013202	0.001603
3.6	3.46	0.0073	3.345	0.024419	0.002182
4.19	4.67	0.0121	3.895	0.04713	0.003107
4.88	6.56	0.0189	4.535	0.085712	0.004168
5.69	9.4	0.0284	5.285	0.150094	0.005374
6.63	13.42	0.0402	6.16	0.247632	0.006526
7.72	18.82	0.054	7.175	0.38745	0.007526

9	25.63	0.0681	8.36	0.569316	0.008146
10.48	33.62	0.0799	9.74	0.778226	0.008203
12.21	42.34	0.0872	11.345	0.989284	0.007686
14.22	51.21	0.0887	13.215	1.172171	0.006712
16.57	59.69	0.0848	15.395	1.305496	0.005508
19.31	67.4	0.0771	17.94	1.383174	0.004298
22.49	74.15	0.0675	20.9	1.41075	0.00323
26.2	79.61	0.0546	24.345	1.329237	0.002243
30.53	83.97	0.0436	28.365	1.236714	0.001537
35.56	87.48	0.0351	33.045	1.15988	0.001062
41.43	90.36	0.0288	38.495	1.108656	0.000748
48.27	92.73	0.0237	44.85	1.062945	0.000528
56.23	94.67	0.0194	52.25	1.01365	0.000371
65.51	96.17	0.015	60.87	0.91305	0.000246
76.32	97.26	0.0109	70.915	0.772974	0.000154
88.91	97.99	0.0073	82.615	0.603089	8.84E-05
103.58	98.46	0.0047	96.245	0.452351	4.88E-05
120.67	98.77	0.0031	112.125	0.347587	2.76E-05
140.58	99.01	0.0024	130.625	0.3135	1.84E-05
163.77	99.25	0.0024	152.175	0.36522	1.58E-05
190.8	99.5	0.0025	177.285	0.443212	1.41E-05
222.28	99.74	0.0024	206.54	0.495696	1.16E-05
258.95	99.9	0.0016	240.615	0.384984	6.65E-06
301.68	100	0.001	280.315	0.280315	3.57E-06

Table 3.1 particle size distribution of H/ZSM-5 using (MALVERN MASTERSIZER)

Check on mass fraction = 1

Mean particle size by mass (D[4,3]), microns = 20.88144

Specific surface area per unit volume, microns^{-1} = 0.593527

Sauter mean diameter (D[3,2]), microns = 10.10907

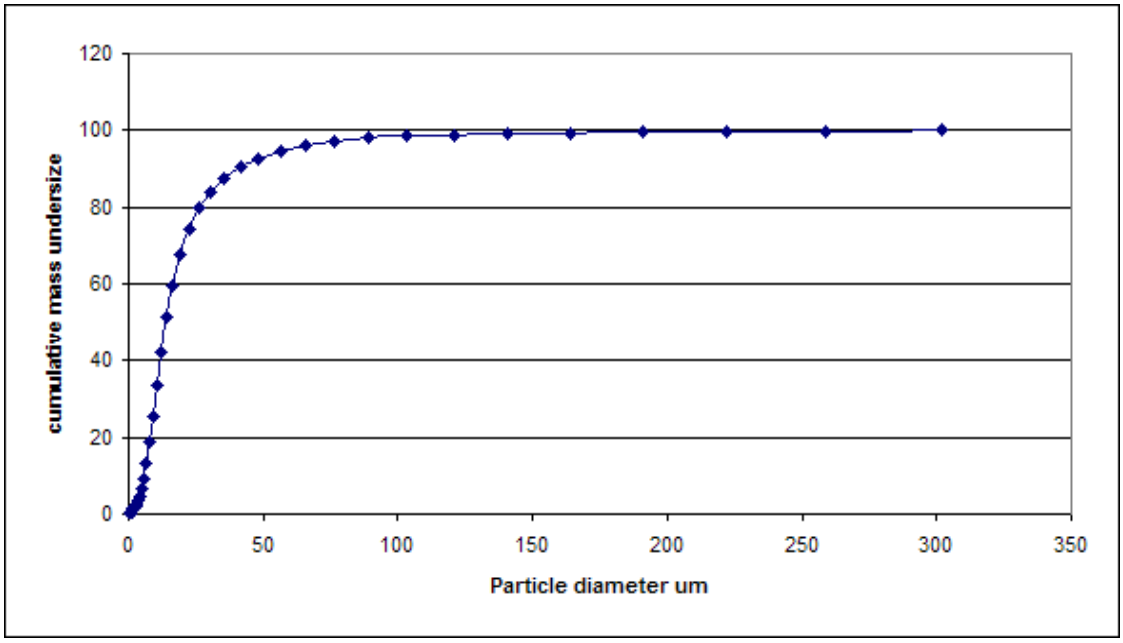


Figure 3.1 the cumulative curve of particle size distribution of H/ZSM-5

Notation

Mi = Mass fraction or Relative mass $\frac{xi^3 \times fi}{\sum xi^3 \times fi}$

Xi= Mid- point (microns)

(D[4,3]) = Mean particle size by mass (microns) $\sum mi \times xi$

S_V = Specific surface area per unit volume (microns^{-1}) $6\sum \frac{mi}{xi}$

(D[3,2]) = Sauter mean diameter (microns) $\frac{6}{S_v}$

Appendix C.2: Active sites concentration

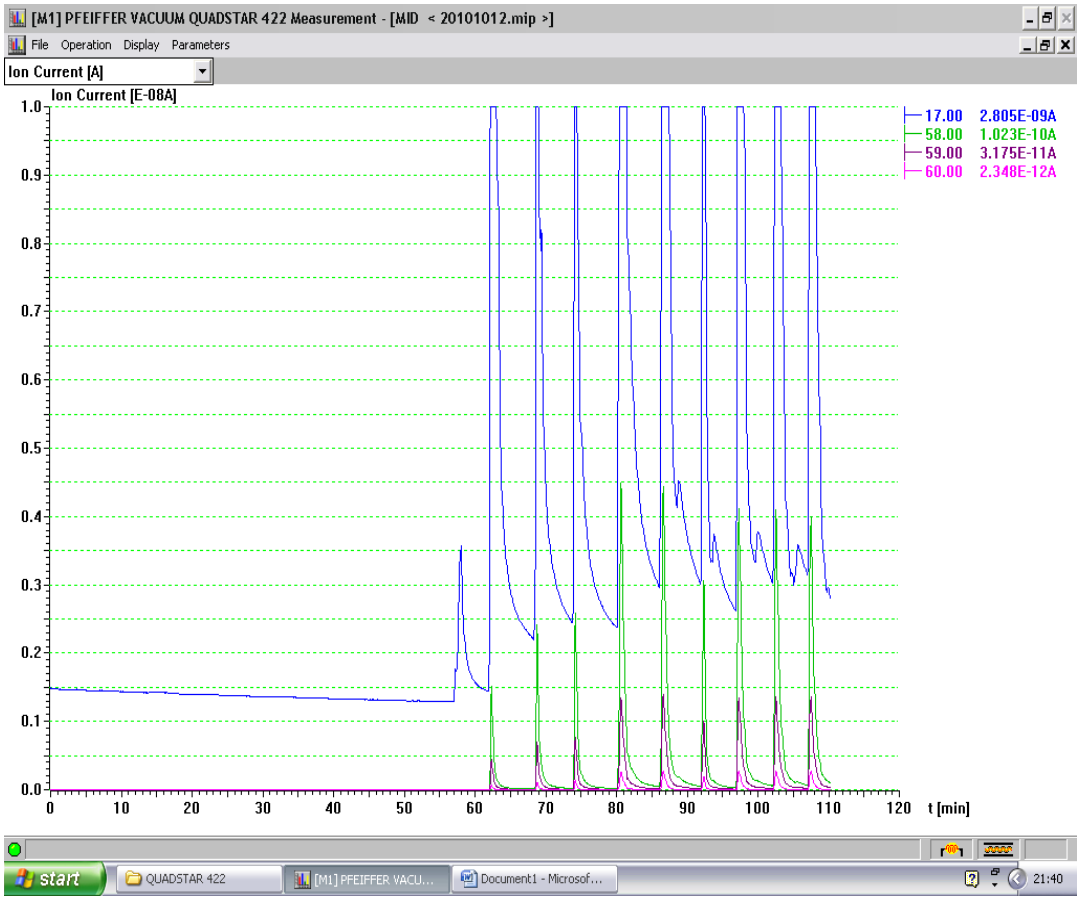


Figure 3.2. Isopropylamine injection at 200°C using 0.5g 1%FeZ30catalysts

As example for the active site concentration:

After obtaining the peak area using 0.1%FeZ30 by Mass Spectroscopy (A_{pms}) . The acid site concentration (N_{as}) can be calculated :

$$N_{as} = A_{PMS}\left[\left(\frac{V_{cal}}{A_{cal}}\right)\left(\frac{L}{10^3 cc}\right)\left(\frac{mol}{22.414L(STP)}\right)\left(\frac{10^6 Mmoles}{mole}\right)\right]$$

$$N_{as} = 3.3\times10^{-9}\left[\left(\frac{15}{4\times10^{-8}}\right)\left(\frac{L}{10^3 cc}\right)\left(\frac{mol}{22.414L(STP)}\right)\left(\frac{10^6 Mmoles}{mole}\right)\right]$$

$$N_{as} = 552.11 Mmoles/g \times (6.023\times10^{23} mol^{-1})$$

$$0.33\times10^{20} site/1g \Rightarrow 16\times10^{18} site/0.5g$$

Appendix D: Experimental results

Appendix D.1: Experiments (The stability of the feed composition of benzene)

To evaluate the stability of the feed composition stream as a function of time, feed samples were taken at every hour. The flow rate are 10 ml/min of N_2O and 50 ml/min of He, flow through the benzene bubbler, temperature set at 50°C), with preheated (oven 1 and oven 2) at 300 and 450°C consequently.

Experiment	**He (**ml/min)	**N_2O (**ml/min)	**Total Flow Rate (**ml/min)
EXP.1	50	10	60

Table 4.1 Benzene feed composition as a function of time on stream.

Time (h)	**Area of benzene**	**Concentration of benzene (**mol/m3)
1.66	4406	1.20
5	4444	1.21
15	4418	1.2
Average	4423	1.2

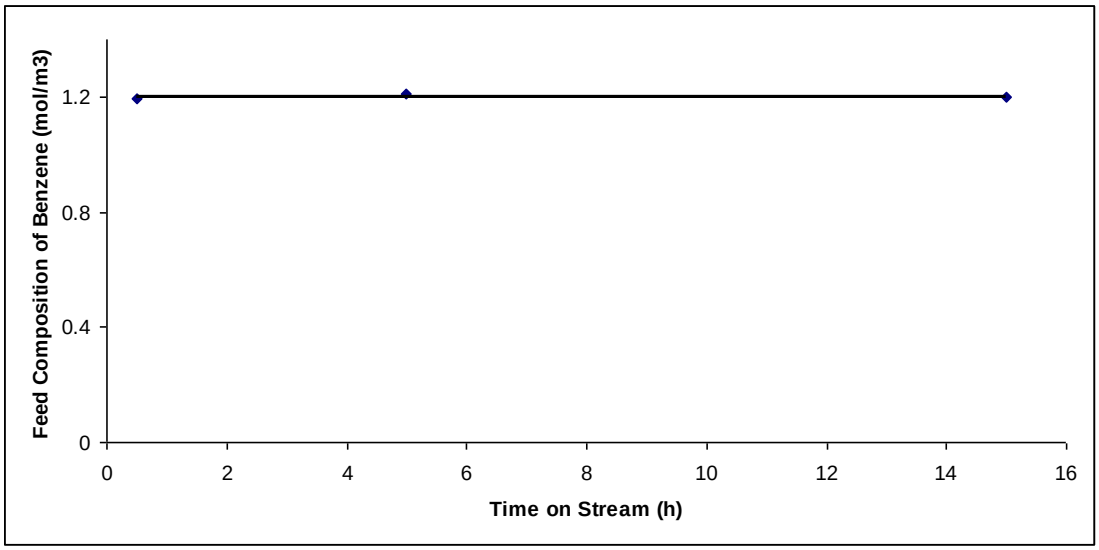


Figure 4.1 The stability of the feed composition of benzene as a function of time with preheated oven 1 and oven 2 : 350 and 450°C consequently.

Experiments (hydroxylation of benzene to phenol)

A matrix of experiments has been done to evaluate the effect of temperature and different iron contents (0.1 and 1 %) on phenol selectivity using 0.2 g of (Fe/Z30 –cal 900°C/154µm).

1- First experiment at 450°C (0.1% Fe/Z30- cal 900°C/154µm)

Experiments	**He** ml/min	**N_2O** ml/min	**Total Flow Rate** ml/min
EXP.1	50	10	60

Table 4.2. Benzene effluent and conversion, Phenol yield, selectivity and concentrations as a function of time using (0.1% Fe/Z30 –cal 900°C/154µm). reaction temperature 450°C/ catalyst (0.2g)

Time (h)	Area of benzene effluent	Area of Phenol	Benzene Effluent Concentrations (mol/m3)	Phenol Concentrations (mol/m3)	Benzene Conversion (%)
1	2022	3552	0.23	0.60	79
2	2256	3318	0.35	0.56	71
3	2531	2414	0.46	0.41	62
4	2405	2281	0.41	0.38	66
5	2445	2187	0.42	0.37	65
10	2430	2112	0.42	0.36	65
15	2313	1612	0.37	0.27	69
20	2468	1686	0.43	0.28	64

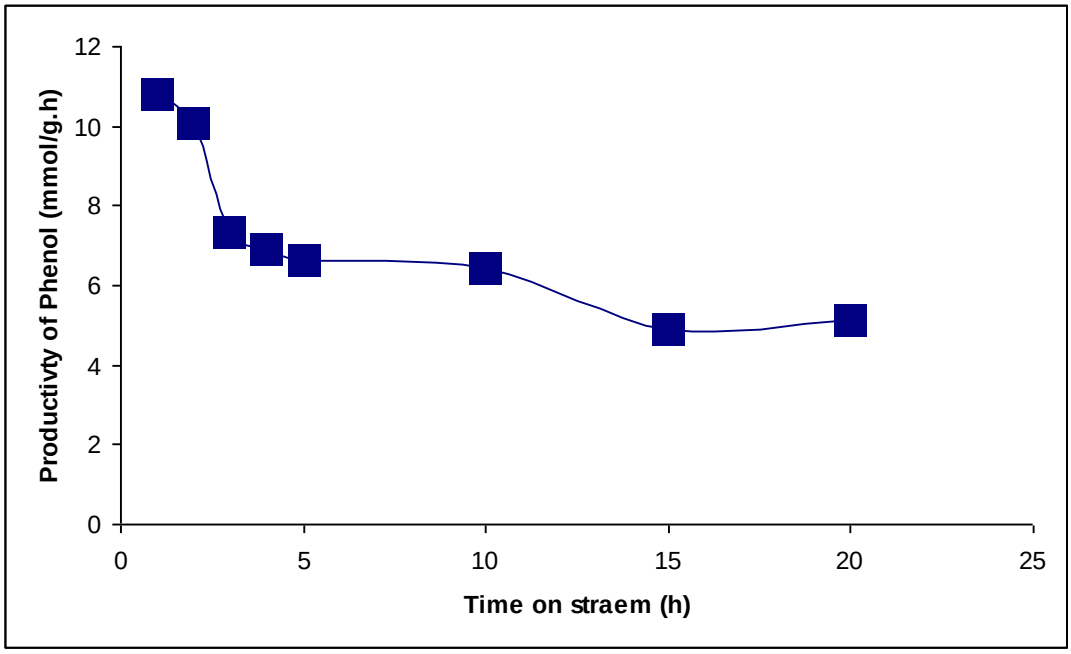


Figure 4.2 Phenol productivity vs time on stream (reaction conditions: 450°C, atmospheric pressure, feed gas =60ml/min). using 0.2 g of 0.1% Fe/Z30 –cal 900°C/154µm.

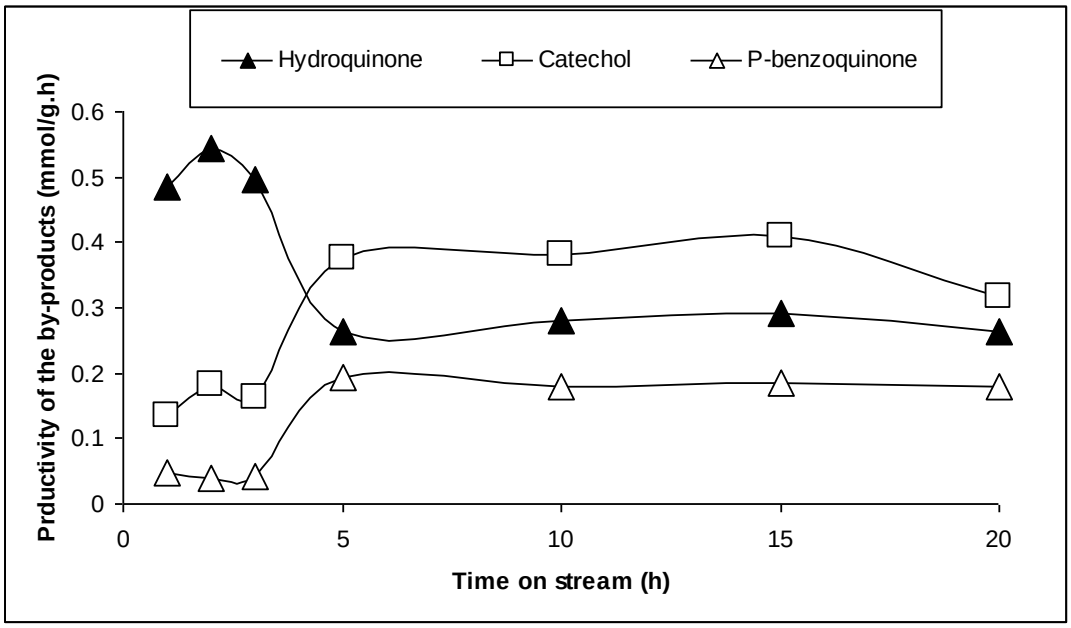


Figure 4.3 By-products productivity vs time on stream (reaction conditions: 450°C, atmospheric pressure, feed gas =60ml/min). using 0.2 g of 0.1% Fe/Z30 –cal 900°C/154µm.

Experiments (hydroxylation of benzene to phenol)

The experiments using 0.2 g of (0.1% Fe/Z30 –cal 900°C/154µm) at 350°C has been done.

1- First experiment at 350°C ((0.1% Fe/Z30 - cal 900°C/154µm)

Experiments	**He** ml/min	**N_2O** ml/min	**Total Flow Rate** ml/min
EXP.1	50	10	60

Table 4.3. Benzene effluent and conversion, Phenol yield, selectivity and concentrations as a function of time using (0.1% Fe/Z30 –cal 900°C/154µm). reaction temperature 350°C/ catalyst (0.2g)

Time (h)	**Area of benzene effluent**	**Area of Phenol**	**Benzene Effluent Concentrations (mol/m3)**	**Phenol Concentrations (mol/m3)**	**Benzene Conversion (%)**
1	1574	2247	0.08	0.38	92
2	2509	1947	0.45	0.32	57
4	2554	1593	0.47	0.27	55
5	2723	1413	0.53	0.24	49
10	2456	1559	0.43	0.27	59
15	2612	1316	0.49	0.22	53
20	2787	1395	0.56	0.24	46

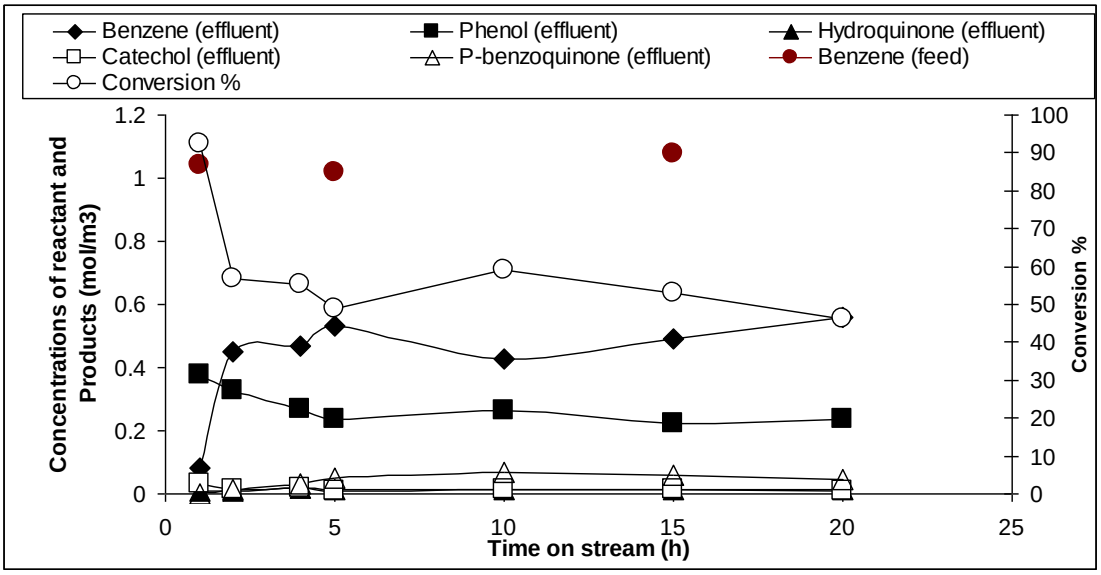


Figure 4.4. Benzene and phenol concentrations vs. time on stream (reaction conditions: 350°C, atmospheric pressure, feed gas =60ml/min, 154µm) 0.2g of 0.14% Fe/Z30 –cal 900°C/154µm.

Rate of Formation of Phenol(Productivity)

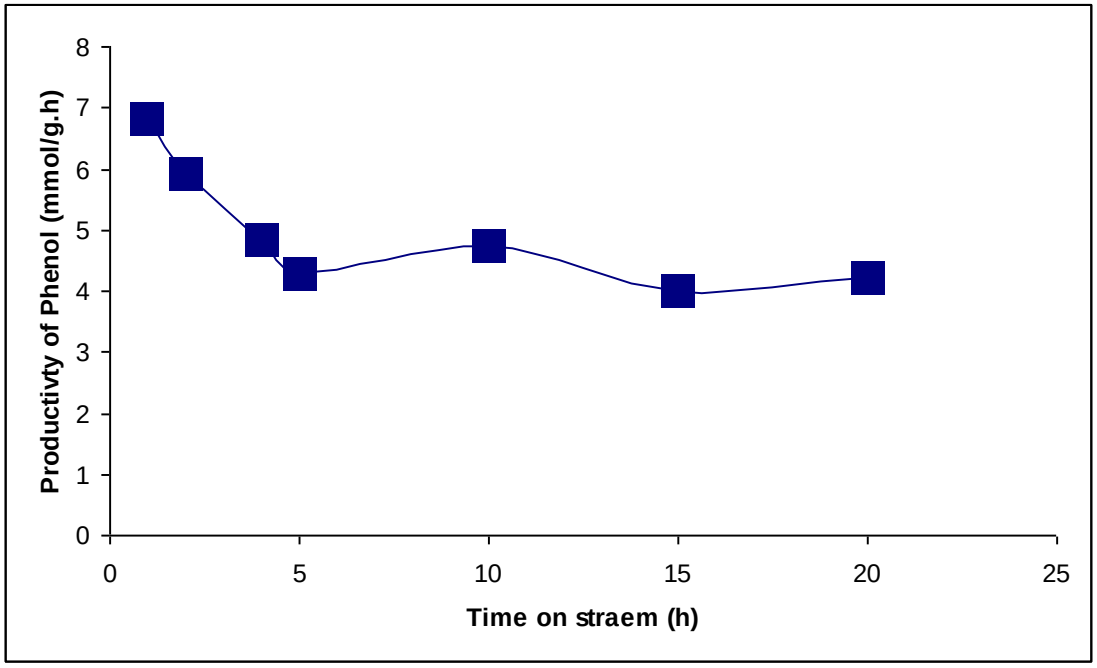


Figure 4.5 Phenol productivity vs time on stream (reaction conditions: 350°C, atmospheric pressure, feed gas =60ml/min). using 0.2 g of 0.14% Fe/Z30–cal 900°C/168µm.

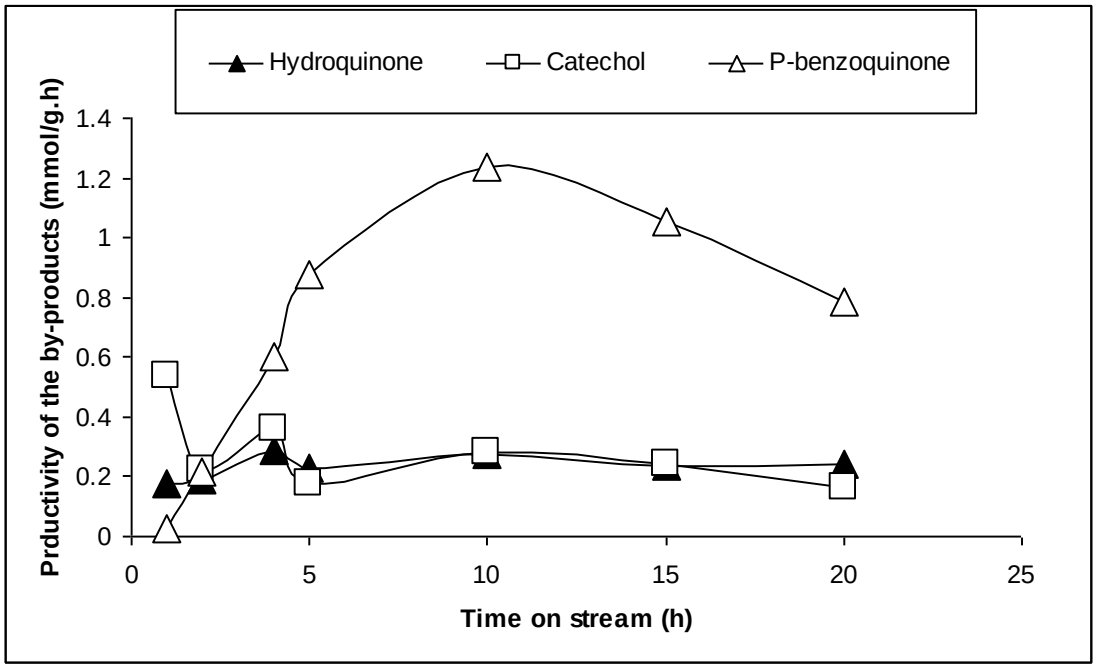


Figure 4.6 By-products productivity vs time on stream (reaction conditions: 350°C, atmospheric pressure, feed gas =40ml/min). using 0.2 g of 0.14% Fe/Z30 –cal 900°C/154µm.

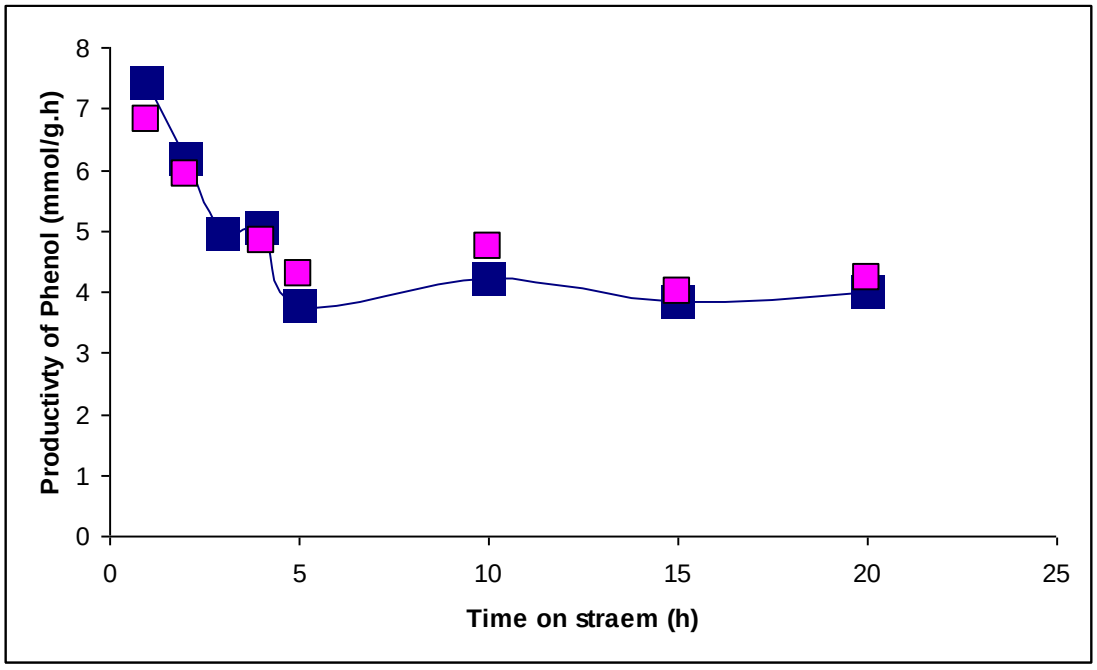


Figure 4.7 Phenol productivity for experiments number 1 & 2 vs time on stream (reaction conditions: 350°C, atmospheric pressure, feed gas =60ml/min). using 0.2 g of 0.14% Fe/Z30–cal 900°C/154µm.

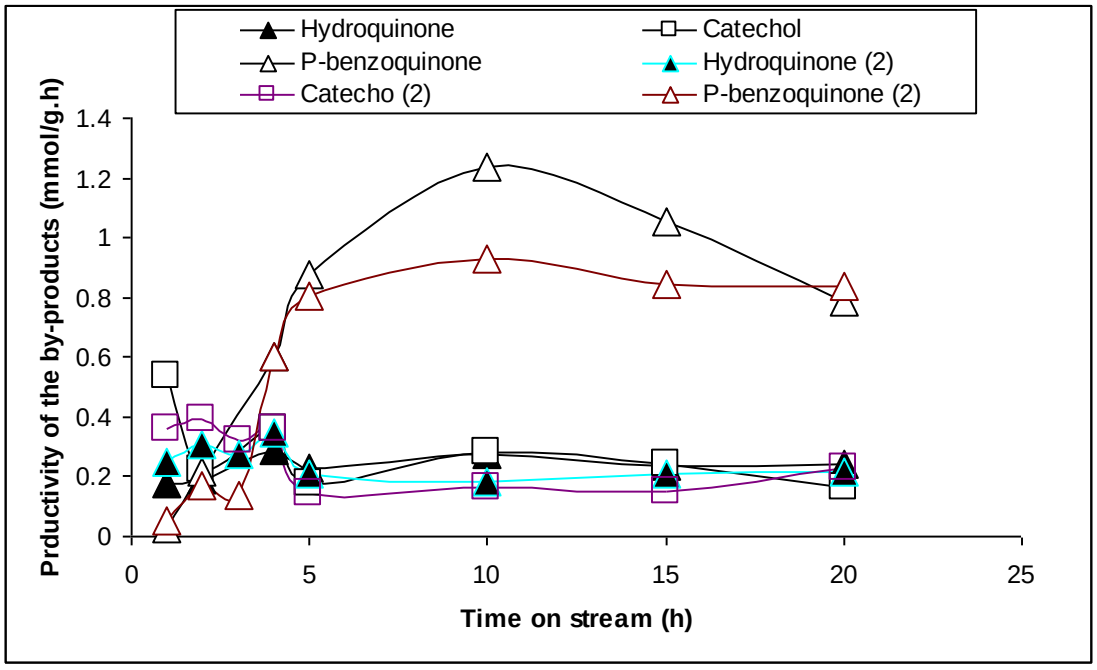


Figure 4.8 By-products productivity for experiments 1 & 2 vs time on stream (reaction conditions: 350°C, atmospheric pressure, feed gas =40ml/min). using 0.2 g of 0.14% Fe/Z30 –cal 900°C/154µm.

Appendix E. Published work

Al-Hazmi, N., Malik, D.J. and Wakeman, R.J., "Hydroxylation of benzene to phenol using nitrous oxide", *Proceedings of the 19th International Congress of Chemical and Process Engineering CHISA 2010*, 1, 19th International Congress of Chemical and Process Engineering CHISA 2010, Prague, Czech Republic, 2010, 27-36.